Indian Journal of Natural Sciences www.tnsroindia.org.in ©IJONS

Vol.9 /Issue 51 / December / 2018 *International Bimonthly* *ISSN: 0976 – 0997*

RESEARCH ARTICLE

Sero-Prevalence of Foot-and-Mouth Disease in Cattle by 3ABC NSP ELISA

Karim Sadun Al-Ajeeli[1]*, Amer Khazaal Al-Azawy[1], Ghazwan Khudhair AL-Anbagi[2] and Layth Mohammed Salih Abdul-Rasoul[3]

[1]Department of Microbiology, College of Veterinary Medicine, University of Diyala, Iraq
[2]Veterinary Directorate, Diyala Veterinary Hospital, Baquba, Diyala, Iraq.
[3]Veterinary Directorate, Central Veterinary Laboratory (C.V.L), Iraq.

Received: 16 Aug 2018 Revised: 19 Sep 2018 Accepted: 22 Oct 2018

***Address for Correspondence**
Karim Sadun Al-Ajeeli
Department of Microbiology,
College of Veterinary Medicine,
University of Diyala, Iraq.
Email: alajeelikarim@gmail.com

ABSTRACT

This study was conducted during the period from September 2017 to May 2018, and aimed to estimate the seroprevalence of FMDV in cattle of Diyala province.Bovine serum samples were collected from 450 animals of five different areas of Diyala province. These samples were grouped according to age, pregnancy status, vaccination, gender and location. All the samples were subjected to 3ABC ELISA test for the purpose of screening of such samples to antibodies against non-specific proteins (NSP) of foot and mouth disease (FMD). About 25.33%(114/450) of them were positive by ELISA test. No significant differences were observed between positive and negative 3ABC results but there was significant difference between positive 3ABC results of pregnant cattle and non-pregnant cattle samples ($P<0.05$). The positive samples from vaccinated animals (41) were higher than those from non-vaccinated (39) but no significant differences between the two positive groups in relation to vaccination status. High prevalence of FMDV antibodies was observed in female 82.5%(94/114) in comparison to that of male 17.5% (20/114). Significant differences were observed between vaccinated and non-vaccinated groups of same sex. In regard to age grouping and FMDV 3ABC seroprevalency, high seroprevalence of positive 3ABC was observed with age group of more than 4 years old 40.4% (46/114) followed by more than 2-4 years old 26.3% (30/114). Age groups of male less than 6 months and 7-12 months of age showed high seroprevalency 30% (6/20) and 45%(9/20) in comparison of same age groups of female more than 2-4 years and more than 4 years showed high seroprevalence of 31.9%(30/94) and 48.9% (46/94) respectively. In regard to location of animal sampling, significant difference in seroprevalenc of samples collected from cattle in Al-Khalis district in comparison to those collected from cattle in Baqubadestrict. The other three destricts of Al-Moukdadia, Baladrouz and Khanaqin were insignificantly correlated. High prevalence of

FMDV 3ABC antibodies among cattle need to use an effective control measures and an evaluation of FMDV circulating serotypes among Iraqi livestock.

Keywords: FMDV, Cattle, 3ABC-ELISA, Iraq, risk-factors**.**

INTRODUCTION

Foot-and-Mouth disease (FMD) is one of the most important diseases of animal husbandry that affected cloven-hoofed ruminants and pigs. It is viral disease that characterized formation of vesicles in skin junction (coronate) with hooves (Foot) and mucous membrane of mouth and tongue (Mouth). Other parts like teats were also affected (1). The disease is very important from economic point of view. Its economic importance was attributed to losses from high morbidity, treatment vaccination and veterinary services, secondary infections, losses in body weight gain of infected animals, mortality that might reach 2% in adults and 20% (2) to 50% (1) among young animals, reduction in milk production , increased abortions that might lead to fertility impairment (3) , and restriction regulations that applied on countries affected with FMD outbreaks (4,5,6,7). More than 100 countries were reported endemic by FMD. Some developed countries were reported free, whereas it was the main problem in most developing countries (8).The disease was caused by an RNA virus that classified as a member in the genus *Aphthovirus*. This genus was grouped with the family *Picornaviridae.* Its RNA genome is single stranded, linear and positive sense. There are seven serotypes of the virus named: A, O, C, Asia 1 and three Southern African Territories (SAT) serotypes recognized as SAT1, SAT2, and SAT3. These serotypes were included subtypes and confined to specific geographical distribution (9,10).

In Iraq, cattle and sheep husbandry and rearing is one of the important national economic facts. Most Iraqi foods supplement of meat was depending on such industry. Accordingly, spread of a viral disease of such type (FMD) might greatly affected animal production and led to huge economic losses among such animals as it was reported many FMD outbreaks in last decades(5,6). During 1988 in Iraq, FMD virus was isolated, serotyped, and characterized by (11). During the period of 1998 t0 2000 many outbreaks among Iraq cattle were reported and the virus was isolated from Holstien cattle and identified as serotype O (12). In 2009 an FMD outbreaks among cattle were occurred, and some of collected samples were sent to Pribright laboratories. The isolated virus was identified as a subtype related to Turkish FMD isolate. This A/IRQ/24/2009 isolate was found to 99.69% matched to A/IRQ/10/2009, and A/KUW/6/2009. The same isolate was found to be closely related in 95.46% identity to A/IRN/1/2005 and, in 84.75% to A/SAU/41/91 isolate, and finally it was related in 82.16% identity to A22/IRQ/24/64 (vicinal strain) (13).Recently many FMD infections were reported among cattle in some villages of Diyala province. Some of these animals were subjected to vaccination programs by veterinary services. Occurrence of FMD in vaccinated animals in Iraq had been reported nine years ago and attributed to misuses of scientific and accurate methods for FMD control. Additionally, random doses of the vaccine were used, and such vaccine did not match the antigenicity of circulating field FMDV in Iraq (14 ,15) . Accordingly, the present study aimed to: Serologic screening of FMD in cattle of Diyala province by 3ABC kit that differentiates infected animals regardless their vaccination status.

MATERIALS AND METHODS

This study was conducted in Diyala province from the period of September 2017 to May 2018.The main objective of this study is to estimate the sero-prevalence of Foot-and Mouth disease in vaccinated and unvaccinated cattle.

Collection of samples

Samples were collected from both sexes and from both native cattle breed aswell as cross breed of five main areas of Diyala province (Table 1). Four hundred and fifty serum samples were collected from apparently healthy animals according to their genders, age, type of nutrition, status of vaccination, and pregnancy (Table 2). Blood samples were collected by using sterile disposable syringes of 18 gage needle size and clot activator blood plain tube. After disinfection of skin site of jugular vein region by using cotton and 70% of ethyl alcohol, blood collection was done aseptically by jugular vein puncture. The collected blood samples were transported in cooler box to the laboratory and then the cleared sera were separated by cooled centrifugation at (3000 rpm) for 10 minutes, the cleared serum sample were labeled, numbered, and kept frozen (-20)°C till used.

Processing of Serum Samples and Detection of FMDV antibodies

Frozen serum samples were thawed at room temperature; this was followed by taking 10 µl from each sample separately and diluted to 1/100 in dilution buffer. Processed collected samples, positive control and negative control were subjected to IDEXX FMD-3ABC Bo-Ov ELISA test kit according to the instructions of the manufacturer (IDEXX laboratories, USA.) for the detection of FMDV antibodies in such collected samples.

Statistical analysis

Data were calculated by SPSS for windows TM version 24.0. . as well as Chi-square, and $P<0.05$ was considered to be significant (16) .

RESULTS

In overall seroprevalnce of FMDV 3ABC antibodies 114 (25.33%) bovine samples were positive to ELISA out of 450 collected samples from bovine in five different localities of Diyala province.

The effect of Pregnancy

Serum samples collected from pregnant and non-pregnant cattle and subjected to 3ABC ELISA test showed that 85(42.7%) samples were positive to the test out of 199 samples (Table 3). These samples were from pregnant and non-pregnant cattle and estimated as 45 (52.9%) and 40 (47.1%) respectively. No significant differences were observed between positive and negative 3ABC results also there was no significant difference between positive 3ABC results of pregnant cattle and non-pregnant cattle samples($P<0.05$) .

Pregnancy and Vaccination

In regard pregnancy, FMDV vaccination and 3ABC positivity rate, 45 samples (41 vaccinated and 4 non-vaccinated) from pregnant cattle (Table 4) were positive to 3ABC test, and 40 samples (39 vaccinated and 1non-vaccinated) from non-pregnant cattle were positive to 3ABC test. No significant differences were noticed between pregnant and non-pregnant cattle in regard to vaccination status and positivity to 3ABC test.

The effect of Gender

Twenty serum samples out of 137 collected from male cattle were positive to 3ABC test, whereas 94 out of 313 samples from female cattle were positive to the same test (Table 5). No significant differences were observed between

positive and negative 3ABC results, neither between males nor between females as a separate gender, but there was significant difference between positive 3ABC results of male group and female group of serum samples (P<0.05).

Gender and Vaccination

The number of 3ABC positive male and female samples was 114 out of 450 samples. They were 91 FMDV vaccinated animals (5 male and 86 female) and 23 non-vaccinated animals (15 male and 8 female) (Table 6). significant differences were observed between male and female groups in positivity rate of 3ABC test in regard to vaccination, similarly vaccinated and non-vaccinated animals of the same gender were showed differences at level of P<0.05.

The effect of Age

The results of positive samples to FMDV antibodies according to age groups of A, B, C, D, and E showed that the number was (9, 12,17,30, and 40 respectively (Table 7). There were significant differences between each 3ABC positive and 3ABC negative results groups of A, B, D, and E (P<0.05), but not with Age group C.

Age groups and Vaccination status

The number of serum samples that were collected from FMD vaccinated animals and positive to 3ABC test were 356 out of 450. The rest 94 were not vaccinated but also positive for 3ABCtest (Table 8). The results showed significant differences in 3ABC positive results between vaccinated and non-vaccinated animals of the age groups A,B, and E (P<0.05), but not within the age groups of C and D.

Age groups and Gender

The 3ABC positive results according to the gender of tested animals showed that 20 samples were positive from male and 94 were positive to the test from female (Table 9). There were significant differences between male and female within each age group of A,B,D, and E (P<0.05), but not with the male and female age group C.

3ABC positivity rate and Location

The 114 samples positive to 3ABC test were compared in table (10). The number of 3ABC positive sample were 20, 23, 14, 34, and 23, and were collected from Baquba, AL-Mouqdadia, Baladrouz, AL-Khalis and Khanaqin respectively. Significant difference was observed in 3ABC positivity rate in samples collected from Bauquba and AL-Khalis, but no significant differences in 3ABC positivity rate were noticed in other compared locations.

DISCUSSION

The 3ABC kit was designed to detect FMDV antibodies against nonstructural proteins of the virus that were produced during the past and present infections with any of FMDV serotypes in unvaccinated animals (17) . The test also can be used differentiated the FMD vaccinated animal from the FMDV-infected carrier one (18,19) .Non-structural proteins of FMD like 3ABC, 3D, 3B and 3A can be detected in less than 10 days post recent infection in cattle and also can be detected in long duration up to 2 years (20,21,22,23,24) Recently, many workers were used 3ABC ELISA test to estimate the seroprevalence of FMDV antibodies in cattle (25,26,27]. Serum samples that were positive to 3ABC test of present study were 114 (25.33%) of total 450 serum samples collected from cattle and subjected to 3ABC ELISA test. This finding was higher than that reported by many workers (28 , 29 , 30 , 31 , 32) who were reported 19.33%, 16%, 12.8%, 17.6%,14.05% and 19.33% respectively among serum samples collected from cattle

and subjected to the same test. Higher than present findings wasalso reported in many other locations, like 61% in Uganda (33) and overall 72.62% in Nigeria (34). This higher or lower seropostivity might be attributed to nature of animal population, and control programs of FMDV infection in their country of study. Furthermore, (27) attributed such variation in sero-prevalence to variation in management system, intervention and agro-climatic condition.In Iraq, a seroprevalnceof 78.6% was reported in cattle of Basrah(35) .Their findings also were higher than that reported by(36,37,35,38) in cattle of different parts of Iraq. Overall FMDV seroprevalence of 75% was reported in Al-Diwaniyah and Al—Najaf, whereas, 100% seropostivity was reported in Karbala (38). The 3ABC positive samples collected from pregnant and non-pregnant cattle were 85 samples.Non-significant difference between positive 3ABC results of pregnant cattle and non-pregnant cattle samples ($P<0.05$) was estimated when 45 samples from pregnant cattle were positive to 3ABC test in comparison to that of non-pregnant cattle. The finding of present study was coincide to the finding of (32), who stated that sex and pregnancy did not have any association with the disease. Contrary to the findings of (39).that caution the difference might be attributed to stress and hormonal factors of pregnancy.

In the present study 20 samples (17.5%) from male and 94 (82.5%) from female were positive to 3ABC test. Accordingly, the seropositivity in female was higher than that of male and statistically significant at the level of $P<0.05$. The high seroprevalence in femal of present study came in consistent with many other reports, high seropostivity to FMDV antibodies in female in comparison to male was reported by many researchers (29, 40, 41, 32) and attributed to thephysiological factors like lactation, pregnancy, and estrus (32) . The high and low seroprevalence of FMDV according to gender seems to be of contrary values when some other workers reported high seropostivity in male than female cattle (42,31). In another reports by (42 and 27] mentioned that no statistical differences were noticed between male and female cattle seropositivity to FMDV. In Basrah province of Iraq high seroprevalence in female cattle 78.6% than in male 60.4% was also reported (43) and supported by the same findings of (40) . Contrary, some other reporters mentioned no significant correlation in seropostivity to FMDV between male and female bovines in middle part of Iraq (38, 35). The use of age grouping as a risk factor in the seropositivity to FMDV by 3ABC ELISA showed no significant differences within the positivity of these groups, but significant differences were reported between negativity and positivity to 3ABC test ($P<0.05$) except for one group of 1-2 years old cattle. The results showed that the seropositive samples were increased with the increase of age, and high percentage was reported in age group of more than 4 years and followed by the age group of 2 to 4 years old. These finding came in agreement with findings of (27) who reported that high seroprrvalence to FMDV was in ages more than 4 to 10 years in comparison to young animals and adult in more than 10 years old. They more added that no significant differences were found in relation to age groups of seroprevalence to FMDV.

In association of age grouping and gender inseropositivity to 3ABC test, the present study showed in general that female positive samples 94 (82.5%) were higher than those of male samples 20 (17.5%) and the findings were in agreement to many authors in regard to age grouping (43,27)when they were reported high prevalence of FMDV NSPS antibodies in adult cattle than young, but in contrary with findings of (44) who mentioned that such seroprevalce was high in young animals. This might attributed to management programs when young animals were mixed with the adult. Some other reporters mentioned that seroprevalence to FMDV in bovine was age associated (45,46,31,47). In contrast to the finding present study, another report mentioned that young animals were more susceptible to FMD than adults (44). The high seroprevalence of adult in present study might be attributed to possibility of reinfection with different circulating serotypes of FMDV, and the adult cattle got the infection by contact with other infected animals either in grazing areas or due to movement from one region to another (27). Low seropostivity of young animals might be attributed to methods of rearing when farmers separated young from adult and appeared with low possibility to contact other infected animals (42).The association of vaccination to serprevalence of FMDV antibodies to NSPs with pregnancy, no significant differences were noticed between pregnant and non-pregnant cattle in regard to vaccination status and positivity to 3ABC test, but it was noticed that 85 vaccinated cows (41 pregnant and 39 non-pregnant) were positive to 3ABC test. The same observation was reported association of gender and vaccination to seropostivity in 3ABC test when high number (93 out of 114) of

vaccinated animals was positive to the test in comparison to 21 (3ABC positive) non-vaccinated animals. These findings came in agreement with that reported by (26) in detection of NSPs of FMDV in vaccinated animals that suggested their reinfection with FMDV. The animals of present study might be gained the infection from other circulating serotype of FMDV that was not represented in current vaccine used (27).In conjunction to locality the sero-positivity of bovine samples of present study were as 17.5% in Baquba, 20.2% in AL-Muouqdadia, 12.3% in Baladrouz, 29.8% in Al-Khalis, and 20.2% in Khanaqin. Furthermore, statistically no significant differences were observed in seroprevalence and number of samples in relation to locality, but such significant difference was observed between positive samples of Baquba district and Al-Khalis districts when 20 serum samples of cattle from Baquba were positive to 3ABC test in comparison to 30 samples in Al-khalis district.

Significant differences (P<0.05) of seroprevalence according to locality were reported by (32) from Pakistan who reported lower seroprevalence in Chakwal 11% and Khanewal 17.66% in comparison to high prevalence of Faisalabad 29.33% and this might be attributed to differences in population of animals and free movement of animals (48).In present study, Al-Khalis have had larger population of animals with free movement of livestock in comparison to Baquba district. Similar findings were reported by (42) who found significant differences (P<0.05) between South Omo than Sidama and GamoGofa areas in Athiopia. (46) reported significant differences among seropositivity of samples in relation to locality when they were reported seroprevalence of 30.2% in Benaatsemay district in comparison to 6.3% seroprevalence of Malle and DebubAari districts of Athiopia. In contrast (27) found no statistical differences in seroprevalence of FMDV antibodies in relation to origin of animals, they reported high prevalence to FMDV antibodies in bovine from pastoral areas of free animal movement more than those animals from areas with restricted animal movement.

CONCLUSIONS AND RECOMMENDATIONS

FMDV in bovine of Diyala province appeared with high seroprevalence (25.33%) when 114 out of 450 tested animal serawere positive by 3ABC test to NSP antigens which means the possibility of FMDV reinfection of such animals including the vaccinated bovine. This might indicated exposing of the bovine to circulating FMDV of different serotype from those of the vaccine. Accordingly, isolation and sequencing of circulating FMDV is recommended to differentiate them and to apply effective control programs that associated with restriction of animal movement from borders to Iraq and using suitable vaccination programs.

REFERENCES

1. MacLauchlan, N.J. and Dubovi, E. (2011): FENER'S Veterinary Virology. 4th ed.USA. Acadamic Press, pp: 32.
2. Radostits, O. M.; Blood, D. C. and Gay, C. C. (2007): Veterinary Medicine, A Text Book of the Disease of Cattle, Sheep, Goats, Pigs and Horses. 8th ed. London: BalliereTindall, pp: 1223-1227.
3. Admassu, B.; Getinet,K.; Shite, A. and Mohammed, S. (2015): Review on Foot and Mouth Disease: Distribution and Economic Significance in Ethiopia: *Acad. J. of Anim. Dis.* 4(3): 160-169
4. Geering, A.W. and Lubroth, J.(2002): Preparation of Foot- and-Mouth Decease Contingency Plans. Food and Agriculture Organization of the United Nation(FAO); Rome pp 7-20.
5. Dosky, A. M; Ahmed, B. D. ; Seitzer, U. and Ahmed, J.(2006): Foot and Mouth Disease, Rinderpest, Peste des Petits Ruminants and Avian Influenza in the Erbil, Dohuk, and Sulaimania Governorates of Iraq ; *J. Vet. Med. 53:23–25.*
6. Al Gharawyi, F. K.(2009): Epidemiological study of Foot and Mouth Disease in Iraq. Master thesis, college of veterinary medicine, *university of Al-Qadissiya, 2009*
7. Knight, T.; Jonesa, B. and Rushtonb, J. (2013): The economic impacts of foot and mouth disease what are they, how big are they and where do they occur? Preventive Veterinary Medicine 2013 November 1:112 (3-4):161-73.

8. Jamal, S. M. and Belsham, G. J. (2013). Foot-and-mouth disease: Past, present and future. *Veterinary Research* 44:116 - 129.
9. Vosloo, W.; Bastos, A.D.S. and Boshoff, C.I.(2006): Retro-spective genetic analysis of SAT-1 type foot-and-mouth disease outbreaks in southern Africa. *Arch. of Virology, 151:285–289.*
10. Valdazo-González, B.; Knowles, N. J.; Hammond, J. and King, D. P. (2012): Genome sequences of SAT2 foot-and-mouth disease viruses from Egypt and Palestinian Autonomous Territories (Gaza Strip). Journal of Virology86(16): 8901–8902. Virus by RT-PCR and ELISA. Kufa. Journal of veterinary medicine sciences.,Vol (5) . No(2) 2014.
11. Al-Bana, A.S. and Shouny, M.O.(1988).Foot and mouth disease in Iraqi native gazella: virus isolation. Serotyping and characterization. The Iraqi J.Veet.Med.,12:13-24.
12. Al-Janabi, M.A. (2001).Isolation and identification of Foot and Mouth Disease virus from cattle and sheep and study the infectivity of the virus of different types of cells from human and animals. M.Sc. Thesis In veterinary Microbiology, College of Veterinary Medicine, University of Baghdad. (In Arabic).
13. FAO.(2010): FAO World Reference Laboratory for Foot and Mouth Disease (Pirbright laboratory) *www.wrlfmd.org.*
14. FAO.(2009): Situation of FMD in the Middle East. (Compilation of information from OIE (official notifications), or reports to EuFMD /FAO by countries or by the FAO/OIE/EC FMD Reference Laboratory, Institute for Animal Health, Pirbright, UK. 38th General Session of the EuFMD – 28-30 April 2009. FAO, Rome.
15. WrLfmd.(2009): Molecular Epidemiology Report, FAO World Reference Laboratory for FMD Genotyping Report (IAH -P -EP-MEG-FOR-005 -1), *P1of 1, January 2009.*
16. Steel, R. G. and Tarries, J. H. (1980).Principle and procedure of statistical 2th ed., Mc grow Hill book. Co. In. New York.
17. OIE. (2012): Manual of Standards for Diagnostic Tests and Vaccines, 4th edition. Part 2. Section 2.1. OIE Listed Diseases. *Chapter 2.1.1. Foot and Mouth Disease* p. 77–92. , p. 190–216. *In* OIE Manual of diagnostic tests and vaccines for terrestrial animals. *Office International des Epizooties,* Paris, France.
18. Clavijo, A.; Wright, P. and Kitching, P.(2004): Developments indiagnostic techniques for differentiating infection from vaccination in footand- mouth disease. *The Vet. J. 2004; 167(1): 9 - 22.*
19. Lu, Z.; Cao, Y.; Guo, J.; Qi, S.; Li, D.; Zhang, Q.; Ma, J.; Chang, H.; Liu, Z.; Liu, X. and Xie, Q. (2007): – Development and validation of a 3ABC indirect ELISA for differentiation of foot-and-mouth disease virus infected from vaccinated animals. *Vet. Microbiol*.,125 (1–2), 157–169. doi:10.1016/j.vetmic.2007.05.017.
20. Diego, A.; Brocchi, E.; Mackey, D. and Simone, F. (1997). The use of non-structural polyproteins 3-ABC of FMD virus as a diagnostic antigen in ELISA to differentiate infected from vaccinated cattle. Arch. Virol. 142: 2021- 2023.
21. Silberstein, E.; Kaplan, G.; Taboga, O.; Duffy, S. and Palma, E. (1997): Foot-and-mouth disease virus-infected but not vaccinated cattle develop antibodies against recombinant 3AB1 nonstructural protein. Archives of Virology 142 (4), 795-805.
22. Sørensen, K.J.; Madsen, K.G.; Madsen, E.S.; Salt, J.S.; Nqindi, J. and Mackay, D.K.J. (1998): Differentiation of infection from vaccination in foot-and-mouth disease by the detection of antibodies to the non-structural proteins 3D, 3AB and 3ABC in ELISA using antigens expressed in baculovirus. Archives of Virology 143 (8), 1461-1476.
23. Moonen, P.; van der Linde, E.; Chenard, G. and Dekker, A. (2004): Comparable sensitivity and specificity in three commercially available ELISAs to differentiate between cattle infected with or vaccinated against foot-and-mouth disease virus. Veterinary Microbiology 99 (2), 93-101.
24. Robiolo, B.; Seki, C.; Fondevilla, N.; Grigera, P.; Scodeller, E.; Periolo, O.; Torre, J.L. and Mattion, N.(2006): Analysis of the immune response to FMDV structural and non-structural proteins in cattle in Argentina by the combined use of liquid phase and 3ABC-ELISA tests. Vaccine. 2006;24:997–1008.
25. Bora, M.; Sharma R. and Kakker, N.K. (2014) . Detection of Anti-nonstructural protein antibodies against Foot and- Mouth Disease Virus in the bovine population of Haryana during FMD control programme in the year 2012. *Haryana Vet.* (June, 2014) 53 (1), 8-12
26. Colling ,A.; Morrissy, C.; Barr, J.; Meehan, G.; Wright L.; Goff W.; Gleeson, L.J.; van der Heide, B.; Riddell, S.; Yu, M.; Eagles, D.; Lunt, R.; Khounsy, S.; Long, N. T.; Vu, P. P.; Phuong, N. T.; Tung N.; Linchongsubongkoch, W.; Hammond, J.; Johnson, M.; Johnson, W.; Unger, H.; Danielsa, P. and . Crowtherh, J.R . (2014). Development and

validation of a 3ABC antibody ELISA in Australia for foot and mouth disease. Australian Veterinary Journal Volume 92, No 6, June 2014: 192–199.

27. Belina,D.; muktar,Y.; Girma,B. and Mengistu,S. (2016) . Sero-Prevalence of Bovine Foot and Mouth Disease in Selected Districts of Eastern Showa Zone, Oromia Regional State, Ethiopia Global Journal of Science Frontier Research Volume (16) Issue (4) Version (1) .2016
28. Hafez, S.M.; Farag,M.A.; Mazloum K.S. and Al- Bokmy, A.M. (1994). Serological survey of foot and mouth disease in Saudi Arabia. Rev. Sci. Tech. Off. Int. Epiz. 13 (3): 711-719.
29. Gelaye, E.; Ayelet, G.; Abera, T. and Asmare, K. (2009). Seroprevalence of foot and mouth disease in Bench Maji zone, Southwestern Ethiopia. J Journal of Veterinary Medicine and Animal Health, 1 (1): 005- 010. http://www.academicjournals.org/journal/JVMAH/
30. Dukpa, K.; Robertson, I.D. and Ellis, T.M. (2011). The seroprevalence of foot-and-mouth disease in the sedentary livestock herds in four districts of Bhutan. Prev. Vet. Med. 100(3-4): 231-6.
31. Mohamoud, A.; Tessema, E. and Degefu, H. (2011). Seroprevalence of bovine foot and mouth disease (FMD) in Awbere and Babille districts of Jijiga zone, Somalia regional state, eastern Ethiopia. Afr. J. Microbiol. Res. 5(21): 3559-3563.
32. Nawaz, Z.; Arshad, M.; Rahman, S. and Iqbal, Z. (2014) . Epidemiology of Foot and Mouth Disease in buffaloes and cattle ofPunjab using non- structural proteins ELISA.Pak. J. Agri. Sci., Vol. 51(2), 497-501; 2014
33. Mwiine, F.N.; Ayebazibwe, C.; Olaho-Mukani, W.; Alexandersen, S. and Tjornehoj, K.(2010). Prevalence of Antibodies against foot-and-mouth disease virus in cattle in Kasese and Bushenyi districts in Uganda. Inter. J. Anim. Vet. Adv. 2(3): 89-96.
34. Lazarus, D.D.; Schielen, W.J.G.; Wungak, Y.; Kwange, D. and Fasina, F.O. (2012). Sero-epidemiology of foot-andmouth disease in some border states of Nigeria. Afric. J. Microbiology Res. 6(8): 1756-1761.
35. AL-Jobori,Y.A.A.(2012). Diagnostic Study of Foot and Mouth Disease in Cattle by ELISA and Reverse Polymerase Chain Reaction Technique in ALDiwaniyaCity.M.Sc.Thesis College of Veterinary Medicine, University of Al-Qadissiya.
36. Adil, M. A.(2011).Heat-Intolerance Syndrome as a Sequel of Foot-and- Mouth Disease in Cattle . M.Sc. Thesis/ College of Veterinary Medicine- University of Basrah.
37. Abood, B.K. ;Shlash, K.H. and Hussein, Z.S.(2009). Study of prevalence of FMD in cattle in middle and south of Iraq and detection of the causative serotype . Al-Anbar journal of Veterinary Sciences. 2: 82-86 .
38. Al – Budeiri, M. K. (2012). Isolation and identification of predominant serotypes of foot and mouth disease virus in middle of Iraq .M.Sc.Thesis, College of Veterinary Medicine, University of Al-Qadissiya.
39. Susan, E.A. (1998). The Merck Veterinary Manual, 8th Ed. Whitehouse Stat NJ Merck and Co. Inc. p.1879.
40. Hailu, M.; Mengistie, T.; Negussie, H.; Alemu, S. and Asaminew, T. (2010). Incidence of foot and mouth disease and its effect on milk yield in dairy cattle atandassa dairy farm. Northwest Ethiopia. Agri. Biol.J. 1: 969-973.
41. Chepkwony, E.C.; Gitao, C.G. and Muchemi, G.M. (2012) .Seroprevalence of foot and mouth disease in the Somali eco-system in Kenya. Int. J. Anim. Veter. Adv. 4 (3): 198-203.
42. Megersa, B.; Beyene, B.; Abunna, F.; Regassa, A.; Amenu, K. and Rufael, T. (2009). Risk factors for foot and mouth disease seroprevalence in indigenous cattle in southern Ethiopia: the effect of production system. Trop. Anim. Health Prod. 41: 891–898.
43. Al-Rodhan, A. M. and Salem, Z. M.(2014). Molecular and serological identification of Foot-and-Mouth Disease Virus Serotypesin Cattle of BasrahProvince . Bas.J.Vet.Res.Vol.1,No.1.2014.
44. Radostits, O. M.; Gay, C .C.; Blood, D. C. and Hinachcliff, K. W. (2000). Veterinary medicine, a textbook of the diseases of cattle, sheep, goats, pigs and horses,foot and mouth Disease,9th ed.., California, Elsevier,Pp: 1059-1064.
45. Gebretsadik, Z. (2009) . Study of seroprevalence of foot and mouth disease in Tigray Regional state, Northern Ethiopia. DVM thesis, Faculty of Veterinary Medicine, Haramaya University, Ethiopia. Pp: 12.
46. Molla, B.; Ayelet, G.; Asfaw. Y.; Jibril, Y.;Ganga, G. and Gelaye, E. (2010). Epidemiological Study on Foot-and-Mouth Disease in Cattle: Seroprevalence and Risk Factor Assessment in South Omo Zone, Southwestern Ethiopia. Trans-boundary and Emerging Disease, 57 (5): 340 347.

47. Kibore, B.; Gitao, C. G.; Sangula, A. and Kitala, P. (2013). Foot and mouth disease sero-prevalence in cattle in Kenya. Journal of Veterinary Medicine and Animal Health, (9): 262-268. http://www.academicjournals. org/journal/JVMAH/article-full-text-pdf/.
48. Anjum, R.; Hussain, M.; Zahoor, A.B.; Irshad H. and Farooq, U (2006). Epidemiological analyses of foot and mouth disease in Pakistan. *Int. J. Agric. Biol. 5: 648- 651.*

Table (1) Distribution of samples according to the areas of Diyala province

Areas	Serum samples of cattle		
	Male	Female	Total
Baquba	26	64	90
Khalis	32	58	90
Muqdadia	28	62	90
Kanaqen	29	61	90
Baladrose	22	68	90
Total	137	313	450

Table (2) Number of serum samples collected from cattle according to gender, vaccination, ration, age and pregnancy

Factor Groups		Gender		Total
		Male	Female	
Pregnancy	Pregnant	-------	101	101
	Non-pregnant	-------	212	212
	Male	137	-----	137
Total				**450**
Vaccination	Vaccinated	88	268	356
	Non -vaccinated	49	45	94
Total		137	313	450
Age	(A) Less than 6 months	42	42	84
	(B) 7-12 months	52	53	105
	(C) 1-2 years	35	54	89
	(D) More than 3-4 years	7	82	89
	(E) More than 5 years	1	82	83
Total		**137**	**313**	**450**

Table (3) Seroprevalence of FMDV antibodies by 3ABC Test in Pregnant and Non-pregnant cattle

Pregnancy	3ABC.Test		Total
	+Ve	-Ve	
Pregnant	45 (52.9%) Aa	56 (49.1%) Aa	101
Non pregnant	40 (47.1%) Aa	58 (50.9%) Aa	98
Total	85(42.7%)	114 (57.3%)	199

Table (4) Seropositivity rate to FMDV antibodies by 3ABC Test in cattle according to pregnancy and vaccination

3ABC positive and pregnancy	Vaccination		Total
	Vaccinated	Non vaccinated	
Pregnant	41(51.3 %) Aa	4(80 %) Aa	45
Non pregnant	39(48.8 %)Aa	1(20 %)Aa	40
Total	80 (94.1%)	5 (5.9%)	85

Table (5) Seroprevalence of FMDV antibodies by 3ABC Test in Male and Female cattle

Gender	3ABC.Tes		Total
	+Ve	-Ve	
Male	20 (17.5 %) Bb	117 (34.8 %) Bb	137
Female	94 (82.5 %) Aa	219 (65.2 %)Aa	313
Total	114(25.3%)	336 (74.7%)	450

Table (6) Seropositivity rate to FMDV antibodies 3ABC Test in Infected cattle according to gender and vaccination

3ABC Positivity and Gender	Vaccination		total
	Vaccinated	Non vaccinated	
3ABC+ve Male	5(5.5 %) aA	15(65.2 %) bB	20
3ABC+ve Female	86(94.5 %) aB	8(34.8 %) bB	94
Total	91 (79.8 %)	23 (20.2 %)	114

Table (7) Seroprevalence of FMDV antibodies by 3ABC Test in Cattle according to the age

Age Group	3ABC. Test		Total
	+Ve	-Ve	
(A) Less than 6 months	9(7.9%) a	75(22.3%) b	84
(B) 7 – 12 month	12(10.5%) a	93(27.7%) b	105
(C) 1 – 2 years	17(14..9%) a	72(21.4%) a	89
(D) More than 2 - 4years	30(26.3%) a	59(17.6%) b	89
(E) More than 4years	46(40.4%) a	37(11%) b	83
Total	114 (25.3%)	336 (74.7%)	450

Table (8) Seropositivity rate to FMDV antibodies by 3ABC Test in cattleaccording to age group andvaccination status

Age Group	Vaccination		Total
	Vaccinated	Non vaccinated	
(A) Less than 6 months	2(2.2 %) a	7(33.3 %) b	9
(B) 7 – 12 month	5(5.4 %) a	7(33.3 %) b	12
(C) 1 – 2 years	14(15.1 %) a	3(14.3 %) a	17
(D) More than 2 years - years	28(30.1 %) a	2(9.5 %)a	30
(E) More than 4 years	44(47.3 %) a	2(9.5 %) b	46
Total	93	21	114

Table (9) Seropositivity rate to FMDV antibodies by 3ABC Test in cattle according to age and gender

Age Group	Male 3ABC +Ve	Female 3ABC +Ve	Total
(A) Less than 6 months	6(30 %) a	3(3.2 %) b	9
(B) 7 – 12 month	9(45 %) a	3(3.2 %) b	12
(C) 1 – 2 years	5(25 %) a	12(12.8 %) a	17
(D) More than 2 - 4years	0(0 %) a	30(31.9 %) b	30
(E) More than 4 years	0(0 %) a	46(48.9 %) b	46
Total	20 (17.5%)	94(82.5%)	114

Table (10) Number of 3ABC positive cattle sera according to location

3ABC+ / Area	Baquba	AL-Mouqdadia	Baladrouz	AL-Khalis	Khanaqin	Total
3ABC+	20a	23 a,b	14 a	34 b	23 a,b	114
%	17.5%	20.2%	12.3%	29.8	20.2%	100%

Indian Journal of Natural Sciences www.tnsroindia.org.in ©IJONS

Vol.9 /Issue 51 / December / 2018 *International Bimonthly* *ISSN: 0976 – 0997*

RESEARCH ARTICLE

Hybrid Biomaterial Based on PANI/$CaCO_3$ Nanoparticles as a Novel Anticancer Drug in Combination with NIR Laser in the Treatment of Breast Cancer Cells Line

Mohanad I. Kamil[1]*, Salma M. Hassan[1] and Sabah M. Hadi[2]

[1]Physics Department, College of Science, University of Baghdad, Iraq.
[2]Biology Department, College of Science, University of Baghdad, Al-jadiria, Iraq.

Received: 14 Aug 2018 Revised: 17 Sep 2018 Accepted: 22 Oct 2018

***Address for Correspondence**
Mohanad I. Kamil
Physics Department,
College of Science,
University of Baghdad, Iraq.
Email: mohanad.irzooqi@yahoo.co

ABSTRACT

Breast cancer is by far the commonest cancer in women; more than 1 milion women worldwide are diagnosed with breast cancer every year.Although there have been significant advancein breast cancer treatment over the past several decades.Conducting polyaniline (PANI)absorbsmild energy and transforms it into localized warmth to produce cell loss of life while encapsulation with inorganic materials. Amongst inorganic substances, $CaCO_3$ micro debris showcase a highencapsulation efficiency and solubility in acidicmedia. Hybrid biomaterial turned into prepared based totally on PANI-$CaCO_3$ – Cys nanoparticles for photo thermal therapy. The hybrid nano-material turned into synthesized through $CaCO_3$ and carboxymethyl cellulose in a chemical way. The characteristics have been examined using Ultraviolet spectrophotometer, FTIR and AFM. Invitro anticancer activity of each compound in the direction of MCF-7 strains was done using MTT assay indark and irradiatedconditions. Hybrid PANI-$CaCO_3$-Cys nanoparticles show off low toxicity to most cancers cells in dark and increasewith NIR laser.The consequences of this have a look at advice that hybrid PANI-$CaCO_3$–Cys nanoparticles with NIR laser can be used for huge medical packages and offer new drug recompense a chemotherapy drug.

Keywords:- NIR laser, Nanoparticles, Hybrid PANI-$CaCO_3$-Cys, MCF-7**.**

INTRODUCTION

Discovery of conductive polymers have given a brand new measurement to the prevailing generation. Polymers are acknowledged thus far as a category of warmth touchy, bendy, electrically insulating and amorphous substances.

Electrically carrying out Polymers seem like best applicants for numerous packages, as a lot of their residences sidestep issues familiar with conventional RAM (ferrites, carbon black), together with corrosion, weight, matrix incompatibility, and environmental integrity [1]. Further to being corrosion resistant and mild weight, many crucial residences of carrying out polymers can be tailor-made for numerous packages. The energy to weight, opportunity, resistance to corrosion, has given carrying out polymers benefit over metals[2]. Polymers are typically recognized for his or her insulating belongings due to covalent bond found in saturated carbon compounds. due to the fact acceptable residences may be comfortably attained through tailoring the polymer shape and additionally through incorporating components; scientists had been enthusiastic to discover the opportunity of remodeling insulating polymers into engaging in or semiconducting substances envisaging such unique traits like low density, ease of fabrication, flexibility of layout, low electricity and necessities for fabrication and processing [3]

Cancer is leading to the death that accounts for more than 25% of the deaths in Iraq[4]. Currently, conventional cancer therapies including surgical excision, medical therapies such as chemotherapy and radiotherapy, and combination methods have their inherent drawbacks. Surgical excision usually fails to remove all cancerous cells resulting in serious morbidity. In addition, surgery is limited to large numbers of tumors which are adjacent to critical tissue structures. Furthermore, the severe side effects of chemotherapy and radiotherapy make the patient lots of sufferings[5]. in the beyond decade, photo thermal therapy (PTT) that employs warmth generated from the absorbed optical power through mild-soaking up retailers has attracted high-quality interest because of a lot of its blessings which includes high specificity, minimum invasiveness, and occasional toxicity to regular tissues, and sturdy anti-tumor efficacy [6]. until now, numerous inorganic phototherapeutic retailers, which include gold Nano substances and carbon Nano substances, all with robust optical absorbance within the close to-infrared (NIR) tissue-transparency window, have proven encouraging photo thermal healing efficacy in preclinical animal experiments. but, the ones inorganic Nano substances that aren't biodegradable may want to continue to be within the body for lengthy intervals of time, elevating critical issues concerning their capacity long-time period toxicity, which limits their capability packages inside the health center [7]. This studyaimed to enerate biocompatible, hierarchicalhybrid nanomaterial, composedof PANI modified ithL-cysteineand $CaCO_3$, that's capable of incorporate the lively photo thermal nanomaterial and then investigated its activity on MCF-7 cell lines.

MATERIALS AND METHODS

Materials

Aniline ($C_6H_5.NH_2$) purity 98% from (HOPKIN&WILLIAMS) was distilled, Ammonium persulphate $(NH_4)_2S_2O_8$ purity 98% from (HIMEDIA-India) was used without further purification, L-Cysteine hydrochloride monohydrate ($C_3H_7NO_2S.HCL.H_2O$) purity 98% from (HIMEDIA-India), carboxymethyl cellulose, Calcium chloride dehydrate ($CaCl_2$) (from BDH- England) was usedwithout any purification , Sodium carbonate monohydrate (Na_2CO_3), NH4OH, and Dimethyl sulfoxide (DMSO) $(CH_3)_2SO$ purity 99.6% (BDH-England). Allaqueous solutionswere prepared singdistillwater.

Synthesis of PANI/$CaCO_3$ Hybrids Materials

Synthesis of PANI nanoparticles

The synthesis of PANI nanoparticle done based on the Neira-Carrillo, et al[8] with some modification. To preparethe PANI nanoparticles, in the beginning, aniline is distilled. after which 7 mmol ofaniline had been combined with 20 mL ofdistilled water and saved underneath amagneticbarstirrer for 30 min. Then, the combination turned into cooled to zero°C. An queous solution ofammonium peroxydisulfate 7 mmol turned into dissolved in 80 mL of freshlydistilledwaterand brought tothe anilinesolution. The reaction combination stirred for 1 h to finish

thepolymerization. the consequent PANI was accumulated on a filter out paper 0.2 µm and washed with distilled water, anddried underneath a vacuum for 1 day. The PANI rinsed with 0.1 M NH_4OH solution after which accumulated and dried as defined within the preceding sentenceto achieve emeraldine base, the deprotonated shape of PANI.

Synthesis of PANI-Cys

The polymer functionalized by way of nucleophile addition. The polymer was immersed right into a stirred 1 M aqueous solution of L-cysteine for twenty-four h at room temperature, after which filtered with 0.45µm filter out, washed with distill water then dried, and saved at room temperature. the solution A turned into synthesized primarily based on $CaCO_3$ and carboxymethyl cellulose CMC additives by way of blending 100mL of aqueous 0.025M $CaCl_2$ with 2 mL of CMC 5% W/V underneath a magnetic stirrer for 15 min. The solution B turned into organized by way of dissolving Na_2CO_3 in 100 mL of aqueous approach to achieve a 0.025 M solution.

Synthesis of $CaCO_3$-PANI-Cys Hybrids Materials

PANI-Cys combined with 100 mL of solution B underneath magnetic stirrer till a homogenous suspension acquired. This suspension (solution B+PANI-Cys) turned into delivered to 100mL of solution A underneath ultra-sonication at 80 W for 10 min. $CaCO_3$-PANI-Cys substances had been filtered with 0.45 µm filter out and washed with distilled water.

Characterization

Fourier transform infrared (FTIR) spectra were measured 8000 series (400 – 4000 cm^{-1}), in Department of Chemistry, College of Science, University of Baghdad.The FTIR was used to analyze the characterization of the PANI, $CaCO_3$ and $CaCO_3$-PANI-Cys in KBr pellets. UV-vis spectra were measured by using Shimadzu spectrophotometer UV 200-1100 nm, in Department of Chemistry, College of Science, and University of Baghdad. UV-vis spectrometer was absorption spectra of the sample at wave length rang 200-1100 nm. Finally, AFM (GENEX, USA) analyses were conducted to determine the particle size and morphology.

Cytotoxicity Assays

To decide the cytotoxic impact, the MTT viability assay turned into carried out on 96-well plates. Cellular strains had been seeded at 1 × 104 mL^{-1}. After 24 h, a confluent monolayer became accomplished; cells had been handled with examined compound. cellular viability measured after 72 hrs of remedy via casting off the medium, adding 28 µL of 2 mg/mL solution of MTT (and incubating the cells for 1.5 h at 37 °C. After casting off the MTT solution, the crystals ultimate within the wells have been solubilized via the addition of 130 µL of DMSO (Dimethyl Sulphoxide) accompanied through 37 °C incubation for 15 min with shaking [9]. The absorbency determined on a microplate reader at 492 nm (check wavelength); the assay was executed in triplicate. The inhibition rate of cellular growth (the proportion of cytotoxicity) turned into calculated as the following equation:-

Inhibition rate = A-B/A

Where **A** and **B** are the optical density of control and the optical density of test

Laser Treatment of Cancer Cells

The laser specifications used in the experiment were determined at the laboratories of the laser Institute at the University of Baghdad. The presence of the laser was detected using a detector card and determining its power at a height of half a meter using photometer THOR LABS[10]. As the previous assay, the cancer cells line were seeded on 96-well plates with density1 × 10^4 mL^{-1}. Then cells were incubated with $CaCO_3$-PANI-Cys hybrid for 1 hrs. The treated cells with tested compound were irradiated using NIR wave length 805nm irradiation with a light fluency almost of 568mW/cm^2 for 10 and 30 min. furthermore, non-treated cancers cells were irradiated with the laser.

Statistical analysis

The obtained data were statically analyzed using unpaired t.test with GraphPad Prism 6. The values were presented as the Mean ± S.E of the three replicate of each experiments[11].

RESULTS AND DISCUSSION

Characterization

FTIR spectroscopy wasused to determine the change in the chemical structure of pristine polymer after conjugated with $CaCO_3$ and cysteine, The FTIR results of pristine polymer is shown in Fig(1). The PANI spectrum displayed all feature polyaniline absorptionbands: 1557 cm^{-1} (assigned to –C=N- stretching vibration of quinonimine) and 1500 cm^{-1} (C=C stretching vibrationof aromatic). additionally visible turned intothe band at 1305 cm^{-1}correspondsto the stretchingvibration of C-N, the band at 1150 cm^{-1} (aliphatic amines), whichcorresponded to the hoop stretching N-Q-N, wherein Qirepresents the quinidi ring. The extensive conduction band inside the variety of 1812 cm-1 to 2941 cm^{-1} changed into assignedto the digital transition within the unfastened providers of thepolymer. The FTIR spectrum of compound PANI-Cys confirmed extra absorption bands marked with an asterisk within the graph at ~645 cm^{-1} that might be assigned to the C-S linkage of the cysteine institution to the polymer As seen in Fig(2). Moreover, new bands at 1665 cm^{-1} and 1314 cm^{-1} correspond to stretching of the C=O and C-O found in cysteine. The infrared spectrum found out that PANI-Cys exhibited new useful agencies in contrast with unmodified PANI, confirming powerful amendment of the polymer.

FTIR of the hybrid compound turned into additionally accomplished., the FTIR spectrum of the hybrid nanomaterial exhibited robust absorption bands at 1447 cm^{-1} and 719 cm^{-1}, resulting from the presence of $CaCO_3$ and the excessive amount of carbonate within the $CaCO_3$-PANI-Cys that keep away from the visualization of PANI-Cys absorption bands that corresponds to the $CaCO_3$ As seen in Fig (3). The optical properties for $CaCO_3$-PANI-Cys have been investigated by using UV-visible absorbance and transmittance spectra, in the region of 200-1100nm. The optical energy gap has been evaluated as seen in Fig (4). The optical absorption spectra are normally determined by a UV-visible spectrophotometer. The functionof UV-visible absorption is based on measuring theintensities of two transmitted beams, one beamtransmitted from the sample andanother transmitted from the referencecavity. In order toinvestigatethe calcination effect on theopticalpropertiesof nanoparticles, all calcined sampleswere taken from thedispersion of nanoparticles andmeasured theabsorptionspectra in the range of 200–1100nm at roomtemperature, which are as shown inFig (4). It is clear from the absorption spectra that the maximum absorbance wavelengths (_max)which can be seen at wavelength 375 and 606, that there are two top peak could be seen at the UV-spectroscopy results data. The maximum absorbance wavelength is associated with the conduction band energy according toQuantum theory of metal nanoparticles. Surface topology of the synthesize $CaCO_3$-PANI-Cys hybrid nanoparticles were studied by Atomic Force Microscope (AFM) analysis. The AFM results image of the morphology for the surface of the $CaCO_3$-PANI-Cys in the three dimensions represented in Fig (5). The results display a uniform surface, which indicate that the particle had uniform dimension.

The average grain size on the surface was calculated by granularity cumulating distribution chart that the grain size was (86.75) nm for $CaCO_3$-PANI-Cys as shown in Fig (6).

In-Vitro Anticancer activity

Cytotoxicity assay

Thiazolyl Blue Tetrazolium Bromide (MTT)assay is a colorimetric methodbasedon the conversionof the yellow tetrazoliumsalt topurple formazan crystals bymetabolic activity of activecells [12]. The cytotoxic effects of hybrid $CaCO_3$-PANI-Cys on the viability of two type's human cancer cell lines (MCF-7) for 48 h were examined by MTTassay. Asignificant inhibition could be obtained for proliferation MCF-7 cellline as shown in Fig.(7) afteri48 h. The cell prolife ration of treated cell was significantly lower when compared with untreated control cells. Afteri48 hrs of treatment hybrid $CaCO_3$-PANI-Cys with concentrations range 1.2 μgmL^{-1} – 5 $mgmL^{-1}$. The highest concentration exhibited cytotoxicity on cell line that the inhibition rate was 64%, mean while the efficiency of the lowest concentration on the cell line decreased.This study suggests that hybrid $CaCO_3$-PANI-Cys nanoparticle could enhance the delivery into the cells because of increasing bio availability and solubility in water, and the effectiveness lead to make each compound activity in cell growth inhibition enhanced [13].The apoptogenic property of the active compounds was investigated through morphological changes in MCF-7.Thus, determination of the morphological changes to define apoptosis was visualized using inverted phase contrastmicroscope. After incubation with testedcompounds for 48 h, morphological alterations in MCF-7 wereobserved in Fig (8) in comparison with control cells. Visualization of theuntreated cellsshowed that its' maintainedtheir original morphologyform, most of the control cells wereadherent to the tissue culture plate .In contrast, MCF-7 cancer cells which treated with hybrid $CaCO_3$-PANI-Cys with lowest concentration exhibited slightly efficiencyon the morphological for cell linestrains. Meanwhile, the highest concentration exhibited high efficiency onthe proliferation and morphologicalof cancers cell lineafter treatment for 48 h and revealed typical apoptoticfeatures such as membrane blabbing, it loses of contact withadjacent cells and decreasing in the number of cell [14].

Photo thermal therapy in MCF-7

The aim of this part of study is to determine the cytotoxicity of $CaCO_3$-PANI-Cys hybrid nanoparticles with effect of NIR laser on cell line. One concentration of hybrid nanoparticles is used 10 µg/ml without and with NIR laser for the two period of time 10 min and 30 min, Fig (9),shows the viability results examined by MTT colorimetric assay of MCF-7 cancer cell lines after of exposure with $CaCO_3$-PANI-Cys. The results illustrated that treatment with $CaCO_3$-PANI-Cys with NIR laser inhibited the growth of cells significantly and was more potent as compared to those $CaCO_3$-PANI-Cys only without NIR laser. Alternatively, cells incubated with $CaCO_3$-PANI-Cys and irradiated with NIR laser for 10 min showed cytotoxicity 62% and for 30 min showed cytotoxicity 77%. These results indicated that the $CaCO_3$-PANI-Cys with high photo thermal conversion efficiency and photo stability could be used as a photo thermal agent.

PANI is one of the most widely used anticancer drugs, particularly against cancer cell. In our study we used Hybrid $CaCO_3$-PANI and combined with L- Cysteine and following irradiation with NIR for 10 and 30min to improving this hybrid material as anticancer drugs.It's clearly indicates that the hybrid material is required for photo-thermal conversion of the laser irradiation, which induced cell death [15].A clear reduction in cell density was observed for cells irradiated in presence of Hybrid $CaCO_3$-PANI-Cys when compared to Hybrid $CaCO_3$-PANI-Cys alone or laser alone. The results indicatingthat the membrane was still intact, since there was no heat shock performed. However, when cells are challenged with photothermal agents for the NIR, almost all cells show clear signs of losing cell integrity and extensive cell death can be observed [16]. The results confirmed that irradiated Hybrid CaCO3-PANI-Cys, Especially those adsorbed to the cell membrane, promote a local functions and formation of pores in the

membrane which affects not only cellular membrane but also cell viability. This happens either by denaturation of proteins or nucleic acids in the cytoplasm, or by affecting cellular and\or organelles membranes,laser cause structural damage that accelerates the metabolism of hybrid material[17].This study suggests that NIR Laser improves the efficiency of $CaCO_3$-PANI-Cys through higher absorption by cells and effectiveness of $CaCO_3$-PANI-Cys in cell growth inhibition was enhanced.

CONCLUSIONS

Polymers have gained a splendid region inside the biomedical area as substances for the fabrication of numerous gadgets and for tissue engineering programs. Hybrid $CaCO_3$-PANI-Cys substances composed of PANI nanoparticles functionalized with L-cysteine have been synthesized and successfully integrated into $CaCO_3$. The CMC became used to maintain the form, composition, and long time balance of hybrid substances and to supply the burden close to the most cancers cellular, which turned into launched within the low pH regions that the cells set off. FTIR showed that PANI-Cys integrated into the Nano pores of $CaCO_3$. AFM commentary of $CaCO_3$ confirmed described edges, a easy surface, and a spherical to ovular form starting from of 500nm to 5µm in size. In vitro research of the hybrid $CaCO_3$-PANI-Cys biomaterials did result in modifications in cellular viability on the studied concentrations without laser, however the mixture of a laser within the NIR area and $CaCO_3$-PANI-Cys markedly growing cytotoxicity. In precis, we concluded that the consequent hybrid biomaterial can be used a PTT agent for most cancers ablation.

Declaration of Interest

The authors declare that there are no conflicts of interest. The authors alone are responsible for the content and writing of the paper

REFERENCES

1. D. Nguyen, and H. Yoon, Recent advances in nanostructured conducting polymers: from synthesis to practical applications, *Polymers*, 2016;8 (4):118.
2. T. Ohtsuka, Corrosion protection of steels by conducting polymer coating, *International Journal of Corrosion*, 2012;7:16-21.
3. M. Naebe, J. Wang, A. Amini, H. Khayyam, N. Hameed, L. Li, Y. Chen, and B. Fox, Mechanical property and structure of covalent functionalised graphene/epoxy nanocomposites, *Scientific reports*, 2014;4:4375.
4. A. Hagopian, A. Flaxman, T. Takaro, S. Al Shatari, J. Rajaratnam, S. Becker, A. Rector, L. Galway, B.Al-Yasseri, and W. Weiss, Mortality in Iraq associated with the 2003–2011 war and occupation: findings from a national cluster sample survey by the university collaborative Iraq Mortality Study, *PLoS Medicine*, 2013;10(10).
5. S. Liauw, P. Connell, and R. Weichselbaum, New paradigms and future challenges in radiation oncology: an update of biological targets and technology, *Science translational medicine*, 2013;5:(173)sr2.
6. Z. Bao, X. Liu, Y. Liu, H. Liu, and K. Zhao, Near-infrared light-responsive inorganic nanomaterials for photothermal therapy, *asian journal of pharmaceutical sciences*, 2016;11 : 349-364.
7. M. Vats, S. Mishra, M. Baghini, D. Chauhan, R. Srivastava, and A. De, Near infrared fluorescence imaging in nano-therapeutics and photo-thermal evaluation, *International journal of molecular sciences*, 2017;18 : 924.
8. A. Carrillo, E. Yslas, Y. Marini, P. Quitral, M. Sánchez, A. Riveros, D. Yáñez, P. Cavallo, M. Kogan, and D. Acevedo, Hybrid biomaterials based on calcium carbonate and polyaniline nanoparticles for application in photothermal therapy, *Colloids and Surfaces B: Biointerfaces*, 2016;145 : 634-642.
9. G. Sulaiman, A. Tawfeeq, and A. Naji, Biosynthesis, characterization of magnetic iron oxide nanoparticles and evaluations of the cytotoxicity and DNA damage of human breast carcinoma cell lines, *Artificial cells, nanomedicine, and biotechnology*, 2017 :1-15.

10. R. Fekrazad, N. Naghdi, H. Nokhbatolfoghahaei, and H. Bagheri, The combination of laser therapy and metal nanoparticles in cancer treatment originated from epithelial tissues: a literature review, *Journal of lasers in medical sciences*, 2016;7 : 62.
11. M. Jabir, G. Sulaiman, Z. Taqi, and D. Li, Iraqi propolis increases degradation of IL-1β and NLRC4 by autophagy following Pseudomonas aeruginosa infection, *Microbes and infection*, 2017.
12. T. Riss, Cell Viability Assays. Assay Guidance Manual (Eli Lilly & Company and the National Center for Advancing Translational Sciences, 2004.
13. F. Aqil, R. Munagala, J. Jeyabalan, and M. Vadhanam, Bioavailability of phytochemicals and its enhancement by drug delivery systems, *Cancer letters*, 2013;334 :133-141.
14. M. Archana, T. Yogesh, and K. Kumaraswamy, Various methods available for detection of apoptotic cells-A review, *Indian journal of cancer*, 2013;50:274.
15. L. Lin, X. Yang, G. Niu, J. Song, H. Yang, and X. Chen, Dual-enhanced photothermal conversion properties of reduced graphene oxide-coated gold superparticles for light-triggered acoustic and thermal theranostics, *Nanoscale*, 2016;8: 2116-2122.
16. R. Mendes, P. Pedrosa, J. Lima, A. Fernandes, and P. Baptista, Photothermal enhancement of chemotherapy in breast cancer by visible irradiation of Gold Nanoparticles, *Scientific reports*,2017;7 :10872.
17. C. He, S. Wang, Y. Yu, H.Shen, Y. Zhao, H. Gao, H.Wang, L. Li, and H. Liu, Advances in biodegradable nanomaterials for photothermal therapy of cancer, Cancer Biology & Medicine, 2016;52:2095-3941.

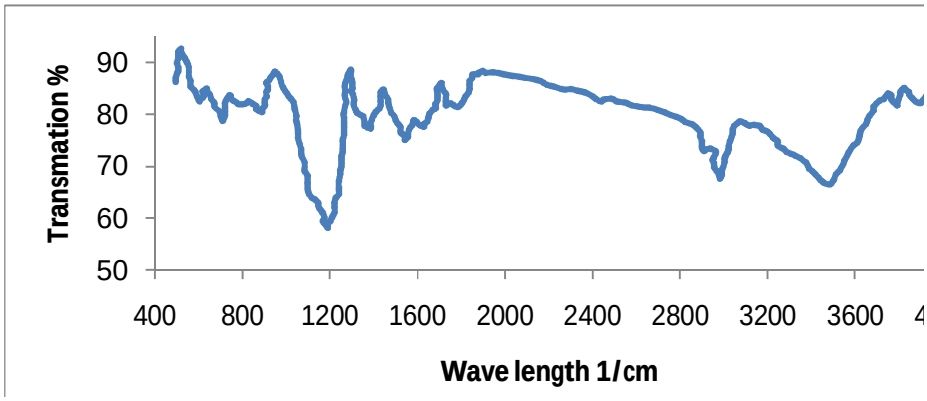

Figure.1. FTIR spectra of PANI

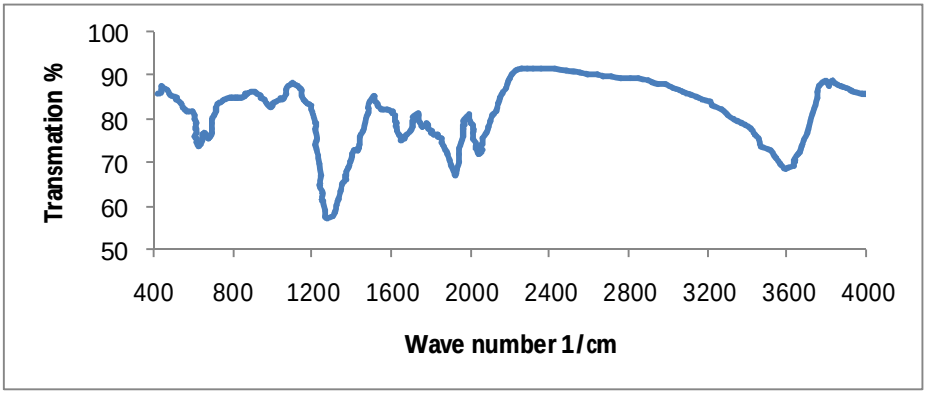

Figure.2. FTIR spectra of PANI-Cys

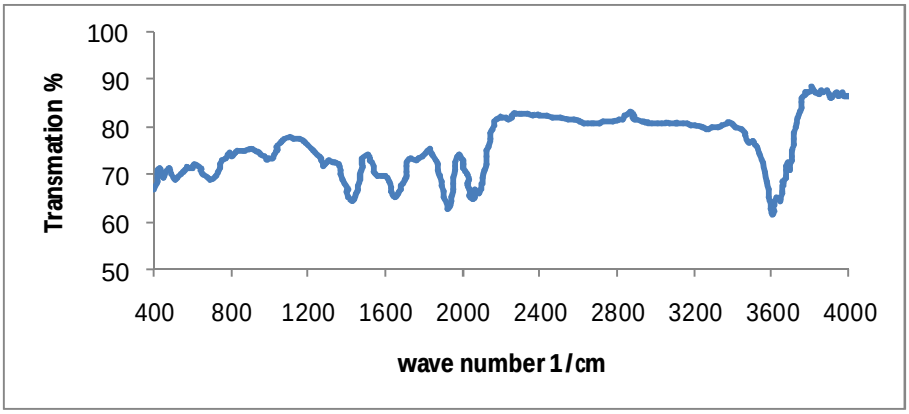

Figure.3. FTIR spectra of $CaCO_3$-PANI-Cys.

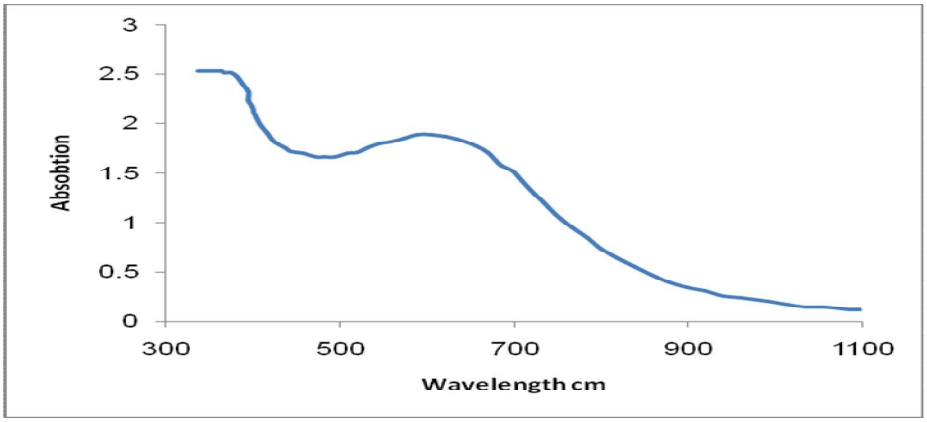

Figure 4.The absorption of UV-Vis spectrophotometer.

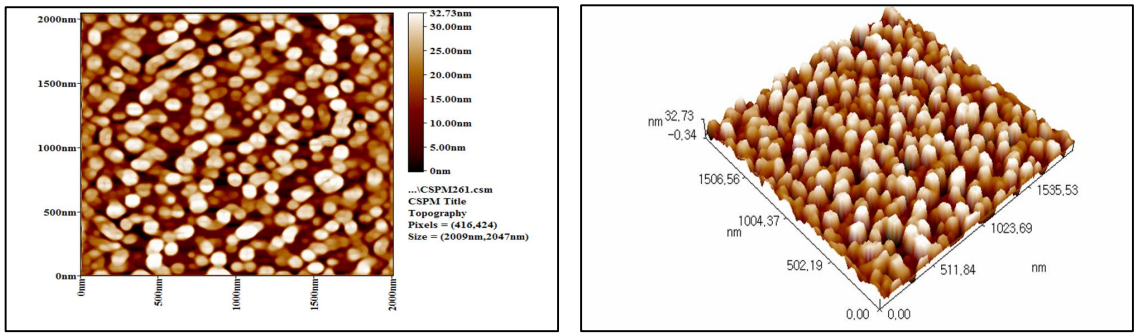

(A) **(B)**

Figure (5): (A) and (B) 3D view of AFM image of $CaCO_3$-PANI-Cys hybrid nanoparticles

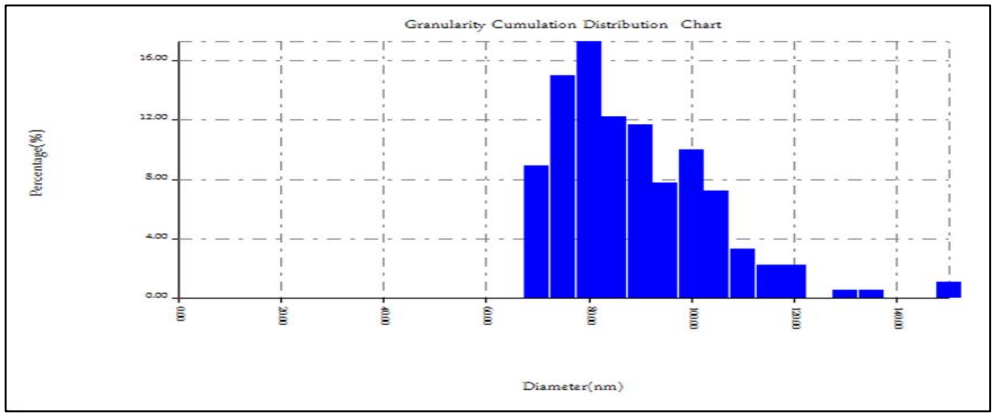

Figure (6): the granularity cumulating distribution for $CaCO_3$-PANI-Cys prepared.

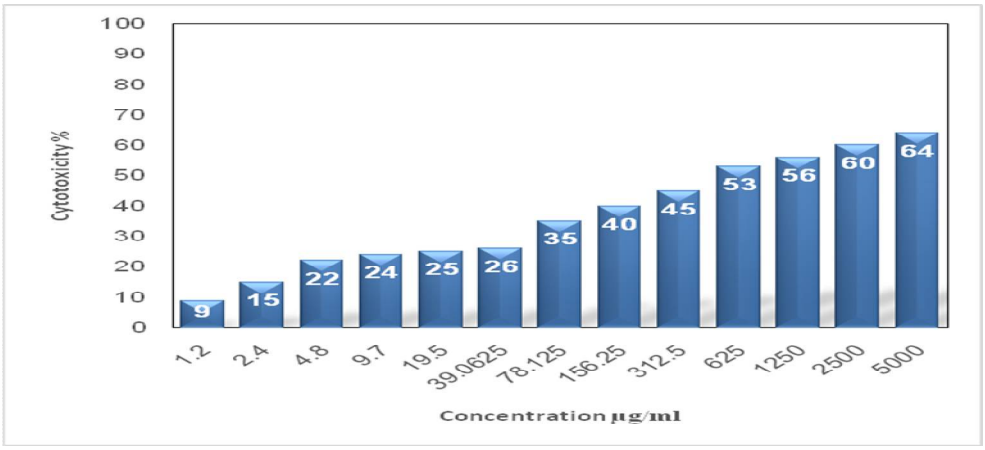

Figure (7) Cytotoxicity effect on MCF-7 cell line.

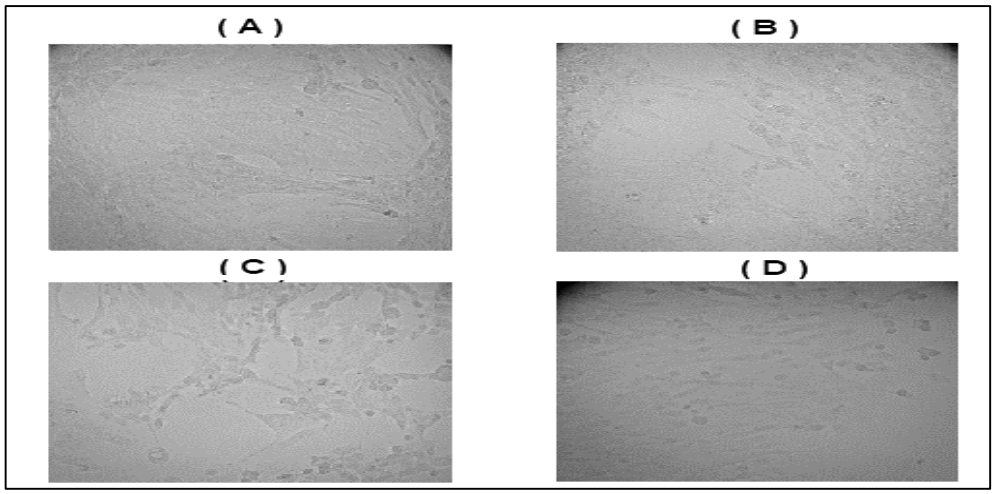

Figure (8). Microphotographs of MCF-7 cell line after the cytotoxicity test: (a) reference, (b) 9.7 µg/ml $CaCO_3$-PANI-Cys, (c) 625 µg/ml $CaCO_3$-PAIN-Cys, (d) 5000µg/ml $CaCO_3$-PANI-Cys

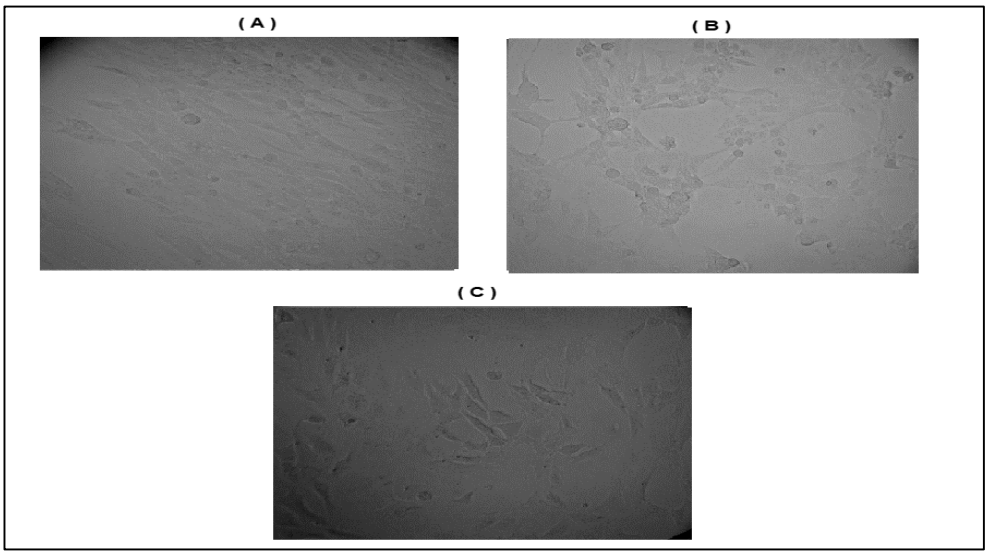

Figure (9). Microphotographs of MCF-7 cell line after the cytotoxicity test

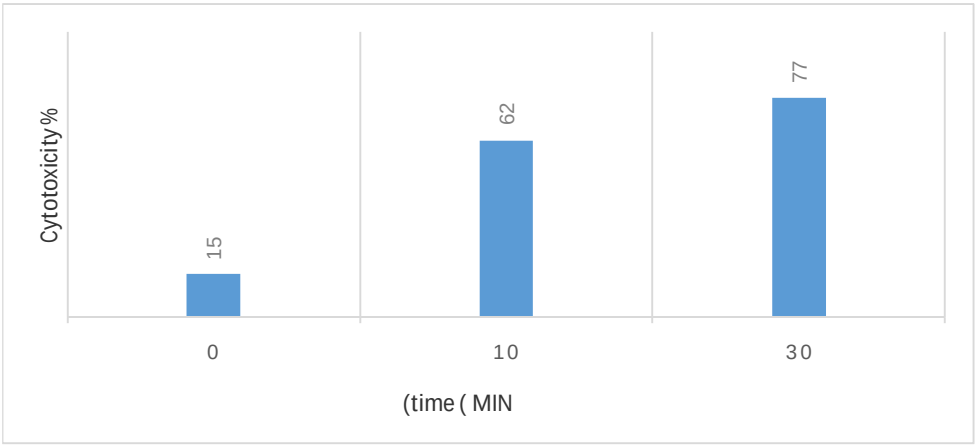

Figure 10. Effect of laser with concentration 10 µg/ml of $CaCO_3$-PANI-Cys on MCF-7. Control without laser then 10 min and 30 min irradiated.

Indian Journal of Natural Sciences www.tnsroindia.org.in ©IJONS

Vol.9 /Issue 51 / December / 2018 *International Bimonthly* *ISSN: 0976 – 0997*

RESEARCH ARTICLE

Occurrence of Prolonged Oestrus in Cattle Breeding Farm, Thumburmuzhy During January 2015 to December 2017

Shakir Arafath K*, Abdul Azeez C. P., Promod K, Magnus Paul K,Vinu David P, Sunanda C and Justin Davis

Department of Animal Reproduction, Gynaecology and Obstetrics, College of Veterinary and Animal Sciences, Pookode, Wayanad-673 576, Kerala, India.

Received: 20 Sep 2018 Revised: 24 Oct 2018 Accepted: 28 Nov 2018

***Address for Correspondence**
Shakir Arafath K
Department of Animal Reproduction,
Gynaecology and Obstetrics,
College of Veterinary and Animal Sciences,
Pookode, Wayanad-673 576, Kerala, India

ABSTRACT

The cows exhibiting oestrus duration of more than 36 h were considered as having prolonged oestrus. Assessment of the data in the registers maintained at Cattle Breeding Farm, Thumburmuzhy for a period of three years revealed an occurrence of prolonged oestrus from January 2015 to December 2017 in cows and heifers were 26.87 and 17.93 per cent, respectively with an overall occurrence of 24.30 per cent. During these three years, there is a non-significant ($p > 0.05$) increase in the incidence of prolonged oestrus in both cows and heifers in the farm. Statistical analysis of the data on the incidence of prolonged oestrus in the farm revealed significant difference ($p < 0.05$) between cows and heifers with higher occurrence among cows during this period.

Key words: Oestrus duration, Prolonged oestrus, Incidence of prolonged oestrus

INTRODUCTION

Livestock sector is an important subsector of the agrarian economy in India, which contribute nearly 25.60 per cent of the agrarian gross domestic product. Infertility has been a major problem affecting the reproductive efficiency of crossbred cattle causing huge economic loss to the livestock farmers. As per Cattle Sterility Office, Aluva, bulletin 2012-2013, defective oestrous cycles account for 27.31 per cent of the infertility conditions reported in Kerala, of which prolonged oestrus constitute 13.10 per cent. Repeat breeding is one among the major problems associated with decreased fertility in dairy cattle and about 30 to 40 per cent repeat breeder crossbred cattle display prolonged oestrus (37 to 60 h vs 24 to 36 h; Dadarwal *et al.,* 2005). Proper timing of Artificial Insemination (AI) is very difficult in cows exhibiting prolonged oestrus, leading to repeat breeding. Diagnosis requires sequential per rectal palpation of

the ovaries, which may interfere with ovulation or cause premature rupture of the follicles. Frequently, ultrasonography as well as hormonal assay may also be required for specific diagnosis, which is difficult under field conditions.

MATERIALS AND METHODS

Data regarding the occurrence of prolonged oestrus in all the breedable crossbred cattle were collected from the registers maintained at Cattle Breeding Farm, Thumburmuzhy for a duration of three years from January- 2015 to December- 2017. Cows which exhibited oestrus duration of more than 36 h were considered as prolonged oestrus (Dadarwal *et al*., 2005). All the postpartum cows in the farm were closely monitored for any of the visual signs of oestrus like restlessness, mounting behaviour, sniffing the vulva of other cattle, chin resting, standing for mounting by other cattle and vaginal discharge.

RESULTS AND DISCUSSION

Data regarding the occurrence of prolonged oestrus among all breedable crossbred cattle at CBF, Thumburmuzhy for a period of three years from January 2015 to December 2017 were collected from the registers maintained at the farm and are presented in the Table 1 and Fig.1.In the year 2015, among 112 cows and 52 heifers in the farm, 26 cows (23.21 per cent) and seven heifers (13.46 per cent) exhibited prolonged oestrus. There was progressive increase in the per cent of both cows and heifers exhibiting prolonged oestrus through subsequent years. In 2016, 33 out of 121 cows (27.27 per cent) and eight among 45 heifers (17.78 per cent) exhibited prolonged oestrus, while in 2017, it was further increased up to 29.69 per cent and 22.91 per cent in cows and heifers, respectively. The total occurrence of prolonged oestrus from January 2015 to December 2017 in cows and heifers were 26.87 and 17.93 per cent, respectively with an overall occurrence of 24.30 per cent. During these three years, there is a non-significant ($p > 0.05$) increase in the incidence of prolonged oestrus in both cows and heifers in the farm.

Statistical analysis of the data on the incidence of prolonged oestrus in the farm revealed significant difference ($p<0.05$) between cows and heifers with higher occurrence among cows during the period between January 2015 to December 2017. Higher occurrence (30 to 40 per cent) of prolonged oestrus among repeat breeding crossbred cattle were reported by Dadarwal *et al.* (2005). Dhas (2005) obtained similar results with an occurrence of 21.62 per cent of prolonged oestrus in crossbred cattle under farm conditions. Mathew (2011) also reported a higher occurrence of prolonged oestrus among repeat breeder cattle at the rate of 41.37 per cent under farm situations.Parvathy (2015) observed that occurrence of 24.73 and 16.57 per cent of prolonged oestrus among cows and heifers, respectively with overall occurrence of 21.78 per cent. Similarly, in present study also, occurrence of prolonged oestrus was higher in cows (26.87 per cent) compared to heifers (17.93 per cent), which may be due to greater probability of endocrine irregularities in cows due to production stress.

ACKNOWLEDGEMENTS

The authors acknowledge the facilities and funding provided by the Head of the Cattle Breeding Farm, Thumburmuzhy, Dean, CVAS, Pookode and the DAR, KVASU.

REFERENCES

1. Animal Husbandry Department Cattle Sterility Office Bulletin. 2012 - 2013 p-10.
2. Dadarwal, D., Singh, J., Honparkhe, M., Cheede G.S and Kang R.S. 2005. Investigations on repeat breeding crossbred cattle with history of prolonged estrus. *Indian J. Anim. Sci.* 75(8): 922–24.

3. Dhas, G.J.S. 2005. Fertility trials on induced oestrum in repeat breeding cattle with prolonged oestrum. *M.V.Sc thesis*, Kerala Agricultural University, Thrissur, 39p.
4. Mathew. 2011. Comparison of human placental extract, human chorionic gonadotrophin and gonadotrophin releasing hormone on fertility of repeat breeding cattle. *M.V.Sc. thesis*, Kerala Veterinary and Animal Sciences University, Trichur 52p.
5. Parvathy, S. 2015. Effect of prostaglandin administration on progesterone levels during oestrous cycle in crossbred cattle showing prolonged oestrus. *MVSc. Thesis.* Kerala Veterinary and Animal Sciences University, Pookode,117p.

Table 1. Occurrence of prolonged oestrus among crossbred cattle at Cattle Breeding Farm, Thumburmuzhy for a period of three years from January 2015 to December 2017

Year	Total number of cattle		Number of animals having prolonged oestrus		Per cent of prolonged oestrus animals (%)	
	Cow	Heifer	Cow	Heifer	Cow	Heifer
2015	112	52	26	7	23.21	13.46
2016	121	45	33	8	27.27	17.78
2017	128	48	38	11	29.69	22.91
χ^2 – value					1. 29^{ns}	1.52^{ns}
p – value					0.52	0.48
Total	361	145	97	26	26.87	17.93
z – value					2.26*	
p – value					0.024	
Overall occurrence					24.30	

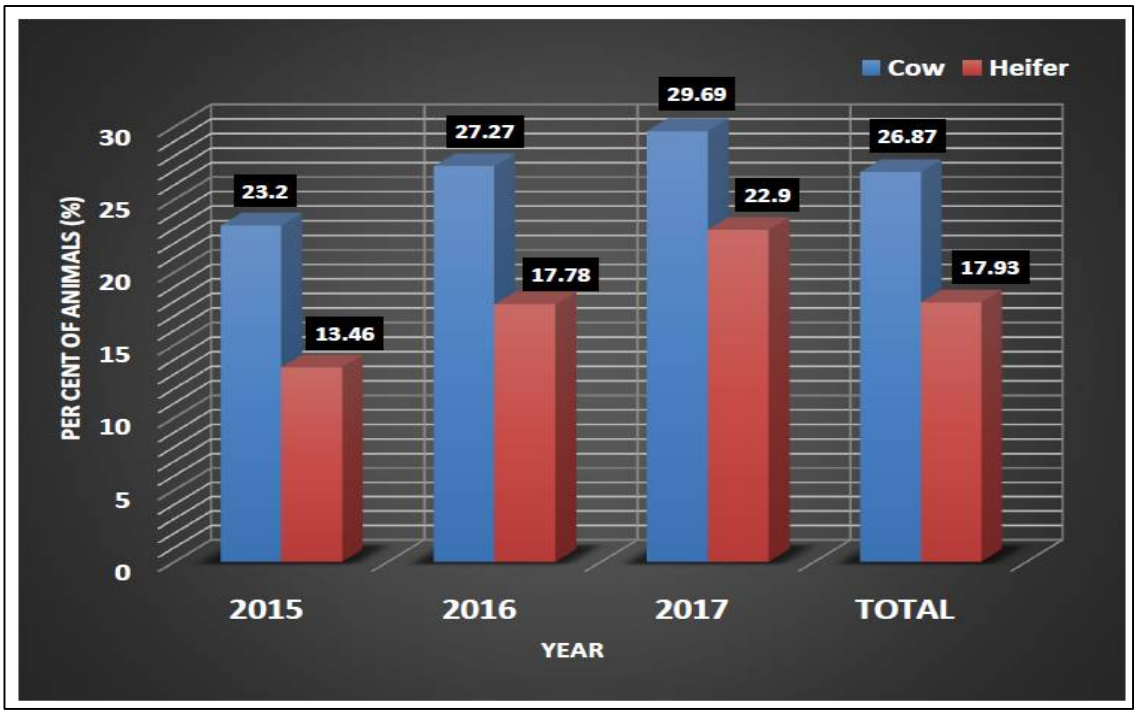

Fig 1. Occurrence of prolonged oestrus among crossbred cattle at Cattle Breeding Farm, Thumburmuzhy for a period of three years from January 2015 to December 2017

Indian Journal of Natural Sciences www.tnsroindia.org.in ©IJONS

Vol.9 /Issue 51 / December / 2018 *International Bimonthly* *ISSN: 0976 – 0997*

RESEARCH ARTICLE

Predicting Sediment Accumulation in Euphrates River: A Case Study of the Upstream of Al-Hindiya Barrage, Iraq

Ali Hassan Hommadi[1]* and Fadhil M. Dahir[2]

[1]M.Sc.in Water Resource, Ministry of Water Resources, Iraq,
[2]Kerbala Technical Institute, AL-Furat Al-Awsat Technical University, 56001 Kerbala, Iraq.

Received: 18 Aug 2018 Revised: 20 Sep 2018 Accepted: 23 Oct 2018

***Address for Correspondence**
Ali Hassan Hommadi
M.Sc.in Water Resource,
Ministry of Water Resources, Iraq,
E-mail:alihassan197949@yahoo.com

ABSTRACT

The search conducted to calculate the accumulation of sedimentation in river at upstream(U/S) of Alhindiya barrage through three years (2012, 2017 and 2018) and compare with three years also knowledge the amount of sediment through each year and knowledge the year gets on high accumulation of sedimentation . Alhindiya barrage site on Euphrates river and divide the river two river Sat- Alhila and Shat- Alhindiya. The barrage site on Shat- Alhindia with more the head regulators on two rivers (Old Alhusienia regulator,New Alhusienia regulator, Kifil regulator, Shat- Alhila regulator and mousaib regulator). This regulators site in U/S of barrage. In this search shown the sedimentation through 2018 more than 2012 and 2017 by 41.35% and 23.43%, respectively. Reduction in water level happen the island and reduction in river section and this will increase the amount of sedimentation because reduce of depth(shallow depth) water and river section (narrow of river width) lead to reduction of discharge and share water in downstream reigns (south governorates).

Keywords: Alhindiya barrage, Sediments fluvial.

INTRODUCTION

The accumulation of sediment river (fluvial) in U/S of Alhindiya barrage helps on reduce the capacity of reservoir, reduce river depth and cross section this in turn reduce the discharge and waterlogging land adjacent also reduce the water amount to the other governorates which site in downstream of barrage because of block sediment to water streams. The scouring and settling increased due to water scarcity and decrease of river cross section caused to increase of velocity and decrease cross section and discharge. To solve the problem the sedimentation work ministry of water resource excavation and move it from cross section of river by excavator inside river was floating and it do on mixing of water with fluvial to exit outside the river section by big pipes on basins was done before execution of

excavation in river to fill in fluvial. This work carried out by Ministry of water resource. Liu et al., 2017 mentioned in studies the sediment problems in many rivers for example Nile stream Basin, Mississippi stream Basin, Volga stream Basin andothers Rivers Basins. The study search about the problems that happen bysediment and sediment how management the sediment around the world. Many rivers inworld have problems for examplereducing sediment loads chiefly because of the building of barriers such as dam and river structures, acceleration in soil erosion and sediment filling and trapping of sediment in basin of reservoir this causing decreasein volume of storage. In their studyshow working best methods to control on sediments and management.Franz et al., 2017 state about work model of the Coastal protection structures are built to save the beach from erosion. Also mention about study sediment transport and study the morphological variation in coastal region below the composite influence of the waves and water currents. They used models to prevent the coastal from erosion and reduction the sediment transport depending on morphologic the coast of the Costa da Caparica. The coastal region sited near the upstream of a mesotidal with high tidal water currents allowed for evaluation of the hydrodynamics also evaluation the sediment transport in calm water states not found waves and under high wave states.

Kadhim, 2013 studied influence of sediments river source on some alluvium lands characteristics abutting on River of Shatt Alarab. Two sections were taken the section one at Alharitha area the sample depending on taking Shatt Alarab only and section two at Al seeba area taking Shatt Alarab River and Alkaroon River. The result of searching in soils was shown the changes in morphology characteristics depending on landscape site. The physical Characteristics of second section showed sudden changing of texture increasing in clay and silt particles and decreasing in sand sedimentation rate according. The bulk density was increases with increasing the depth. The results of chemical analysis was shown increasing in that organic matter in section two. low – medium values in the section one which take from River of Shatt Alarab while the soils in the second stripe shown of a high salinity values because of Alkaroon river in second section exit water was high salinity (40.7 ds/m) while River of Shatt Alarab salinity test was 9.37ds/m . the sedimentation and salinity of Alkaroon effect on River of Shatt Alarab salinity.AL-JARRAH, 2009 studythe sediment pollution and influencing on river via many mounts of sediment that bearvia the water then stilling in bed and banks made the islands in streams with negative influencesin cross section of river for example the narrow and shallow of the stream, they utilize the remote Sensing technology to estimate influence through more period of years. In their study choose in north, middle and south of Tigris River by satellite records and maps.theygoton maps in various periods and via mechanism of sediment got the exact areastogrow island and the bluster sites in future filledvia sediments. The increasing in sediment in channels due to low discharge and the high narrow of streams and increase innumbers of islands also increase in areas of islands. The sugist to solve problem excavation the sediment from riverand put sudden Discharge very big amounts of water from water dams to pay out of stream.

Awaz et al., 2009 study on the 292km length of Euphrates river begin from Al-Hindiya barrage to Al-Kifil township in 5 locations in length of river and measure the concentration and distribution of some carbon pollution through steeling in sediment. K.G. Ranga Raju,1996 state the sediment problems in canal from a big capacity reservoir may be free sediment or it may include on fine sediment in suspension. If the canal sidewas non-erodiblethe designer has to ensure that the expected load input the canal is movedto downstream without gaining deposited on the bottom canal. Sediment was sand, gravel and silt, alsoin design must the shear stress on the side and bed is not high to move of soil. Sediment problems inreservoir One of the problems representof performance of reservoirs is the calculation of gradualincreasing in storage capacity because of sedimentation. The method includes the calculation of the sediment yield in year from the catchment.The limitation of the part of this that will deposit in the reservoir based on the term called a trap efficiency.Tocalculate sediment yield use the relation a trap efficiency and the usingthe Empirical Area Reduction method enables limitation of sedimentation rates to preliminary design.Wilcock et al., 2009Calculate sediment transport rate in gravel-bed rivers. They found the problem in traps was did not efficient the transport of fine material in bed. Sand and very fine gravel wasdid not efficient trapped in a pit due to transport fine bed material tends to be more active and a bitbest mixing than coarse bed-material transport. They found the fine material take long time more than coarse material and stay suspended to long distance. Marion et al., 2006 used the experimental

work about local scouring sited in toe of bed sills that was building in steep, gravel Bed Rivers in mountains. They evaluate the influence of upstream (U/S) sediment supply on the scour depth and figure. The engineering properties of three holes of scour were below conditions of steady flow rate and steady sediment apply. They put144 scour holes to test. The effect of jet erosion on scour engineering is also discussed. The effect the average of U/S sediment moving can be calculated for in the variable that description of the morphological jump and description the effect of sediment moving on the evolution of the scouring.Taylor and Owens, 2009assess the sediment sources, track and storage in river. The sediment management in urban systems and basins of river and general environmental variation on sediment operations and management. The sediment is moved in urbanized basins was contaminating. There is a need tomonitoring of sediment in urban river and basins. They need to technology and studies to get on sources and transfers of deposited sediment method.

MATERIALS AND METHODS

In this study used The device was utilized in calculation the river sediments called ECO- SOUNDER as figure (1) to calculate bed level in water of river. but the elevation of sides slope out the water calculate by level device as shown the following.

1. The ECO- SOUNDER device put on water surface and operation by battery after send sounder wave and receives will calculate time go and go back wave multiply with wave velocity to get on the depth of water and level of bed nextcompare bed level with design bed get on depth of sedimentation in point on the station then inter in excel and drawing finally calculate area and volume of sediments.
2. To measure the bed level need to boatand measure tape to limited the station (distance from starting) and level of bed and side slope inside water by ECO- SOUNDER also need to level device to measure the elevation of side slope outside the water.
3. Collect design Data and as plot an existing of upstream of barrage to compare reduction of section area.
4. Level surveying device used and reading staff with two person to read the ground level of river bed (this classic measuring with measuring tape to measure the stations) but ECO- SOUNDER device simplifies the measure operation put it in surface of water but the side slope of river outside the water measure byLevel surveying device as shown in **figure (8)**.
5. The design(real)bed level was 24.9m, bank level was 33.9m and water level in upstream was 31.6m. The method to calculate area by work strip of river and work multiply x with y then y with x after than take the average finally sum the strip areas to calculate total area of section. The volume was calculated by trapezoidal method to sections areas of river. We take station 0+400 in figures (3,4 and 5) as examples to show method draw and calculate area of sediment in cross section.

The field work and consumption amount of sediment

The work carried out in right side bank of Euphrates river at new Alhindiya barrage in quarry of excavation rivers office of Ministry of water resource which provided us with the data. The new Alhindiya barrage farof old Alhindiya barrageabout 1.700 km from U/S to food 500000 ha from agriculture lands (420000 ha in Shat- Alhila, 25000 ha in Kifl canal, 30000ha in Bani Hassan canal and 25000 ha in Hussienia canal). The quarry of sedimentation site at latitude ♂32 43‘1" N and longitude ♂4415’58"E. The design discharge of barrage was 2500 m^3/s and max. Water level of U/S was 32.55m and normal water level of U/S was 31.90m.Table (1) Soil physical characteristics for site work Doing in college of agriculture of university of Baghdad in soil and water resource department laboratories of high degree. Figure (2) shows the Google earth of site work.

The increasing in last years in sedimentation was shown in figure(6). The sedimentation through 2018 more than 2012 and 2017 by 41.35% and 23.43%, respectively. This increase may be result from reduction of water level an showing the island and reduction of discharge and may be change morphologic and geophysics of soil bank which happing it

the scouring. The figure (9) shown the elevation of sedimentation in center line of river on 500m distance compare with design bed level and water level in upstream of barrage through three years (2012, 2017and 2018).

CONCLUSIONS

1. Increasing in sedimentation offluvialin 2018 more than 2017 and 2012 and the increasing gradually year after year and the reason reduce of water level because of increasing of temperature degree and reduce the discharge (share of water) from States neighbors by construction dams on Euphrates river in their lands. The office of rivers excavation raises sediment each year after than the sediment deposits again.
2. The reason of increasing of sedimentation in river because of change in geologic and morphologic in bank (in vertical on depth and horizontal) that is happening which erosion (scouring) .
3. Excavation operation in upstream ofEuphrates river in Anbar governorate sites are reducing because events terrorism and stopped this helped on increasing the suspending load and accumulate in Alhindiya barrage.
4. Reduction in water level happen the island and reduction in river section and this will increase the amount of sedimentation because reduce of depth water and river section.
5. The sedimentation through 2018 more than 2012 and 2017 by 41.35% and 23.43%, respectively.

Recommendation

1. Work engineering and geomorphologic surveyingto banks was more erosion on Euphrates length and cladding with stone.
2. Work excavation in north of Euphrates to reduce the accumulated sediment in Alhindia barrage which make to narrow the river section and the depth become shallow thus reducing the amount of water that received the south governorates and hinder.
3. Work economic study to the amount of costs that disposal of the operation excavators, other machines and office management compared with the sale of sediment and are they found economic feasibility? Also determine the returned the sediment that sales to fill costs operation the excavators and other machines.

REFERENCES

1. AL-JARRAH, OMAR BURHAN, 2009 "Continous detecting of growing of the middle river islands by using the remote sensing technique and the negative effects to the river" journal of AL-Anbar university of science vol.3, no.3.
2. Awaz B . Mohammed , Maysoon M.S. Al–Taee and Fikrat M. Hassan, 2009 "The Study Of Some PAHs Compounds In Euphrates River Sediment From Al-Hindiya Barrageto Al- Kifil City – Iraq" Vol. 4 College of Science/ Babylon Univ. 4th Scientific Conference.
3. Franz, Guilherme, Matthias T. Delpey, David Brito, Lígia Pinto, Paulo Leitão, and Ramiro Neves, 2017 "*Modelling of sediment transport and morphological evolution under the combined action of waves and currents"* Ocean Sci., 13, 673–690, 2017, Lisboa, Portugal.
4. K.G. Ranga Raju, 1996 "*Sedimentation of Rivers, Reservoirs and Canals* " FRESH SURFACE WATER – Vol. III - ©*Encyclopedia of Life Support Systems* (EOLSS), *Civil Engineering, University of Roorkee, Roorkee, India.*
5. Kadhim, Mohammed A., 2013 " Effect of Sediments Fluvial Source in Some Properties of Alluvial Soils abutting for Shatt Alarab River" College of Agriculture - Univ . of Basrah, journal of Theqar to science, vol. 3(4). pp 65-78.
6. Liu, Cheng, Desmond E. Walling, Manfred Spreafico, Jayakumar Ramasamy, Hans Dencker Thulstrup, Anil Mishra, 2017 "*Sediment Problems and Strategies for their Management*" Published by the United Nations Educational, Scientific and Cultural Organization, 7, place de Fontenoy, 75352 Paris 07 SP, France.

7. Peter Wilcock, John Pitlick, Yantao Cui, 2009" Sediment Transport Primer Estimating Bed-Material Transport in Gravel-bed Rivers" Wilcock, Peter; Pitlick, John; Cui, Yantao.Gen. Tech. Rep. RMRS-GTR-226. Fort Collins, CO: U.S. Department of Agriculture, Forest Service, Rocky Mountain Research Station. 78 p.
8. Marion, Andrea, Matteo Tregnaghi and Simon Tait, 2006"Sediment supply and local scouring at bed sills in high-gradient streams " WATER RESOURCES RESEARCH, VOL. 42, W06416.
9. Taylor, Kevin G. & Owens, Philip N., 2009"Sediments in urban river basins: a review of sediment–contaminant dynamics in an environmental system conditioned by human activities" J Soils Sediments (2009) 9:281–303.

Table (1) Soil physical characteristics for site work

Type of test	Result
Apparent (bulk) specific gravity(G)	1.45
Sand (%)	80
Silt (%)	10
Clay (%)	10
Texture	Loamy sand
Eciw (ds/m)	0.88
Ece (ds/m)	0.92

Table (2) the quantity of sedimentation ofSediments fluvial in upstream of Alhindia barrage of 2012. The data collected from excavation rivers office follow the Ministry of Water Resource.

Station	Section area (m^2)	Average section area (m^2)	Section length (m)	Sediment volume (m^3)
0+050	568.8			
0+100	619.2	594	50	29200
0+150	460.1	539.65	50	26982.5
0+200	601.1	530.6	50	26530
0+250	356.4	478.75	50	23937.5
0+300	519	437.7	50	21885
0+350	605.3	562.15	50	28107.5
0+400	780.7	693	50	34650
0+475	826.4	826.4	75	60277.5
				Sum =251570 m^3

Table (3) the quantity of sedimentation ofSediments fluvial in upstream of Alhindia barrage of 2017.The data collected from excavation rivers office follow the Ministry of Water Resource.

Station	Section area (m^2)	Average section area (m^2)	Section length (m)	Sediment volume (m^3)
0+050	960.25			
0+100	922	941.125	50	47056.25
0+175	863.5	892.75	75	66956.25
0+250	722	792.75	75	59456.25
0+325	775	748.5	75	56137.5
0+400	865.75	820.375	75	61528.125
0+450	745.75	805.75	50	40287.5
				Sum 328421.875 m^3

Table (4) the quantity of sedimentation ofSediments fluvial in upstream of Alhindia barrage of 2018.The data collected from excavation rivers office follow the Ministry of Water Resource.

Station	Section area (m^2)	Average section area (m^2)	Section length (m)	Sediment volume (m^3)
0+050	1079			
0+100	1101	1090	50	54500
0+175	1047	1074	75	80550
0+225	1041	1044	50	52200
0+275	892	966.5	50	48325
0+350	901.5	896.75	75	67256.25
0+400	1099	1000.25	50	50012.5
0+475	930	1014.5	75	76087.5
				Sum 428931.25m^3

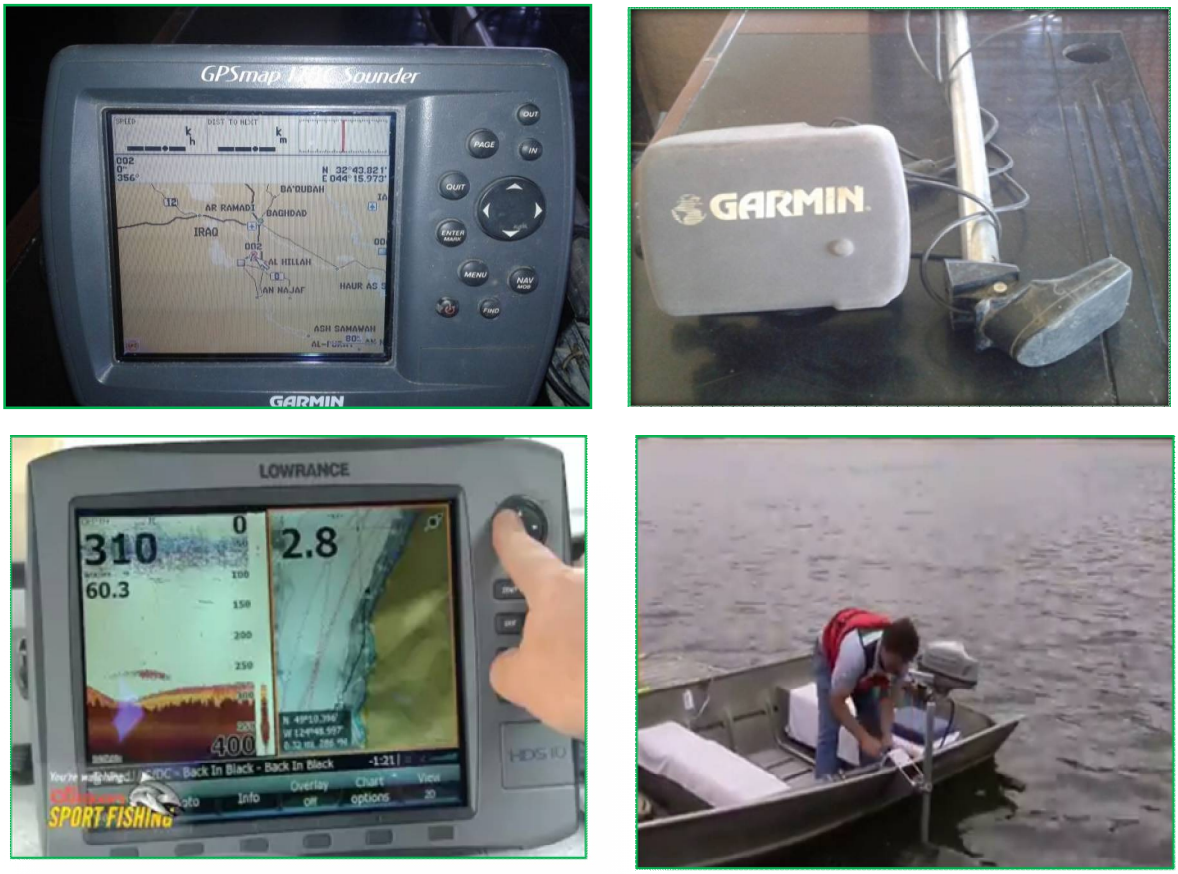

Figure (1) shown the image of device Echo sounder.

Figure(2).Google map for the site work

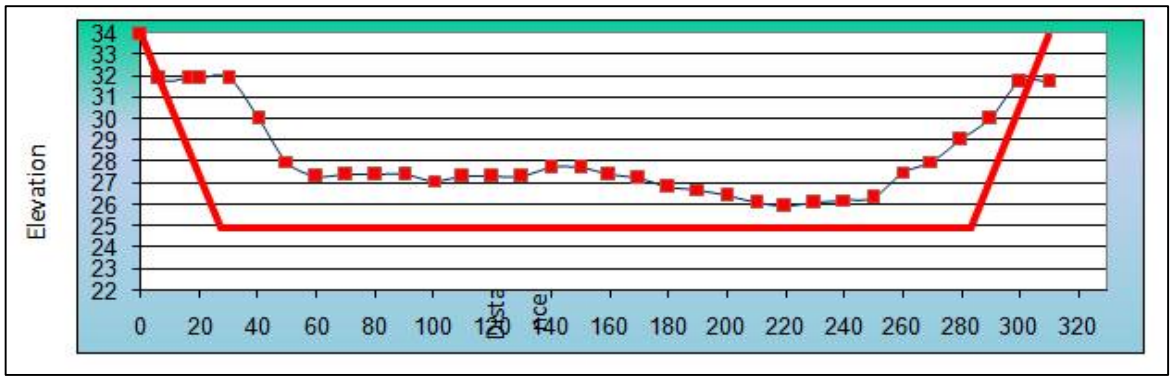

Figure (3) shown the cross section of sediments fluvial in station 0+400 in 2012

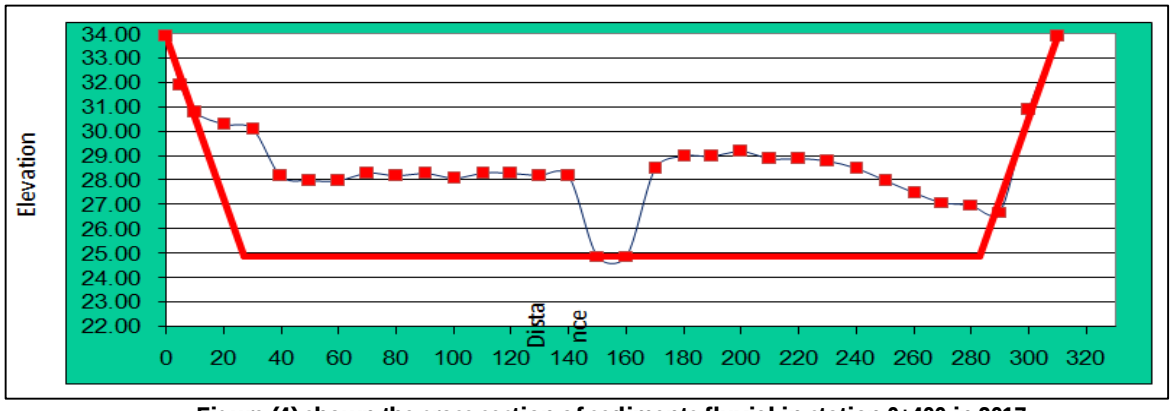

Figure (4) shown the cross section of sediments fluvial in station 0+400 in 2017.

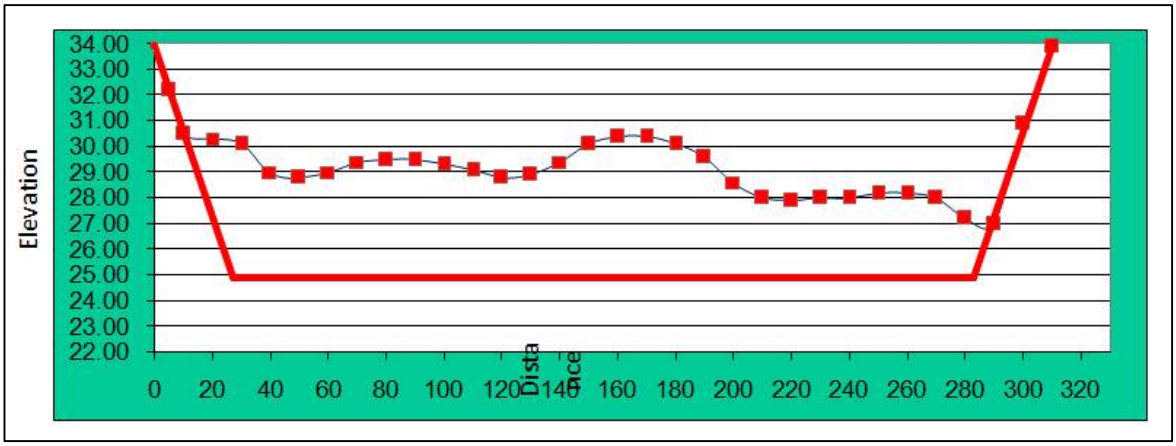

Figure (5) shown the cross section of sediments fluvial in station 0+400 in 2018.

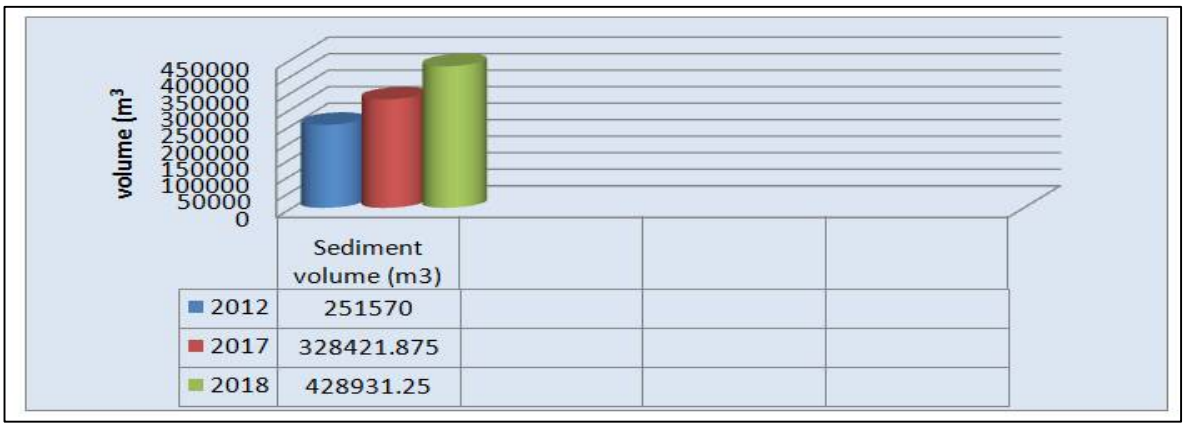

Figure (6) volume of sedimentation in three years (2012, 2017 and 2018).

Figure (7) the image of site of work and excavator.

Figure (8) the image of level device with staff reading.

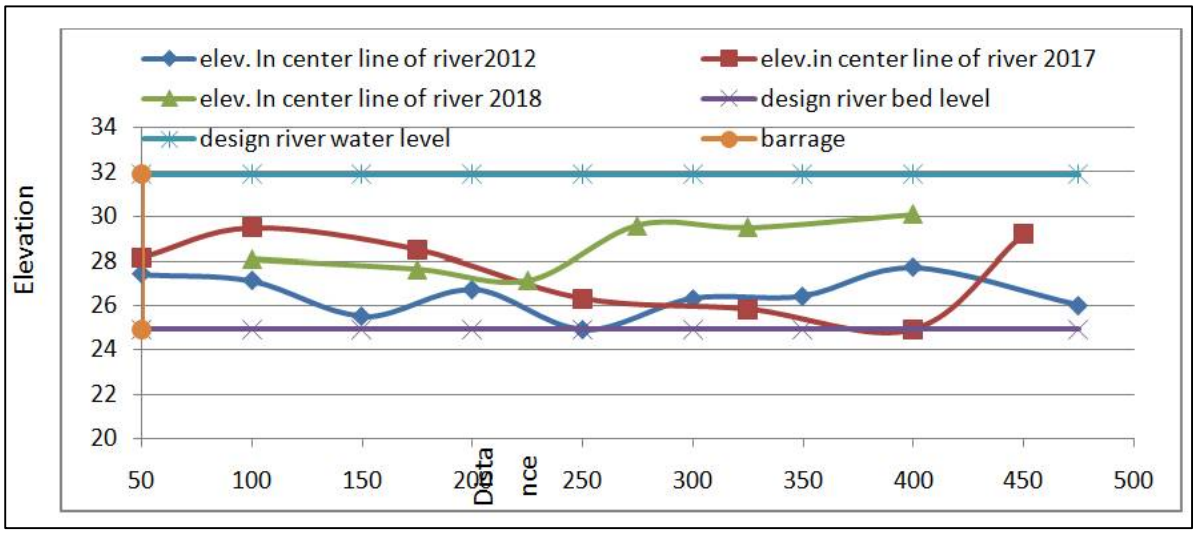

Figure (9) the sedimentation water level in center line at distance 500m from barrage through 2012,2018 and 2018.

Indian Journal of Natural Sciences www.tnsroindia.org.in ©IJONS

Vol.9 /Issue 51 / December / 2018 *International Bimonthly* *ISSN: 0976 – 0997*

RESEARCH ARTICLE

The Feasibility Study Economic and Technical Fields of Poultry in the Province of Diyala Depend on Analysis the Returns – Costs (CBA)a Comparative Study Between Sexing Poultry and other / Case Study – 2018)

Bilal Najah Jubiar[1]*, Mhana Abdullah Mahmood[2], Siraa Hameed Nayyef[1] and Ahmed Ebrahim Ahmed[3]

[1]Department of Agricultural Research, Ministry of Agriculture, Iraq.
[2]College of Agriculture, University of Diyala, Iraq.
[3]The Directorate of Agriculture in Diyala, Station Research Al Ghalbya, Iraq.

Received: 16 Aug 2018 Revised: 18 Sep 2018 Accepted: 24 Oct 2018

***Address for Correspondence**
Bilal Najah Jubiar
Department of Agricultural Research,
Ministry of Agriculture, Iraq.

ABSTRACT

To reach specific level of sufficiency in poultry breeding was of heeding specialists in poultry breeding ,using of the new techniques in poultry breeding very importance ,so we determined two aims are for this research: first aim the economic feasibility of sexing poultry (cock and hen) and get economic benefit from sexual separation, and the second aim is forecasting the production and consumption quantity of poultry meat for the period 2018 2022) ,We noticed from the prediction results the Iraq was import quantities of poultry meat to meet the demand and this is a major crisis and loss of scarcity currency may be exceeded by the right planning and expected to continue this food gap until the year 2022 and up to 354 thousand tons The results of cost analysis – returns (CBA)ofsexing poultry was economically feasible, The fields of sexing poultry exceled on other fields are not sexing poultry with high net returns except field NO. (2) so there can be investment opportunities for the production of poultry meat in Iraq, The recommendations of the research is to provide full support for the production projects of poultry breeding and facilitate enter the investors with this projects to prove opportunities of profits to the interested businessmen.

Key words: analysis of CBA, sexing chicken, Diyala province.

INTRODUCTION

Poultry meat have an importance in the markets and for consumers cause it is less expensive than other types of meat. Poultry is characterized by a rapid cycle of production and then the cycle of capital and as a result of genetic

improvement in the poultry sector so poultry breeding is important for researchers and specialists to find the best ways to improve the production of poultry meat and eggs and feasibility study for poultry to get On the best economic return .The poultry breeding take a major role in providing food security to a large part of the world's population because it is supplied with meat and egg exporters (Samurai, 2003, 12). It is a source of animal protein as well as a tender and easy digestion of poultry meat. With essential nutrients (Al-Atabi, 2008, 113). The technical ideas in this research is to improve the reality of poultry production to reduce losses and increase profits has been sexing poultry will be clarified with detailed and later in this research.

Objective of the research

The objective is to benefit economically from the process of sexing poultry by feasibility study and study the size of the food gap between the consumption and production of poultry meat at the level of Iraq for the period (1990-2017) and forecast the quantities of production and consumption of poultry meat for the period (2018-2022).

Research problem

The production of poultry meat is low locally when meet with demand. This is the problem suffers by specialists and researchers. The increasing demand for poultry meat is meet with import. The country is facing large financial loss. If this loss is invested in the development of the poultry sector so must be reach to solutions fordeveloped poultry meat production sector using advanced methods of poultry breeding.

Search hypothesis

The research assumes that there is a large economic return from the process of poultry breeding than the return obtained by traditional methods of poultry production and the research assumes that local production is increasing the sexing poultry.

Literature Reviews

The review of previous research that specialized in poultry breeding is very important in this research, which dealt with the method of breeding different from the traditional methods and to know the difference between what the researchers get previously, here we highlight some of their results as follows: Al-Qaisi and Al-Rabi'i (2011),astudy to know the using efficiency of labor and capital in poultry production in Diyala governorate, which used criteria for evaluating the efficiency of use resources for meat poultry projects as(profit, net profit, net farm income, (,return farm management, return of a labor, net totalvalue,net present value). It was found that all groups of possession achieved positive returns except the last groups (8.5-10)hens. On the other hand it was found when applying the capital recovery period, the results differentiated from one group to another , And when calculating the return of the dinar investor found above amounted to about 2.1 dinars in group (4-1) thousand birds. AL-Mashhadani, 2002, 2013-222), done a study using the criteria (profit, income, capital recovery period, return of the invested dinar) to know the economic feasiblity of the meat poultry projects. The results showed that all projects achieved positive returns, dinar return between (215 - 404) fils and that the period of capital recovery was 2.2 - 4.2 years and the best groups ofcapacities relatively large .

Poultry sexing

It is a process for separate hens and cocks at a certain age, especially at the age of one day after hatching, where sexing poultry to know the quality of the chick, whether cock or hen and then direct this gender to the purpose of

production, which leads to increase the return of poultry breeding, sexing poultry is a very important process in the poultry breeding, through which production can be directed according to the productive requirements of the stocks.

The benefits of sexing process

There are many benefits we can get it from the sexing we chose the most important are

1. In the white chicken breeds (table eggs), the hens are sorted out from cocks and then the hens are directed to breeding in order to produce the eggs of the table while the cocks are disposed of because they are not genetically capable of producing meat.their low conversion efficiency. In most cases, cocks are executed.
2. In the breeds of meat production may benefit from the sexing process and the breeding of cocks separate from hens, where it is scientifically proven that cocks faster to grow than hens and the application of sexing is hard and difficult because of the high density of stocks of meat production and often does not process the sexingfor stocks of meat production.
3. The process of sexingeconomically is reduce the cost to the least possible through get rid of unwanted sex before being spent on breeding without benefit of any return, for example in the meat breeds are kept cocks only as long It is grew faster than hens their weighs greater than hensalso the kind ofcocks meat was favorite to the consumeras for layer breeds the case differentbecause we get rid from cocks who couldn't not produce the eggs are get rid with the age one day without incur any losses to breeding therefore not used Of them, and thus we will keep the request sex and bear his costsbreeding because he will give a greater return then.
4. There are many ways for sexing poultry Physiological and physical and else, these ways good for expert in poultry breeding technically as for economically all sexing ways same the costs and haven't big variance so it good for technical expert in poultry breeding and needn't mentioned here we recognize at basically at economic side.

Economic importance for sexing

Lambert, Knox(1926)and Fanguf(1928) find The sexual ratio of the chickens of poultry family were equal at 50:50, with house breeding weren't made this ratio any problem practically that cocks use for produce meat and hens for produce eggs (Redman &Kaleta, 2008,391-399). Sexing process of poultry meat (even layers) have big economic importance , in poultry meat the cocks consumed more feed compare with hens,But the cocks reach the standard weight less days than hens, although the consumption of feed more, the short cycle of growth makes the cost of production low, the costs of additional days to raise chickens is greater than the cost of additional feed consumed, and the short days to market costs The cocks have a relatively larger weight of hens as we mentioned, because their metabolism is higher than that of hens. In marketing, the average weight of cocks is about 3.5 kg while the same period of breeding The hens reach an average weight of about 2.3 kg This difference in weights and differences in cost as well as the physiological quality of cocks meat for hens is of great economic importance, so the sexing process helps the breeder to direct his production towards the most profitable projects, by excluding the hens chicks at the age of one day before spends The cost of breeding and then give it less weight, and keepcocks chicks that are desirable by the consumer in terms of quality and economically profitable product.

As for the layers, despite the benefits mentioned above of poultry , which the sameon layers also, but the opposite is the case where the product here tries to keep the hens that give the eggs instead of the cocks, instead of spending the product costs large on the chicken meal and then After a period of breeding, it is discovered that 60% of this meal is cocks, and that the product needs a small number of cocks to be vaccinated only, so there is a great loss in breeding the meal, while the meat of layers is not desirable to the consumer and in this case, Avoid loosby the sexing process, as well as There are many organizations to protect the animal strongly support the sexing process because the occurrence of the situation mentioned above, the product is forced to kill chickens that can't be marketed and this is contrary to the international conventions and conventions that advocate the protection of the animal.

That the process of taking advantage of the cocks chicks resulting from the layers is not economically feasible, so 40 to 50 million chicks are killed directly after hatching only in Germany and about 2.5 billion chicks around the world annually. About 85% of the world's layer'cocks are used as animal feed in zoo (Aslam, 2014).The cocks resulting from hatching eggs of modern layers breeds have very slow growth potential, need large quantities of food and produce small quantities of meat of poor quality (Champers, 1990; Damme and Ristic, 2003; Gerkin O'Khoner, 2003). Both sexes are used to produce meat in poultry, but the body mass varies significantly between cocks and hens, so the sexing is essential (Lesso & Summers, 2009, 78). In the United States, about 50 million broilers are produced per day But only 27% are sexing for the purpose of separate sex to breeding
(Ricks & Others, 2003, 931-938).

Food Importance of Poultry Meat

Poultry meat is one of the richest sources of animal protein, which is one of the characteristics of the quality of human food in the developed countries, where the proportion of protein in the meat of chickens (19%) and sheep meat (17%) and in beef (18.7%). (Jawad,1984,29). Chicken meat is one of the basic ingredients of food for all consumers in the country. The National Nutrition Research Center of the Iraqi Ministry of Health estimated the basic requirements of individual animal products as follows:

Most economic studies in the country mention to increase demand at chicken meat because increase population growth rates , increase income growth rates and high standard living , increase demand on meat chicken and Low levels of domestic productionAnd the failure of the marketing process of the available ones, the country allow the entry of large quantities of poultry meat through imports, which makes the domestic product is not competitive at the local level due to poor production and marketing, these and other matters threaten food security and lead to serious risks and imbalances in the balance of trade, Therefore, the country must have attention to be taken seriously and effectively in the field of agricultural investment and the supply the required support for national agricultural products.

Production, consumption and size gap of poultry in Iraq for the period (1981 - 2016)

The inability of local production of poultryhasn't been the result of recent years, but the gap has been going on since the eighties of the last century and so far, The gap is expected to continue for the coming years if increasing population and the increasing demand for poultry, unless investors resort to modern methods of producing meat broilerand to determine the amount of this gap between the consumption and production of meat broiler then give the appropriate recommendations, it was necessary to study this gap in Iraq and know its economic effects. The table below shows the production and consumption of meat broiler from it know the nutrition gab for meatbroiler. In the Table (2), we note that the highest production of chicken meat was in 1990 (about 170) thousand tons while the lowest quantity of production in 1994 (about (7) thousand tons, The large difference between the quantities of production and the fluctuation in it is due to many factors, the most important epidemiological diseases that kill the chickens, which cause a great loss and in the absence of such epidemic diseases, the quantities of production increase significantly. As for the consumption of chicken meat, it has been noticed recently that consumption is constantly rising and this increase in consumption is related to the increase in population. Table 2 shows that the highest consumption was in 2014, reach about (420) Thousand tons, while the lowest quantity of consumption is in the year (1997), amounting to about (41) thousand tons. figures(1) and (2) showed the general trend of both production and consumption of chicken meat as follow: By combining these two scales in one figure, we can see the size of the food gap. This is clear in Figure 4

In the Figure 4, there is a large food gap between the production of chicken meat in Iraq and consumption, and this gap has been increasing in the last ten years, which means the situation is getting worse over time and this is due to several factors, The growth rate of production lowest of growth rate demand for chicken meat, which was caused by

the rapid population growth, and the lowest production gap occurred in 1990, which amounted to about (76) thousand tons if the production levels in this year is relatively high, although not covered by domestic demand, and higher Food gap occurred in 2016 if it reached 326 thousand tons of chicken meat was covered through Import from abroad. This means that the production units need modern technologies that increase the local production and competition of the broad production. It also needs treatment by the responsible state through supporting the local product and making the investment process in poultry a profitable process by receiving the necessary quantities of breeders Without restrictions or routine conditions after the development of certain criteria for meat received, the crisis of chickenmeat worsens with the passage of time and with the populationincrease, and the chicken meat alternative to red meat for low-income and development process is very important must be a decision makers To find solutions to feed a large and important segment and minimize spent the money that goes abroad.

Predicting production and consumption of poultry meat for the period (2018-2025)

To predict the production and consumption of chicken meat quantities in Iraq and as long as we have missing values in the table (2) of production and consumption so we suggested that the time series is made for a period (2005-2017) for lack of missing values during this period and even the results are based on the fact numbers and is not discretionary, and in order to do the prediction the values consumption and production quantities in Iraq have been adopted specimen ARIMA to estimate the prediction in the production and consumption volumes in this study, and requires a specimen Arima make sure the stability chain (Naqaar and Awad 2011, 127) and this was test stability two series , It was The results are as follows:using the minitab program. We obtained the following results: In Figure (5) clear that a general trend of the two series and that they are not stable around the arithmetic mean. This is confirmed by the ADF test after its application Table (3), which shows the Dicky-Fuller test expanded to test the stability of the time series, it is clear that the two systems are unstable. In order to make the two statins stable, the first difference of the two methods was taken. The results are as follows: In Table 4, it is clear that the two series stabilized after computethe first difference. The calculated (t value) of statistic Diki-Folar was greater than the critical values, so the next step do the Auto regression for two series for find condition of predictability. We were seek ARMA Model Family In order to obtain a model that fits our time series, Jenkins & Box depended on the Auto relation (ACF) and the function Auto relation(P.A.C.F) (Box, Jenkins, 1976, 40). The two function of Auto-regression of two variables as follows: The two function of Auto-regression in Figure (6) show that they meet the conditions of prediction. This meanscan be used twoseries to predict the adoption of the first differences by using minitab program, which provides the Box-Jenks methodology for predicting the time series. Figure (6) can suggest ARIMA. Where predicted the consumption and production values for the next five years by adopting the model. The results were as follows:

From the figures (7&8) findpoultry production in Iraq will continue to increase, but this increase is very weak and does not meet the country's need for poultry. Production in 2022 will reach 113 thousand tons only. This low level of production is Is a real crisis for poultry, unless depend on methodology and planning different also new methods and techniques help produce a wide range of self-sufficiency in poultry. These include the poultry sexing, which is expected to get high economic returns than traditionalbreedingthat found it sample analysis in the part The last of this search. On the other sidewithpoultry consumption, we find the estimated values of consumption shown in Table (5) the consumption is increasing continuously and may be reach 476 thousand tons in 2022. This means the continued need for imports to fill the shortfall in poultry demand. requires big knowledge to consumers in order to modify the food pattern in order to suppress this continuous growth in chicken consumption, which in turn reduces the loss of hard currency lost by Iraq due to import from abroad. Table (5) shows the food gap will continue to increase, although production will increase but there is a greater increase in consumption meet the development of small production. Although gap is continuing for a long time and for a long time in the future. There has been no true policy and plans for the development of the poultry breeding in Iraq on the other hand the modification more consumption of meat in general and poultry in particular.

Descriptive analysis of sample

To know the characteristics of the sample used in the analysis, Table (3) shows some of the details of this sample. In Table (3) we find that farm(2) has the highest production capacity of about 30,000 birds / meal, and the number of halls in three farms were(2) rooms while the farm(2) was the number of (4) halls.These farms are management under a group of researchers and producers distinguished in the production of poultry meat, and these farmswere under scientific research constantly because sexing poultry had a set of scientific requirements can't be any breeders did it.

Cost-Benefit Analysis (COST- BENEFIT ANALYSES) (CBA) for sexing and non-sexing chick fields

We were studdingand analyzingThe factors influencing the breeding of sexing and non-sexing chick in poultry fields represented with financial features by using cash value to product and return input of chick breeding to find best way and how can be a obtain profits so method can use it for evaluate it is cost –benefit analyses (CBA) which is a method of systematic economic analysis to evaluate the techniques used to achieve the best economic return and thus improve the level of Farmers' living This method includes a systematic assessment of the social benefits of a given project as a result of the cost of the project. This is a technique that links program costs or project to its main results or benefits. For the expression of both the benefits and costs in monetary units. This assessment is at the farm level and in the short term. This approach is taken because the previous analysis proved that the market system often fails to achieve the optimal allocation of resources because the external effects are not taken into consideration.- Returns from the most widely available methods of economic evaluation. This method is used to assist decision makers in decision-making in many different areas of economic and social policy in the public sector. The main difference between this method and the economic methods The other the evaluation is that it seeks to use the monetary values of both the inputs (costs) and outputs (returns) of the project or technology under study.

The calculation of net present value (net revenue) is the most important indicator in the CBA and can give answer If the project improves social welfare, there are two alternative accounts that can be used to supplement the calculation of the first present value: the ratio of costs - returns are calculated by taking the net present value of the proceeds and dividing them into the net present value of the costs as the cost-benefit ratio is useful in the following: First, it Making easy compare similar programs and projects; secondly, the decision maker can decide whether the specific return earned per ID of the cost is sufficient given other alternatives related to investment or budget and from the perspective of economic efficiency, any program with higher costs or better interest than Any other similar project is a better allocation of resources. Decision makers should use interest rates when testing two similar projects in terms of size and scope. Otherwise, the interest rates of variations on the scale may disappear, which may lead to an alternative option Save the largest net benefits to the community and the second alternative account is the return on investment (IRR), or IRR, which is frequently used and can be easily calculated. The internal rate of return is simply the discount rate that would achieve the net present value that is equal to the costs. An organization or government agency or decision maker can evaluate the value of the project based on whether a certain percentage of the return is satisfactory given the other available opportunities. Costs and returns for evaluating the economic feasibility of breeding sexing and non-sexing chick, we were geta set of criteria, the most important of which is net present value (net revenue) and internal rate of return that helps to evaluate whether breeding and isolation of sexing chick of non sexing chick makes farmers better compared to the current situation as shown in the tables below have obtained the following results:

Net returns

Net present value to investment project is refers the different between the present value of the project's cash flows and the present value of the outflows. If the net present value is positive, the present value of the cash flows grater than the present value of the cash outflows would have been more profitable and, conversely, the investment project

is not profitable if the net present value is negative The present value of cash flows is less than the present value of cash outflows. In the case of more than one investment project, the project that gives the highest net present value is preferred (Stokey E. & Zeckhauser R., 1978, 133).

Internal rate of return (IRR)

It expresses the minimum return on capital that makes the net present value of the inflows equal to the cost of the investment project and represents the minimum return on capital that the farmer accepts in order to invest in technology. According to international standards if the IRR is greater than (40%) it is recommended to apply the technology to achieve profitable returns for farmers and to divide the percentage of change in net returns to the percentage of change in total costs (Cellinis & Keej,2010,33).

Return-cost ratio

It can be get by divided the present value of the cash flows of the project on the present value of the cash outflows for this project. When the division is equal (1) it is a normal profit while the division is greater than (1), there is an economic profit and If the division is less than (1) this project isn't economic, (Al Yami, 2005, 19).

Period of capital recovery

This is the period in which the projects recover the investment cost or the period in which the inflows and outflows are equal. if the periodshorter project was better. is calculated from divided the cost of the investment on the average net cash flow (Fahim, 2015 - 233).

Break-Even Point

A break-even analysis is used in feasibility studies because it helps to know the minimum level of production or level of sales can the project continue in the market without deciding stop production or exit the market and the lower theBreak-Even Pointlead to get chance for obtaining profits and the propability less to achieve losses, it's Express the lowest level of production that can be allowed to use the production capacity of the project, and is expressed mathematically as follows (www.arab-api.org)

$$\text{Break-Even Point} = \frac{\text{Fixed costs}}{\text{unit selling price} - \text{unit variable cost}}$$

The result of field No.(1)

We were found the breeding sexing chicks gives best results where total return of production to the sexing chicks was (36645000)ID, which is greater than the total return of production to the nonsexing chick (26938000) ID. net profit (profit) reached(13367500)ID it is grater than net return of breeding non sexing chick,The change in return was 0.5%, there was an increase in return of 0.5 and the change in cost was 0.12, there were an increase in costs 0.12 and the internal rate of return was 4.4. The use of one dinar in the broiler breeding project gives a return of 4.4 ID, return value on costs are1.6, revenues exceed costs The value of (1.6) ID,so considered this project economically feasible, and the period of recovery of the invested capital was 1.7 year, the breeder can recover his capital invested in sexing chickens within a period of one year and seven months. Break-even point to product size reach (168)ID the lowest level of production the breeder can produce to cover its costs only.

Results of field No. (2)

It was found that the breeding sexing chicks lead to a large loss estimated at (4417900) IDbecausehigh total costs required for sexing chick so these costgreater than the total production revenue which consists of the revenues of selling birds and the revenues of waste ,litter, and other revenues. Change in revenue decrease with (7.7%) it's big decreas as the use of one dinar led to a decrease (7.7) ID and decreased the rate of internal return by (16.63), investment of one dinar in breeding sexing chickens lead to a loss of (16.63)ID, and decreased returns to cost by (0.91) Costs field No.(2) is not economically feasible as a result of the losses suffered by the field, and the period of recovery of capital invested (- 12) years where the negative sign reference to a loss of net profits where the breeder needs to a period of 12 years with condition work and access Of raising sexing chicks and get profits so that he can recover his capital invested. In this case the breeder needs to decide whether to continue production by changing the combination of resources and reduce costs or change his project to another alternative project more profitable, the break-even point of product size (611) ID is the lowest level of production can breeders that produced to cover its costs only.

Results of field No. (3)

In this fieldwere achieved revenues and profits. The total return on production was higher of sexing chicks (48609600) ID, which is higher than total revenue product obtained of non sexing chicks. The net revenues were high at (13032600)ID, littlechange in revenue(0.6%) Shows the use of one dinar leads to a decrease 0.6 ID and changes in cost, a low decrease in costs (0.05%) and an internal rate of return (12.5), where the investment one dinar in sexing chicks project leads to an increase of 12.5 ID. (1.4) indicates a 1.4% increase in returns This field has achieved economic profits and profitable returns, and the period of recovery of capital invested 2.7 years, which requires the breeders of sexing chicks to a period of two years and seven months to recover investment costs. Break-even point of sales about (132) ID the lowest level of production can be produced by the breeder cover the costs only.

Results of field No.(4)

This field had achieved total revenue product of breeding sexing chicks (28610000) ID, which is higher than the total revenue of product of non sexing chick, as well as increase in net return and gain of profits (5090000)ID, return was increase by (1.0%) there is an increase in return and decreased The cost at (0.1%), there is a decrease in cost . the internal rate of return (8), which shows the investment of one dinar by sexing process chicks leads to the investor to 8 dinar , the returns on costs (1.2) shows the increase in returns by 1.2 This is a field achieved economic feasibility, and the capital recovery period The investor is 4.6 years, the breeder needs a period of four years and six months to recover his invested capital. The break-even point of the sales size is (164)ID, the lowest level of productcan the breeder produce it to cover its costs.

CONCLUSION

The researcher reaches to some results & conclusion as follow:
The country loss hard currency the cause food gap along study period between production & consumption, this gap continue because increase population with continue also use traditional breeding poultry.The result of predicted cleared food gap will continue for next five yearsalthough expect increase the production but there are more expected increase in consumption future.The result of CBA analyses find sexing poultry give profit higher than traditional breeding that make the breeders doing this projects , the breeder carry the added costs as high price of sexing chicks and get high economic revenue.Recovery capital periodin sexing chicks fields was shorter than the fields non sexing that's make the investors depend this projects have speed with recovery capital.

Recommendations

Continue of increase population with low production level need wide educational & extensional program on tow sides , first side of poultry breeder upon on wide production and inter new technical as sexing ,the other side of consumption must minimizing losing of poultry meat with minimize the waste by consumption this product. Supported poultry project ,facility inter investors of this sector which prove find big opportunities profitability attract business men.Recommend that's necessary adopt sexing poultry when breeding this process help increase the profits , wide the production and minimizing losses of breeding poultry.

REFERERENCES

1. AL samrray ,Marwan Zuheir Rajab ,2003, measurement production efficiency of broiler breeders of program rehabilitation poultry sector ,MSC. Study ,Agri. college ,University of Baghdad,p.2.
2. AL Attaby ,Jabeer Majeed and Ahmed Sajed ALMasody,2008, knowledge level of broiler breeders to significant recommended and relation with some factors in Baghdad governorate ,Iraqi agriculture science journal,39(3),133-121
3. AL Qaisy, Esqander Husaen Ali and SHaimaa Ali Kadhum ALRubaey.2011,efficiency use factors labor and capital in broiler production fields (Jalawlaa district-Deyala governorate),Iraqi agriculture science journal 42 (13),244-254.
4. AL Mishhadany .Abdullah Mohamed,2002,finincal evaluate of poultry project (broiler production fields)Iraqi agriculture science journal,folder33.No.4,p.213-222.
5. Jawad ,Emad Nadum 1984, effected factors on product special sector of broiler,Iraqi economic journal,25,No.3,p.29.
6. Hameed Muhamed Mizel, technical and economic feasibility study of broiler product project in Anbar governorate,2011,p.158).
7. AL Yamy ,Ahmed Merwas,2005, technical analyses cost –benefit successfully method with analyses policy and general programs, Abdul Azeez King University ,economic and management ,2(19),Kingdom of Saudi Arabia.
8. Faheem, Abanob Adel Azmy, feasibility study of poultry farm,ALZaazee11mayo 2015.
9. www.arab-api.org.
10. Ministry planning and development cooperation /central statistical organization.
11. Ministry planning and development cooperation/census.
12. Cellinis. & Keej.2010 . Cost Effectiveness and Cost –Benefit Analysis in Handbook of practical program Evaluation san Francisco , ca , Jossey – Bass.
13. Stokey E.,&Zeckhauser R. , 1987 . Aprimer for policy analysis , New York , w. Norton &company .
14. Box, G. E. P. and Jenkins, G. M. (1976). Time Series Analysi Forecasting and Control, 2nd ed , Holden-Day, San Francisco
15. Kaleta, E. and T. Redmann. 2008. Apporaches to the sex prior to and after incubation of chickens eggs and of day old chicks. WPSJ. 64: 391-399.
16. Aslam, M. 2014. Offspring sex ratio bias and sex related characteristics of eggs in chickens. Thesis. Wageningen University. The Netherlands.
17. Lesson, S. and J. D. Summers. 2009. Broiler berrder production. Nottingham University press. University book. 79.
18. Ricks, C., N. Menda and P. Phelips. 2003. The embryonated egg: A practical target for genetic based advances to improve poultry production. Poult. Sci. 82: 931-938.

Table (1): The needs of meat personnel by the National Center for Nutrition Research

N	subject	The need for the individual
1	red meat	10 kg / year
2	Chicken meat	16 kg / year
3	fish	6 kg / year
4	eggs	9 kg / year

The source: (Mohamed mizael hameed , feasibility study technical and economy to poultry product in Anbar governrate,2011,p.158).

Table(2)Annual production and consumption of meat broilerto period(1990–2017)

Years	NO.population Thousand (1)	Production Ton thousand(2)	Consumption Ton thousand(3)	Nutrition gap(4) 4=3-2	Average per capita consumption Kg (5) 5=1000*(1/3)
1990	17890	170	246	-76	13.75
1991	18419	12	151	-139	8.19
1992	18949	28	141	-113	7.44
1993	19478	26	141	-115	7.23
1994	20007	7	125	-118	6.24
1995	20536	9	151	-142	7.35
1996	21124	-	142	-	6.72
1997	22046	-	41	-	1.85
1998	22702	-	45	-	1.98
1999	23382	-	-	-	-
2000	24086	-	-	-	-
2001	24813	-	-	-	-
2002	25565	-	-	-	-
2003	26340	-	-	-	-
2004	27139	-	299	-	11.01
2005	27963	59.7	307	-247.3	10.97
2006	28810	55.6	317	-261.4	11.00
2007	29682	40.3	326	-285.7	10.98
2008	31895	36.9	351	-314.1	11.00
2009	32105	34.1	353	-318.9	10.99
2010	32831	52.8	361	-308.2	10.99
2011	33619	87.2	370	-282.8	11.00
2012	34406	89.8	378	-288.2	10.98
2013	35193	74.7	387	-312.3	10.99
2014	35981	70.2	396	-325.8	11.00
2015	36768	86.4	404	-317.6	10.98
2016	37556	87	413	-326	10.9
2017	37850	96.1	420	-323.9	11.09

Source:

1) Ministry of Planning and Development Cooperation, Demographics.

2) and(3) Ministry of Planning and Development Cooperation, Central Statistical Organization, Annual Statistical Group for the years 2010-2017.
4) Calculated by the researcher.
5) (-) It's mean The absence of data on the production and consumption of meat broiler during the period (1996-2004).

Table (3) ADF test for data stability

Null Hypothesis: CONSMPTION has a unit root
Exogenous: Constant
Lag Length: 1 (Automatic - based on SIC, maxlag=2)

		t-Statistic	Prob.*
Augmented Dickey-Fuller test statistic		-1.522972	0.4853
Test critical values:	1% level	-4.200056	
	5% level	-3.175352	
	10% level	-2.728985	

*MacKinnon (1996) one-sided p-values.
Warning: Probabilities and critical values calculated for 20 observations and may not be accurate for a sample size of 11

Null Hypothesis: PRODUCT has a unit root
Exogenous: Constant
Lag Length: 1 (Automatic - based on SIC, maxlag=2)

		t-Statistic	Prob.*
Augmented Dickey-Fuller test statistic		-1.289769	0.5938
Test critical values:	1% level	-4.200056	
	5% level	-3.175352	
	10% level	-2.728985	

*MacKinnon (1996) one-sided p-values.
Warning: Probabilities and critical values calculated for 20 observations and may not be accurate for a sample size of 11

Source: From the researcher workby adopt Eviews program.

Table (4) ADF test for data stability

Null Hypothesis: D(CONSMPTION) has a unit root
Exogenous: None
Lag Length: 2 (Automatic - based on SIC, maxlag=2)

		t-Statistic	Prob.*
Augmented Dickey-Fuller test statistic		-2.274297	0.0294
Test critical values:	1% level	-2.847250	
	5% level	-1.988198	
	10% level	-1.600140	

*MacKinnon (1996) one-sided p-values.
Warning: Probabilities and critical values calculated for 20 observations and may not be accurate for a sample size of 9

Null Hypothesis: D(PRODUCT) has a unit root
Exogenous: None
Lag Length: 0 (Automatic - based on SIC, maxlag=2)

		t-Statistic	Prob.*
Augmented Dickey-Fuller test statistic		-2.199117	0.0326
Test critical values:	1% level	-2.792154	
	5% level	-1.977738	
	10% level	-1.602074	

*MacKinnon (1996) one-sided p-values.
Warning: Probabilities and critical values calculated for 20 observations and may not be accurate for a sample size of 11

Source: From the researcher work by Eviews program.

Table (5) Predicting the production and consumption values of chicken meat for the period 2018-2022

years	Expected productionof chicken meat) (thousand tons	Expected consumption of Chicken meat (thousand tons)	Expected Food gap (thousand tons)
2018	100.954	430.328	-329.374
2019	104.516	439.479	-334.963
2020	107.685	449.046	- 341.361
2021	110.735	458.466	- 347.731
2022	113.748	467.938	- 354.190

Source: From the researcher work upon outputstatistical program MINITAB. these predicted values is reflected in forms (7) and (8):

Table (6): Characteristics of the research sample in Diyala Governorate

Items	**Farm(1)**	(2)**farm**	)**3**(**farm**	**Farm (4)**
Production capacity chick / meal	7000	30000	20000	12000
No. of administrators	1	1	1	1
No. of halls	2	4	2	2
Type of ownership	rent	owner	owner	owner

No.meals (meal)	5	6	4	6
sector	special	special	special	special
No. workers in one hall	2	6	3	3

Source: from researcher work upon questioner data.

Analyses (CBA) to breeding sexing and non sexing chicks Field No.(1)

Sexing chicks		Non Sexing chicks	
Fixed costs		Fixed costs	
Field rent	350000	Field rent	350000
Variable cost		Variable cost	
Workers wages	1000000	Workers wages	1000000
Cost buy chicks	4550000	Cost buy chicks	3850000
Feed cost/ton	15225000	Feed cost/ton	13050000
Litter cost	60000	Litter cost	60000
losses	227500	losses	330000
gas	280000	gas	280000
electric	225000	electric	225000
repair	60000	repair	60000
drugs	1200000	drugs	1200000
Other costs	100000	Other costs	100000
Sum costs	23277500	Sum costs	20505000
Production(No. markting birds)	6650	Production(No. markting birds)	6400
Revenue of birds marketing	36575000	Revenue of birds marketing	26928000
Revenue of waste & littre	70000	Revenue of waste & littre	10000
Total revenue product	36645000	Total revenue product	26938000
Net revenue	13367500	Net revenue	6433000
Change in revnue%	0.5		350000
Change in cost%	0.12		
IRR	4.4		1000000
B/C	1.6		3850000

Source: researcher work upon questioner data.

Analyses (CBA) to breeding sexing and non sexing chicks Field No.(2)

Sexing chicks		Non Sexing chicks	
Fixed costs		Fixed costs	
Field rent	2400000	Field rent	2400000
Variable cost		Variable cost	
Workers wages	4500000	Workers wages	4500000
Cost buy chicks	22500000	Cost buy chicks	16500000
Feed cost/ton	21060000	Feed cost/ton	48360000
Litter cost	60000	Litter cost	180000
losses	562500	losses	1925000
electric	75000	electric	225000
repair	750000	repair	200000
drugs	800000	drugs	2400000
kerosene	250000	kerosene	725000
Other costs	70000	Other costs	210000
Sum costs	53027500	Sum costs	77625000
Production(No. markting birds)	8140	Production(No. markting birds)	7600
Revenue of birds marketing	45909600	Revenue of birds marketing	33111750
Revenue of waste & littre	2500000	Revenue of waste & littre	2500000
Other revenue	200000	Other revenue	3500000
Total revenue product	48609600	Total revenue product	39111750
Net revenue	-4417900	Net revenue	-38513250
Change in revnue%	-7.717547		
Change in cost%	-0.463863		
IRR	16.637553		
B/C	0.9166866		

Source: researcher work upon questioner data.

Analyses (CBA) to breeding sexing and non sexing chicks Field No.(3)

Sexing chicks		Non Sexing chicks	
Fixed costs		Fixed costs	
Field rent		Field rent	
Variable cost		Variable cost	
Workers wages	1800000	Workers wages	1800000
Cost buy chicks	14000000	Cost buy chicks	14000000
Feed cost/ton	15000000	Feed cost/ton	13000000
Litter cost	120000	Litter cost	120000
losses	1302000	losses	1680000

electric	125000	electric	125000
repair	100000	repair	100000
drugs	1780000	drugs	1700000
kerosene	800000	kerosene	800000
Other costs	50000	Other costs	50000
Sum costs	35077000	Sum costs	33375000
Production(No. markting birds)	8140	Production(No. markting birds)	7600
Revenue of birds marketing	45909600	Revenue of birds marketing	33111750
Revenue of waste & littre	2500000	Revenue of waste & littre	2500000
Other revenue	200000	Other revenue	3500000
Total revenue product	48609600	Total revenue product	39111750
Net revenue	13532600	Net revenue	5736750
Change in revnue%	0.6		
Change in cost%	0.05		
IRR	11.9		
B/C	1.4		

Source: researcher work upon questioner data.

Analyses (CBA) to breeding sexing and non sexing chicks Field No.(4)

Sexing chicks		Non Sexing chicks	
Fixed costs		Fixed costs	
Cost hall building	500000	Cost hall building	500000
Field rent		Field rent	
Variable cost		Variable cost	
Workers wages	2100000	Workers wages	2100000
Cost buy chicks	3900000	Cost buy chicks	3000000
Feed cost/ton	14400000	Feed cost/ton	12240000
Litter cost	60000	Litter cost	60000
losses	195000	losses	350000
electric	100000	electric	100000
repair	50000	repair	50000
drugs	1600000	drugs	1600000
kerosene	200000	kerosene	200000
gas	315000	gas	315000
Other costs	100000	Other costs	100000
Sum costs	23520000	Sum costs	20615000
Production(No. markting birds)	5700	Production(No. markting birds)	5700
Revenue of birds marketing	28500000	Revenue of birds marketing	20550750
Revenue of waste & littre	60000	Revenue of waste & littre	60000
Other revenue	50000	Other revenue	100000

Total revenue product	28610000	Total revenue product	20710750
Net revenue	5090000	Net revenue	95750
Change in revnue%	1.0		
Change in cost%	0.1		
IRR	8		
B/C	1.2		

Source: researcher work upon questioner data.

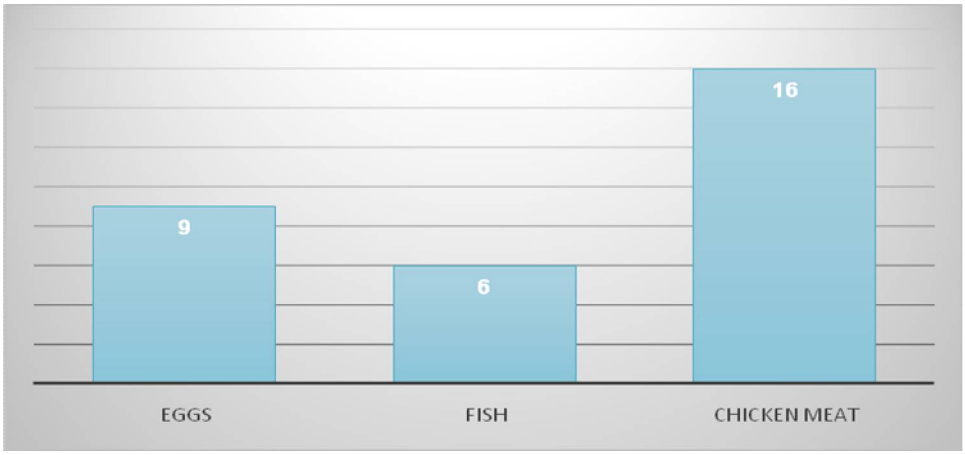

Figure (1) individual need of meat according international center of nutrition research The source: from researcher work upon table (1).

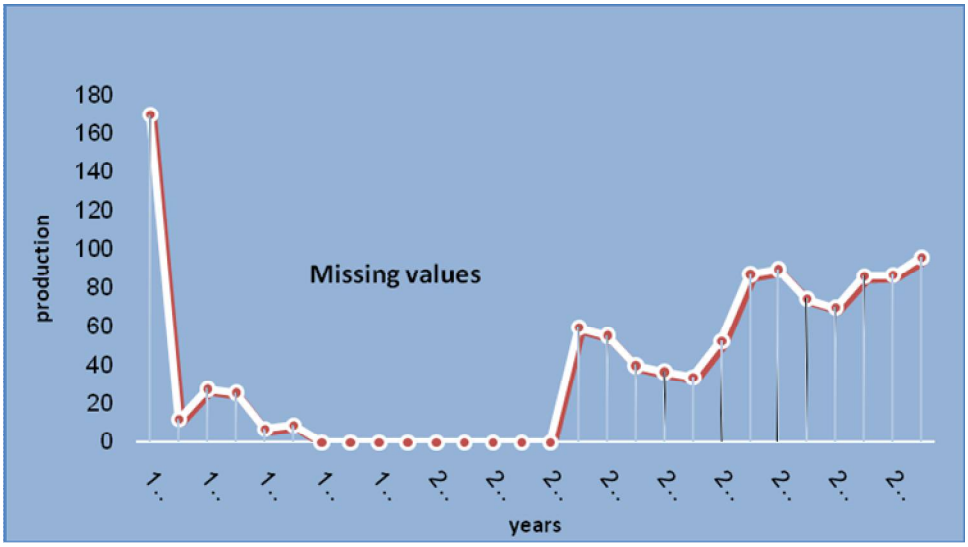

Source: from researcher work upon table (2).

Figure (2) The general trend of production quantities of chicken meat at the level of Iraq for the period (1990 - 2017)

Source: from researcher work upon table (2).

Figure (3): The general trend of quantities of consumption of chicken meat at the level of Iraq for the period (1990 _2017

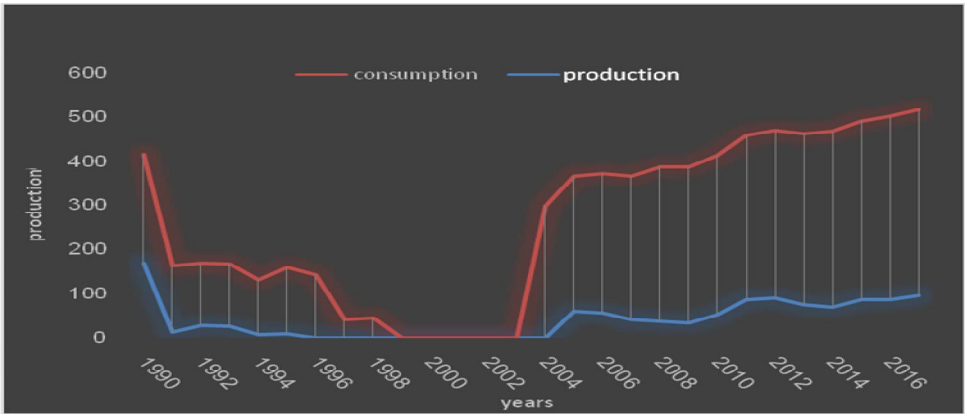

Source: from researcher work upon table (2).

Figure (4): Production, consumption and size of food gap of chicken meat at the level of Iraq for the period (1990 - 2017)

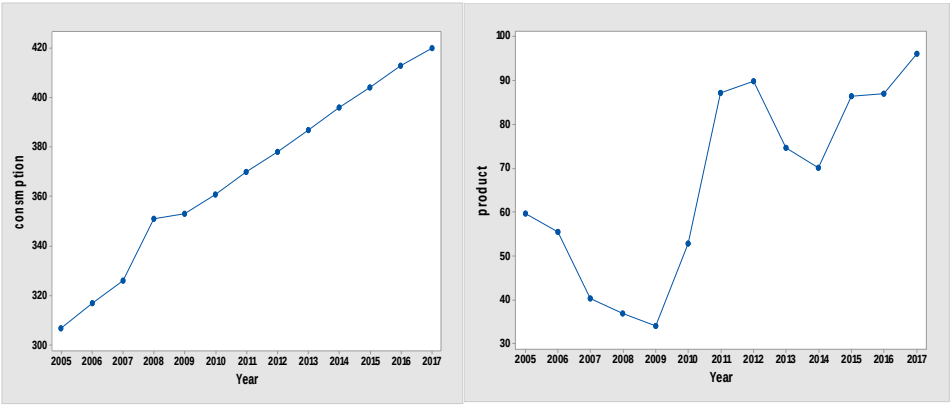

Figure (5) The general trend of consumption and production of chicken meat for the period (2005 - 2017)

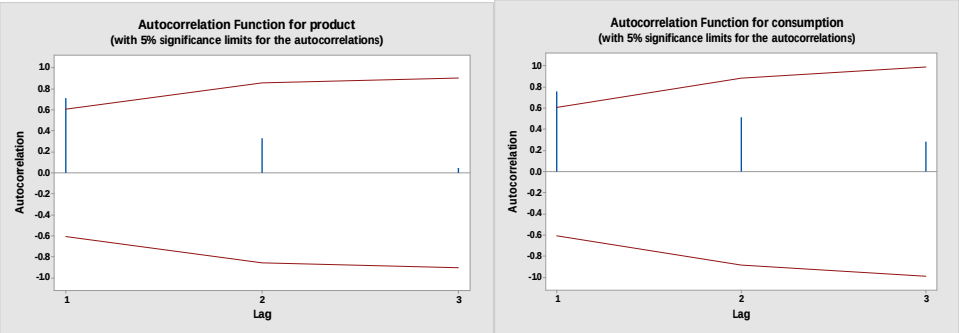

Figure (6) Auto-regression function of production and consumption series of chicken meat

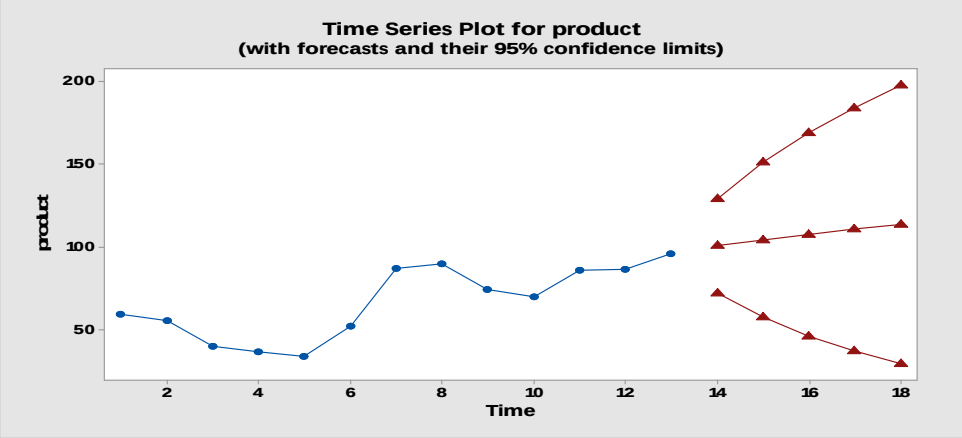

Source: from researcher work upon on table (2)data

Figure (7) Estimated values of chicken meat productionto period(2018-2022)

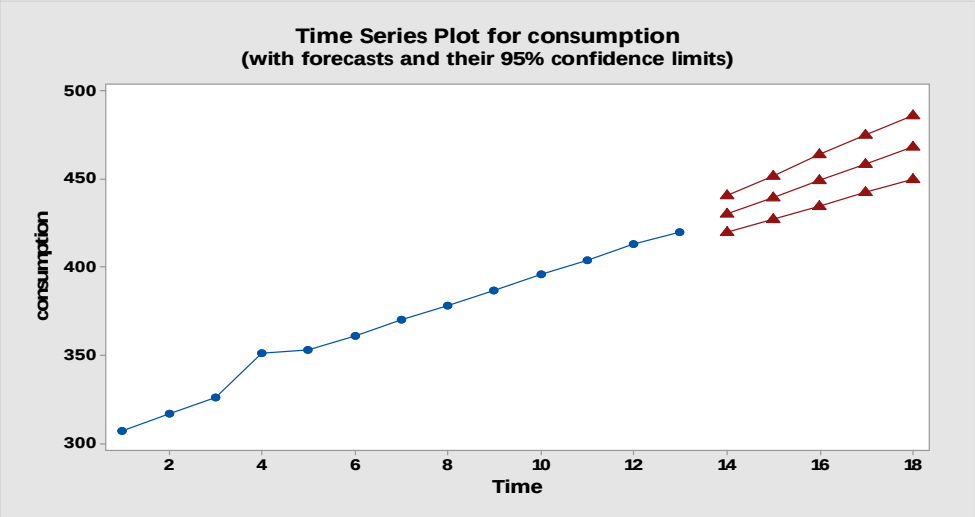

Source: searcher work upon table(2)data

Figure(8)Estimated value of chicken meat consumption to period(2018-2022)

Indian Journal of Natural Sciences www.tnsroindia.org.in ©IJONS

Vol.9 /Issue 51 / December / 2018 *International Bimonthly* *ISSN: 0976 – 0997*

RESEARCH ARTICLE

Ixodid Ticks of Cattle in South India

B. M. Amrutha[1], K. G. Ajith Kumar[1]*, Prashant S. Kurbet[1], Anju Varghese[1], R. K. Pradeep[1], M. Nimisha[1], A. Nandini[1], Angeline Felicia Bora[1], Lanchalung Malangmei[1], C. K. Deepa[1]. Sanis Juliet[2] and Reghu Ravindran[1]

[1]Department of Veterinary Parasitology, College of Veterinary and Animal Sciences, Pookode, Wayanad, Kerala, India
[2]Department of Veterinary Pharmacology and Toxicology, College of Veterinary and Animal Sciences, Pookode, Wayanad, Kerala, India

Received: 24 Sep 2018 Revised: 26 Oct 2018 Accepted: 29 Nov 2018

***Address for Correspondence**
K.G.Ajith Kumar
Department of Veterinary Parasitology,
College of Veterinary and Animal Sciences,
Pookode, Wayanad, Kerala, India.
Email: ajithkumarkg@gmail.com

ABSTRACT

A study was carried out in different geographical locations of two South Indian states *viz*., Kerala and Karnataka to study the prevalence of Ixodid ticks on cattle. A total of 157 and 122 cattle were screened for tick infestation, out of which 116 and 79 animals were infested from Kerala and Karnataka respectively. *Rhipicephalus (Boophilus) annulatus* was the predominant tick species (54.26 per cent) infesting cattle of Kerala followed by *Haemaphysalis bispinosa* (25.58 per cent), *R. (B.) microplus* (12.40 per cent) and *R. haemaphysaloides* (5.42 per cent). Low infesation rate of 0.77 per cent was observed with *R. sanguineus*, *Amblyomma integrum* and *Dermacentor* spp. in Kerala. In Karnataka, the *R. (B.) microplus* was the predominant tick species (77.10 per cent) followed by *H. bispinosa* (18.07 per cent) and *R. haemaphysaloides* (4.81 per cent).

Key words: Ixodid ticks, cattle, Kerala, Karnataka.

INTRODUCTION

Ticks are very important and harmful blood sucking external parasites of mammals, birds and reptiles throughout the world (Furman and Loomis, 1984). There are 939 species of ticks with 727 under Ixodidae, 211 under Argasidae and one species under Nuttalliellidae throughout the world (Rivera *et al*., 2018). Nearly, 12.5 per cent of the world tick fauna are present in South-East Asia (Petney, 1993). A total of 106 tick species were recorded from India out of which 88 species belong to Ixodidae (Geevarghese *et al.,* 1997; Ghosh *et al*., 2007). In India, most of the animals are suffering from multi-species tick infestations (Ghosh and Nagar, 2014). Ticks cause reduction in milk production and weight gain and transmission of pathogenic parasites, thus acting as an impediment to the growth of the livestock (Singh and Chhabra, 1992). Ticks are the important vectors for the transmission of bacteria, viruses, protozoa and helminths of zoonotic significance (de la Fuente *etal*.,2008). Ticks are involved in the transmission of haemoprotozoan

diseases such as babesiosis and anaplasmosis (Jongejan and Uilenberg, 2004). The global loss caused by ticks and tick-borne diseases (TTBDs) was estimated between US$ 13.9 and 18.7 billion annually (de Castro, 1997) while in India the economic loss has been estimated as US$ 498.7 million/annum (Minjauw and McLeod, 2003). Ticks and tick-borne diseases (TTBDs) affect 80 per cent of the cattle population throughout the world, particularly tropical and subtropical countries, including India (de Castro, 1997). The present study was designed to evaluate the prevalence of tick infestation in cattle of Kerala and Karnataka and to identify the most common tick species in these states.

MATERIALS AND METHODS

Study area

The study area included different regions of Kerala and Karnataka. From Karnataka, ticks samples were collected from North and South Karnataka regions. North Karnataka is a geographical region consisting of mostly semi-arid plateau at are elevation of 300 to 730 meters (980 to 2,400 ft.). It include districts like Bidar (latitude 17.74º and longitude 77.31º), Bijapur (latitude 16.82º and longitude 75.71º), Belgaum (latitude 15.85º and longitude 74.50º), Dharwad (latitude 15.45º and longitude 75.00º) and Haveri (latitude 14.8º and longitude 75.40º) whereas Davangere (latitude 14.46º and longitude 75.92º), Shimoga (latitude 13.92º and longitude 75.56º), Chikkamangaluru (latitude 13.31º and longitude 75.77º), Udupi (latitude 13.34º and longitude 74.74º), Mangalore (latitude 12.91º and longitude 74.85º), Hassan (latitude 13.07º and longitude 76.17º) and Bengaluru (latitude 12.97º and longitude 77.59º) belong to Southern part of Karnataka.

From Kerala, tick samples were collected from all the three zones *viz*., Northern zone (Kasaragode- latitude 12.51º and longitude 74.98º, Kannur- latitude 11.87º and longitude 75.37º, Wayanad- latitude 11.68º and longitude 76.13º, Kozhikode- latitude 11.25º and longitude 75.78º and Malappuram- latitude 11.05º and longitude 76.07º), Central zone (Palakkad- latitude 10.78º and longitude 76.65º, Thrissur- latitude 10.52º and longitude 76.21º and Ernakulam- latitude 9.98º and longitude 76.29º) and Southern zone (Idukki- latitude 9.91º and longitude 77.10º, Alappuzha- latitude 9.49º and longitude 76.33º, Kollam- latitude 8.89º and longitude 76.61º and Thiruvananthapuram- latitude 8.52º and longitude 76.93º).

Tick collection and identification

A total of 157 and 122 cattle of Kerala and Karnataka respectively were screened for the presence of ticks. Adult (both male and female) ticks of cattle were collected from different regions of Kerala and Karnataka. Body of animals were searched for the presence of ticks by passing hands through the animal's coat and collected manually without damaging their mouthparts. Ticks were collected in a clean vial and wrapped with a muslin cloth. The sample bottles were labeled. The place and date of collection were noted. Ticks were stored at 4ºC until morphological identification was performed. For identification, the ticks were examined under stereo-zoom microscope (CZM4, Labomed) and compound binocular microscope (Leica, DM 1000 LED). The preserved ticks were processed as per standard protocol (Soulsby, 1982). Briefly, male ticks were boiled in 10 % potassium hydroxide (KOH) solution for 10 minutes, dehydrated using ascending grades of alcohol and then transferred into creosote for clearing. Morphological identification was performed based on diagnostic keys (Miranpuri and Gill, 1983; Walker, 2003; Geevarghese and Mishra, 2011: Estrada-Peña *et al*., 2012; Barker and Walker, 2014).

RESULTS

In the present investigation, a total of 279 cattle from different geographical locations of Kerala and Karnataka were screened for the infestation with hard ticks. Out of 279 animals, 185 were infested. Ticks were observed in all the body parts of cattle especially around the ears, tails, trunk and legs. Morphological identification of ticks from cattle revealed the presence of *Rhipicephalus (Boophilus) annulatus, R. (B.) microplus, R. haemaphysaloides, R. sanguineus. Haemaphysalis bispinosa, Amblyomma integrum* and *Dermacentor* spp. The most predominant tick species infesting cattle

from Kerala and Karnataka were *R. (B.) annulatus* and *R. (B.) microplus* respectively. The percentage occurrence of tick species of cattle in Kerala is shown in the fig. 1 and table 1. *Rhipicephalus (Boophilus) annulatus* was the predominant species (54.26 per cent) observed followed by *Haemaphysalis bispinosa* (25.58 per cent), *R. (B.) microplus* (12.40 per cent) and *R. haemaphysaloides* (5.42 per cent). Low prevalence rate (0.77 per cent) was observed with *R. sanguineus*, *Amblyomma integrum* and *Dermacentor* spp.The percentage occurrence of tick species of cattle in Karnataka is shown in the fig. 2 and table 2. The *R. (B.) microplus* was the most predominant species (77.10 per cent) followed by *H. bispinosa* (18.07 per cent) and *R. haemaphysaloides* (4.81 per cent). Multitick infestation was observed in six and one animals from Kerala and Karnataka respectively.

DISCUSSION

Ticks belonging to the genera *Rhipicephalus (Boophilus)* and *Hyalomma* are most widely distributed in India (Ghosh and Nagar, 2014). Cattle ticks of the subgenus *Rhipicephalus (Boophilus)* are major agricultural pests worldwide, causes billions of dollars in losses annually. *Rhipicephalus (B.) annulatus* and *R. (B.) microplus* are the most well-known and widespread species (Burger *et al*., 2014). In the present study, *R. (B.) annulatus* was the major tick species identified among cattle of Kerala followed by *H. bispinosa* and *R. (B.) microplus*. This result corroborates with previous reports of tick infestation from cattle in Northern Kerala (Shyma *et al*., 2013). Moreover, the present study revealed that *R. (B.) annulatus* and *H. bispinosa* were identified from all the zones of Kerala suggesting their wide distribution pattern.

Though prevalent in most of the Northern and Southern states of the country, *R. (B.) microplus* was not a common tick in Kerala. The common tick species affecting the cattle of Kerala were identified previously were *R. (B.) annulatus*, *R. (B). decoloratus*, *R. (B). microplus, Haemaphysalis bispinosa*, *H. turturis*, *H. intermedia*, *H. spinigera, H. aculeata*, *H. knobigera*, *Rhipicephalus sanguineus*, *R. haemaphysaloides*, *Hyalomma anatolicum*, *H. hussaini* and *Amblyomma integrum* (Rajamohanan, 1980; Prakasan and Ramani, 2007; Shyma *et al*., 2013). However, in the present study *R. (B.) microplus* could be identified from the household cattle of three districts of Kerala *viz*., Alappuzha, Thiruvananthapuram and Palakkad. Earlier, Prakasan and Ramani (2007) reported the occurrence of *R. (B.) microplus* ticks from cattle brought to cattle market in Northern Kerala. Since, majority of the cattle brought to this market are from other Southern states of the country, this report does not represent true *R. (B.) microplus* infestation status in Kerala.

Rhipicephalus (Boophilus) microplus was reported previously from the Northern districts of Kerala *viz*., Kannur, Kasaragod and Kozhikode (Shyma *et al*., 2013). Eventhough *R. (B.) microplus* could not be detected in cattle of Northern Kerala in the present study, this tick species was detected infesting cattle of Southern Kerala (Alappuzha and Thiruvananthapuram).The tick species reported from cattle in Karnataka were *R. (B). microplus* (Rajagopalan and Sreenivasan, 1981; Hiregoudar and Harlapur, 1988; Pradeep *et al*., 2012; Umashri *et al*., 2017), *R. (B.) annulatus* (Umashri *et al*., 2017), *R. haemaphysaloides* (Hiregoudar and Jagannath, 1977; Umashri *et al*., 2017; Manjunatha *et al*., 2017), *H. spinigera* (Bhat, 1989) and *Hyalomma* spp. (Umashri *et al*., 2017). *Rhipicephalus (Boophilus) microplus* was the predominant tick species reported from Karnataka (Hiregoudar and Harlapur. 1988).

CONCLUSION

Morphological identification of ticks from cattle of Kerala and Karnataka states of South India revealed the presence of *Rhipicephalus* (*Boophilus*) *annulatus*, *R*. (*B*.) *microplus*, *R. haemaphysaloides*, *R. sanguineus*, *Haemaphysalis bispinosa*, *Amblyomma integrum* and *Dermacentor* spp. The most predominant tick species infesting cattle of Kerala and Karnataka were *R. (B.) annulatus* and *R. (B.) microplus* respectively.

ACKNOWLEDGEMENTS

This work was supported financially by Indian Council of Agricultural Research (NASF/ABA-6015/2016-17) and Kerala Veterinary Animal Sciences University (Code Number: BT/40/81/MVP/2016/PR)

REFERENCES

1. Barker SC, Walker AR (2014) Ticks of Australia. The species that infest domestic animals and humans. Zootaxa 3816: 1-144
2. Bhat HR (1989) Tick Ecology in relation to Kyasanur Forest Diseases. Progress in Acarology. E.J Brill, Leiden, p 11-33
3. Burger T.D, Shao R, Barker SC (2014) Phylogenetic analysis of mitochondrial genome sequences indicates that the cattle tick, *Rhipicephalus* (*Boophilus*) *microplus*, contains a cryptic species. Mol Phylogenet Evol 76: 241–53
4. de Castro JJ (1997) Sustainable tick and tick-borne disease control in livestock improvement in developing countries. Vet Parasitol 71: 77–97
5. de La Fuente J, Estrada-Pena A, Venzal JM, Kocan KM, Sonenshine DE (2008) Ticks as vectors of pathogens that cause disease in humans and animals. Front Biosci 13: 6938-6946
6. Estrada-Peña A, Venzal JM, Nava S, Mangold A, Guglielmone AA, Labruna MB, De La Fuente J (2012) Reinstatement of *Rhipicephalus* (*Boophilus*) *australis* (Acari: Ixodidae) with redescription of the adult and larval stages. J Med Entomol 49: 794-802
7. Furman DP, Loomis EC (1984) The ticks of California (Acari: Ixodida). University of California Press, California
8. Geevarghese G, Mishra AC (2011) *Haemaphysalis* ticks of India. Elsevier, United States, p 268
9. Geevarghese G, Fernandes S, Kulkarni SM (1997) A check list of Indian ticks (Acari: Ixodoidea). *Indian J Anim Sci* 67: 566-574
10. Ghosh S, Azhahianambi P, Yadav MP (2007) Upcoming and future strategies of tick control: a review. J Vector Borne Dis 44: 79-89
11. Ghosh S, Nagar G (2014) Problem of ticks and tick-borne diseases in India with special emphasis on progress in tick control research: a review. J vector Borne Dis 51: 259-270
12. Hiregoudar LS, Harlapur S (1988) Ticks of Cattle and Buffalos in north Karnataka. Indian Vet J 65: 18-22
13. Hiregoudar LS, Jagannath MS (1977) Ticks of sheep in Challakere area of Chitradurga district of Karnataka State
14. Jongejan F, Uilenberg G (2004) The global importance of ticks. *Parasitology*. 129**:** S3-S14
15. Manjunatha L, Puttalakshmamma BL, Balaraju BL, Dhanalakshmi H, Veena, M (2017) Ecto-Parasite Infestation In Livestock: An Exploratory Study In Hassan, Karnataka. Int J Environ SciTechnol 6: 1438– 446
16. Minjauw B, McLeod A (2003) Tick-borne diseases and poverty: The impact of ticks and tick-borne diseases on the livelihood of small-scale and marginal livestock owners in India and eastern and Southern Africa. DFID Animal Health Programme, Centre for Tropical Veterinary Medicine, UK, pp 124
17. Miranpuri GS, Gill HS (1983) Ticks of India. Lindsay & Macleod, Edinburgh, p 63
18. Pradeep BS, Renukaprasad C, Souza PE (2012) Evaluation of the commonly used acaricides against different stages of the cattle tick *Boophilus microplus* by using different in vitro tests. Indian J Anim Res 46: 248 – 252
19. Prakasan K, Ramani N (2007) Tick parasites of domestic animals of Kerala, South India. AsianJ Anim Vet Adv 2: 74-80
20. Rajamohanan K (1980) Studies on the common ticks affecting livestock in Kerala. Dissertation, Kerala Agricultural University
21. Rajagopalan PK, Sreenivasan MA (1981) Ixodid ticks on cattle and buffaloes in the Kyasanur forest disease area of Karnataka state. Indian J Med Res
22. Rivera A, Marcelo B, Thiago F, Jorge E, Gabriel J, Paula A, Carlos A, Rodrigues B, Hector J, Maria I (2018) Contributions to the knowledge of hard ticks (Acari: Ixodidae) in Colombia. Ticks Tick Borne Dis 9: 57-66
23. Petney TN (1993) A preliminary study on the significance of ticks and tick-borne diseases in South-east Asia. Mitt Österr Ges Tropenmed Parasitol 15:33-42
24. Shyma KP, Stanley B, Ray DD, Ghosh S (2013) Prevalence of cattle and buffalo ticks in Northern Kerala. J Vet Parasitol 27: 55-56
25. Singh S, Chhabra MB (1992) Comparative acaricidal efficacy of coumaphos and fenvalerate against some common livestock ticks. Indian Vet J 16: 94
26. Soulsby EJL (1982) Helminths, arthropods and protozoa of domesticated animals, 7th edn. The English Language Book Society and Bailliere Tindall, London
27. Umashri, Swetha V Lingashetter, Kadadevaru GG (2017) Prevalence of Ixodid ticks from different domestic animals of north Karnataka. Int J Curr Res 9: 56333-56335
28. Walker AR (2003) Ticks of domestic animals in Africa: a guide to identification of species. Bioscience Reports, Edinburgh, p 3-210

Table 1: Rate of infestation of ticks in different districts of Kerala

District	Total no. of animals screened	Total no. of animals infected with each spp. of ticks	Total no. of animals infested	% of infestation	Total no. of multi tick infestation
Wayanad	65	*R. (B.) annulatus* : 35, *R. haemaphysaloides* :5, *H. bispinosa* : 16, *A. integrum* : 1	57	87.69 %	0
Kozhikode	8	*R. (B.) annulatus* : 4, *H. bispinosa* : 1	5	62.50 %	0
Kannur	6	*H. bispinosa* : 3, *R. sanguineus* : 2 *Dermacentor* spp. : 1	4	66.66 %	2
Malappuram	10	*R. (B.) annulatus* : 6	6	60.00 %	0
Kasaragod	8	*R. (B.) annulatus* : 4, *R. haemaphysaloides* :2	5	62.50 %	1
Ernakulam	9	*R. (B.) annulatus* : 3, *H. bispinosa* : 4	6	66.66 %	1
Kollam	3	*R. (B.) annulatus* : 1	1	33.33 %	0
Idukki	5	*R. (B.) microplus* : 1	1	20.00 %	0
Thrissur	20	*R. (B.) annulatus* : 12, *H. bispinosa* : 6	17	85.00 %	1
Palakkad	5	*R. (B.) microplus* : 2	2	40.00 %	0
Thiruvananthapuram	15	*R. (B.) microplus* : 9, *H. bispinosa* : 2	10	66.66 %	1
Alappuzha	3	*R. (B.) microplus* : 2	2	66.66 %	0
Total	**157**		**116**	**73.88 %**	**6**

Table 2: Rate of infestation of ticks in different districts of Karnataka

District	Total no. of animals screened	Total no. of animals infected with each spp. of ticks	Total no. of animals infested	% of infestation	Total no. of multi tick infestation
Chikkamagaluru	10	*R. (B.) microplus* : 8	8	80.00 %	0
Shimoga	15	*R. (B.) microplus* : 11	11	73.33 %	0
Belgaum	6	*R. (B.) microplus* : 3, *H. bispinosa* : 1	4	66.66 %	0
Bidar	20	*H.bispinosa* : 7, *R. heamophysoloides*: 3	9	45.00 %	1
Davangere	2	*R.(B.) microplus* : 1	1	50.00 %	0
Udupi	5	*R. (B.) microplus* : 3	3	60.00 %	0
Mangalore	4	*R. (B.) microplus* : 2	2	50.00 %	0
Hassan	11	*R. (B.) microplus* : 9	9	81.81 %	0
Haveri	13	*R. (B.) microplus* : 6, *H. bispinosa* : 2	8	61.53 %	0
Hubli	3	*R. (B.) microplus* : 1	1	33.33 %	0
Bengaluru	28	*R. (B.) microplus* : 21	21	70.00 %	0
Bijapur	5	*H. bispinosa* : 2	2	40.00 %	0
Total	**122**		**79**	**64.75 %**	**1**

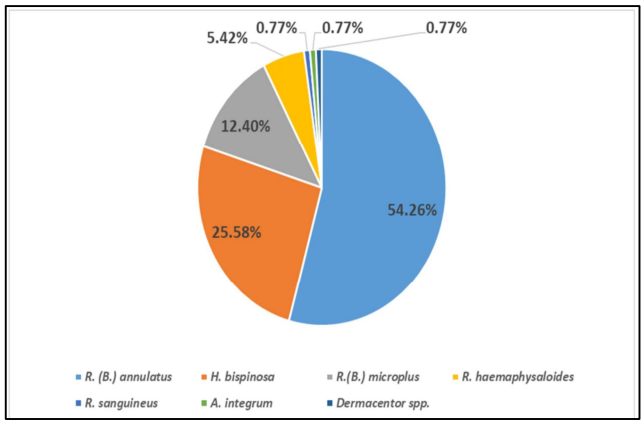

Fig .1. Prevalence of Ixodid ticks of cattle in Kerala

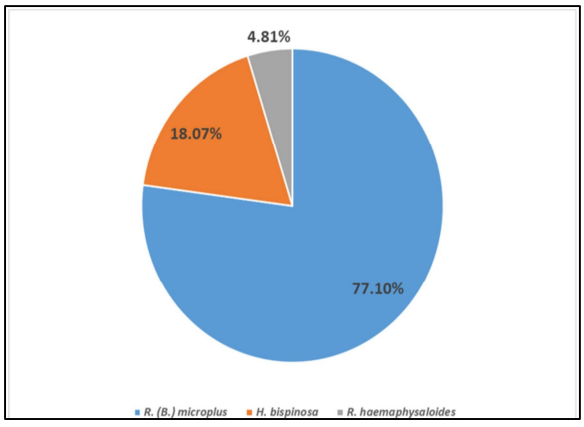

Fig .2. Prevalence of Ixodid ticks of cattle in Karnataka

Indian Journal of Natural Sciences www.tnsroindia.org.in ©IJONS

Vol.9 /Issue 51 / December / 2018 *International Bimonthly* *ISSN: 0976 – 0997*

RESEARCH ARTICLE

Formation Evaluation in Carbonate Reservoir using NMR Logging a Case Study from South Iraq

Ali Duair Jaafar Al-musawi[1]* and Medhat E. Nasser[2]

[1]Department of Geology, Petroleum Geology, College of Science, University of Baghdad, Al-jadreea, Baghdad, Iraq.
[2]Department of Geology, College of Science, University of Baghdad, Baghdad, Iraq.

Received: 23 Aug 2018 Revised: 25 Sep 2018 Accepted: 28 Oct 2018

***Address for Correspondence**
Ali Duair Jaafar Al-musawi
Department of Geology,
Petroleum Geology,
College of Science,
University of Baghdad,
Al-jadreea, Baghdad, Iraq.
E-mail: ali72.jafar@gmail.com

ABSTRACT

Formation evaluation from conventional wireline logs is difficult because of the complex lithology (mixture of calcite and dolomite) and the rock texture (very low primary porosity, closed and open fractures, complex breccia texture and presence of vugs).Conventional porosity and resistivity logs provide engineers in first look at the reservoir, but there are practical limits to the accuracy. Neutron, density, and sonic porosities are more sensitive to lithology than to reservoir fluids. As a result, even small amounts of clay minerals may cause errors inporosity measurements. In addition, reservoirs commonly contain clayboundwater, capillary-bound water, and moveable water.This response characteristic makes a Nuclear Magnetic Resonance (NMR) tool fundamentally different from conventional logging tools. The method consists of combining NMR and conventional wireline logs for two wells of field (x) of south Iraq to estimate of porosity and permeability. Additional combinations with conventional logs can be formed with NMR diffusion measurements to infer movable and capillary-bound water volumes.This research presents two cases of reservoir evaluation by new techniques in TechlogSchlumberger software where conventional logs used to determine the petrophysical properties once and evaluationdone by nuclear magnetic resonance (NMR) in another time. The results are encouraging as these correlations should be applicable to newly drilled wells in similar geological facies in this region where there is no core control.

Keywords: Nuclear Magnetic Resonance (NMR), Porosity Distrbution, petrophysical properties.

INTRODUCTION

Open hole analysis is one of the greatest valued and significant tools obtainable to petroleum geologist. Logging aids describe physical characteristics of rocks for example, porosity, lithology, permeability and pore geometry. Logging data are utilized to detect pay zone to fix thickness and depth of intervals, to distinct amongst gas, oil or water in reservoir and to estimate oil reserve [1]. ButFormation evaluation from standard wireline tools is problematic due to the complex lithology (combination of dolomite and calcite) and the rock texture (very low primary porosity, filled and open fracture, occurrence of vugs and complex breccia texture). An attempt is made to improve the formation evaluation ofMishrif reservoir of oil field (x) in the south of Iraq by integration of the standard open hole logs (GR, Density, Caliper, Neutron, Sonic and Resistivity), core analysis and nuclear magnetic resource (NMR). NMR Logging helps to accurately determine petrophysical properties of reservoir rocks and also regard very cost efficient tool. through the analysis of NMR data, many phases of NMR technique have been used; 1) fluid identification by T1/T2 ratio, 2) determine the types of clay minerals by the difference between NMR derived porosity and total porosity, 3) identify fluids nature and rock properties fromNMR relaxation properties.In order to determine lithology independent porosity and to distinguish between bound and freewater,Analysis of NMR data of low resistivity reservoirs has helped toidentify the productivity of these zones. For the state of low contrast resistivity reservoir where there was littleresistivity contrast between water bearing formation and oil bearing formation,NMR has been able to identify the fluid nature and theheight of the oil column. This was based mainly on high contrast of NMR relaxationparameters.

Formation Evaluation by Conventional Logs

Resistivity, density, gamma ray and neutron logs can be using to calculate and interpretPorosity, permeability, fluids saturation, reservoir lithology, original fluid contacts and other reservoir parameters [2].Porosity and fluid saturation are among the most important reservoir properties used in the reserve estimation of oil and gas. Because of the heterogeneity of most reservoirs, continuous recording of these properties vs. depth is essential for accurate evaluations [3]. Since a complete coring and core analysis of the entire pay zone is impractical, well logging appears to be the most plausible mean to obtain such information. To achieve this task, different logs including resistivity, acoustic and radioactive logs are recorded in the well and well log interpretation is used to obtain the required properties

Relationship between Permeability and Porosity

There is no specific correlation between permeability and porosity values. In many cases the relationship between permeability and porosity is qualitative and is not directly or indirectly quantitative in any way. It is possible to have very high porosity without having any permeability at all, as in the case of pumice stone (where the effective porosity is nearly zero), clays and shales. The reverse of high permeability with a low porosity might also be true, such as in microfractured carbonates. In spite of this fundamental lack of correspondence between twoproperties, there often can be found a useful correlation between them within one formation [4].
The formation analysis results for the well are given in Figures (1) to (3), in the bulk volume analysis track. These figures, which represent Computer Processed Interpretation (CPI), depict as composite the followings:

1. Porosity analysis track, which is divided into effective porosity (phie),water filled porosity in the invaded zone ($B_{VWXO} = phie * S_{XO}$), and water filled porosity in the un-invaded zone ($B_{VW} = phie * S_W$).

- The area between (phie) and (B_{VWXO}) represents the residual hydrocarbon.
- The area between(B_{VWXO}) and (B_{VW}) represents the movable hydrocarbon.
- The area between (phie) and (phieS_W) represents the total hydrocarbon.

2. Bulk volume analysis is divided in to effective porosity (phie), percentage of shale (V_{shale}), and percentage of non-shale matrix (V_{matrix}).

Nmr Porosity

Thedensity/neutron porosity is influenced by both fluids and surrounding rocksunlike NMR porosity which depends only on the fluids content of the formation that factmakes NMR measurements much more capable than conventional logs to furnish clay-corrected porosity, non-productive and productive porosity. The strength of the NMR signal is proportional to the number of hydrogen atoms in NMR tool dependent rock volume. In zones containing light hydrocarbon, where the hydrogen index is less than unity, NMR porosity will typically underestimate true porosity in proportion to the hydrogen index [5].

Porosity Distrbution

In general, the decay covers the sum of relaxation contributions from clay bound water, capillary bound water (irreducible water), free movable water, and diffusion if gas is present and can describe it as a sum of exponential terms with different relaxation time and magnitude. The processing extracts a distribution of (Echo Data Inversion) from the decay curve. So called cutoffs separate the regions. on the basis of T1 and/or T2, porosity and pore size (BVM, BVI). The regions between CBW, BVI, and BVM are separated by "cutoffs," which depend on the specific internal surface and the surface relaxation as shown in figure 1. Recommended values are[6]: Cutoff CBW/BVI: 3 ms (1_5 ms, depends on clay minerals). Cutoff BVI/BVM: for faster decaying clastics about 33 ms, for slower decaying carbonates about 100 ms. In fact, the NMR measurements allow the separation between the different components of the porosity:

a. total porosity (CBW + BVI + BVM).
b. clay-bound water (CBW),
c. capillary bound water (volume of irreducible (BVI))
d. free fluid volume (free movable fluids (FFV or BVM))
e. effective porosity, $\phi e = (BVI + BVM)$.

BVI versus BVM: where The BVI (bulk volume irreducible fluid) and BVM (bulk volume of movable fluid). The observed T2 decay is the sum of T2 signals from independently relaxing protons under different conditions in the pores:

- Shortest T2 typically is related to clay bound water.
- Medium T2 is related to capillary bound water.
- Long T2 is related to free movable, producible fluids.

For porosity partitioning, processed NMR T2 distribution and VISO from formation micro imager (FMI) have been used. The macro porosity FFI from NMR was compared with the VISO from FMI. T2 short cutoff which defines the boundary between micro and meso-porosity is used 100 ms. Whereas, T2 long cutoff which defines boundary for meso and macro porosity was set to 630 ms(based on VISO and T2 distribution). This gave us a good match between the NMR derived macro porosity and FMI derived VISO. The macro porosity was then taken as mean of the VISO from FMI and macro porosity from NMR. MICP data of SCAL analysis is required and will help to calibrate T2 short and T2 long cutoff [7]. the applicationsof NMR supported information about:

1) Information about the main components
   - Clay-bound water CBW (and shale content);

- Irreducible water BVI; BVI represents the specific surface of pores; a low BVI is typical for large pores and high permeability;
- Bulk volume moveable BVM represents the volume of free moveable fluids.

2) The numerical interpretation delivers
   - The effective porosity by integration over BVI and BVM
   - A permeability measure: The ratio BVI/BVM is a measure for the specific internal surface. "Coates equation" gives a permeability estimate.

NMR Permeability

Permeability can be calculated from the T**2**distribution data using one of two commonly accepted mathematical models: the free-fluid or Coates model (Equation-1) can be applied in formations containing water and/or hydrocarbons, while the average-T**2**or Schlumberger model (Equation -2) can be applied to pore systems containing only water and gas. In either case, measurements on core samples are necessary to refine these modelsby determining the correct values of the coefficients, and produce a model customized for local use [7].The NMR estimate of permeability is based on a combination of experimental and theoretical models and relationships. When all other factors are kept constant in these models and relationships, permeability increases as connected porosity increases. The unit of permeability, the Darcy, has dimensions of area, and from practical considerations in petrophysical applications, permeability can be considered as being proportional to the square of some geometrical size. The correlation between capillary pressure curves and permeability strongly support that the pertinent size is that of the pore throat [8].

NMR measures pore body size, but in almost all sandstones and some carbonates, a strong correlation exists between pore body size and pore throat size. The two most commonly used expressions for permeability both vary as ϕ. This power of ϕ is somewhat arbitrary but is loosely derived from Archie's Law, the relationship of permeability to resistivity, and with an additional factor to account for NMR measuring pore body size not pore throat size. In one expression, the Free Fluid (or Coates) model, the size parameter enters implicitly through *T*2cutoff, which determines the ratio of *FFI* to *BVI*, where *FFI* is the free fluid volume and *FFI* = ϕ - *BVI*. In the other expression, the Mean *T*2 or the Schlumberger-Doll Research (SDR) equation model, the size parameter enters through the geometrical mean of the relaxation spectra, *T*2*gm*. The use of these particular size parameters in the respective expressions is based on empirical considerations. Other size measures have also been used. Both models correlate very well to permeability from laboratory data on 100% brine saturated samples. The Mean *T*2 model, however, fails when the pore contains hydrocarbons because then *T*2*gm* is not controlled exclusively by pore size.

The Free Fluid Model

In the Free Fluid (or Coates) model in its simplest form the permeability *k* is given by

$$K_{TIM} = a \times 10000 \times \varphi^b \left[\frac{FFV}{BFV}\right]^c$$ ----------equ.1

FFV = Free fluid volume
BFV = Bound fluid volume
Φ= NMR Porosity (p.u.)
a, b, c = Coefficients that should be tuned for each formation.
The parameters for Timor-Coates permeability in the processing are a=1, b=2, c=4.

The Mean T2 Model

The Mean *T*2 (or SDR) model is given by

$K_{SDR} = a \times \emptyset^b T2LM^c$---------- equ.2

where *T*2*LM* is the geometric mean of the *T*2 distribution
a, b, c = Coefficients that should be tuned for each formation.
Coefficients used for the processing are a=4, b=4, c=2.

RESULTS AND DISCUSSION

The procedures of final interpretation mainly include effective reservoir discrimination, fluid type determination and oil and gas bearing zone identification**.** The complete interval is processed using Techlog 2015.2 the results obtained are summarized in the following Table (1) and figures of (1-3) based on data processed and interpretation by conventional logs, table (2) and figures (4-5) based on Nuclear magnetic resonance (NMR) where:

CMR: Combined magnetic resonance is the same (NMR)

MRP: CMR Effective porosity

BVF: bond fluid volume.

FFV: Free fluid volume.

KSDR: permeability from Schlumberger equation.

KTIM: permeability from Timur equation.

CONCLUSIONS

The following conclusions can be drawn based on the above CMR (NMR) analysis:

1. Borehole condition is generally good and hence not affecting very much the NMR measurement. The measurement is only affected in a few intervals where the hole is rugose or washed out and under this condition, the NMR data cannot be used.
2. The porosity ranges of the entire acquire data intervals are moderate to high, ranging at 19.9-20.5 p.u.in the carbonate formations.
3. The pore sizes are mainly filled with free fluid in more porous zones and capillary/bound fluid in medium porosity zones.
4. Porosity measurement from NMR in shale zones are more accurate when compared to density and neutron as NMR is only sensitive to the hydrogen content in the pore space and is not affected by varying grain density.
5. NMR provides reasonable estimate of free and bound water in most of the zones using a default T2 cutoff of 100 ms for carbonates and 33ms for clastics.

REFRENCES

1. Asquith, G., and Krygowski, D., 2004, Basic Well Log Analysis, 2nd.ed. Sections by Steven Henderson and Neil Hurleg. The American Association of Petroleum Geologist, Tulsa, Oklahoma. AAPG. Methods in Exploration series No.16, 244p.
2. Bandar D. Al-Anzi, The Role of the Modem Petrophysicist, CWLS magazine, Canadian Well Logging Society, Canada, 2006.

3. Asquith, G., and Gibson, C. "Basic Well Log Analysis for Geologists", Methods in Exploration Series, AAPG, 1982.
4. Elena Pasternak, "Porosity–permeability relationship", Allan Hancock College, 2009.
5. Akkurt, R., et al., 1995, NMR logging of natural gas reservoirs, paper N, 36th AnnualSPWLA Logging Symposium Transactions, 12 p. Also published in 1996 in The Log Analyst, v. 37, no. 5, p. 33–42.
6. Chen, S., and Georgi, D.T., 1997, Improving the accuracy of NMR relaxation distributionanalysis in clay-rich reservoirs and core samples, SCA 9702, in 1997 internationalsymposium proceedings: Society of Professional Well Log Analysts, Society of CoreAnalysts Chapter-at-Large, 10 p.
7. George R. Coates, Lizhi Xiao, and Manfred G. Prammer "NMR Logging Principles and applications" Halliburton Energy Services Houston,1999.
8. Kenyon, W.E., 1992, Nuclear magnetic resonance as a petrophysical measurement,Nuclear Geophysics, v. 6, no. 2, p. 153-171. Later revised and published in 1997 underthe title, Petrophysical principles of applications of NMR logging, in The Log Analyst,v. 38, no. 2, p. 21–43.

Table 1. shows the results obtained by conventional logging of well 1. For interval (2862-2876)

Zones	Top	Bottom	Gross	Net	Net to Gross	BVW	Shale Volume	Porosity	Water Saturation
MA2	2862.35	2876.02	13.67	11.05	0.81	0.18	0.044	0.14	0.12
MB1_1	2876.02	2888.49	12.47	2.05	0.17	0.02	0.22	0.12	0.09
MB1_2A	2888.49	2925.51	37.02	22.75	0.61	0.37	0.183	0.12	0.14
MB1_2B	2925.51	2957.01	31.50	22.97	0.73	0.45	0.219	0.13	0.15
MB1_2C	2957.01	2992.20	35.19	26.81	0.76	0.82	0.228	0.15	0.21
MB2_1	2992.20	3006.10	13.90	6.27	0.45	0.20	0.121	0.13	0.26
MB2_2	3006.10	3022.54	16.44	13.10	0.80	0.49	0.052	0.17	0.23
MB2_3	3022.54	3040.56	18.02	18.02	1.00	1.41	0.044	0.25	0.32
MC1_1	3040.56	3064.74	24.18	18.39	0.76	1.85	0.232	0.23	0.43
MC1_2	3064.74	3082.76	18.02	13.91	0.77	1.27	0.225	0.15	0.62
MC1_3	3082.76	3103.57	20.81	7.61	0.37	0.76	0.26	0.15	0.65
MC1_4	3103.57	3125.28	21.71	13.88	0.64	1.54	0.214	0.19	0.60
MC2_1	3125.28	3139.83	14.55	1.82	0.13	0.16	0.07	0.15	0.59
MC2_2	3139.83	3153.26	13.43	4.37	0.33	0.33	0.175	0.13	0.56
MC2_3	3153.26	3218.74	65.48	54.51	0.83	6.84	0.18	0.19	0.65
MC3_1	3218.74	3224.56	5.82	2.54	0.44	0.23	0.247	0.15	0.59
MC3_2	3224.56	3252.54	27.98	18.90	0.68	2.26	0.185	0.21	0.57

Table 2 the results obtained by NMR logging of well 2. For interval (3025-3030)

Depth(m)	BFV_CMR	FFV_CMR	KSDR_CMR	KTIM_CMR	MRP_CMR
3025	0.10	0.12	2.30	39.03	0.23
3025.25	0.11	0.13	2.31	55.43	0.24
3025.5	0.11	0.13	2.05	47.63	0.24
3025.75	0.10	0.10	2.06	22.81	0.21
3026	0.10	0.09	1.55	14.13	0.20
3026.25	0.13	0.10	1.16	16.97	0.23
3026.5	0.16	0.10	1.00	22.42	0.27
3026.75	0.18	0.10	0.90	26.86	0.29
3027	0.18	0.11	0.67	28.35	0.30

3027.25	0.16	0.11	0.75	26.59	0.27
3027.5	0.13	0.11	1.72	32.67	0.24
3027.75	0.10	0.13	3.22	57.85	0.24
3028	0.08	0.14	4.41	87.17	0.23
3028.25	0.08	0.14	4.08	81.14	0.23
3028.5	0.10	0.14	2.48	65.01	0.24
3028.75	0.10	0.13	2.28	58.52	0.23
3029	0.09	0.13	3.12	66.51	0.23
3029.25	0.08	0.14	3.83	71.41	0.22
3029.5	0.09	0.14	3.94	76.32	0.23
3029.75	0.11	0.14	2.67	64.84	0.25
3030	0.12	0.14	1.92	63.01	0.26

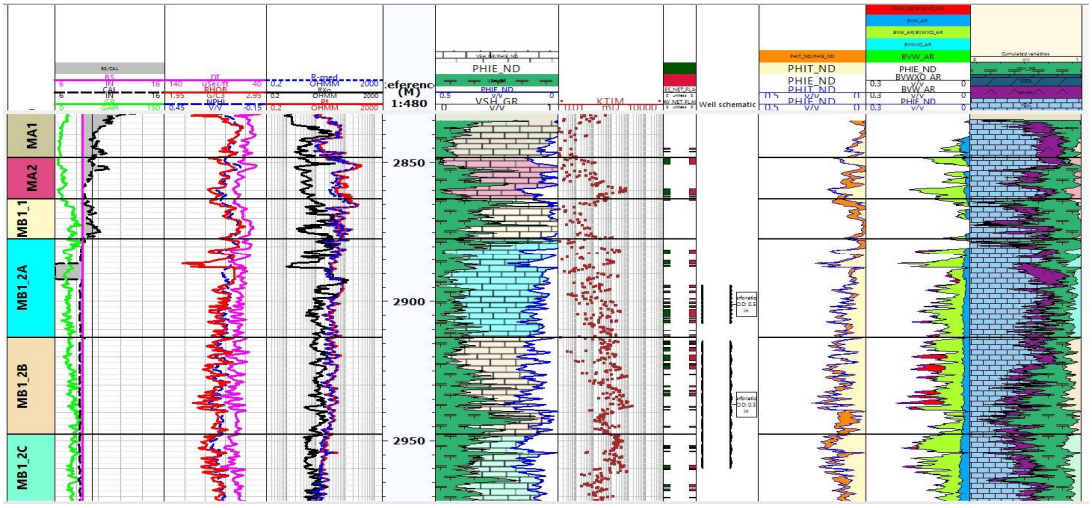

Figure 1 shows the computer process interpretation (CPI) by conventional logs of well-1 for interval (2845-2955m)

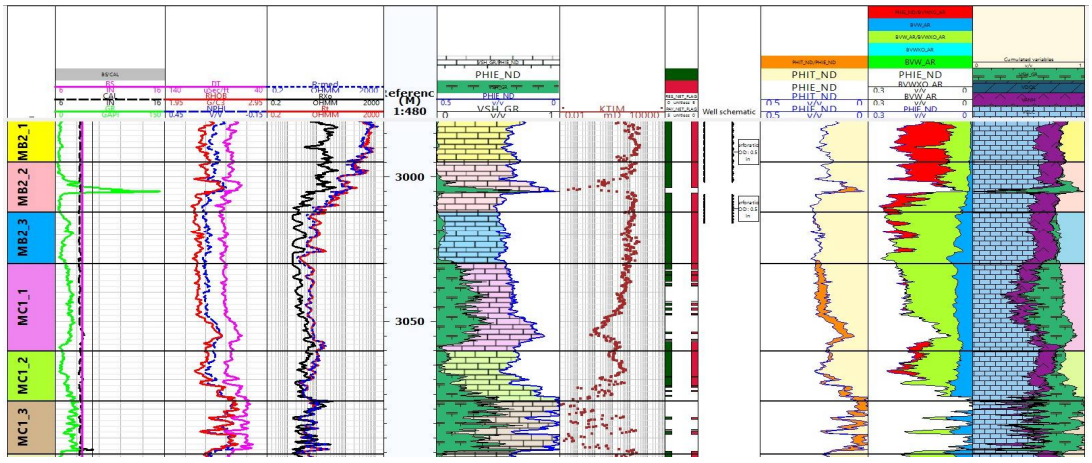

Figure 2 shows the computer process interpretation (CPI) by conventional logs of well -1 for interval (2955-3100m).

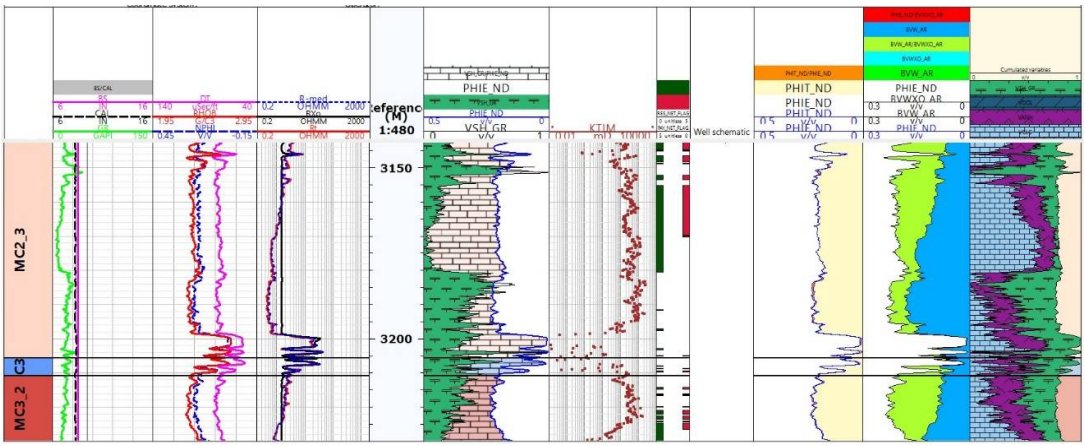

Figure 3 shows the computer process interpretation (CPI) by conventional logs of well -1 for interval (3150-3225m).

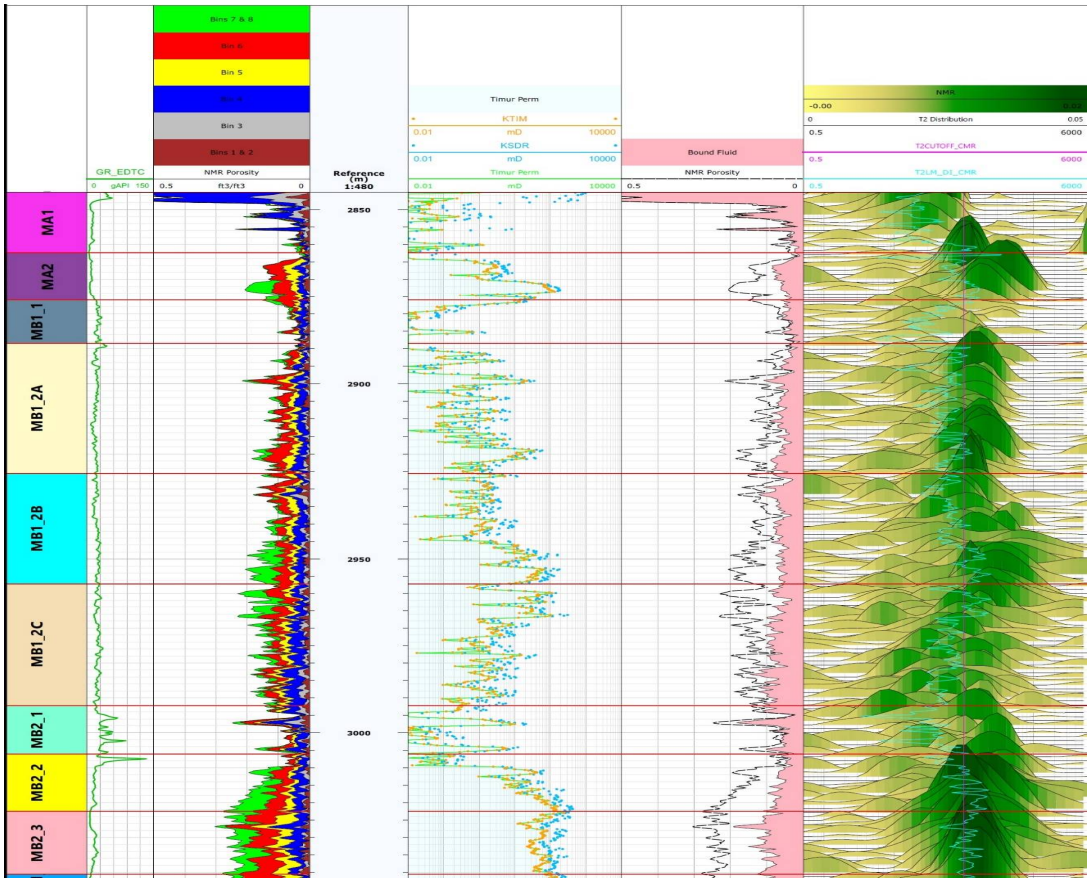

Figure 4. shows the computer process interpretation (CPI) by NMR log of well -2 for interval (2850-3050m).

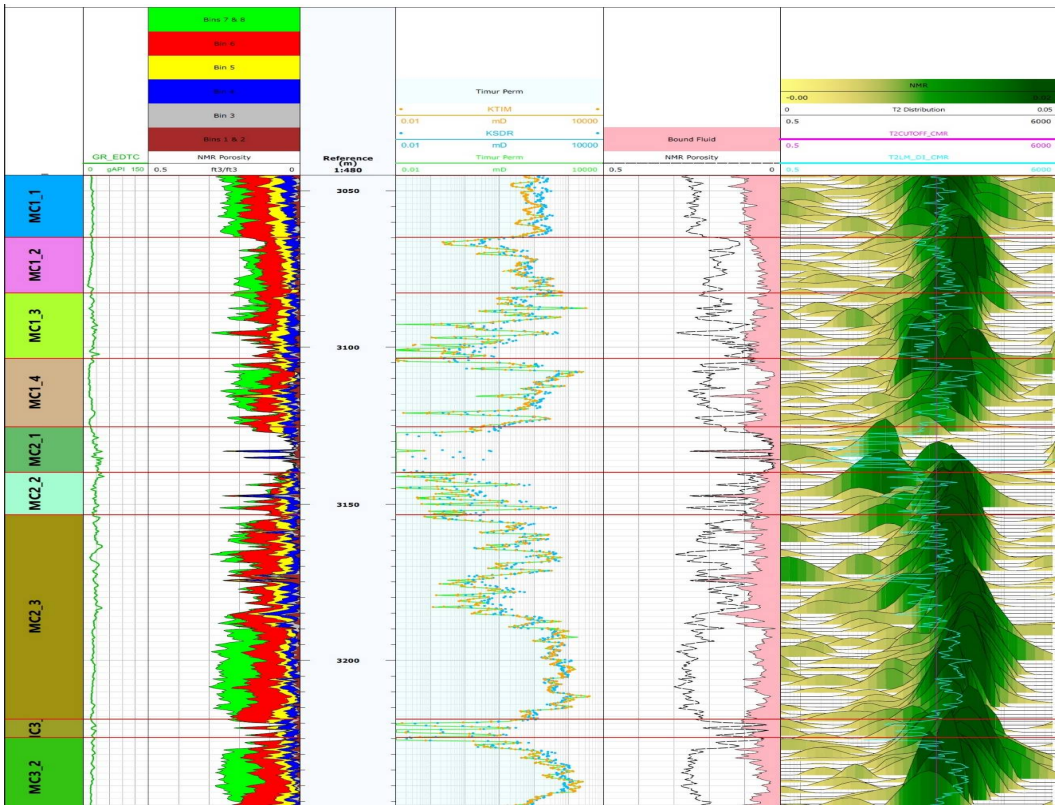

Figure 5. shows the computer process interpretation (CPI) by NMR log of well -2 for interval (3050-3250m).

Indian Journal of Natural Sciences www.tnsroindia.org.in ©IJONS

Vol.9 /Issue 51 / December / 2018 *International Bimonthly* *ISSN: 0976 – 0997*

RESEARCH ARTICLE

Using Multispectral Analysis to Determine the Vegetation Indices and Land Surface Temperature for Baghdad City

Ebtesam F.Khanger

Department of Astronomy and Space, College of Science, University of Baghdad, Iraq.

Received: 20 Aug 2018 Revised: 26 Sep 2018 Accepted: 28 Oct 2018

***Address for Correspondence**
Ebtesam F.Khanger
Department of Astronomy and Space,
College of Science,
University of Baghdad, Iraq.

ABSTRACT

Land surface temperature (LST) is a significant parameter in examining natural, environmental procedures and environmental change at different scales, and is likewise important in the investigations of evapotranspiration, soil dampness conditions, surface vitality adjust, and urban warmth islands. In this research, LST of the city of Baghdad was measured using the band 10 of Landsat 8 satellite for the study area. The land surface temperature was extracted using the transformational equations of the ground radiation values and the temperature of the satellite using the K1 and K2 values from the metadata.The examination demonstrated the significance of utilizing Landsat 8 pictures and the outcomes got indicated generally high contrasts between the locales of the investigation territory, particularly between zones with low vegetation cover and agrarian regions with thick vegetation cover. This is because of the impact of the surface of the Earth (strong) sun oriented radiation more than the air (gas substance).

Keywords: Land Surface Temperature (LST), Land Surface Emissivity (LSE), Normalized Difference Vegetation Index (NDVI), Operational Line Imager (OLI), Thermal Infrared Sensor (TIRS),

INTRODUCTION

The significance of land surface temperature (LST) recovered from high to medium spatial determination remote detecting information for some, natural examinations, especially the applications identified with water assets administration over agrarian destinations, was a key factor for an official choice of including a warm infrared (TIR) instrument on board the Landsat Data Continuity Mission or Landsat-8. This new TIR sensor (TIRS) incorporates two TIR groups in the environmental window in the vicinity of 10 and 12 μm. LST is a standout amongst the most critical factors estimated by satellite remote detecting. Open space information are accessible from the recently operational

Landsat-8 (LST) is identified with surface vitality and water adjust, at neighborhood through worldwide scales, with foremost criticalness for a wide assortment of uses, for example, environmental change, urban atmosphere, the hydrological cycle, and vegetation check in [1] .The temperature emissivity detachment (TES) calculation depends on an exact connection between phantom difference and least emissivity, decided from research center and field emissivity spectra. It is utilized to even out the quantity of obscure parameters and the quantity of estimations with the goal that the arrangement of Planck's conditions for the deliberate warm radiances can be modified. Surface temperatures are free of wavelength and can be recouped from even a solitary band of brilliance information gave environmental qualities can be indicated and surface emissivity is known. Be that as it may, emissivity of land surfaces isn't known from the earlier (aside from water bodies) however ought to be evaluated alongside the temperature. In addition, emissivity esteems shift with wavelength [2].OLI gathers information at a 30-m spatial determination with eight groups situated in the unmistakable and close infrared and in the shortwave infrared districts of the electromagnetic range, in addition to an extra panchromatic band at 15-m spatial determination. TIRS [(3]

Data and techniques used in research

1- Recent Satellite image from US Geological Survey site (USGS) for Landsat 8 with sensor (TIRS) to Baghdad city at date 19/5/2017
2- Iraq map in vector format
3- Arcgis10.2 program

RESEARCH METHODS

The following flow chart illustrate the method of research
The wavelength run for infrared district discovered roughly between 0.70 to 100 µm, which is hundred times more extensive than the unmistakable part. Infrared is subdivided mostly in to two sections in view of its radiation properties: -

- ➢ Reflected infrared
- ➢ Emitted or Thermal infrared

Radiation in the reflected infrared area is utilized for remote detecting purposes in a route like radiation in the obvious segment and this spreads from 0.70 to 3.0 µm while the warm infrared district is not the same as the unmistakable and reflected locale, as this vitality is basic to the radiation that is transmitted from the earth surfaces as warmth and this extents covers between 3.0 to 100µm [4].

Conversions of radiance to Kelvin temperature

In the wake of acquiring the brilliance esteems from the computerized pictures components, figuring temperature , turn out to be simple by applying the opposite of the Plank work as indicated by the accompanying numerical recipe [5,6]

$$T = \frac{K_2}{\ln\left(\frac{K_1}{L_\lambda} + 1\right)}$$

where
T :is degrees Kelvin
K1 : watts/(meter squared * ster * µm), K2: Kelvin

Normalized Difference Vegetation Index (NDVI)

There are various vegetation records created to evaluate vegetation cover with the remotely detected symbolism. A vegetation record is a number that is produced by some blend of remote detecting groups. The most widely recognized otherworldly record used to assess vegetation cover is the Normalized Difference Vegetation Index (NDVI). The fundamental arithmetical structure of an otherworldly file takes for type of a proportion between two ghastly groups Red and close infrared (NIR). This file is computed by subtracting Red reflectance from NIR reflectance, and isolating by the whole of the two. For example, in vegetation territories, the NIR part of the range is reflected by leaf tissue, and the sensor records the reflectance [7]. The NDVI is the most common and known vegetation index and has been computed as:

- **NDVI =** NIR – R/ NIR + R

Estimation of Emissivity

Surface emissivity is an important parameter for estimating long wave radiative budget.[5]

- Assumes pixel dominant land cover is known
- Pixel emissivity can be estimated

Land Surface temperature (LST) estimation

To get the estimation of the Earth surface temperature (LST), pictures were gotten from the Landsat-8 satellite OLI/TIRS sensor in the (19/5/2017) and the dry season, to appraise the dirt surface temperature (LST). Of the US Geological Survey (USGS), where they were dealt with in ArcGIS 10.2.2 and the aftereffect of the groups 10 got by methods for equation (1):

LST= T/1+W*(T/p)*In(e)) ---------- (1)

Where:
T= A satellite temperature;
W=Wavelength of emitted radiance (11.5μm);
p = h*C/S (1.438*10^{-2}m.k).
h = Planck's Constant (6.626*10^{-34} J.s)
s = Boltzmann Constant (1.38*10^{-23}J/K)
C = Velocity of light (2.998 *10^{8} m/s)
Therefore **p = 14380**

Keeping in mind the end goal to utilize the last TST condition, it is important to get alternate parameters which are procured from the accompanying conditions, where it is important to evaluate the satellite brilliance temperature by implies of equation (2):

T = K2/In (K1/ Lλ+1) – 273.15 ----------.(2)

Where
- **T**= Satellite brightness temperature in Kelvin (K).
- **Lλ** = spectral radiance (watts/(m2*ster* μm)).

• **K1** = Band Specific thermal conversion from the metadata (K1 – constant _Band _X, where X is the band number, 10).
• **K2** = Band Specific thermal conversion from the metadata (K2 – constant _ Band _X, where X is the band number, 10).
• **- 273.15** = Conversion of Kelvin to degrees Celsius;

However, to calculate T, it is necessary to perform the conversion of the digital number values of each pixel to spectral radiance, which is given by equation (3):[8,9]

$L\lambda = ML*Q\ cal. + AL$ --------- (3)

Where:
• $L\lambda$ = spectral radiance (watts/(m2*ster*μm));
• **ML** = Band Specific multiplicative rescaling factor from the meta (RADIANCE _MULT_BAND_X, Where X is the band number 10);
• AL = Band specific additive rescaling factor from the metadata (RADIANCE_ADD_BAND_X, Where X is the band number 10);
• **Q cal**.= Quantized and calibrated standard product pixel values (DN);

Finally, to find the value "e" (the last component of the TST equation), which refers to the emissivity of the land surface cover

e = 0.004 * PV + 0.986 --------- (4)

Where:
• **e** = land surface emissivity from NDVI.
• **PV** = Proportion of vegetation, obtained by the following eq.(5) .

$PV = (NDVI - NDVI_{min} / NDVI_{max} – NDVI_{min})^2$ --------- (5)

Where:
NDVI =Normalized Difference Vegetation Index, obtained by equation 6
$NDVI_{min}$ = minimum value do NDVI
$NDVI_{max}$ = maximum value do NDVI

Being:

NDVI = NIR – R/ NIR + R ---------- (6)

Where:
NIR=near infrared wavelength, referring to the spectral band 5
R= wavelength of red , referring to the spectral band 4[10]

RESULTS

The practical part will include finding a map of the land surface temperature (LST) for study area by finding the required parameters mentioned previously in the research. All previous equations were applied using the

ArcMap10.2 program and use option of raster calculator For each equation separately. They are on several steps as described in the next steps.

1. Using Iraq map in vector format to extracting Baghdad map
2. Landsat image for band 4 to study area and surrounding
3. Landsat image for band 5 to study area and surrounding
4. Extraction Landsat image for band 10 to study area by projection Iraq map in vector format on Landsat image for band 10 for study area and surrounding areas then using ArcGIS program to extraction
5. Extraction Normalized DifferenceVegetation Index (NDVI) for study area by using band 4 and 5
6. Finding radiance map for study area from band 10 by using Previous Equations
7. Finding atmospheric temperature for study area for band 10 by using previous equations
8. Extraction map of emissivity to study area for band 10 by using previous equations
9. Finding Proportion of vegetation (PV) to study area from band 10 by using previous equations
10. Finally finding the land surface temperature (LST) map to study area form band 10 by using equation 1 the previous figure of the land surface temperature map. We show the following in table (1)

CONCLUSIONS

1. Identification of elements influencing the land surface temperature is essential. Since the temperature of urban areas was higher than the farmland and this wonders is because of an expansion in arrive surface temperature and along these lines making urban warmth islands are happened.The main cause of increase in urban land surface temperature is change in the structure of the Earth's surface or the so-called change of land use/land cover in these areas.
2. Temperature incensement in long haul makes a ton of harm the urban condition and its occupants also.By identifying effective land use at land surface temperature, the spatial autocorrelation and spatial non stationary to resolve the issue.
3. In this investigation, the absence of vegetation cover had the best effect in expanding the temperature of the earth surface and this is seen in the regions of south-west Baghdad (regions of the edges of Baghdad) and additionally the northeastern districts.
4. The outcomes demonstrated that the mechanical and military businesses, transport and streets significantly affect the temperature of the surface of the earth. This is obvious in the focal zones of Baghdad (the downtown area), where there was a high temperature contrasted with the zones encompassing the Tigris due to its over the top utilization of land (local locations).

REFERENCES

1. Offer Rozenstein , Derivation of Land Surface Temperature for Landsat-8 TIRS Using a Split Window Algorithm Sensors 2014, 14, 5768-5780; doi:10.3390/s140405768
2. Janisson B. de Jesus*, Ighor D. M. Santana ,Estimation of land surface temperature in caatinga area using Landsat 8 data , Available on line at Directory of Open Access Journals , Journal of Hyper spectral Remote Sensing v.7, n.3 (2017) 150-157, www.periodicos.ufpe.br/revistas/jhrs.
3. Michael TsehayeWubet , estimation of absolute surface temperature by satellite remount sensing .), March 2003, international instate for geo-information science and earth observation Enscheda, the Netherlands.
4. Nawal K. Ghazal, Khalid I. Hassoon , .2012 temperature calculation using thermal bands of (ETM+) sensor , Iraqi Journal of Science. Vol. 53.No 2..Pp 435-443
5. AbduwasitGhulam, PhD , 2014 Calculating surface temperature using Landsat thermal imagery, Department of Earth & Atmospheric Sciences, and Center for Environmental Sciences, Saint Louis University ,St. Louis, MO 63103.

6. JesúsA.Prieto-Amparan,Atmospheric 2018correction for satellite remotely sensed data intended for agricultural applications: impact on vegetation indices, Remote Sens.2018, 10,21doi: 10.3390 /rs 10020219, www.mdpi.com/journal/remotesensing.
7. D.W.Wong[a] and M.Sun[a],**2013**,"Handling Data Quality Information of Survey Data in GIS:A Case of Using the American Community Survey Data",[a]George Mason University, **Corresponding Author**: David Wong, Geography and GeoInformation Science, George Mason University, Fairfax, VA 22030 E-mail: dwong2@gmu.edu, Spatial Demography.
8. GiacomoCapizzi, Grazia Lo Sciuto, Marcin Wozniak, RobertasDamasevicius. 2016A Clustering Based System for Automated Oil Spill Detection by SatelliteRemote Sensing, ICAISC (2): 613-623.
9. Schowengerdt, Robert A. 2007. Remote sensing:models and methods for image processing (3rd ed.). Academic Press. p. 2. ISBN 978-0-12-369407-2.
10. Šarić, M., Dujmić, H., & Russo, M. 2013. Scene TextExtraction in HSI Color Space using K meansAlgorithm and Modified Cylindrical Distance.

Table (1) description of the areas According to the researcher

N.	Temperature value	Description of the area
1-	31.16 – 38.27	Water areas
2-	38.27 – 41.75	Intensive agricultural areas
3-	41.75 - 44	Dense residential areas
4-	44 – 46.43	Low density residential areas
5-	46.43 – 53.29	Arid or dry areas

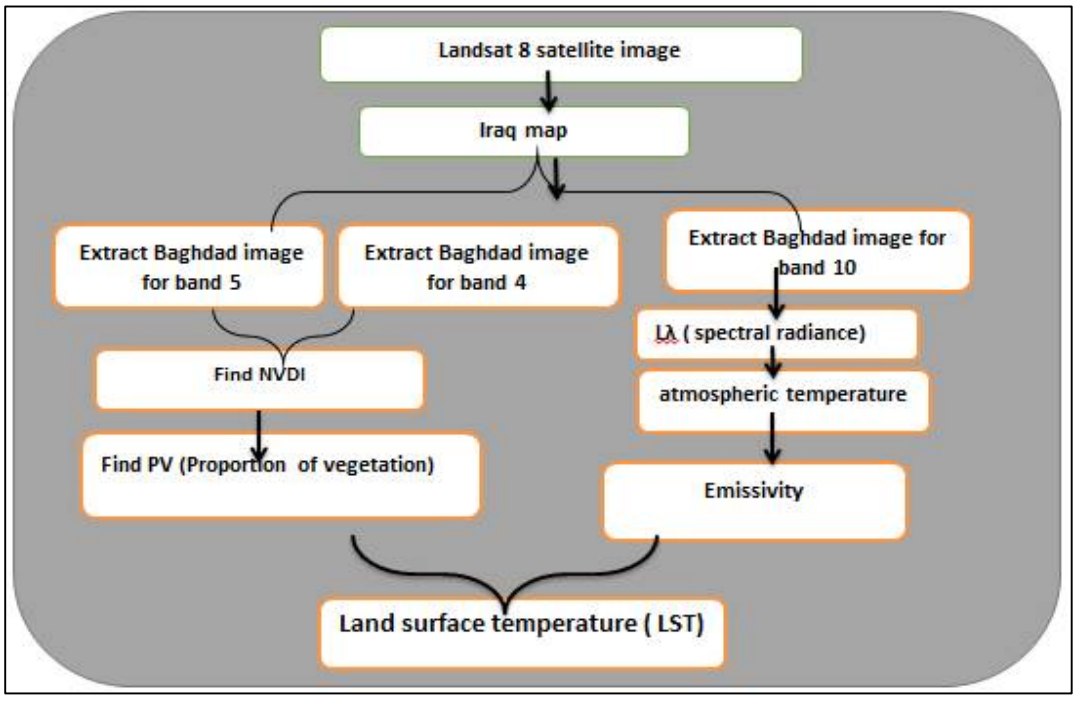

Fig.(1) flow chart of method of research

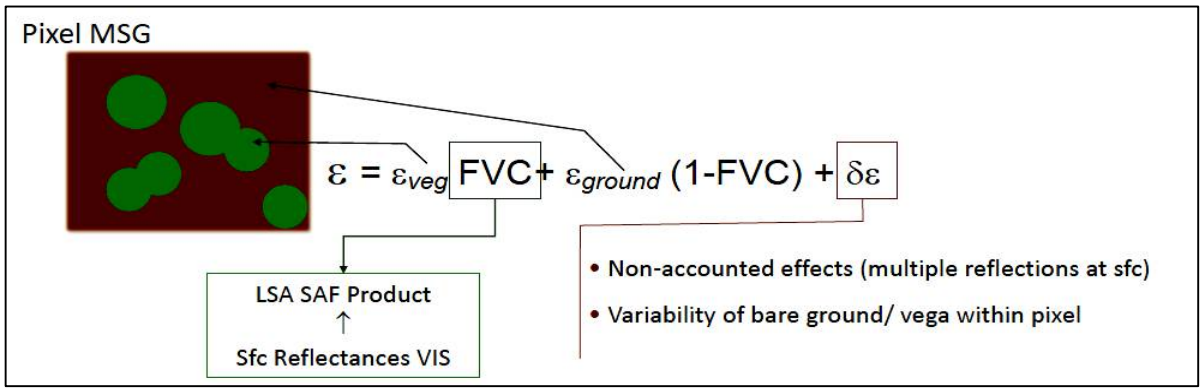

Figure(2) illustrate method Estimation of Emissivity [6]

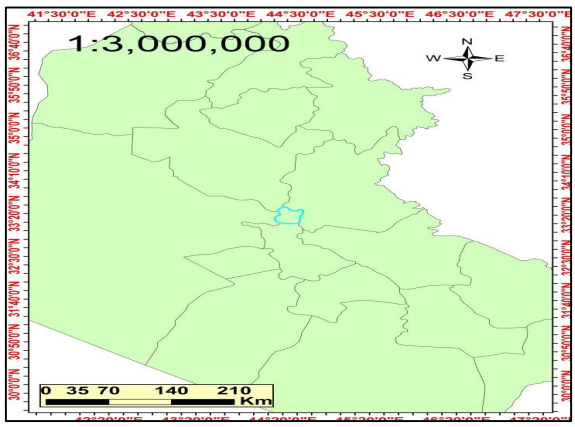

Figure(3) Iraq map in vector format

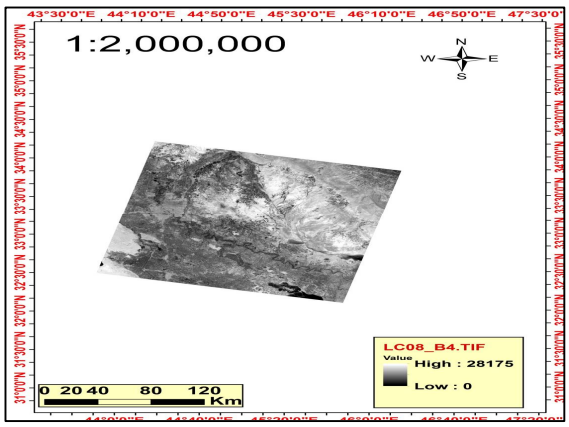

Figure (4) Landsat image for band 4 to study area and surrounding

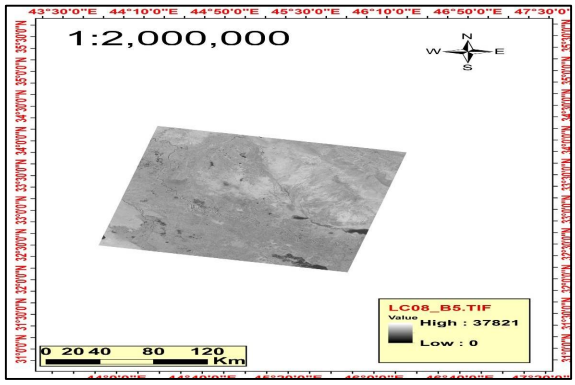

Figure (5) Landsat image for band 5 to study area and surrounding

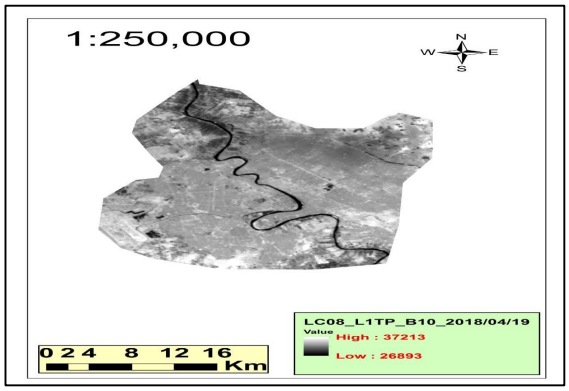

Figure (6) Landsat image for band 10 to study area

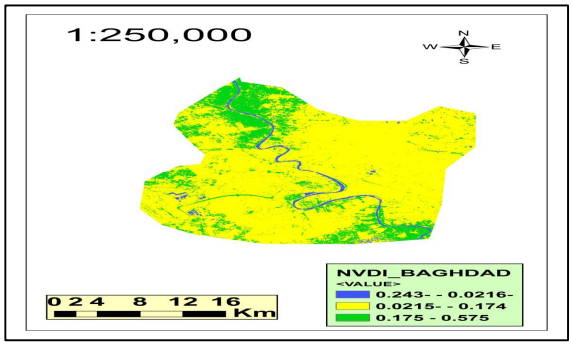

Figure (7) Normalized Difference Vegetation Index (NDVI) for study area by using band 4 and 5. The map shows that the north-western and south-eastern part of Baghdad has the highest value of (NDVI). This is because these areas are agricultural areas

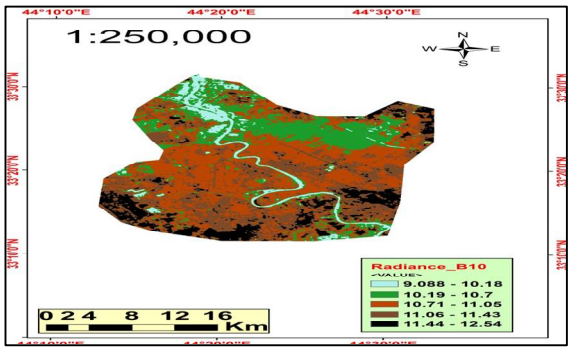

Figure (8) radiance map for study area from band 10 by using Previous Equations. We note from the map that the minimum radiation values were for the water regions and this is known because the water is low emission. While the western areas of the city of Baghdad have the highest value of the emission and the reason, according to the researcher to the lack of vegetative distribution to the drought experienced by these areas

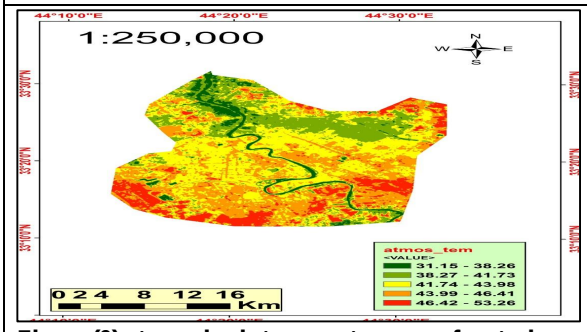

Figure (9) atmospheric temperature map for study area for band 10 by using previous equations

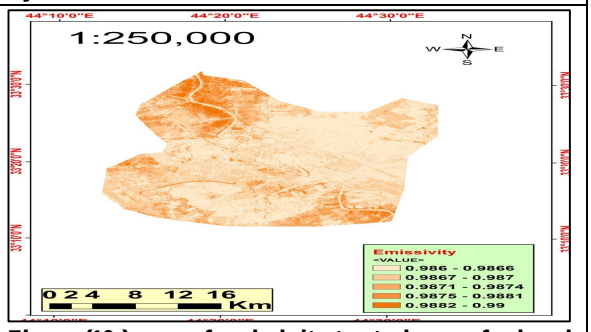

Figure (10) map of emissivity to study area for band 10 by using previous equations

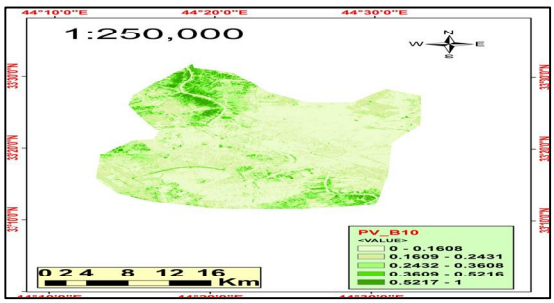

Figure (11) map of Proportion of vegetation (PV) to study area from band 10 by using previous equations.Note from the figure that the characteristics of Proportion of vegetation (PV) have a relationship and a significant correlation with (NDVI) so note the similarity between tow maps

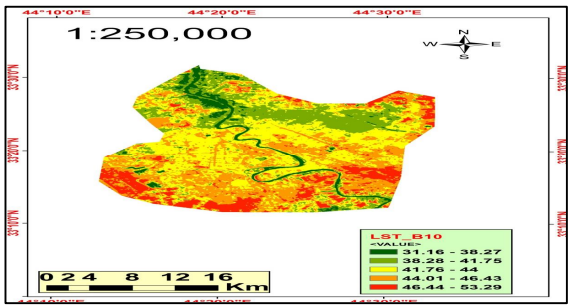

Figure (12)the land surface temperature (LST) map to study area form band 10. From

Indian Journal of Natural Sciences www.tnsroindia.org.in ©IJONS

Vol.9 /Issue 51 / December / 2018 *International Bimonthly* *ISSN: 0976 – 0997*

RESEARCH ARTICLE

Management Practices Followed by Pet Bird Owners of Kerala in India

P.C. Divya, Joseph Mathew, Sabin George*, K.S. Anil, A. Kannan, K. Shyama, and M.K.Muhammad Aslam

Department of Livestock Production Management, College of Veterinary and Animal Sciences, Mannuthy, Thrissur, Kerala – 680651, India.

Received: 18 Sep 2018 Revised: 24 Oct 2018 Accepted: 27 Nov 2018

***Address for Correspondence**
Sabin George
Department of Livestock Production Management,
College of Veterinary and Animal Sciences,
Mannuthy, Thrissur,
Kerala – 680651, India.
E-mail: sabingeorg@gmail.com

ABSTRACT

A study on the existing management practices followed by the pet bird owners was taken up in the Kerala state of India. Data were collected from pet bird owners in their own premises by personal interview using a pre-tested questionnaire. All the birds were used for the breeding purpose and the breeding age varied with species. No out-sources were used for breeding. Age at maturity, the average interval between two clutches, egg per bird in a clutch, incubation period etc. varied with species. Feeding was based on the advice given by the local breeders and not according to standard books or recommendations of veterinarians. All the owners were feeding home-made cereal and pulse-based formulations with mineral and vitamin supplements along with ad-libitum drinking water. Mortality of the chicks occurred due to disease and lack of attention. Except for de-worming, bathing and sun-bath other management practices like vaccination, debeaking, nail and beak trimming was not practiced by the owners. Among all, 48.4 percent of the owners consulted veterinarians for a health check-up and 60.6 percent of the fecal samples were positive for parasitic ova and almost all the birds were free from ectoparasitic infestation. Tail trimming was the only cosmetic treatment practiced.

Keywords: Management practices, Entrepreneurship, Pet bird owners, Random sampling.

INTRODUCTION

Fast changes in the socio-economic conditions of human beings occurred in the last decade have resulted in an increased importance of pet birds and animals. Rearing of pet birds not only act as a tool for stress alleviation in the modern society but also open an avenue for entrepreneurship for unemployed youth. Pet bird owners are on the

increase in India. There are more than 400 varieties of pet birds to choose from. Birds remain the most popular specialty or exotic pet, second only to fish. Although birds have been popular as pets for thousands of years it is now easier than ever to maintain them successfully. The wide range of prepared feed enable bird keepers to offer all types of birds a balanced diet and modern equipment and accessories have greatly eased care, feeding,and breeding of all species. Most of the pet bird owners were resorted to management practices that were often based on traditional knowledge and practices that are convenient to them. The present study was conducted to study the existing management practices followed by the pet bird owners of Kerala, taking Ernakulam district as a sample and to identify the possible areas of intervention to improve the return and welfare of birds.

MATERIALS AND METHODS

A total of 33 pet bird owners from Ernakulam district of Kerala who maintain pet birds were surveyed. A purposive random sampling method of survey utilizing a structured questionnaire and personal interview was conducted in the study area. A detailed questionnaire was prepared to incorporate the details regarding the socio-economic profile of the pet bird owners and the management practices followed such as the selection of birds, housing, feeding, breeding, etc. A pilot study was also carried out to test the efficacy of the questionnaire. The data collected were analyzed for mean and standard error using SPSS package and the results were categorized and tabulated (Snedecor and Cochran 1994)

RESULTS AND DISCUSSION

The housing management of pet birds

Housing facilities provided for the pet birds are given in Table 1. Most of the owners had constructed aviaries instead of cages as aviaries were more comfortable for the birds and this is in agreement with the finding of Gebhardt-Henrich and Steiger (2006).All the owners had their aviaries in the terrace and garden as they had the constraint of space in the urban areas.Concrete formed the stratum for the floor for more than half (57.5 percent) of the surveyed owners. Other materials used for the floor were iron mesh (27.2 percent), wood (6 percent), wire mesh (6 percent) and plywood (3 per cent). Iron mesh was preferred for the wall by 72 percent while 18.1 percent constructed it as three side bricks and one side iron mesh whereas 6 percent used wire mesh and 3 per cent used 2 side bricks and two side plastic mesh. GI sheet forms the roof of most of the aviaries (87.8 percent) while concrete was used by 6 percent and iron mesh formed the roof for 9.1 per cent.The platform of 51.5 percent of the aviaries/cages were raised while 39.4 per cent of the aviaries had their floor at ground level and 3 per cent used hanging cages. Most of the owners used sand (42.4 per cent) as bedding material while 15.1 percent used newspaper as bedding material, 9 per cent used both sand and newspaper and 3 per cent used polyfoam whereas 30.3 percent used no bedding material at all.

Cost of construction of the aviary was 1000-10,000 rupees for 21 percent of the owners, 10,000-40,000 rupees for 39.1 percent and 40,000-1,00,000 for 39.3 percent.There are two types of breeding practiced by the owners-cage breeding and colony breeding. In cage breeding only one pair of birds are kept in a cage and in colony breeding, about 10- 50 birds are kept in an aviary.Kalmar et al. (2010) opined that scientifically based recommendations for species-specific cage dimensions are scarce and enclosures should at least enable the birds to spread their wings and turn around while perched without touching the cage floor or walls with their tail or wings. Although the dimensions were not uniform and scientifically based for all owners this opinion was almost followed by all the owners.

Feeding management of pet birds

The feeding practices followed by the pet bird owners are presented in Table 2. The average proximate principles present in the feed samples collected from the owners are presented in Table 3. Majority of the owners are feeding

home-made foods to the birds. The major ingredients of the feed were cereals and pulses. Cereals include wheat, maize, hulled and de-hulled rice, *Jowar*, *Bajra*, *Thina*, Ragi etc. with wheat being the major ingredient used by most of the owners. Pulses used are Bengal gram, green gram, green peas, groundnut, dal etc. Sunflower seeds were also given by some owners. Different owners had formulated their own ration including the above cereals and pulses according to the availability. Commercial poultry finisher pellets were used by 12 percent of the owners as a feed ingredient. Poultry layer feed was used by 3 percent of the bird owners. Soft food was fed by 3 percent who were rearing African love birds. The ingredients of the soft food include one egg, three teaspoon bread powder, three teaspoons commercial protein health mixture and five drops multi-vitamin supplement. Green leaves like *Tulsi*, green grass, drumstick leaves etc. was given by many of the owners.Vegetables other than green leaves and Azolla was fed by one of the owners who rear pheasants.

Cereals and pulses were fed to the birds when the birds are 1.5 months old. All the owners were providing vitamin and mineral supplements. Calcium is supplemented by using shell grit or cuttlefish bone or egg shell powder or commercially available Calcium supplements by all of the owners. All the owners think that calcium is essential for breeding of the birds.Salt was given by 42.4 percent of the owners. Other supplements provided by the owners include turmeric powder (51.5 percent), ash (36.3 percent) and brick powder (18.1 percent). The feeding schedule matched to the previous reports that diets should be designed to provide a minimum of 10 percent to 14 percent of dietary protein for adult birds and 15 percent to 20percent for growing birds(Harper and Skinner, 1998). All the owners got advice about feeding on the local breeders. None of the owners were feeding as per recommendations of veterinarian/ standard books.This is because there is no NRC publication exists that describes the nutritional requirements of ornamental or companion birds (Reid and Perlberg, 1998). The major ingredients of the feed were cereals and pulses. This is in agreement with the opinion of Harper and Skinner (1998) that most of the small psittacine and passerine species are granivorous.

All the owners provided ad-libitum drinking water to their birds and majority of them change water daily in the morning after cleaning the waterers. Type of waterers used was plastic (21.2 percent), earthen(21.2per cent), steel(12 percent), automatic hopper type(36.3 percent), Aluminum (3 percent), both plastic and earthen (6 percent). Type of feedersused was plastic(24.2 percent), earthen(45.4 percent), steel(24.2percent), wooden (6 percent), both plastic and earthen (3 percent).

Breeding management of pet birds

The breeding data collected in the survey are detailed in Table4.It was observed that all the owners used the birds for breeding purpose. Age at which the birds are used for breeding varies with species. Almost all the owners breed the birds throughout the year. 6 percent of the owners providedVitamin-E supplement for better breeding performance. None of the owners are using any out sources for breeding purpose. While selecting birds for breeding the owners will consider the appearance of the birds, their pedigree and previous performance. Mode of incubation practiced by 96.9 percent of the owners was natural while 3 percent are practicing artificial incubation also. To increase hatchability percentage 75.7 percent of the owners practice candling. Almost all the owners reported that the hatchability percentage was 90 percent.

CONCLUSION

Cage breeding is found to be better than colony breeding as it prevents inbreeding and immature breeding. For growing and breeding birds, additional protein and mineral supplementation in addition to the routine diet should be given.Standard protocols should be developed for healthcare. Awareness on the prospects of pet bird rearing among women must be given. Steps should be taken by the government to issue a licenses to the pet bird owners. As there is no NRC publication regarding the nutritional requirements of companion birds, educational institutions

should take necessary steps to conduct researches regarding the same and should formulate species-specific diets for birds. Awareness should be given to the stake holders regarding the best way of breeding pet birds.

REFERENCES

1. Gebhardt-Henrich SG,SteigerA, 2006.Effects of aviary and box sizes on body mass and behaviour of domesticated Budgerigars (*Melopsittacusundulatus*). Animal Welfare15: 353-358.
2. HarperEJ, Skinner ND, 1998. Clinical Nutrition of Small Psittacinesand Passerines. Seminars in Avian and Exotic Pet Medicine7(3):116-127.
3. Kalmar ID, JanssensGPJ, Moons CPH, 2010.Guidelines and Ethical Considerations forHousing and Management of Psittacine Birds Used in Research.ILAR Journal51(4):409-423.
4. Ried RB, Perlberg W, 1998. Emerging trends in pet bird diets. Journal of AmericanVeterinary Medical Association212(8):1215-1249.
5. Snedecor GW, Cochran WG, 1994.Statistical Methods. 8th Ed., The Iowa State University Press, USA.

Table 1: Housing system of pet birds in Kerala

Sl. No	Variables	Options	Percent
1	Whether constructed an aviary/cage? (%)	Yes	100
		No	0
2	Time of construction in years (%)	1-5	30.3
		5-10	39.4
		10-15	15.1
		>15	15.1
3	Location of the cage/aviary (%)	Terrace	33.3
		Garden	42.4
		Both	24.2
4	Consultation before constructing the cage/aviary	Veterinarian	0
		From books	3
		Local breeder	96.9

Table 2: Feeding practices of pet birds

Sl No	Variables	Options	Percent
1	Feeding of the birds done by	Adult male member	54.5
		Adult female member	9
		Both	30.3
		Servant	3
2	The frequency of feeding for both chicks and adults	One	30.3
		Two	66.6
		Three	3
3	Advice on feeding	Local breeder	100
		Veterinarian	0
		Books	0
4	Feed supplements given	Cuttlefish bone/Shell grit/Eggshell powder	100
		Turmeric powder	42.4
		Salt	51.5

		Ash	36.3
		Brick powder	18.1
		Sand	6
5	Type of feeder used	Plastic	24.2
		Earthen	18.2
		Wooden	6
		Plastic and earthen	3
6	Type of waterer used	Plastic	21.2
		Earthen	21.2
		Steel	12
		Automatic hopper	36.3
		Plastic and earthen	6
		Aluminum	3

Table 3: Proximate principles present in the feed samples collected

Sl. No	Proximate principles	Values (Mean ± SD)
1	Moisture	8.51±0.23
2	Ash	3.31±0.45
3	Acid Insoluble ash	1.69±0.47
4	Crude protein	13.89±0.45
5	Crude fiber	27±0.38
6	Ether extract	4.9±0.51
7	Nitrogen-free extract	74.01±1.23

Table 4: Breeding of birds

Sl No	Variables		Percent
1	Whether the birds are used for breeding?	Yes	100
		No	0
2	Age at which the birds are used for breeding	Pigeons	6-8 months
		Budgerigars	6-8 months
		Cockatiels	18 months
		Finches	3 months
		African lovebirds	6 months
		Diamond dove	4-5 months
		Pheasants	10 months
		African grey parrot	5-6years
3	Whether the non-seasonal birds are used for breeding throughout the year?	Yes	100
		No	0
4	Whether you are giving additional feed supplements for the breeding birds?	Yes	6
		No	94
5	Use of outsources for breeding	Yes	0
		No	100
6	Average number of eggs per bird	Pigeons	1-2
		Budgerigars	4-6
		Cockatiels	2-8

		Finches	2
		African lovebirds	3-4
		Diamond dove	2
		Pheasants	40-60
		African grey parrot	2-5
7	Mortality of chicks	Yes	100
		No	0
8	Mode of incubation	Natural	96.9
		Artificial	3
9	Nest box used	Plastic	42.4
		Earthern	57.5

Indian Journal of Natural Sciences www.tnsroindia.org.in ©IJONS

Vol.9 /Issue 51 / December / 2018 *International Bimonthly* *ISSN: 0976 – 0997*

RESEARCH ARTICLE

Radiographic Evaluation of Healing of Critical Size Defects of Femur Treated with Tri-Phasic Composite Bio-Ceramic Implants in Rat Models

Dinesh P T[1]*, Syam K. Venugopal[2], John Martin K.D[3], Devanand C.B[4], Usha N. Pillai[5] and N. Divakaran Nair[6]

[1]Ph.D. Scholar, Department of Veterinary Surgery & Radiology, College of Veterinary & Animal Sciences, Pookode, Wayanad, Kerala – 673 576.India.
[2]Professor & Head, University of Veterinary Hospital, Kokkalai, Thrissur, Kerala, India.
[3]Professor, Department of Veterinary Surgery & Radiology, College of Veterinary & Animal Sciences, Mannuthy, Kerala, India.
[4]Professor & Head, Department of Veterinary Surgery & Radiology, College of Veterinary & Animal Sciences, Mannuthy, Kerala, India.
[5]Professor & Head, Department of Clinical Medicine, College of Veterinary & Animal Sciences, Mannuthy, Kerala, India.
[6]Professor (Retd.), Department of Pathology, College of Veterinary & Animal Sciences, Mannuthy, Kerala, India.

Received: 18 Sep 2018 Revised: 24 Oct 2018 Accepted: 27 Nov 2018

***Address for Correspondence**
Dinesh P T
Ph.D. Scholar,
Department of Veterinary Surgery & Radiology,
College of Veterinary & Animal Sciences,
Pookode, Wayanad,
Kerala – 673 576.India.
Email:dineshpt@kvasu.ac.in

ABSTRACT

Management of diaphyseal defects is still a perplexing problem faced by orthopedic surgeons. Development of synthetic bone graft substitutes has revolutionized the treatment of such fractures. Development of bone graft substitutes have reduced the incidence of complications encountered as in auto and allografting. HASi is one such material which requires extensive pre-clinical evaluation. Radiographically the graft was found integrated both proximally and distally by four weeks and complete radiographic healing was observed by 16 weeks. Radiographic evaluation of critical size rat femoral segmental defects prove that the material is showing good integration and aids in proper healing of the defect on time.

Key Words: - critical size defects, tri-phasic composite bio-ceramic implants, radiographic evaluation

INTRODUCTION

Bioceramic graft substitutes find wide range of applications in veterinary clinical practice like correction of bone defects resulting from dissection of bone tumours, osteomyelitis, severe comminuted fractures and osteoporotic diseases. Development of Silica based ceramic coated calcium hydroxyapatite has revolutionised the field of bone grafting. Studies by Nair 2009 have proved this material to be oestrogenic and osteoinductive. The graft material augments the healing process by stimulating the proliferation of osteoblasts (Zhang et al., 2010) and undergoes gradual degradation in par with osteogenesis (Nair et al., 2009). The study was intended to evaluate the healing of critical size femoral diaphyseal defects using tri-phasic silica containing ceramic coated hydroxyapatite in rat models.

MATERIALS AND METHODS

The study was conducted in accordance with the guide lines laid by the *Committee for the Purpose of Control and Supervision of Experiments on Animals (*CPCSEA) as per the principles of guide for care and management of experimental animals. The study was approved by the Institutional Animal Ethics Committee of College of Veterinary & Animal Sciences, Pookode of Kerala Veterinary and Animal Sciences University. The study was conducted in eighty adult male Wistar rats with an average weight of 200g. A critical size segmental defect of 6.0 mm was created in the right femur of all the animals under general anaesthesia using a combination of xylazine and ketamine hydrochloride given intraperitoneal at the dose rate of 9.0 mg/Kg and 90.0 mg/Kg body weightrespectively (IACUC Guidelines: Anaesthesia of lab animals). The defect was filled with a pre-sized tri-phasic composite bio-ceramic coated with silica and retained in position using 1.5mm, five hole micro plates. Postoperatively, all the animals were given cephalexin at the dose rate of 20mg/Kg body weight twice a day orally for seven days. Analgesia was effected by administering butorphanol at the dose rate of 2.0 mg/Kg body weight intramuscularly for three days and meloxicam @ 2.0 mg/Kg body weight intramuscular for seven days.

Immediate postoperative radiographs were taken to assess the extent of reduction of the fracture. Healing of the defect was assessed by orthogonal radiographic views of the affected limb, during 2^{nd}, 4^{th}, 8^{th}, 12^{th} and 16^{th} week postoperative, under light anaesthesia using isoflurane (3 %) in oxygen. The parameters used for radiography were 45 kV and 9.5mAS at 100 cm FFD. Five radiographs each at different stages of healing were given to six persons who were unaware of the stage of healing and scored as per Sadegh*et al.,* 2015. The observers were divided into two groups in which three were novice and three were experienced persons in assessing the radiographic healing. The scores ranged from 0 to 10 where "0" denoted "No- healing" and "10" denoted "Complete healing". The criteria used were formation of bone, union of proximal and distal fragments with grafts and bone remodelling.

RESULTS AND DISCUSSION

Immediate postoperative radiographs (Fig.1) in all the animals showed good reduction of the fragments with the graft material in position. The implant used to hold the material in position was found intact and *in situ* through out the period of observation. Radiographic results depicted that the fixation of porous HASi cylinders using 1.5 mm micro plates and screws was effective in holding the implant and the graft in position. Porous ceramics were brittle and tend to fracture in the centre. Hence, inorder to preventfracture of the implant, excessive load on the materials should be avoided during the early stages of healing (Zhang *et al*., 2001).In the present study, by the end of second week, the graft material density was higher than that of the bone and the radiolucent zone was visible both proximally and distally (Fig.2). The material was found integrated with the host bone by four weeks. Proximal and distal fracture lines were not visible radiographically (Fig.3). Similar observations were made by Parizi*et al.* (2012), where they treated rabbit ulnar critical defects with corals and human platelet rich fraction of blood. Divya *et al.* (2017) made similar observations while treatingclinical cases of goat segmental defects with Silica based ceramic

coated calcium hydroxyapatite incorporated with strontium. In the present study, by eight weeks, the defect was found radiographically healed without any periosteal reactions noticed (Fig. 4). In a study conducted in goat femoral segmental defect models treated with HASi, Nair (2009) observed that the density of the graft material decreased in par with new bone formation. By 16 weeks, complete bone healing was observed in the present study. Similar findings were reported by Sadegh*et al.* (2015) when decalcified bone matrix was used as graft material in rabbit tibia. Nandi *et al.* (2008) observed complete radiographic healing of goat tibia by 90 days. They used plain HA as graft for filling the segmental defects. The graft material showed complete resorption by 30 days.

Scoring of Radiographic healing

To quantify the radiographichealing, a scoring system as proposed by Sadegh*et al.* (2015)was used. Radiographs were given to six persons who were unaware of the stage of healing. The scores ranged from 0 to 10 where "0" denoted "No- healing" and "10" denoted "Complete healing". The criteria used were formation of bone, union of proximal and distal fragments with grafts and bone remodelling. In the present study, the total score observed were 0.57 ± 0.15 at two weeks, 3.25 ± 0.25 at four weeks, 6.83 ± 0.28 at eight weeks, 8.94 ± 0.15 at twelve weeks and 9.54 ± 0.16 at sixteen weeks in a score card of maximum 10 points.The results of the present study indicated good progressive healing and integration of the graft material with the host bone. Material degradation equivalent with the formation of new bone was also noticed radiographically.

REFERENCES

1. Divya Suresh, Syam,K. V., George Chandy, Sooryadas,S and Deepa,P.M. 2017. Radiographical evaluation of Sr-HASi bioceramic substitute for critical size bone defect in a goat – Clinical study *J. Vet. Anim. Sci.* 48: 40 - 42
2. IACUC Guideline rodent anaesthesia& analgesia formulary available at https://animal.research.uiowa.edu/iacuc-guidelines-anesthesia (29/06/2017)
3. Nair, M.B. 2009. Bone reconstruction of goat femur segmental defects using tissue-engineered bioceramic scaffolds with osteogenically induced mesenchymal stem cells and platelet-rich plasma. *Ph.D. thesis*, Sri Chithira Thirunal Institute for Medical Science and Technology, Trivandrum, 235p.
4. Nandi, S.K., Kundu, B., Ghosh, S.K., De, D.K. and Basu, D. 2008. Efficacy of nano-hydroxyapatite prepared by an aqueous solution combustion technique in healing bone defects of goat. *J. Vet. Sci.***9**: 183-191.
5. Parizi, A.M., Oryan, A., Sarvestani, S.Z. and Bigham, A.S. 2012. Human platelet rich plasma plus Persian Gulf coral effects on experimental bone healing in rabbit model: radiological, histological, macroscopical and biomechanical evaluation. *J. Mater. Sci. Mater. Med.***23**: 473–483.
6. Sadegh, A, B, Karimi, I, Shadkhast, M, Hosein, M and Mahdavi, 2015, Hydroxyapatite and demineralized calf fetal growth plate effects on bone healing in rabbit model *J Orthopaed. Traumatol.* 16:141–149
7. Zhang, C., Wang, J., Feng, H., Lu, B., Song, Z. and Zhang, X. 2001. Replacement of segmental bone defects using porous bioceramic cylinders: A biomechanical and X-ray diffraction study. *J. Biomed. Mater. Res.* **54**: 407-11.

Table 1. Scoring of Radiographic healing

Stage of Healing	Bone Formation	Proximal Union	Distal Union	Remodeling	Total score
2 Weeks	0.17	0.13	0.33	0.00	**0.57**
4 Weeks	1.50	0.96	0.92	0.54	**3.25**
8 Weeks	2.87	1.40	1.63	0.93	**6.83**
12 Weeks	3.39	2.00	2.00	1.56	**8.94**
16 Weeks	3.92	2.00	2.00	1.63	**9.54**

Fig.1.(A)Immediate postoperative radiograph

Fig.2.(B)Radiograph at 2nd week

Fig.3.(A)Radiograph at 4th week

Fig.4.(B) Radiograph at 8th week

Fig.5.(A) Radiograph at 12th week

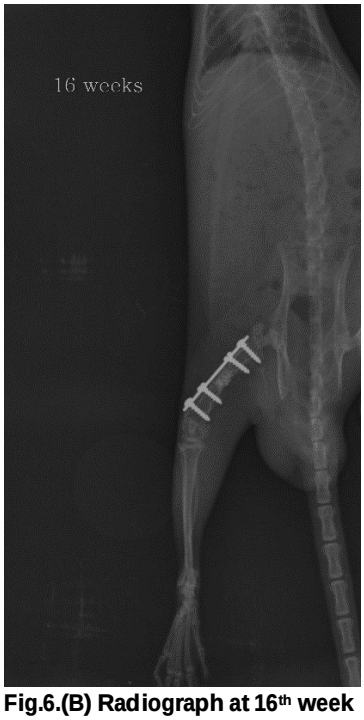

Fig.6.(B) Radiograph at 16th week

Indian Journal of Natural Sciences www.tnsroindia.org.in ©IJONS

Vol.9 /Issue 51 / December / 2018 *International Bimonthly* *ISSN: 0976 – 0997*

RESEARCH ARTICLE

Determination of the Electron Density Variation for Ionosphere Layer Over Iraqi Zone Using IRI Model

Khalid A. Hadi* and Asma'a A.Hamead

Department of Astronomy and Space, College of Science, University of Baghdad, Baghdad, Iraq

Received: 24 Aug 2018 Revised: 27 Sep 2018 Accepted: 29 Oct 2018

***Address for Correspondence**
Khalid A. Hadi
Department of Astronomy and Space,
College of Science,
University of Baghdad,
Baghdad, Iraq

ABSTRACT

In this research, the impact of the solar activity on the variation of the ionosphere layer has been studiedfor different heights (100, 200, 300 …1000) km of the ionosphere layer over Iraqi zone. The study has been made by determining the electron density (Ne) parameter variation. The calculations have been conducted using IRI-2016 modelfor several sites that cover the studied Iraqi zone during the minimum and maximum years of the solar cycles (22, 23 and 24).The determinations have been made for fifty five sites located within Iraq area; the capital Baghdad has been chosen to represent the transmitter station while the other communication points which are located on different distances and directions around the transmitter station have been represented as receiver stations. Also, a mathematical formula that describe the correlation between the ionospheric electron density and critical frequency parameters have been investigated for the annual times of the tested years. The mathematical correlation equation between the tested parameters has been found to be a polynomial equation of the third order. The result of the conducted study demonstrated that the electron density parameter is generally increased during noon time and the southern part of the studied zone showed higher values of electron density than the northern regions that may due to the solar radiation also.

Key Words: Electron Density, IRI model, Solar Activity, Ionosphere layer.

INTRODUCTION

The ionosphere is a region composed of electrically charged particles ranging between 60 to 1000 km and more, it is very important because of its effect on the propagation of radio waves [1]. The ionosphere layer is depending on the electron density, so this layer is subdivided into three layers: the D, E, and Fregions. Each region is subdivided into layers called the D, E, Es, F1, F2. Also, the presence of these layers varies during the day and night .The D-layer is the

lowest part of the ionosphere, extending roughly from the height of (50 - 90) km above the surface of the earth [2].The E-layer is located at an altitude of (90-150) km. Ionization of this layer begins near the sunrise reaches maximum ionization at noon and stops shortly after sunset [3]. Also there is an unexpected layer known as E Sporadic (Es). This layer appears day and night with an average life of between two hours and three hours. Its altitude may vary anywhere between 80 and 120 km [4].The F-layer is considered to be one of the most ionized ionospheric layers, usually range from about (140-500) km and above. The F layer is the only one that remains ionization during daylight hours [4]. Ionization in this region remains at night, due to the large increase in the rate of free particle path way in this region. This gives layer F distinct importance from the rest of the layers for the transmission of High Frequency (HF) waves over long distances during the day and night [5]. The coming sunlight causes the division of this layer into two distinct layers first layer (F1) is the lower part of the F layer, which is at a height of (150-250) km. This layer occurs during the daytime. The maximum HF waves are penetrated through the F1 layer [6]. The second layer (F2) is the highest layer of the ionosphere and is located at a height of (250-400) km. The electron density of the F2 layer may vary because it is the highest area. This layer is the main mechanism for reversing HF signals during the day and night [2].

Ionospheric Electron Density

Electron density behavior versus altitude is a useful parameter for describing different regions of the ionosphere, with the relative maxima and minima used to identify the ionospheric layers [7].The relationship between electron density and frequency can be expressed roughly by the following equation [8].

$N_e = 1.24 \times 10^4 f_N^2$ …….. (1)

Where:
N_e = electron density (e/cm^3)
f_N^2= plasma frequency (MHz).

When the ionosphere horizontally stratified, as N_e is increased upward, the plane wave is reflected vertically at a height that satisfies equation (1). According to this technique, the vertical distribution of the electron density can be measured as much as possible in the ionized layer (F2peak). The electron concentration in the peak F2 is designated as (NmF2) [8]. The frequency corresponding to NmF2 is called the *critical frequency* or the *frequency of penetration* (f_oF2) which can be expressed in the following equation[9].

$f_oF2 = 9 * \sqrt{Ne_{max}}$ …….. (2)

Where:
f_o: critical frequency
When the plasma frequency exceeds the critical frequency, it passes through the ionosphere without reflection. Therefore, ground measurements provide only the distribution of the electron density to the peak F2 on the "bottom side" of the ionosphere and cannot provide information about the peak F2, which is about 300 km [8].

International Reference Ionosphere model (IRI)

The International Reference Ionosphere (IRI) project was initiated by the Commission for Space Research (COSPAR) and the International Union of Radio Science (URSI) in the late 1960s, using a standard ionosphere model based on all available data sources around the world from terrestrial observations as well as satellites [10].As requested by these international unions, IRI was built as an empirical model representing the syntheses of most of the available ground and space measurements of ionospheric characteristics. IRI represents monthly averages of electron and ion densities and temperatures in the altitude range of 50 km–2000 km. It also provides the vertical total electron content

(TEC) from the lower boundary (60–80 km) to a user-specified upper boundary. Additional IRI output includes the ion drift near the magnetic equator and the probability for the occurrence of a F1 layer [2]. From the beginning, the model has become available in electronic format as FORTRAN and recently also as an interactive web interface accessible from the IRI home page [11].The latest version of the IRI-2016 model was selected in this paper because this model represents the best model and solution in the ionosphere [12].

RESULTS

In this work, the impact of solar activity on the behavior and variations of the ionosphere layers has been studied over Iraqi region during the minimum and maximum years of the solar cycles (22, 23 and 24). The minimum tested years of the three solar cycles are (1986, 1996 and 2008) and the maximum years are (1989, 2001, and 2014) respectively. The solar activity is represented by the sunspot number and solar flux. The monthly sunspot numbers and the monthly values of the adjusted solar flux ($F_{10.7}$)of the selected year are shown in table (1) [13]. In this study, Baghdad city (44.37°E, 33.35 °N) has been picked to represent as a transmitting station with other forty five different selected receiving stations laid within the studied region. The selected link locations used in the local communications study are illustrated in figure (2). Geographical location coordinates (longitude and latitude), spherical geodesic parameters (path length - bearing transmitter to receiver (T_x to R_x) and bearing receiver to transmitter (R_x to T_x) and distance for connection links over Iraqi region are listed in table (2):-

The behavior of the annual variations of the ionospheric electron density parameter for the twelve months of the selected years (1989,2001,2014) at maximum solar cycles (22,23 and 24) and the years (198,1996,2008) of theminimum same solar cycles have been determined. The calculations have been conducted using the (IRI-2016model). The adopted model have been tested for the selected locations; the predicted values of the ionospheric parameter have been calculated for the altitudes (100,200, 300 …1000)km. A statistical analytical study have been made on the generated datasets of the predicted values from the international modelby taking into consideration the local time (LT) for the city of Baghdad (transmitter station). Table (3) shows a sample of the statistical analysis results that illustrate the annual statistical variations of the electron density (Ne) for the height (100) km.

Figure (2), show samples of the statistical analysis results of the annual time variations for the (Ne) parameter that have been conducted for the maximum and minimum years of the solar cycles (22, 23 and 24). The maximum tested years of the three solar cycles are (1989, 2001, and 2014) and the minimum years are (1986, 1996 and 2008) respectively, for heights (100, 200, 300 … 1000) km. The relationship between the ionospheric electron density and critical frequency parameters have been investigated to get a suitable mathematical correlation equation for these parameters that can give predictable values. Depending on the results of the annual statistical analysis study that have been made on the generated datasets using the IRI-2016 model for the maximum and minimum years of the studied solar cycles, the mathematical correlation equation between the tested parameters have been found to be expressed as a polynomial formula, so the suggested mathematical correlation equation between the studied parameters can be presented by the following equations:

$$y = \sum_{k=0}^{n} a_k x^k \quad \text{..... (3)}$$

$$Y = a_0 + a_1 x^1 + a_2 x^2 + \cdots + a_n x^n \quad \text{..... (4)}$$

So, the suggested correlation formulas can be presented as follow:

$$N_e = a_0 + a_1 (f_0F_2) + a_2 (f_0F_2)^2 + \cdots + a_n (f_0F_2)^n \quad \text{..... (5)}$$

According to the result of the statistical analytical study, the correlation formula has been found to be a polynomial equation of "Third Order". The theoretical values of the ionospheric electron density have been calculated using equation (1). Table (4) shows sample of the correlation coefficients [(a_0, a_1, $a_2$and a_3), the correlation parameter (R^2) and the calculated values of the Root Mean Square Error (RMSE) which have been calculated using the following equation:

$$MSE=\frac{1}{n}\sum_{i=0}^{n}(X_i - Y_i)^2 \quad \text{..... (6)}$$

Where:

Xi = present values, Yi = Predict or Theoretical Values.

The comparison between the annual values of the (Ne) ionospheric parameter that have been calculated using the suggested formula (5) "predicted" with the ionospheric values that have been generated using the international model (IRI) and the theoretical values which have been calculated using equation (1) have been shown in figures (3) and (4),that show samples for thiscomparison between the annual values of the (Ne) parameter for the maximum tested years(1989, 2001, and 2014) and the minimum years (1986, 1996 and 2008) of the three solar cycles (22, 23 and 24) respectivelyfor the location of Baghdad city.

DISCUSSION AND CONCLUSION

Using Different methods, Geographical location coordinates (longitude and platitude) and many geodesic parameters [distance, path length and bearing (transmitter to receiver and vice versa)] have been calculated for all tested connecting links between transmitter and receiver station over the studied area (Iraqi zone).The results of the analytical study that have been made for the datasets generated using IRI-2016 model for the ionospheric electron density parameter will be discussed. The calculation of the Ne parameter has been achieved for the Iraqi local zone by considering Baghdad province as a transmitter station and many other different cities around the transmitter station have been represented as receiving stations.An analytical study of the annual changes of the Neparameter for the minimum and maximum years of the solar cycles (22,23 and 24)and for the heights (100, 200, 300 …. 100) Kmhas been illustrated in Figs(2). The results of this study show that there is an obvious anomaly in the electronic density during these years at the heights (200 and 300) km. The behavior of the (Ne) parameter showed that the values of the Ne parameter in 1989 werehigher than that of the years 2001 and 2014at the maximum years of the solar cycles (22,23and 24)within the range of ($3x10^{12}$). While, the values in the minimum years of the studied solar cycles showed that the Ne values in 1986 were higher than that of the years 1996 and 2008 within the range of ($8x10^{11}$). The increment in the values of the Ne parameter was May due to the increment in the values of the sunspot numbers and solar flux of the studied years.

The comparison results between the annual values of the (Ne) ionospheric parameter that have been calculated using the suggested formula "predicted values" with the ionospheric values that have been generated using the international model (IRI-2016) and the theoretical values which have been calculated using a theoretical equation showed that the behavior of electron density values for the IRI-2016 model is similar to the predicted values while it difference from the values calculated using theoretical equation.The behavior of the Ne parameter displayed kind of anomalies for the height (200, 300, and 400) km, then with increasing the height the values became more stable.
According to the previous discussion, the following conclusions can be recorded:

1- The behavior of electron density varieswith the changes of the solar activity that associated with the sunspots number and strength of the solar flux.
2- The electron density increases with the height, so it reaches its maximum value at an altitude of 400 km, then begin to decline with the increase of the height.
3- In the height of 200 and 300 km the variation of the electron density observed kind of anomaly behavior during the low and high solar activities.

4- The comparison results between the annual values of the (Ne) ionospheric parameter had different values for the same behavior during various altitudes, and also notices kind of anomaly in the electron density in the heights of 100, 200, 300 and 400 km

REFERENCES

1. A. Belehaki, I. Stanislawska, and J. Lilensten, "An Overview of Ionosphere-Thermosphere Models Available for Space Weather Purposes", Space Science Reviews, Vol. 147, 2009.
2. A. Komjathy, "Global Ionospheric Total Electron Content Mapping Using the Global Positioning System" , Department of Geodesy and Geomatics Engineering Technical Report No. 188, University of New Brunswick, Fredericton, New Brunswick, Canada, (1997).
3. T. R. Gilliland, G. W. Kenrick, and K. A. Norton, "Investigations ofKennelly-heaviside layer heights for frequencies between 1600 and 8650 kilocycles per second" , Proceedings of the Institute of Radio Engineers, vol. 20,1932.
4. Recommendation and Reports of the CCIR, Geneva, vol. VI, Rep.725-2, pp. 1-12, 1986.
5. H. R.R.Razoki, "Study the effect of solar cycle variation on the behavior of (F2) ionosphere layer for high frequency communication (HF)",M.Sc. Thesis, Department of Astronomy Space, College of Sciences, University of Baghdad, 2005
6. M.I. Mohammed, "Investigation of the variation of maximum usable frequency (MUF) to ensure a good communication link between two locations", M.Sc. Thesis, Department of Astronomy and Space, College of Science, University of Baghdad, 2011.
7. B. Zolesi and L. R. Cander, "Ionospheric Prediction and Forecasting", Springer Geophysics DOI: 10.1007/978-3-642-38430-1_2, Springer-Verlag Berlin Heidelberg 2014
8. Wu Mao-Fou,"Topside Ionosphere Electron Density Concentration: Observation and Theory", Ph.D. Thises, University of Chicago, 1970.
9. Z. Mosna, P. Sauli, and O. Santolkk, "Analysis of Critical Frequencies in the Ionosphere ", WDS'08 Proceedings of Contributed Papers, Part II, 2008.
10. D. Bilitza, D. Altadill,V. Truhlik, V. Shubin, I. Galkin , B. Reinisch , and X. Huang , "International Reference Ionosphere 2016: From ionospheric climate to real-time weather predictions", American Geophysical Union, 2017.
11. D. Bilitza, B.W .Reinisch, "International Reference Ionosphere 2007: Improvements and new parameters", Advances in Space Research, vol. 42, pp. 599–609, (2008).
12. D.Bilitza, S. Watanabe, V. Truhlik, D. Altadill, "IRI-2016: Description and Introduce", 41st COSPAR Scientific Assembly, Istanbul Congress Center (ICC), Turkey, 2016.
13. The Sunspot Cycle, Marshall Space Flight Center, NASA, USA, November 2018. http://solarscience.msfc.nasa.gov/SunspotCycle.

Table 1: Monthly sunspot number and adjusted solar flux (F10.7)of the min. and max. Years of solar cycle 24 [13]

Smoothed Sunspot Number (SSN)						
Month	1986	1989	1996	2001	2008	2014
Jan	15.2	210.1	16.8	158.3	6.6	109.3
Feb	14.3	208.7	16.2	152.5	5.6	110.5
Mar	14.3	170.4	15.4	155.1	5.1	114.3
Apr	15.1	166.3	13.6	160.7	5.1	116.4
May	15.8	195.4	12.9	163.7	5.3	115.0
Jun	15.2	284.5	13.5	167.4	4.8	114.1
Jul	15.1	180.5	13.4	172.0	4.0	112.6
Aug	14.4	232.0	13.1	175.8	3.8	108.3
Sep	13.5	225.1	13.3	177.1	3.2	101.9
Oct	14.7	212.2	14.0	177.3	2.4	97.7
Nov	16.6	238.2	15.4	180.3	2.3	94.7
Dec	18.3	211.4	16.2	179.1	2.2	92.2

Solar Flux ($F_{10.7}$ cm)						
Month	1986	1989	1996	2001	2008	2014
Jan	73.25	235.38	74.52	167.50	74.02	162.69
Feb	83.58	222.39	71.83	146.72	71.03	170.13
Mar	77.02	205.07	70.67	178.14	72.99	150.50
Apr	75.06	189.56	69.42	192.46	70.15	143.94
May	72.61	190.14	70.13	147.52	68.32	130.11
Jun	67.59	239.58	69.86	174.11	65.85	122.37
Jul	70.21	181.86	71.36	131.72	65.67	137.90
Aug	68.37	217.09	72.48	166.85	66.17	124.56
Sep	68.71	225.90	69.45	134.08	67.00	146.57
Oct	82.95	208.68	69.23	210.54	68.21	154.99
Nov	77.14	235.13	79.06	214.57	68.53	155.74
Dec	72.64	213.00	75.69	241.16	69.05	159.02

Table (2): Geographical and geodesic parameter values of the connection links over Iraqi zone

Reciver station	Location		Distance Km	Path length Rad.	Bearing					
					T_X to R_X			R_X to T_X		
	Longitude (E)	Latitude (N)			Method(1)	Method(2)	Average	Method(1)	Method(2)	Average
Tel Afar	42.36	37.04	448.40	0.0705	336.48	335.88	336.18	155.32	155.88	155.60
Amedi	43.38	37.02	416.97	0.0656	347.68	347.44	347.56	167.10	167.44	167.27
Soran	44.48	37.01	405.95	0.0639	2.29	1.28	1.79	182.40	181.28	181.84
Al-Ba'aj	41.38	36.02	403.48	0.0634	318.09	317.24	317.67	136.39	137.24	136.81
Sinjar	42.4	36.02	346.96	0.0546	329.08	328.60	328.84	147.95	148.60	148.28
Nineveh 1	43.41	36.02	309.03	0.0486	343.67	343.36	343.51	163.12	163.36	163.24
Koysenjaq	44.43	36.02	296.08	0.0466	1.79	0.88	1.33	181.84	180.88	181.36
Sharbazher	45.49	35.8	290.02	0.0456	20.11	20.47	20.29	200.73	200.47	200.60
Ana	41.39	35.02	331.42	0.0521	304.80	303.99	304.40	123.12	123.99	123.56
Nineveh 2	42.44	35.02	257.08	0.0404	316.66	316.11	316.39	135.57	136.11	135.84
Baiji	43.45	35.02	203.94	0.0321	335.42	335.25	335.33	154.89	155.25	155.07
Tooz	44.5	35.02	185.48	0.0292	3.87	3.40	3.64	183.95	183.40	183.68
Kalar	45.49	35.02	211.41	0.0332	28.37	28.82	28.60	208.99	208.82	208.91
Al-Qa'im	41.39	34.23	292.89	0.0460	290.29	289.46	289.87	108.62	109.46	109.04
Haditha	42.44	34.23	204.02	0.0320	299.17	298.59	298.88	118.09	118.59	118.34
Samarra	43.49	34.23	127.58	0.0201	320.02	319.93	319.97	139.52	139.93	139.73
Al Khalis	44.54	34.23	98.67	0.0155	7.91	8.60	8.26	187.99	188.60	188.30
Khanaqin	45.5	34.23	142.20	0.0223	46.21	46.64	46.43	226.83	226.64	226.74
Ar Rutba1	39.29	33.44	472.35	0.0742	272.57	271.17	271.87	89.86	91.17	90.51
Ar Rutba2	40.34	33.44	374.97	0.0589	272.59	271.48	272.04	90.37	91.48	90.93
Al Anbar 1	41.39	33.44	277.61	0.0436	272.84	272.02	272.43	91.20	92.02	91.61
Heet	42.44	33.44	180.28	0.0283	273.67	273.14	273.40	92.60	93.14	92.87
Albu Bali	43.49	33.44	83.18	0.0131	277.09	276.86	276.98	96.60	96.86	96.73
baghdad	44.37	33.35	17.89	0.0028	55.88	56.06	55.97	235.97	236.06	236.02
Baladrooz	45.59	33.44	112.72	0.0177	84.62	84.95	84.79	265.29	264.95	265.12
Ar Rutba3	39.29	32.65	480.65	0.0755	262.13	260.73	261.43	79.35	80.73	80.04
Al Anbar 2	40.34	32.65	384.42	0.0604	259.48	258.37	258.93	77.28	78.37	77.83
Al Anbar 3	41.39	32.65	289.26	0.0454	255.25	254.44	254.85	73.63	74.44	74.03
Al Anbar4	42.44	32.65	196.76	0.0309	247.29	246.76	247.02	66.23	66.76	66.50
Rahhaliyah	43.49	32.65	113.58	0.0179	227.25	226.87	227.06	46.77	46.87	46.82
Mahaweel	44.54	32.65	79.01	0.0124	169.94	169.14	169.54	350.02	349.14	349.58
Kut	45.59	32.65	136.89	0.0215	124.25	124.57	124.41	304.91	304.57	304.74
Ali Al-Gharbi	46.59	32.65	220.10	0.0346	110.03	110.65	110.34	291.23	290.65	290.94
Ar Rutba4	40.34	31.98	407.27	0.0640	249.21	248.10	248.65	67.03	68.10	67.56
Al Anbar 5	41.39	31.98	318.26	0.0500	242.29	241.48	241.89	60.68	61.48	61.08
Al Anbar 6	42.44	31.98	236.63	0.0372	230.58	230.04	230.31	49.53	50.04	49.79
Al Anbar 7	43.49	31.98	173.18	0.0272	208.78	208.69	208.74	28.30	28.69	28.50
Al-Shamiya	44.54	31.98	152.59	0.0240	174.70	174.38	174.54	354.78	354.38	354.58
Afaq	45.59	31.98	189.40	0.0298	142.97	143.35	143.16	323.62	323.35	323.48
Amara1	46.65	31.98	261.06	0.0410	125.01	125.61	125.31	306.23	305.61	305.92
Amara2	47.7	31.98	345.70	0.0543	115.18	116.08	115.63	296.97	296.08	296.52
Al Anbar 8	42.44	31.07	311.64	0.0490	216.28	215.77	216.03	35.25	35.77	35.51
Najaf1	43.49	31.07	266.19	0.0419	198.58	198.29	198.44	18.11	18.29	18.20
Najaf2	44.54	31.07	253.15	0.0398	177.88	176.60	177.24	357.93	356.60	357.26
Al-Khidhir	45.59	31.07	277.12	0.0436	155.48	155.80	155.64	336.12	335.80	335.96
AL-Aritham	46.65	31.07	330.75	0.0520	139.26	139.86	139.56	320.47	319.86	320.17
Al-Qurna	47.5	31.07	387.14	0.0608	129.99	130.79	130.39	311.65	310.79	311.22
Najaf3	43.49	30.28	350.46	0.0552	194.28	193.85	194.06	13.80	13.85	13.82
Al-Salman1	44.54	30.28	340.58	0.0536	177.60	177.46	177.53	357.68	357.46	357.57
Al-Salman2	45.54	30.28	357.43	0.0562	162.03	162.19	162.11	342.64	342.19	342.41
Al-Zubair1	46.65	30.28	402.09	0.0632	147.30	147.84	147.57	328.50	327.84	328.17
Al-Zubair2	47.5	30.28	450.00	0.0708	138.29	139.16	138.72	319.93	319.16	319.55
Al Muthanna1	44.54	29.49	428.04	0.0674	177.44	177.97	177.71	357.54	357.97	357.76
Al Muthanna2	45.55	29.45	441.67	0.0695	165.35	165.61	165.48	345.95	345.61	345.78
Al-Zubair3	46.65	29.49	478.83	0.0753	152.79	153.33	153.06	333.97	333.33	333.65

Table (3) Sample of statistical analysis result of the annual (Ne) parameter at 100 Km height of Baghdad city

Ne (m^{-3}) at height 100 Km (Baghdad)			
Local time	**Annual 1989**	**Annual 2001**	**Annual 2014**
0	3.86E+09	3.48E+09	2.85E+09
1	3.87E+09	3.48E+09	2.85E+09
2	3.89E+09	3.50E+09	2.86E+09
3	3.93E+09	3.53E+09	2.88E+09
4	4.09E+09	3.70E+09	3.11E+09
5	1.02E+10	9.55E+09	8.63E+09
6	2.98E+10	2.85E+10	2.65E+10
7	6.19E+10	5.84E+10	5.31E+10
8	1.00E+11	9.38E+10	8.38E+10
9	1.30E+11	1.22E+11	1.08E+11
10	1.53E+11	1.42E+11	1.25E+11
11	1.64E+11	1.53E+11	1.35E+11
12	1.68E+11	1.57E+11	1.38E+11
13	1.64E+11	1.53E+11	1.35E+11
14	1.52E+11	1.42E+11	1.25E+11
15	1.30E+11	1.21E+11	1.08E+11
16	9.99E+10	9.39E+10	8.43E+10
17	6.22E+10	5.83E+10	5.32E+10
18	3.03E+10	2.89E+10	2.69E+10
19	1.07E+10	1.00E+10	9.09E+09
20	4.18E+09	3.80E+09	3.18E+09
21	3.93E+09	3.53E+09	2.88E+09
22	3.89E+09	3.50E+09	2.86E+09
23	3.87E+09	3.48E+09	2.85E+09

Table (4) shows sample for the correlation coefficients of the Ne and f_0F_2 parameters for the annual times of Baghdad city for the heights (100-1000) Km of the year 2014

bbghdbd-2014							
Equbtion: Ne= b3(foF2)^3 - b2((foF2)^2 + b1(foF2) - bo							
Hieght =100km		Correlation Coefficients					
LT	ao	a1	a2	a3	R^2	RMSE-pred	RMSE-theo
0-4	0.044	-0.003	-	-	0.8143	0.02197	10.12023
5_13	0.445	-0.295	0.051	-0.002	0.9989		
14_18	10.035	-2.336	0.137	-	0.998		
19_23	0.1134	-0.0258	0.002	-	0.9929		
Hieght =200km		Correlation Coefficients					
LT	ao	a1	a2	a3	R^2	RMSE-pred	RMSE-theo
0-4	2.210	-0.726	0.061	-	0.99	0.12556	7.47551
5_13	-92.111	51.457	-10.677	0.972	0.9998		
14_18	-599.3	178.320	-17.618	0.581	0.9985		
19_23	-26.452	12.01	1.8369	0.0939	1		
Hieght =300km		Correlation Coefficients					
LT	ao	a1	a2	a3	R^2	RMSE-pred	RMSE-theo
0-4	0.203	0.423	-	-	0.608	0.10724	1.02066
5_13	-14.361	6.643	0.684	0.031	0.9999		
14_23	-6.794	-0.193	0.385	-0.017	0.9992		
Hieght =400km		Correlation Coefficients					
LT	ao	a1	a2	a3	R^2	RMSE-pred	RMSE-theo
0-4	-4.373	1.441	-	-	0.9887	0.0963	3.5306
5_13	-25.027	11.178	-1.470	0.067	0.9982		
14_23	-23.560	10.144	-1.229	0.053	0.9995		
Hieght =500km		Correlation Coefficients					
LT	ao	a1	a2	a3	R^2	RMSE-pred	RMSE-theo
0-4	-2.356	0.781	-	-	0.9937	0.05578	7.11893
5_13	-10.171	4.692	-0.621	0.029	0.9983		
14_23	-12.116	5.404	-0.668	0.029	0.9997		
Hieght =600km		Correlation Coefficients					
LT	ao	a1	a2	a3	R^2	RMSE-pred	RMSE-theo
0-4	1.077	0.377	-	-	0.9967	0.01967	8.86019
5_13	-4.110	1.924	-0.250	0.019	0.9987		
14_23	-6.703	2.858	-0.344	0.015	1		
Hieght =700km		Correlation Coefficients					
LT	ao	a1	a2	a3	R^2	RMSE-pred	RMSE-theo
0-4	0.547	0.202	-	-	0.9982	0.01983	9.66462
5_13	1.198	-0.271	0.027	-	0.9949		
14_23	-3.932	1.631	-0.188	0.008	1		
Hieght =800km		Correlation Coefficients					
LT	ao	a1	a2	a3	R^2	RMSE-pred	RMSE-theo
0-4	-0.318	0.121	-	-	0.999	0.01782	10.06975
5_13	-0.941	0.447	-0.055	0.003	0.9993		
14_23	0.595	-0.097	0.012	-	0.9957		
Hieght =900km		Correlation Coefficients					
LT	ao	a1	a2	a3	R^2	RMSE-pred	RMSE-theo
0-4	-0.204	0.080	-	-	0.994	0.0088	10.29395
5_13	0.320	-0.066	0.009	-	0.9978		
14_23	0.308	-0.046	0.007	-	0.9964		
Hieght =1000km		Correlation Coefficients					
LT	ao	a1	a2	a3	R^2	RMSE-pred	RMSE-theo
0-4	-0.142	0.056	-	-	0.9996	0.0097	1042843
5_13	0.183	-0.036	0.006	-	0.9985		
14_23	-1.134	0.439	-0.048	0.002	0.997		

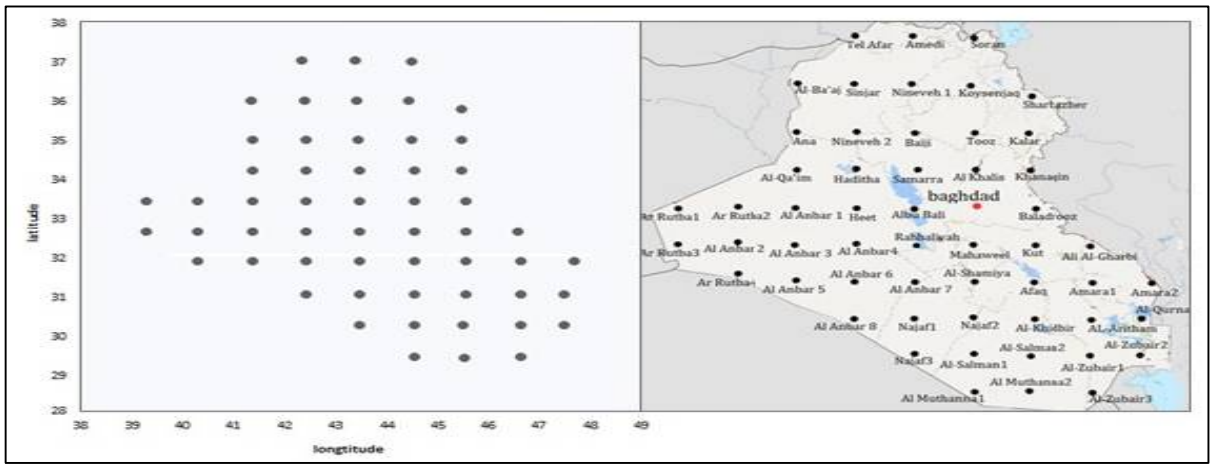

Figure(1) Show the locations of the transmitter/receiver stations over Iraqi area

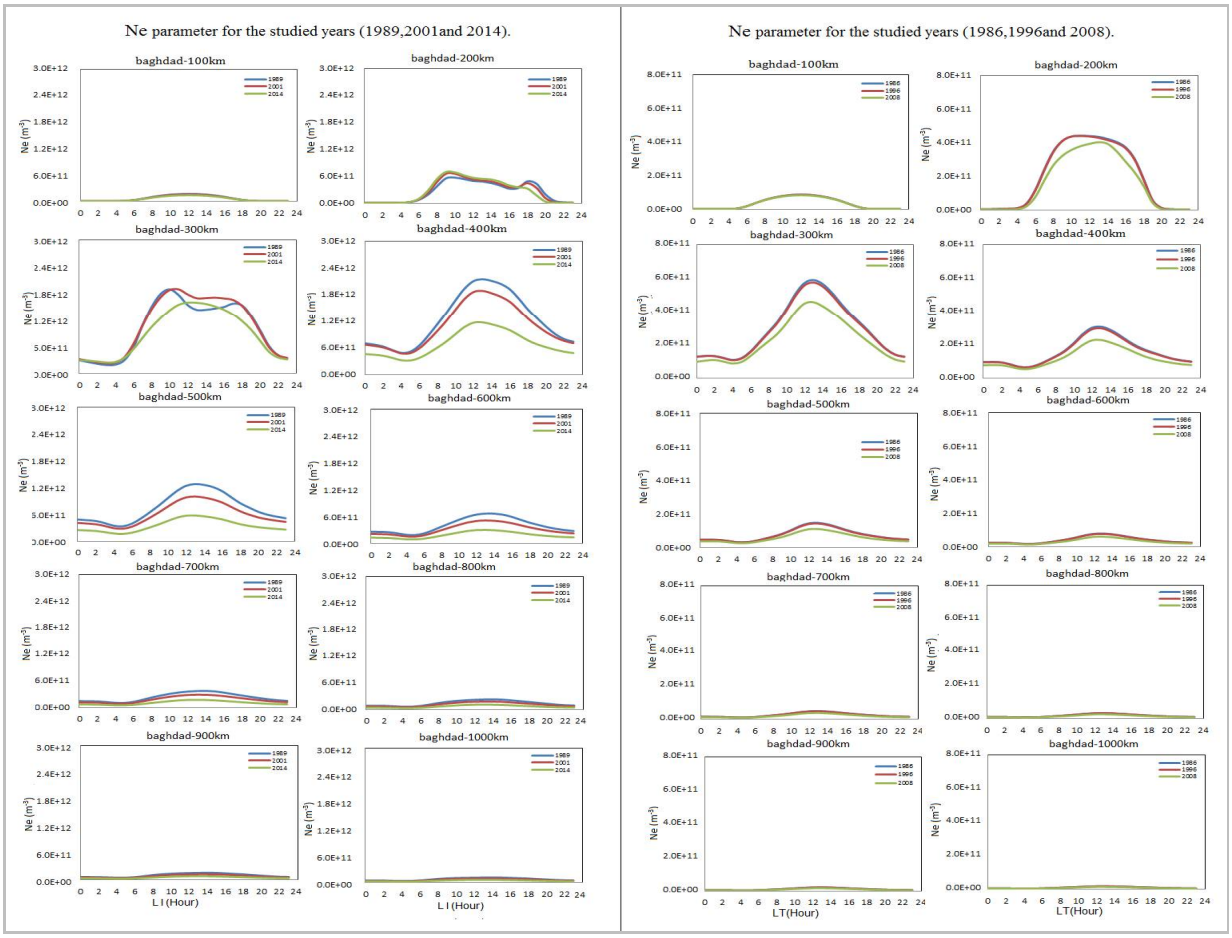

Figure (2) Samples of the annual variations of the electron density (Ne) parameter.

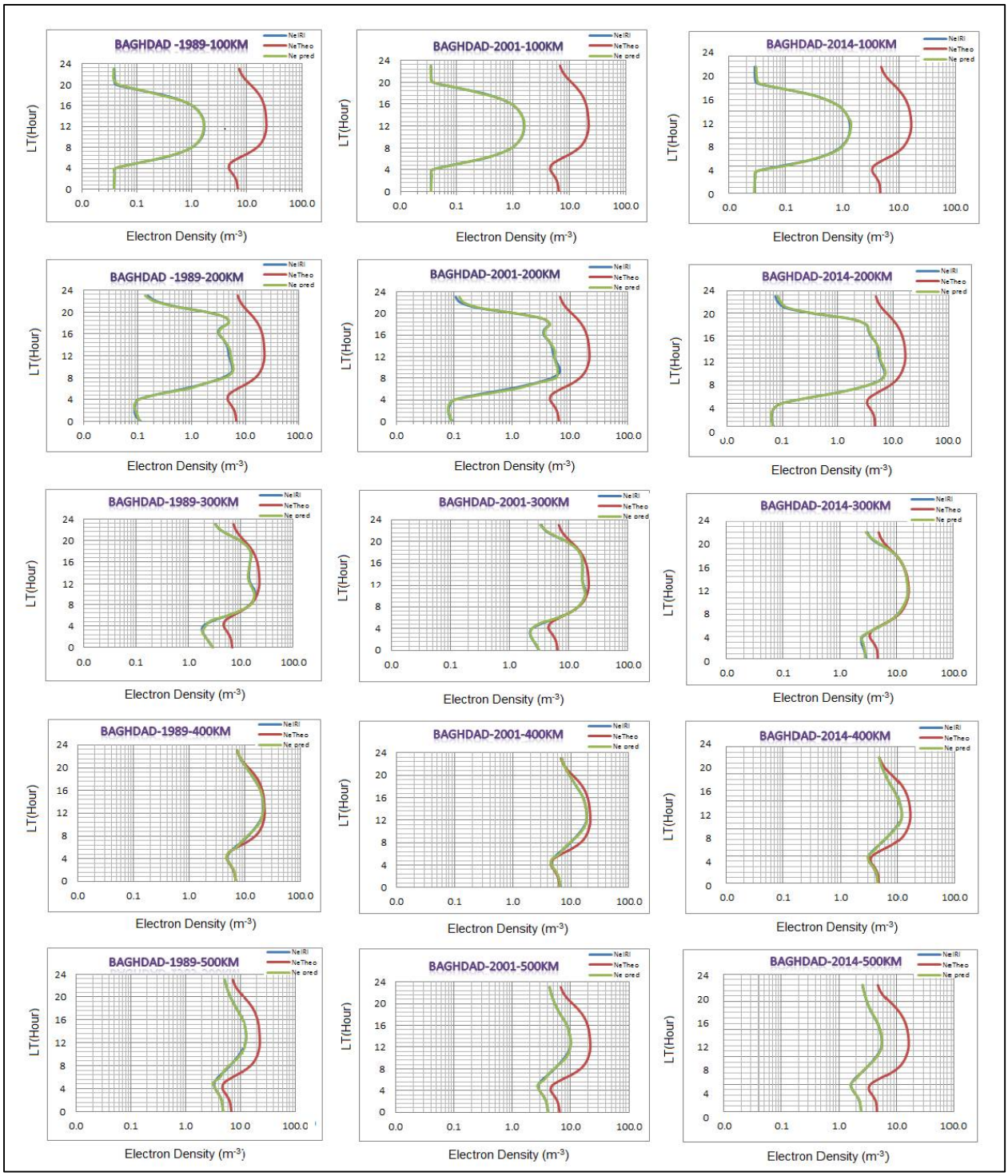
BAGHDAD -1989-100KM
BAGHDAD-2001-100KM
BAGHDAD-2014-100KM
BAGHDAD -1989-200KM
BAGHDAD-2001-200KM
BAGHDAD-2014-200KM
BAGHDAD-1989-300KM
BAGHDAD-2001-300KM
BAGHDAD-2014-300KM
BAGHDAD-1989-400KM
BAGHDAD-2001-400KM
BAGHDAD-2014-400KM
BAGHDAD-1989-500KM
BAGHDAD-2001-500KM
BAGHDAD-2014-500KM
NeIRI
NeTheo
Ne pred
LT(Hour)
Electron Density (m-3)
0.0
0.1
1.0
10.0
100.0
0
4
8
12
16
20
24

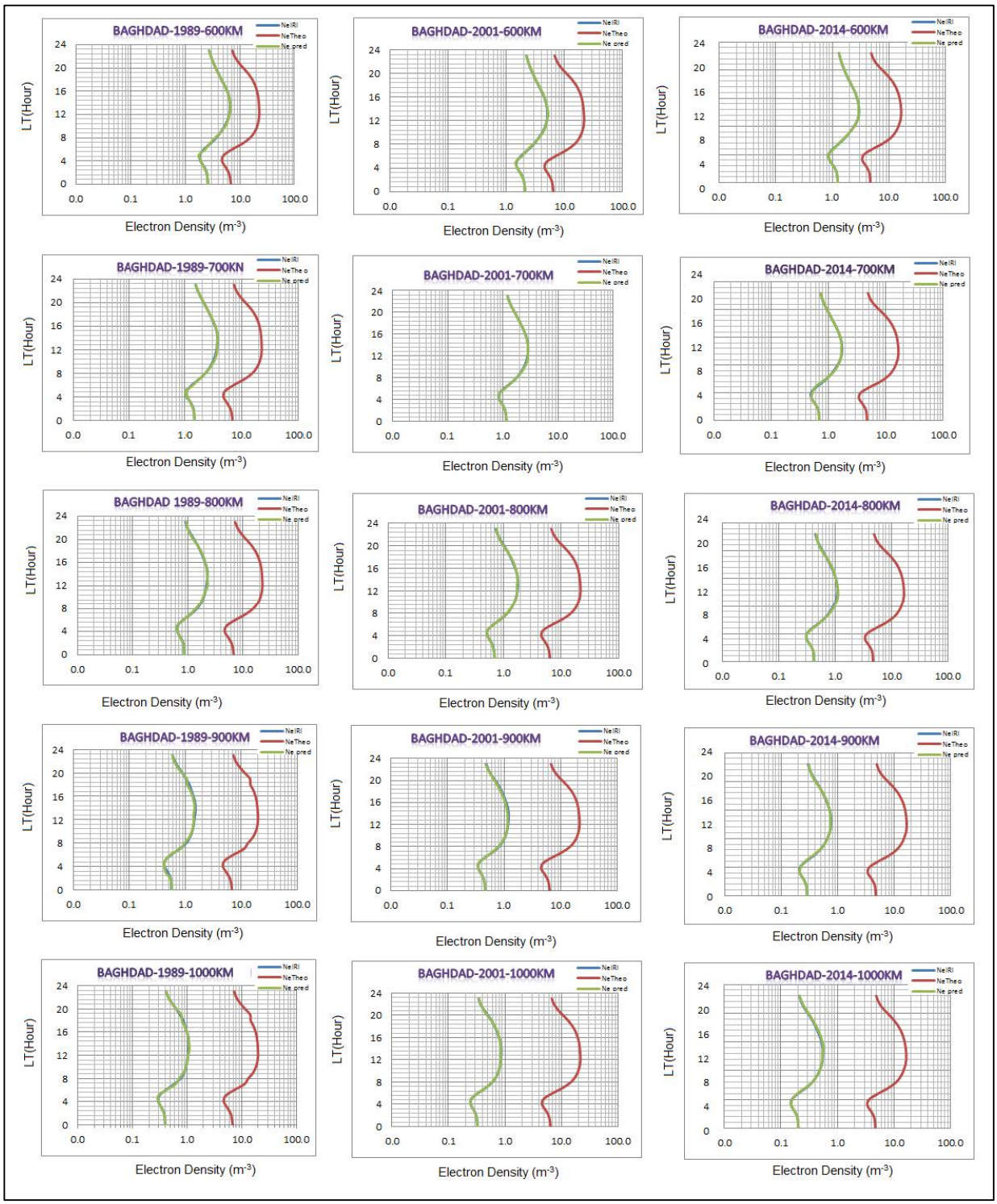

Figure (3) Comparison between the (IRI, predicted and theoretical) values of the (Ne) parameter for Baghdad cityfor the heights (100-1000) kmfor the years (1989, 2001 and 2014)

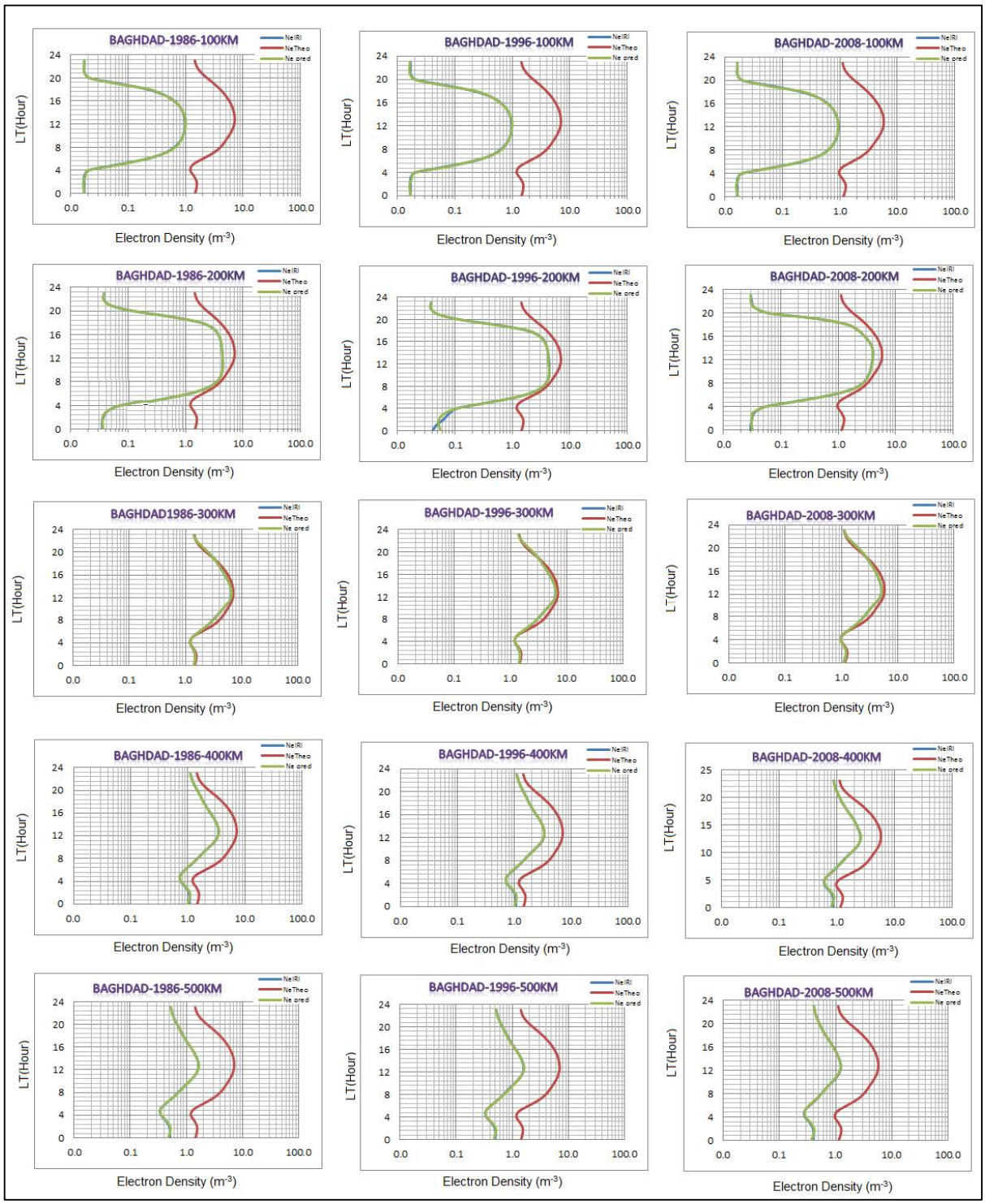
BAGHDAD-1986-100KM
BAGHDAD-1996-100KM
BAGHDAD-2008-100KM
BAGHDAD-1986-200KM
BAGHDAD-1996-200KM
BAGHDAD-2008-200KM
BAGHDAD1986-300KM
BAGHDAD-1996-300KM
BAGHDAD-2008-300KM
BAGHDAD-1986-400KM
BAGHDAD-1996-400KM
BAGHDAD-2008-400KM
BAGHDAD-1986-500KM
BAGHDAD-1996-500KM
BAGHDAD-2008-500KM
NeIRI
NeTheo
Ne pred
LT(Hour)
Electron Density (m-3)

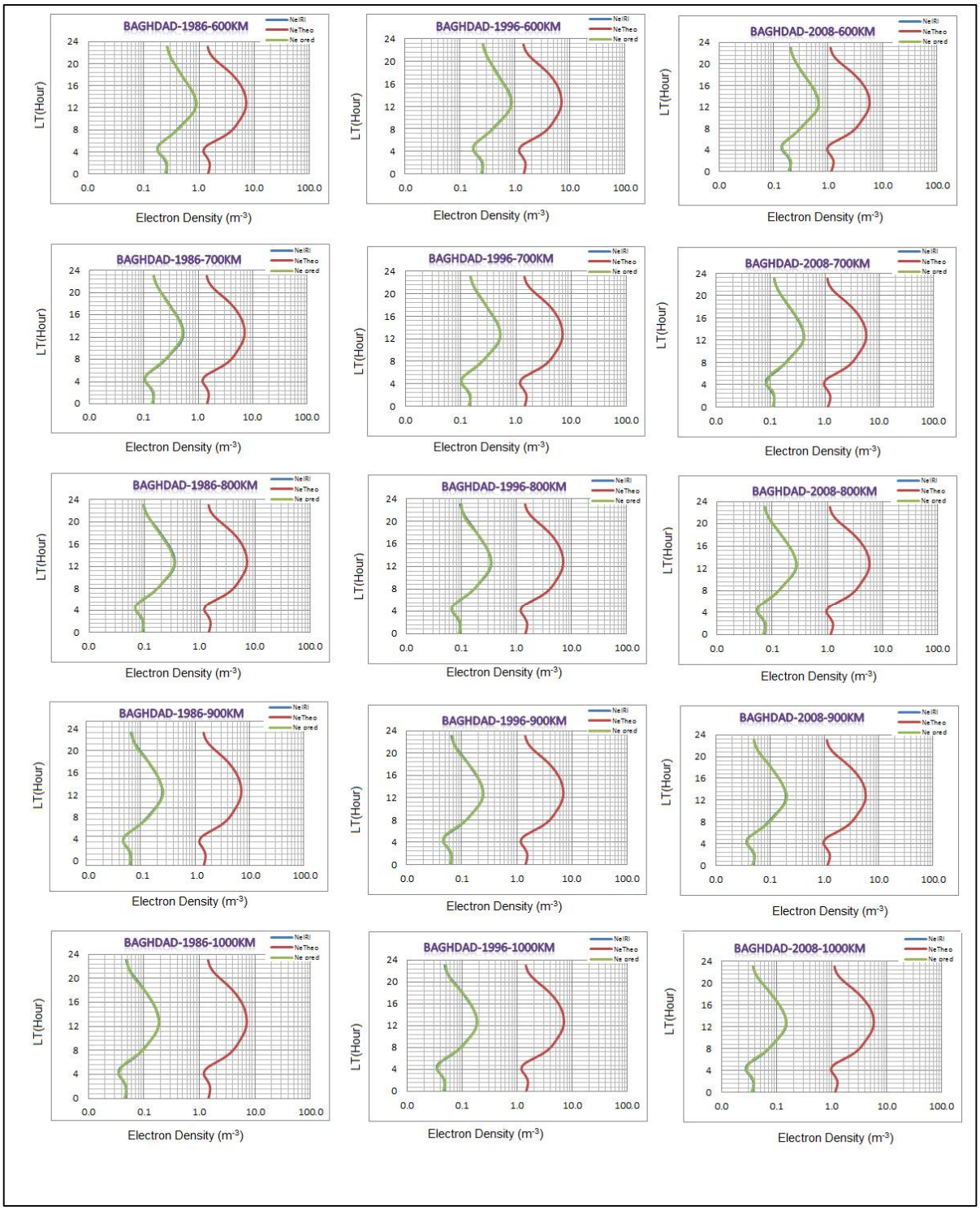

Figure (4) Comparison between the (IRI, predicted and theoretical) values of the (Ne) parameter for Baghdad city for the heights (100-1000) km for the years (1986, 1996 and 2008)

Indian Journal of Natural Sciences www.tnsroindia.org.in ©IJONS

Vol.9 /Issue 51 / December / 2018 *International Bimonthly* *ISSN: 0976 – 0997*

RESEARCH ARTICLE

Change Detection Study of Al Razaza Lake Region by Image Classification Using Gaussian Mixture Model

Ban S.Ismaal[1]*, Ban A.Alazaq[2], Zena F.Rasheed[3] and Ebtesam F.Khanjer[4]

[1,2,4] Department of Astronomy and Space, College of Science, University of Baghdad, Iraq
[3]College of Engineering, University of Baghdad, Iraq.

Received: 25 Aug 2018 Revised: 28 Sep 2018 Accepted: 30 Oct 2018

***Address for Correspondence**
Ban S.Ismaal
Department of Astronomy and Space,
College of Science,
University of Baghdad, Iraq.
E-mail : dr.efk33@yahoo.com

ABSTRACT

In this paper we had classified the Razaza lake and the area around it in Karbala province to produce the Land cover and Land use. The classification method used in this paper is named, supervised classifier, based on Gaussian mixture model which, often used in probability classification problems to model such distributions. We used this technique to detect the Geographic changes of Al Razaza lake region and the area around it on the different date in year 2002 and year 2008. The experiment demonstrate that this method used get a better classification result and less affected by the noise

Key Words: lake, paper, Gaussian mixture, Geographic, technique.

INTRODUCTION

Remote-sensing research focusing on image classification has long attracted the attention of the remote-sensing community because classification results are the basis for many environmental and socioeconomic applications. Scientists and practitioners have made great efforts in developing advanced classification approaches and techniques for improving classification accuracy. The well known and common classification methods that, usually, followed by remote sensing data users are those categorized as supervised and unsupervised methods [1]. The studyarea is located, which includes Razaz Lake and the area surrounding itto the south of Baghdad,is located west of the city of Karbala. Razaza linked from the north by Habbaniyah Lake by Nazim al-warawrCanal, and surrounded bythe other three sides of the land of desert interspersed with some hills and there are some villages,urbans saw mills in the area andthe roads link Ingareas with each other.There are some tourist houses and a very specific number of casinos in the eastern side of the lakeis supplied. The Euphrates Riveris located on the eastern side of the lakea few kilometers from and resides onits banks, farms, orchards, villages and poultry farms. The Razaza lake and the surrounding area lying

15 km west of Karbala [2]. Fig.(1) and fig(2) show Al Razaza lake region and the area around it on the different date in year 2002 and year 2008.

Proposed Classification Method

In this section, the proposed method is presented. Is the general multi-dimensional Gaussian mixture model is described and solved by Expectation-Maximization (EM) algorithm.

For a joint-volume with N voxels, each voxel is a n dimensional vector. The voxel intensity vectors are denoted by $x_i(i = 1,2,\dots,N)$ Recall that the goal is to estimatethe class probabilities on each voxel according to the intensity vectors. The probability distribution of the kth tissue class is denoted by,

$p_k(x|\Theta_k)$

which is governed by a set of parameters Θ_k. Given the parameters of all the classes, the probability distribution of each voxel can be described as a mixture of probability distributions as follows:

$$p(x|\Theta_k) = \sum_{k=1}^{k} a_k\, p_k(x|\Theta_k) \qquad \text{……..(1)}$$

where a_k denotes the mixture coefficients. The parameter set of this distribution is Θ = (a_1, ……, a_k, Θ_1,….., Θ_k) with the constraint that

$$\sum_{k=1}^{k} a_k = 1$$

Typically, $p_k(x|\Theta_k)$ is modeled by a Gaussian distribution with mean μ_k and covariance matrix Σ_k That is :

$$p_k(x|\Theta_k) = p_k(x|\mu_k, \Sigma_k) \qquad \text{……..(2)}$$

$$= \frac{1}{\sqrt{\det(2\pi\Sigma_k)}} e^{-(x-\mu_k)^T \Sigma_k^{-1}(x-\mu_k)/2}$$

Maximum likelihood (ML) estimation is a common used method to find the probability distribution parameters. The log-likelihood expression for this density from the data X is given by:

$$\log(L(\Theta|X)) = \log \prod_{i=1}^{N} P(x_i|\Theta) \qquad \text{……..(3)}$$

$$= \sum_{i=1}^{N} \log\left(\sum_{k=1}^{K} a_k\, p_k(x_i|\Theta_k)\right)$$

Finding the ML solution directly from Eq. (3) is difficult because it contains the log of the sum. The EM algorithm is a good way to solve this problem [3]. The iterative solution for finding the parameters at the (t+1)th iteration step is as follows:

$$a_k^{t+1} = \frac{1}{N}\sum_{i=1}^{N} P(k|x_i, \Theta^t) \qquad \text{.....(4)}$$

$$\mu_k^{t+1} = \frac{\sum_{i=1}^{N} x_i\, p(k|x_i, \Theta^t)}{\sum_{i=1}^{N} p(k|x_i, \Theta^t)} \qquad \text{.....(5)}$$

$$\sum\nolimits_k^{t+1} = \frac{\sum_{i=1}^{N} = P(k|x_i, \Theta^t)\,.(x_i - \mu_k^{t+1})(x_i - \mu_k^{t+1})^T}{\sum_{i=1}^{N} p(k|x_i, \Theta^t)} \qquad \text{.....(6)}$$

$$P(k|x_i, \Theta^t) = \frac{a_k^t p_k(x_i|\Theta_k^t)}{p(x_i|\Theta^t)}$$

$$P(k|x_i, \Theta^t) = \frac{a_k^t p_k(x_i|\Theta_k^t)}{\sum_j^k a_j^t\, p_j(x_i|\Theta_j^t)} \qquad \text{.....(7)}$$

Taking the mixing parameters a_k as prior probabilities, the probability of each class can be computed using Bayes' rule:[4,5,6]

RESULTS

The proposed method of classified (the general multi-dimensional Gaussian mixture model is described and solved by Expectation-Maximization (EM) algorithm). is perform by visual basic. Frist input a vectorial volume X, the number of classes K. Second, Initialization of $\Theta, p_k(x|\Theta_k)$. Any classification method could be used , we choose K-means. Third, calculate the prior probability by Eq.(7). Fourth, compute the new parameter data according to Eqs. (4), (5), and (6). Finaly, repeat steps Second- Fourth until reaching the end condition. **w**e can notice that the final regions are not homogeneous as expected because of the noise. Six initial land use and land cover classes producing from this method (Water bodies, Rural areas, grass land, vegetable-field, bar land, and Plateaus) .successful land use and land cover classification allowed to identify relationship between land use and land cover change and urban expansion. These results illustrate in fig.(3) and fig.(4).

CONCLUSION

The classification process was applied on image satellite using a geographic information systems program. In order to isolate the areas of water and monitoring the area covered by water. Then compared the results of classification for each year with the other year, the classification results indicated:-

1. Studing the topography of the area around Alrazaza Lake to conclusion, decline water in the lake.
2. Catchment area around the lake supplied it quantity from rainfall that cannot be overlooked, but because of the low rainfall led to low water levels which is influential.
3. Because of the scarcity of water and causing water to recede significantly in Razaza Lake. Therefore, fish and many animals that lived in the lake have become almost non-existent, and this has affected many of those working in fishing and also those who work in the grazing.

REFERENCES

1. A. S. Chintan, M.K. Arora, and K. V. Pramod, "International Journal of Remote Sensing", 25, (2004), 481-487.
2. A. A. Zaeen, "Using remote sensing techniques to monitoring and evaluate the water cover in AL-Razzaza lake: Iraq at different periods" Iraqi Journal of physics, 2012, vol. 10, no. 17, pp. 45-52.
3. Hui Tang, Jean-Louis Dillenseger, and Li Min Luo "A Vectorial Image Classification Method Based On neighborhood Weighted Gaussian Mixture Model"
4. R. Fisher, S.Perkins, A.Walker and E. Wolfart "Classification" 2003
5. Schowengerdt, Robert A Remote sensing:models and methods for image processing (3rd ed.). Academic Press. p. 2. ISBN 978-0-12-369407-2. 2007
6. Šarić, M., Dujmić, H., & Russo, M Scene TextExtraction in HSI Color Space using K meansAlgorithm and Modified Cylindrical Distance. 2013

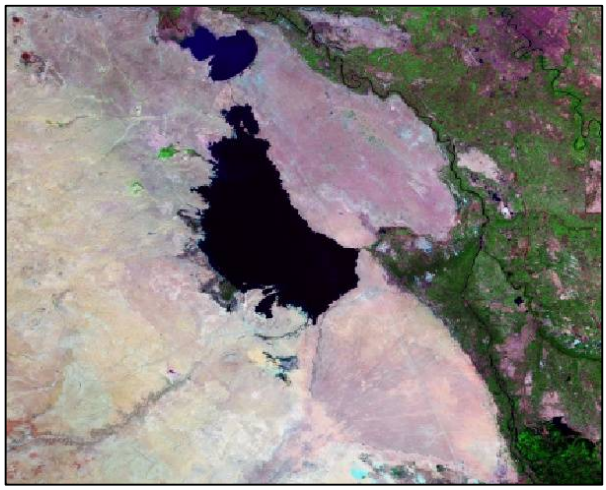

Figure (1): Landsat satellite image for Razaza Lake producted in 2002 and surrounding area.

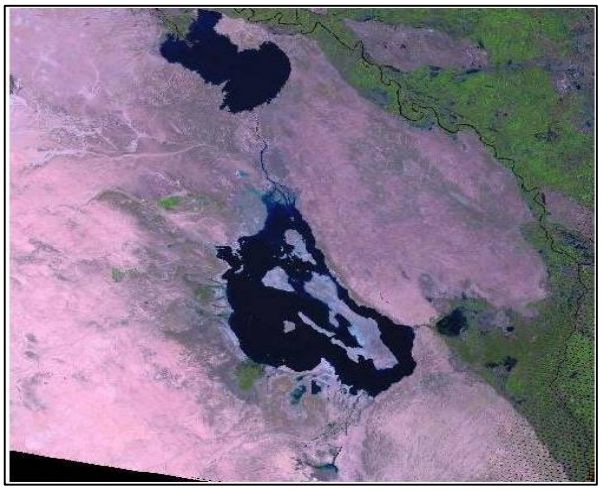

Figure (2): Landsat satellite image for Razaza Lake producted in 2008 and surrounding area

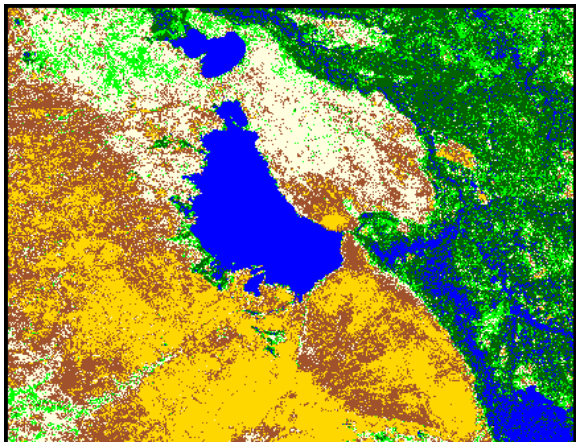

Figure (3): Applied classification method on the scene taken from Landsat+ satellite Image at 2002

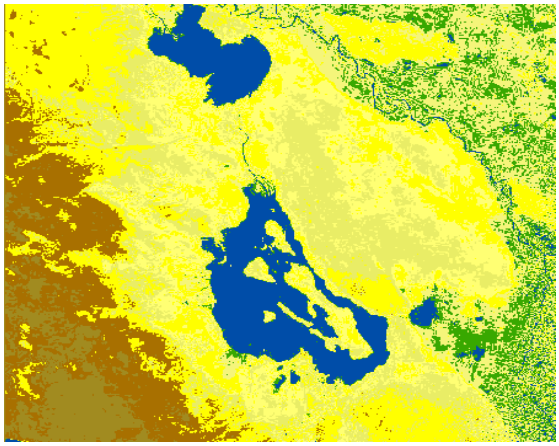

Figure (4): Applied classification method on the scene taken from Landsat+ satellite Image at 2008.

Indian Journal of Natural Sciences www.tnsroindia.org.in ©IJONS

Vol.9 /Issue 51 / December / 2018 *International Bimonthly* *ISSN: 0976 – 0997*

RESEARCH ARTICLE

Complete Guidence for Traveling People using Multi- Source Big Social Media Dataset

M.ArunKumar[1]*, A. Nagarajan[2] and J.Jeganathan[1],

[1]Assistant Professor, Department of Information Technology, PSNA College of Engineering and Technology, Dindigul, Tamil Nadu, India.

[2]Professor, Department of Mathematics, PSNA College of Engineering and Technology, Dindigul, TamilNadu, India.

Received: 18 Aug 2018 Revised: 23 Sep 2018 Accepted: 25 Oct 2018

***Address for Correspondence**
M.ArunKumar
Assistant Professor,
Department of Information Technology,
PSNA College of Engineering and Technology,
Dindigul, Tamil Nadu, India.
Email: Kmarun_vicky@yahoo.co.in

ABSTRACT

Travelling, tourist and community visit are the major activities of human moving from one place too therplaces for prayer, entertainment, education, and occasions and so on.Mostofthe travelling people find out an unknown location in newly travelling city, they enquire road-side people or use social websites. Information obtained from social websites and other person guidance can provide upto60% location information.The main objective of this paper is to provide a high recommendation based guidance for travelling people through out the world.The guidance provides detailed information about the place, time to visit, distance to be travelled, direction and cost.This approach provides a better guidance for decision making in the origin itself. Motto of Travelling from oneplace to otherplace in the world varies. People take a tour for education, community, search in gand entertainment. GPS, GPRS are some the technologies helping people to travel from one place too therplace but these technologies needs technical updates interms of mobile and coverage.The existing systems follow the travel recommendations but they struck in certain place and cannot extend by them selves. In this paper, an Automatic Topical Package Model (ATPM) is proposed for the travelers where it gives the complete informationa bout their destination place.

Keywords: NLP,ATPM,POI,CF,GPS,ATCF.

INTRODUCTION

Travelling, tourist and community visit are the major activities of human move from oneplace to other places for prayer, entertainment, education, occasions and soon. Most of the travelling people find out an unknown location in newly travelling city, they enquire road-side people orusesocial website.Information obtained from social websites and otherperson guidance can provide upto60% location information. Using recommendation is an important problem in both research and industry.

Relatedwork

GPS Estimation for the Places of Interest from

Social Users' Uploaded Photos

Social media has become a very popular way for people to share their photos with friends. Because most of the social images are attached with GPS (geo-tags), a photo's GPS information can be estimated with the help of the large geo- tagged image set while using a visual searching based approach. This paper proposes an unsupervised image GPS location estimation approach with hierarchical global feature clustering and local feature refinement. It consists of two parts: an offline system and an online system. In the offline system, ahierarchical structureis constructed for a large-scale offline social image set with GPS information. Representative images are selected for each GPS location refined cluster, and an inverted file structure is proposed. Inthe online system, when given an input image, its GPS information can be estimated by hierarchical global clusters selection and local feature refine mentin the online system.Both the computational cost and GPS estimation performance demonstrates the effectiveness of the proposed hierarchical structure and inverted file structure in our approach.

AuthorTopicModel-Based Collaborative FilteringforPersonalized POI Recommendations

From social media has emerged continuous needs for automatic travel recommendations. Collaborative filtering (CF) is the mostwell-known approach. However, existing approaches generally suffer from various weaknesses. For example, sparsity can significantly degrade the performance of traditional CF. If auser only visits very few locations, accurate similar user identification becomes very challenging due to lack of sufficient information for effective inference. Moreover, existing recommendation approache soften ignore richuser information like textual descriptions of photos which can reflect users' travel preferences. The topicmodel (TM) method is an effective way to solve the –sparsityproblem, ll but is still far from satisfactory. In this paper, an author topic model- based collaborative filtering (ATCF) method is proposed to facilitate comprehensive points of interest (POIs) recommendations for socialusers. Inourapproach, user preference topics, suchas cultural, cityscape, or landmark, are extracted from the geo-tag constrained textual description of photos via the author topic model instead of only from the geo-tags (GPS locations). Advantages and superior performance of our approach are demonstrated by extensive experiments onalarge collections.

Probabilistic sequential pois recommendation viacheck-in data

While on the go, people are using their phones as a personal concierge discovering what is around and deciding what to do. Mobile phone has become are commendation terminal customized for individuals. While existing research predominantly focuses on one-steprecommendation— recommending the next single activity according to current context, this work moves one step beyond by recommending as eriesofactivities,whichisa packageof sequential Points of Interest (POIs).The recommended POIs are not only relevant to user context (i.e.,current location, time,andcheck-in), but also personalized to his/her check-in history. We presents aprobabilistic approach, which is

highly motivated from a large-scale commercial mobile check-in data analysis, to ranking a list of sequential POI categories (e.g., –Japanese food‖ and–bar‖) and POIs (e.g.,–Ilovesushi‖). The approach enables users to plan consecutive activities on the move. Specifically, the probabilistic recommendation approach estimates the transition probability from one POI to another, conditioned on current context and check-in history in a Markov chain.Toalleviatethediscretization errorandsparsityproblem,we furtherintroduce contextcollaboration and integrateprior information. Experiments on over 100 kreal-world check-in records and 20k POIs validate the effectiveness of the proposed approach.

Design

Data Description in GPS trajectory

This GPS direction data set was gathered in (Microsoft Research Asia) Geolife extend by 178 clients in a time of more than four years (from April 2007 to October 2011). A GPS direction of this data set is spoken to by a group in gof time-stamped focuses, each of which contains the data of scope, longitude and elevation. These directions were recorded by various GPS lumber jacks and GPS phones, and have an as sortment of testing rates.

Trajectory file

Each and every organizer of this data set stores a client's GPS log documents, which were changed over to PLT design. Each PLT document contains a solitary direction and is named by its beginning time.To stay away from potential dis array of time zone, weutilize GMT in the date/ time property of every point, which is not quite the same a sourpast discharge.

Checkindata

Big Data Testing Strategy

Testing Big Data application is progressively a confirmation of its information preparing as opposed to testing the individual elements of the product item. With regards to Big information testing, execution and utilitarian testing are the key.

Geotags

Geotagging is the way toward adding land data to different media as metadata.The information as a rule comprises of directions like scopeand longitude, yetmay even incorporate bearing, elevation, separation and placenames. Geotagging is most generally utilized for photos and can help individuals getaton of particular data about where the photo was taken or the correct area of a companion who signed on to an administration.

Blogs

Ablog is a regularly redesigned online individual diary or journal. It is a place to express you to the world. A place to share your musings and your interests. Truly, it's anything you need it to be. For our motivations we'll say the tablogis your that you will upgrade on a continuous premise. Blogis a short frame for the word weblog and the two word sare utilized conversely.

Module Description

To defeat the issues confronted in the current methodologies, here it is proposed a Topical Package Model (TPM) learning technique to consequently mine client travel enthusiasm from two online networking, group contributed photographs and travel logs. To address the primary test, we consider client's topical enthusiasmas well as the utilization capacity and inclination of going by time and season. Since, it is difficult to directly measure the similarity between user and route, we build a topical package space, and mapbothuser's and route's textual descriptions to the topical package space to get user topical package model (user package) and route topical package model (route package) under topical package space**.** The main contributions of this paper are concluded as: Our work is a personalized travel recommendation rather than a general recommendation. We automatically mine user's travel interest from user contributed photo collections including consumption capability, preferred time and season which is important to route planning and difficult to get directly. We recommend personalized POI sequence rather than individual travel POIs. Famous routes are ranked according to the similarity between user package and route package, and to pranked famous routes are further optimized according to social similar users' travel records. We propose Topical Package Model (TPM) method to learn users and route's travel attributes. It bridges the gapof user interest and routes attributes. We take advantage of the complementary of two big social media for this.

Travel recommendation

Topic package space is a kind of space in which the four travel distribution sofeach topic are described by representative tags mined from travelog ues which describe POIs with in the same topic. A topical package is creating dusing online and offline inputs. The offline inputs provide travelogues and community contributed photos. The online input provides the collection photos in various domains like temple, beach, park and Iceland etc. First, we select sentences containing numbers.And then we utilizenatural language processing (NLP) to learn the featureofeach sentence. We use–faridanimat lab NLP ǁ to process each sentence. The basic idea is as follows. For eachsentence, first, we pass it through–comment Sanitizer ǁ. Then we initialize global hash map. For each word in the resulting string, first, wepass the word to –porter Stemmer ǁ .Then if the word is not in your hash map, addit. If it is, just addoneto its value. Do the same thing for the global hashmap. Then we take the values in your hash map that have value>=n, for example, n=3, and store thos e keys as a header. For each hash map of a sentence, we present it using headers.

Personalized travel recommendation

The second step is to train a text classifier with positive samples and negative samples. We manually mark 500 positive samples and 500 negative samples. We define thes entences, which contain cost information (e.g., ticket fee) as positive samples. Sentences, which contain numbers not related to cost, are defined as negative samples. After training the classifier, we put the sentences containing numbers in to the classifier to test whether a sentence is related to cost. We use the sentences which are both related to cost and from the travelogues of the topic to mine the cost information about this topic. We calculated the mean value of then umbers appeared in these sentences. It mainly consists of the ticket cost of the POI and some times also including catering cost and transportation cost. Notice that although the tickets fee for adults and children are different, the mean cost could still distinguish cheap and expensive things. Due to the structure of travelogues, that topic layer is the parent layer of POI layer, we first mine the cost and time distribution for each POI, then use the average cost and time distribution to present the topic.

Travel sequence and travel package recommendation

The entire proposed approach hastwomodulesas

Location based CF firstly mined similar users according to location co-occurrence and Second, POIs are recommended according to similar users' voting. To do this, it is constructed a topical package space by the combination of two social media: travelogues and community- contribute photos. To construct topical package space, travelogues are used to mine representative tags, distribution of cost and visiting time of each topic, while community-contributed photos are used to mine distribution of visit ingtimeo feach topic.

Advantages

Fast Guidance for travelling people Efficiency in term softime and Cost Increase the country incomeby providing very good tourist guide for people from abroad countries

CONCLUSION

The existing studies have n't well solved the two challenges suchas: Most of the travel recommendation works only focused on user topical interest mining but without considering other attributes like consumption capability. And the next challenge, existing studies focused more on famous route mining but with out automatically mining user travel interest. Despite everything it remains a test for most existing attempts to give both "customized" and "consecutive" travel bundle proposal. However, there are still some limitations of the current system. Firstly, the visiting time of POI mainly presented the open time through travelogues, and it was hard to get more precise distributions of visiting time only through travelogues. Secondly, the current system only focused on POI sequence recommendation and did not include transportation and hotel information, which may further provide convenience for travel planning. In the future, we plan to enlarge the dataset, and thus we could do there commendation for somenon-famous cities. We planto utilize more kinds of social media (e.g., check-indata, transportation data, weather fo recast etc.) To provide more precise distributions of visiting time of POIs and the context-awarerecommendation.

REFERENCES

1. H.Liu,T. Mei,J.Luo,H.Li, and S.Li,–Finding perfect rendezvous onthe go: accurate mobile visual localization and its applications to routing,‖ in Proceedings of the 20thA CM international conference on Multimedia. ACM,2012,pp.9–18.
2. J.Li,X.Qian,Y.Y.Tang,L.Yang, and T.Mei,–Gps estimation for places of interest from social users' uploaded photos,‖ IEEE Transactionson Multimedia,vol.15,no.8,pp.2058–2071,2013.
3. S.Jiang, X.Qian, J.Shen, Y.Fu, and T.Mei,–Author topic model based collaborative filtering for personalized poi recommendation,‖ IEEE Transactions onMultimedia,vol.17,no. 6,pp.907–918,2015.
4. J. Sang, T. Mei, andC. Sun, J.T. and Xu, –Probabilistic sequential poisrecommendation via check-in data,‖ in Proceedings of ACM SIGSPATIAL International Conference on Advances inGeographic Information Systems. ACM,2012
5. Y.Zheng, L. Zhang, Z. Ma, X. Xie, and W. Ma,—Recommending friends and locations based on individual location history,‖ ACM Transactions on the Web, vol. 5, 2011
6. H. Gao, J. Tang, X. Hu, and H. Liu, —Content- aware point of interest recommendation on location- based social networks,‖ in Proceedings of 29th International Conference on AAAI. AAAI, 2015.
7. Q. Yuan, G. Cong, and A. Sun, —Graph-based point-of-interest recommendation with geographical and temporal influences,‖ in Proceedings of the23rd ACM International Conference on Information and Knowledge Management. ACM, 2014, pp. 659–668

8. H. Yin, C. Wang, N. Yu, and L. Zhang, —Trip mining and recommendation from geo-tagged photos,‖ in IEEE International Conference on Multimedia and Expo Workshops. IEEE, 2012, pp.540–545.
9. Y. Gao, J. Tang, R. Hong, Q. Dai, T. Chua, and R. Jain, —W2go: a travel guidance system by automatic landmark ranking,‖ in Proceedings of the international conference on Multimedia. ACM,2010, pp. 123–132
10. X. Qian, Y. Zhao, and J. Han, —Image location estimation by salient region matching,‖ IEEE Transactions on Image Processing, vol. 24, no. 11, pp. 4348–4358, 2015
11. A. Cheng, Y. Chen, Y. Huang, W. Hsu, and H. Liao, —Person-alized travel recommendation by mining people attributes from community- contributed photos,‖ in Proceedings of the 19th ACM international conference on Multimedia. ACM,2011, pp. 83–92.
12. Q. Liu, Y. Ge, Z. Li, E. Chen, and H. Xiong,—Personalized travel package recommendation,‖ in IEEE 11th International Conference on Data Mining. IEEE, 2011, pp. 407–416.

Fig. 1.Geotaggedphotos

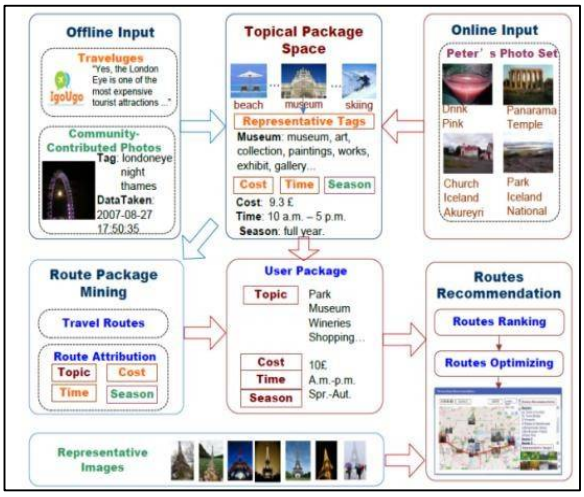

Fig 2. Route Recommendations

Indian Journal of Natural Sciences www.tnsroindia.org.in ©IJONS

Vol.9 /Issue 51 / December / 2018 *International Bimonthly* *ISSN: 0976 – 0997*

RESEARCH ARTICLE

Influence of Target Metal and Laser Pulse Energy on the Plasma Temperature and Electron Density in LIPS Technique

Qusay Adnan Abbas*

Department of Physics, Collage of Science, University of Baghdad, Baghdad, Iraq.

Received: 26 Aug 2018 Revised: 28 Sep 2018 Accepted: 02 Nov 2018

***Address for Correspondence**
Qusay Adnan Abbas
Department of Physics,
Collage of Science,
University of Baghdad,
Baghdad, Iraq.
Email ; Qusayiraqi@yahoo.com

ABSTRACT

The optical emission spectroscopy from laser induced Al and Fe plasmas generated by a 1064 nm radiation at different argon pressure, was recorded between 320 and 740nm. The population level distribution and the corresponding temperatures were obtained using Boltzmann plots method. While the electron densities were determined using Saha-Boltzmann method. The influence of target properties, laser energy and gas pressure on the emission spectra, electron temperature and electron density were studied. Our observations show that increasing of the emission intensity with increasing of pulse laser energy. The target properties did not effect on the behavior of emission intensity with pulse laser energy. The properties of target and pressure have different behavior on the strongest emission intensity of plasma. the ionization energy of metal target shown inversely proportional with electron temperature. The electron temperature shows slight reduction with increasing of pulse laser energy for both plasmas. The target properties did not effect on the behavior of the variation of electron density with increasing of pulse laser energy. Moreover, the electron density of plasma would be greater for smaller metal ionization potential.

Keywords: LIPs, Electron Temperature, Electron Density, OES, Boltzmann plot method, Saha- Boltzmann method.

INTRODUCTION

Laser-induced plasmas (LIP) (usually termed Laser Induced Plasma/Breakdown Spectroscopy (LIPS or LIBS) technique has proved to be useful spectroscopic sources for the direct elemental characterization of almost every type

of material [1]. The basic principle of LIPS is based on exciting matter target (solid, liquid or gas) to plasma state through irradiation by high power laser pulses[1,2].This technique represent one of the important technique in the field of elemental analysis, because of its simplicity and usually inexpensive hardware [3,4]. Additionally, LIBS requires little or no sample preparation and can provide simultaneous multi-element analysis. Therefore, LIBS has been used for a wide variety of applications, such as material analysis [4], preparation of thin films [5] environmental monitoring [6,7], biological identification [8-10] and other application of LIBS could be seen in references[11,12].

Among the various diagnostic techniques which are convenient tools for detecting various transient species from UV up to IR spectral regions, optical emission spectroscopy (OES) has definite advantages pertaining to high spatial and temporal resolution without perturbation of the laser-induced plasma [13]. OES was used to analysis the emission light that emitted from plasma plume which generated by irradiation pulse laser with target. In this work, OES is used to analysis of emitted light of plasma plume which generated from irradiated of Al and Fe targets by Q-switched Nd:YAG laser in vacuum. The influence of target metal, gas pressure and laser energy pulse on the plasma temperature and electron density will investigate in more details.

MATERIALS AND METHODS

The experimental set up of LIPs system that used for the detection and identification of spectral lines of laser-produced Al and Fe plasmas in vacuum demostrated in figure (1). The targets were irradiated by Q-switched Nd: YAG pulses laser (9 ns duration time, 6 Hz frequency, and wavelength at 1064nm) with energy pulse ranging from 100 to 400 mJ to generation of Al and Fe plasmas. The laser was focused on targets by using the convex lens of focal length 10 cm to induce plasma plume. The rectangular targets (length of 4 cm and width of 2 cm) are placed on the holder inside a vacuum chamber. The vacuum chamber consisted from a cylindrical stainless steel tube with four ends. The two ends closed by Pyrex windows, by two stainless steel flanges, and with small quartz window fixed in it is center, that allows for a laser pulse to shoot the targets. Two small pipes connected to pumping systems, one of them connected to pressure gauge which used to determination of vacuum pressure while the other was used to deliver the argon gas (with purity of 99.9%).

RESULTS AND DISCUSSION

Emission Spectra of Al and Fe plasmas

Optical emission spectroscopy technique is mainly based on collecting the emission from ionic, atomic species in a Al and Cu plasmas spark. All elements emit in the spectral range of 320-740 nm.

Aluminum Target

Figure (2) illustrated the effect of gas pressure on the emission light spectra that emitted from Al target that irradiated by Q-switched Nd:YAG laser at 1064 nm wave length for different pulse energy. This spectrum clearly shows that many peaks appearance which associated to atomic and ionic species of Al element. The intensity of all peaks that appear from surface irradiation of Al target by laser increased with increasing of pulse energy. This increasing attributed to transfer of laser energy to the target either by directly by excited electrons, indirectly by photons or through other types by collisions [14]. Figure (3) shows LIBS spectra intensity of two strongest intensities peak associated to Al III at wavelength 452.79nm and 569.69nm versus increasing pressure. The results show there is a slight increase in intensity of both wavelengths when the Ar pressure is increased above 0.2 torr. However, Pressures near 0.4 torr and above result in rapid reduction in emission intensity with increasing pressure for both wavelengths. The increasing of emission intensity with increasing pressure can be explained as; as the pressure increases, so does the frequency of collisions between Ar and Al, which results in increased emission intensity of both strongest Al III

lines. This result agrees with reference [15]. The reduce in the line intensities observed with increasing of pressure may be due to the fact that the density of the ablation plasma produced under a high pressure ambient argon atmospheres is very high, the self-absorption of the spectral lines emitted within the "optically-thick" ablation plasma could be very important and leads to the apparent reduction in emission line intensities.

Iron Target

Figure (4) illustrates the effect of gas pressure and pulse laser energy on the emission spectra of Fe plasma. Many Peak lines of atomic and ionic species of Fe element can observe in this figure. The increases of all types of collisions and the absorptions of laser beam photons by the Fe target are responsible for the increasing of emission intensity of plasma. Figure (5) demonstrate LIBS spectra intensity of two strongest intensities peak associated to Fe I at wavelength 481 nm and 492 nm versus increasing pressure. The curves of the figure (5) indicate that the increase of pressure causes to rapid reduction in the emission light when the Ar pressure is increased above 0.2 Torr. In addition, pressure near 0.4 Torr and above result shows a slight increase in intensity of both wavelengths. Reduce in the emission intensities attributed to the self-absorptions of the spectral lines emission of Fe plasma which finally leads to reduction in the emission intensity. While the increasing of emission intensities that associated with increasing of pressure may be attributed to the increasing of many types of collisions between Ar and Fe with increasing of Ar pressure. The comparison between Figures (3) and (5), shown that the variation of the properties of the laser target causes to variation of LIBS characteristics.

Influence of Target Properties on the Electron Temperature

In this section, the electron temperature (Te) of Al and Fe plasmas is determined by employing Boltzmann plot method of the selected Al –III and Fe-I lines. If we consider the plasma in local thermal equilibrium (LTE) case, so the Boltzmann plot method represents the probable method to determine the electron temperature. The Boltzmann plot method can be written as [16, 17]:

$$Ln\left(\frac{I_Z\lambda_{ki,Z}}{g_{k,Z}A_{ki,Z}}\right) = \frac{1}{k_B T_e}E_{k,Z} + ln\left(\frac{h\,cL_{n,Z}}{4\pi P_z}\right) \quad \text{.....1}$$

where the index z refers to the ionization stage of the species (where z=0 and 1 corresponding to the neutral and singly ionized atom, respectively), kB, Iz , λ ki,z Ek,z ,gk,z,Aki,z, , h, c, L and A is the Boltzmann constant, the integrated intensity of a species in ionization stage Z, the transition line wavelength, the energy of the upper level k, degeneracy of the upper level k, the transition probability, the Planck constant, speed of light, the characteristic length of the plasma and the partition function of the species in ionization stage Z, respectively. This equation yields the linear plot (Boltzmann plot method), where the electron temperature determined from the slope of lift- hand side of equation (1) against the upper level energy.

Aluminum Plasma

The electron temperature (Te) measurement for Al plasma is developed from Boltzmann plot method using six Al III emission spectral lines at wavelengths (361, 415.1, 451.2, 452.8, 569.7 and 572.4) nm at pulse laser energies 200, 400, 600, 800 and 1000 mJ. Table (1) shows the spectral lines of Al III and their atomic data. Using equation (1) and table (1) and plotting $Ln\left(\frac{I_z\lambda_{ki,z}}{g_{k,z}A_{ki,z}}\right)$ versus Ek,z should yields a straight line with a slope equal to (-1/ KB Te).

Iron Plasma

By using the same method that described in section 3.2.1, the electron temperature was calculated. However, the electron temperature for Fe plasma is determined using seven emission spectral lines at the wavelengths (404.6, 467.7, 472, 481, 492, 501.4 and 516.7) nm and pulse laser energy 200, 400, 600, 800 and 1000 mJ. Table (2) indicates the emission spectral lies of Fe I and their atomic data. By using the same technique that used in the previous section, the electron temperature of Fe plasma was calculated.

Influence of Target Properties on the Electron Temperature

Figure (6) display influence of target properties on the variation of electron temperature versus laser energy for Al and Fe plasmas at different laser energy. Many features can be seen in this figure, the electron temperature is inversely correlated to the ionization energy of metal target. This behavior can be explain as; For metals with lower ionization energy, It was found that Te notably increases mainly due to the smaller amount of energy imparts for the ionization of vapor plume and more accessible energy is available to heat plasma. Consequently, it leads to the higher electron temperatures. Moreover, the change of Te with increasing of gas pressure showed a slight reduction of Te with increasing of laser energy for both plasmas. This behavior may be due to the increasing of electron-atom collisions which lead to decrease in the electron temperature.

Influence of Target Properties on the Electron Density

By using atom and ion spectral lines emitted from the Al and Fe plasmas, the electron density is calculated from the Saha-Boltzmann equation as [19]:

$$n_e = \frac{I_Z^*}{I_{Z+1}^*} 6.04 \times 10^{21} (T)^{3/2} \times \exp\left[\left(-E_{k,Z+1} + E_{k,Z} - x_Z/k_B T\right)\right] \text{ cm}^{-3} \quad \text{.....2}$$

where $I_Z^* = I_Z \lambda_{ki,Z} / g_{k,Z} A_{ki,Z}$ and x_z is the line intensity from the k-i transition and the ionization energy of the species in the ionization stage Z, respectively.

Figure (7) demonstrated the effect of pulse laser energy on the electron density at Al and Fe plasmas for different pressures. The data indicates that the increasing of pulse energy shown a slight increment in the electron density for both plasmas under study. Moreover, the electron density of plasma would be greater for smaller metal ionization potential mainly caused by the mass ablation and consequent denser vapor plasma plume create higher electron density.

CONCLUSIONS

In summary, the influence of pulse laser energy on the emission spectra of Al and Fe plasmas that produced by Q-switched Nd: YAG laser with 1064nm at different argon pressure was investigated. The data shows that the increasing of laser energy shows increasing of the emission spectra for both plasmas at different gas pressure. This result means that the properties of laser target did not effect on the behavior of emission spectra. The target properties and gas pressure has different behavior on the strongest emission intensity of plasma. Moreover, the effect of target properties on the electron temperature shows the inversely proportional of the electron temperature with the ionization energy of metal target. While the variation of electron temperature with gas pressure shown a slight reduction of electron temperature with increasing of pulse laser energy for both plasmas. Finally, the influence of target properties on the behavior of electron density with the pulse laser energy and the electron density values was

investigated too. The data shows that the target properties did not effect on the behavior of the variation of electron density with increasing of pulse laser energy. Moreover, the electron density of plasma would be greater for smaller metal ionization potential.

ACKNOWLEDGMENTS

The results presented here were obtained during experiments carried out on laser facilities access through the Plasma Laboratory in department of Physics- Collage of Science- University of Baghdad. I sincerely thank all the technical and administrative staffs of this laboratory for their assistance and their essential contribution for obtaining these results

REFERENCES

1. M. A. Khater,"Influence of Laser Pulse Energy on VUV Emission from Laser Plasmas Under Various Ambient Conditions", Rom. Journ. Phys., vol. 58, no. 1–2, pp. 181–192, 2013.
2. Q. A. Abbas," Optical Emission Spectroscopy Study of Fe Plasma at Atmospheric Pressure", PARIPEX – Indian Journal of Research, vol. 6, Issue 3, pp. 604-606, 2017.
3. A. M. El Sherbini, A. S. Al Amer, A. T. Hassan and T. M. El Sherbini," Measurements of Plasma Electron Temperature Utilizing Magnesium Lines Appeared in Laser Produced Aluminum Plasma in Air", Optics and Photonics Journal, vol. 2, pp. 278-285, 2012.
4. A. J. Effenberger and J. R. Scott," Effect of Atmospheric Conditions on LIBS Spectra", Sensors,vol. 10, pp. 4907-4925, 2010.
5. J. Haverkamp, R. M. Mayo, M. A. Bourham, J. Narayan and C. Jin and G. Duscher, " Plasma plume characteristics and properties of pulsed laser deposited diamond-like carbon films", JOURNAL OF APPLIED PHYSICS, vol. 93, no. 6, pp. 3627-3634, 2003.
6. X. Yu, Y. Li, X. Gu, J. Bao, H. Yang and L. Sun, " Laser-induced breakdown spectroscopy application in environmental monitoring of water quality: a review", Environ Monit Assess, vol. 186, pp. 8969–8980, 2014.
7. E. Asamoah and Y. Hongbing, "Influence of laser energy on the electron temperature
1. of a laser-induced Mg plasma ",Appl. Phys. B, vol. 123, no. 22, pp. 1-6, 2017.
8. S. J. Rehse, H. Salimnia and A. W. Miziolek," Laser-induced breakdown spectroscopy (LIBS): an overview of recent progress and future potential for biomedical applications ", Journal of Medical Engineering & Technology, vol. 36, no.2, pp. 77–89, 2012.
9. M. Baudelet, L. Guyon, J. Yu, J. P. Wolf, T. Amodeo, E. Fréjafon and P. Laloi," Femtosecond time-resolved laser-induced breakdown spectroscopy for detection and identification of bacteria: A comparison to the nanosecond regime ",JOURNAL OF APPLIED PHYSICS, vol. 99, pp. 084701-1-084701-9, 2006.
10. V. K. Singh, V. Kumar, J. Sharma, Y. Khajuria, and K. Kumar," Importance of Laser Induced Breakdown Spectroscopy for Biomedical Applications:A Comprehensive Review", Mater. Focus, vol. 3, no. 3, pp. 169-182, 2014.
11. D. M. Díaz Pace, G. Bertuccelli, and C. A D'Angelo," Characterization of laser - induced plasmas by atomic emission spectroscopy ", Journal of Physics: Conference Series 274, 012076, pp.1-21, 2011.
12. M. Capitellia, A. Casavolaa, G. Colonnab, A. De Giacomoa, "Laser-induced plasma expansion: theoretical and experimental aspects ",Spectrochimica Acta Part B, vol. 59, pp. 271–289, 2004.
13. J. J. Camacho, M. Santos, L. Dıaz and J. M. Poyato," Optical emission spectroscopy of oxygen plasma induced by IR CO2 pulsed laser ", J. Phys. D: Appl. Phys., vol. 41, pp.1-13, 2008.
14. M. R. Leahy-Hoppa, J. Miragliotta, R. Osiander, J. Burnett, Y. Dikmelik, C. McEnnis and J. B. Spicer," Ultrafast Laser-Based Spectroscopy and Sensing: Applications in LIBS, CARS, and THz Spectroscopy ",Sensors, vol. 10, pp. 4342-4372, 2010.

15. A. J. Effenberger and J. R. Scott," Effect of Atmospheric Conditions on LIBS Spectra ",Sensors, vol.10, pp. 4907-4925, 2010.
16. W. T. Mohamed," Study of the Matrix Effect on the Plasma Characterization of Six Elements in Aluminum Alloys using LIBS With a Portable Echelle Spectrometer ", PROGRESS IN PHYSICS, vol. 2, pp. 42-49, 2007.
17. M. Hanif, M. Salik and M. A. Baig, "Diagnostic Study of Nickel Plasma Produced by
2. Fundamental (1064 nm) and Second Harmonics (532 nm) of an Nd: YAG Laser," Journal of Modern Physics, vol. 3, pp. 1663-1669, 2012.
18. https://www.nist.gov/pml/atomic-spectra-database.
19. V. K. Unnikrishnan, K. Alti, V. B. Kartha, C. Santhosh, G. P. Gupta and B. M. Suri, " Measurements of plasma temperature and electron density in laser-induced copper plasma by time-resolved spectroscopy of neutral atom and ion emissions",PRAMANA- journal of physics,vol:74, no. 6, pp. 983-993, 2010.

Table (1): Emission spectral lines of Al III and their ionic data [18]

Wavelength (nm)	Spectrum	Ag (s^{-1})	E_i (eV)	E_k (eV)
361	Al III	2.90E+08	14.377022	17.808269
415.1	Al III	1.15E+09	20.555031	23.541636
451.2	Al III	8.36E+08	17.808269	20.555031
452.8	Al III	1.66E+08	17.818203	20.555031
569.7	Al III	3.51E+08	15.642348	17.818203
572.4	Al III	1.73E+08	15.642348	17.808269

Table (2): Emission spectral lines of Fe I and their atomic data [18]

Wavelength (nm)	Spectrum	Ag (s^{-1})	E_i (eV)	E_k (eV)
404.6	Fe I	6.45E+05	2.27860464	5.3411181
467.7	Fe I	6.00E+03	1.55735732	4.20888324
472	Fe I	4.73E+05	2.99035242	5.61584513
481	Fe I	6.00E+05	3.57321887	6.1501651
492	Fe I	1.25E+08	2.86539122	5.38520737
501.4	Fe I	4.60E+06	4.28330823	6.75602278
516.7	Fe I	1.60E+04	0	2.39920469

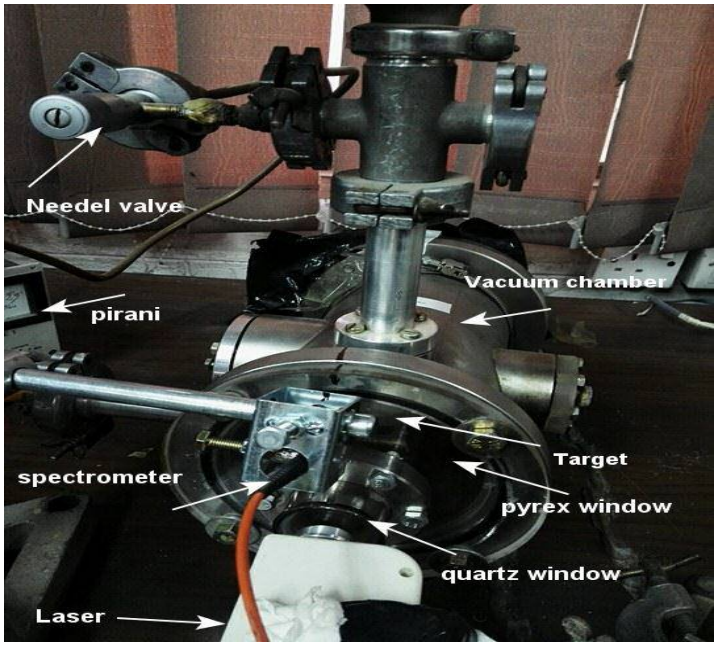

Figure (1): The experimental set up of LIBS system

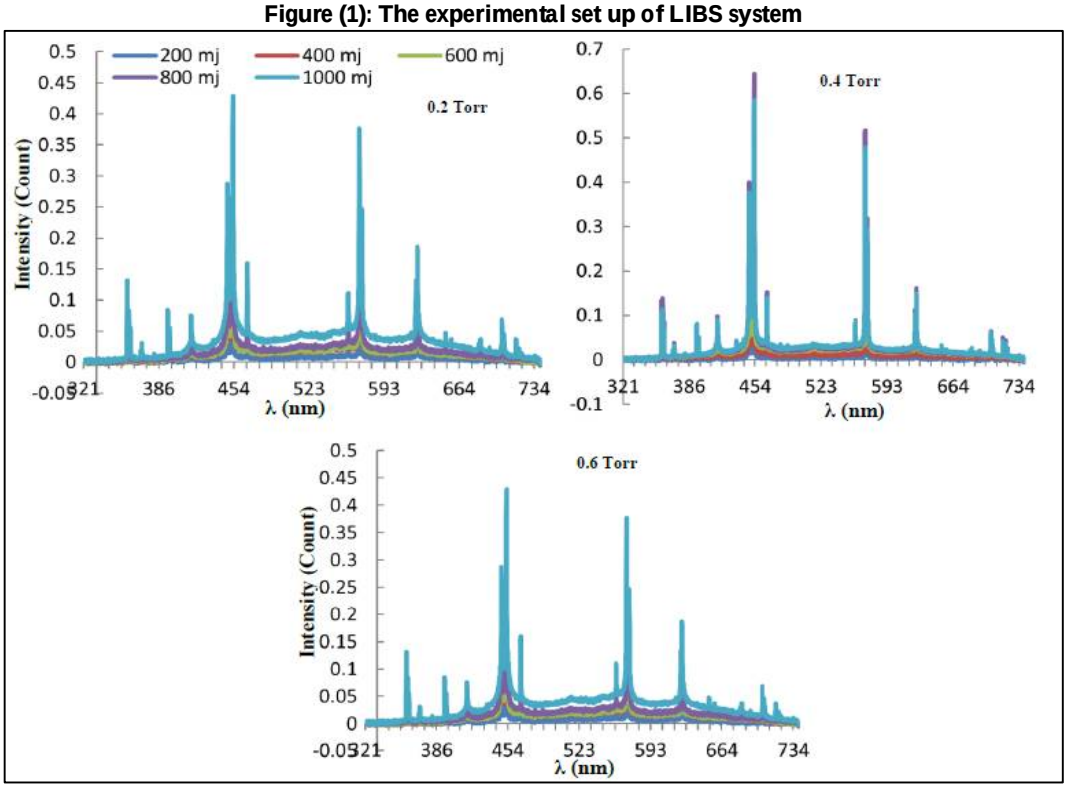

Figure (2): Influence of gas pressure on the emission spectra of Al plasma at different pulse energy

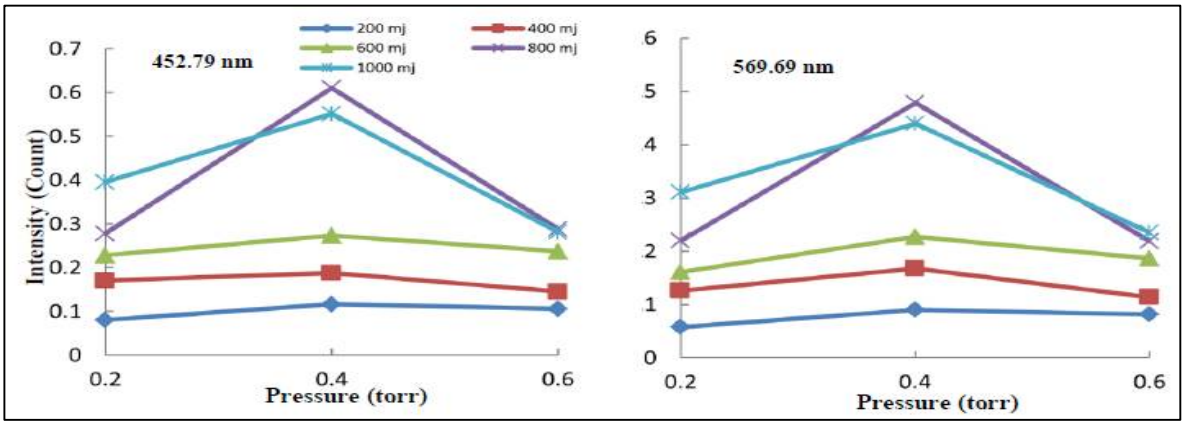

Figure (3): Emission intensity versus gas pressure for 452.79 and 569.69 nm of Al III

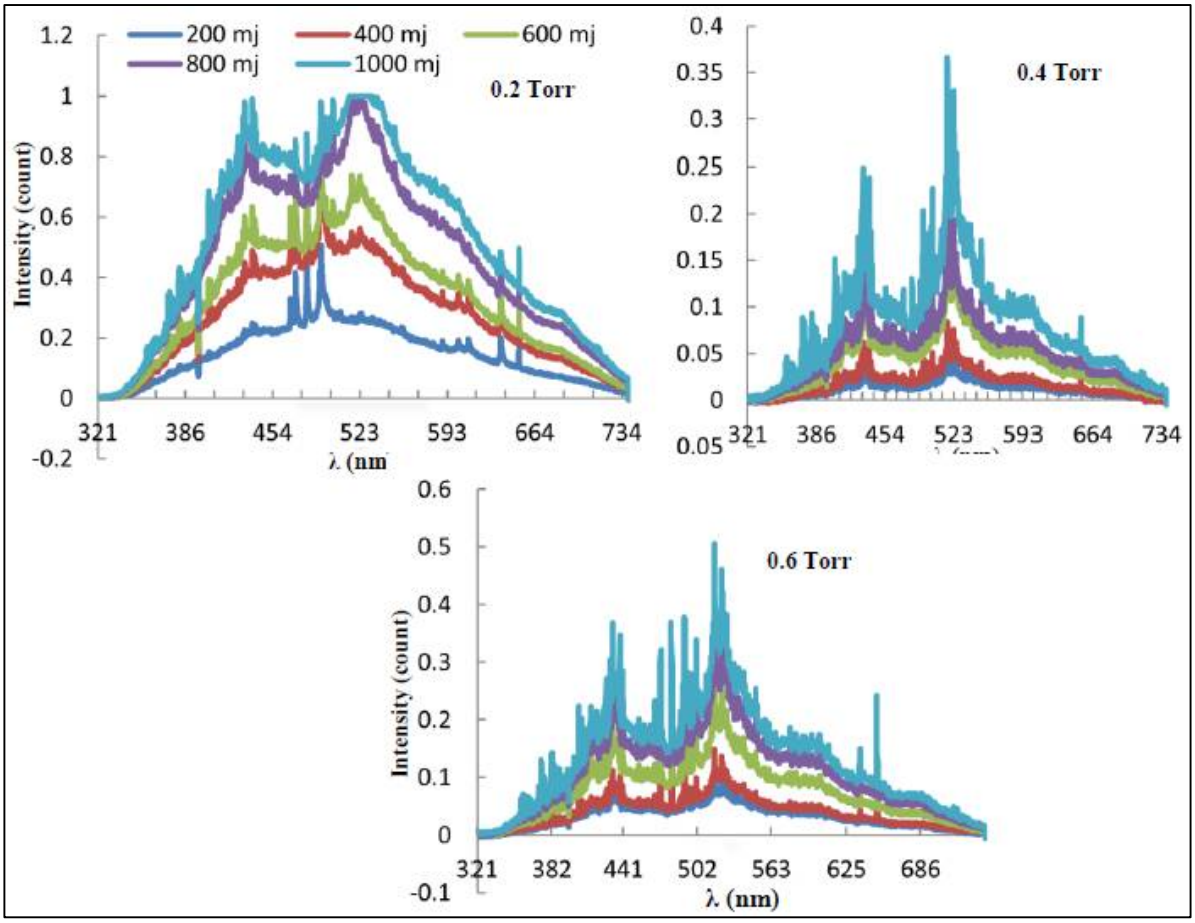

Figure (4): Effect of pressure on the emission light of Fe plasma at different pulse laser energy

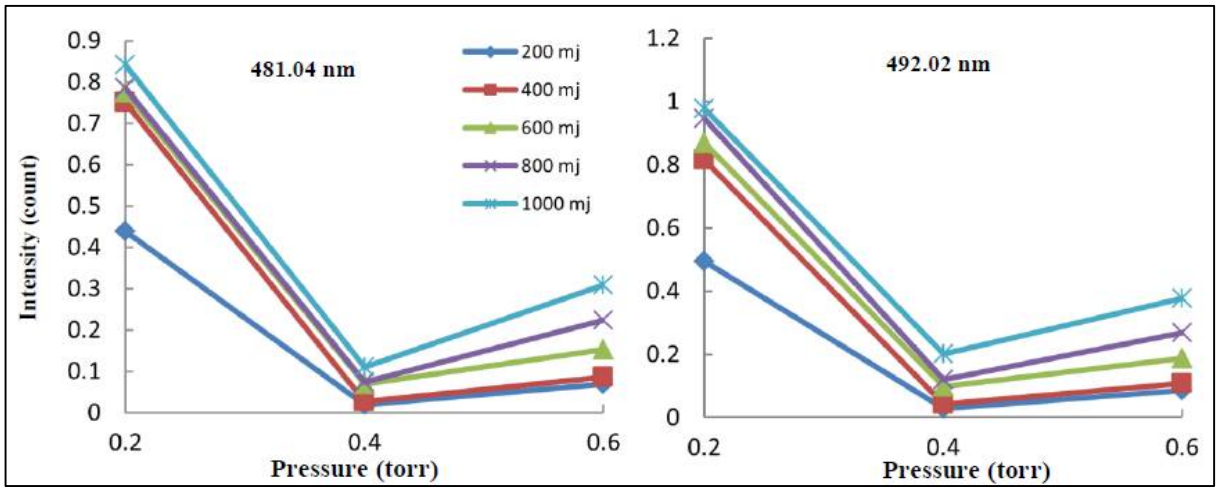

Figure (5): LIBS emission intensities of Fe at different pulse energy and gas pressure of the wavelength 481.04nm and 492.02 nm

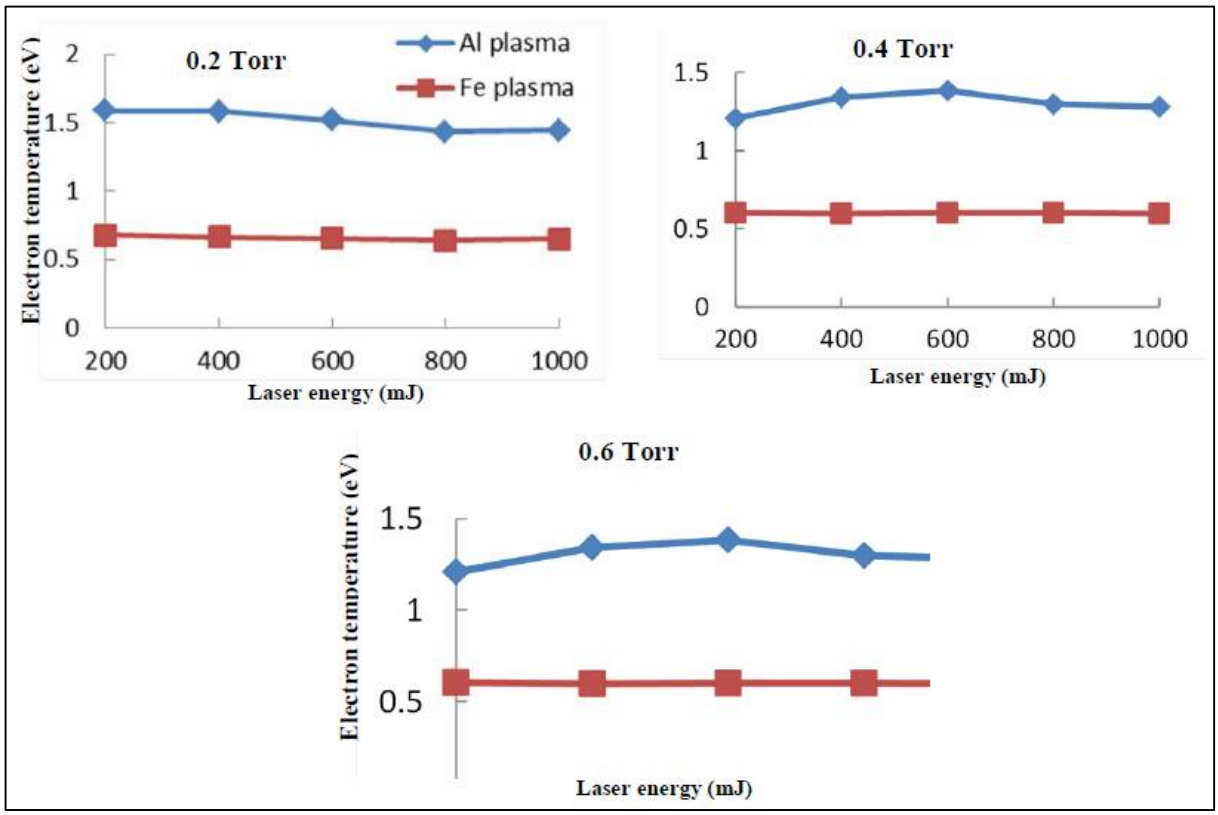

Figure (6): Variation of electron temperature with laser energy at different gas pressure

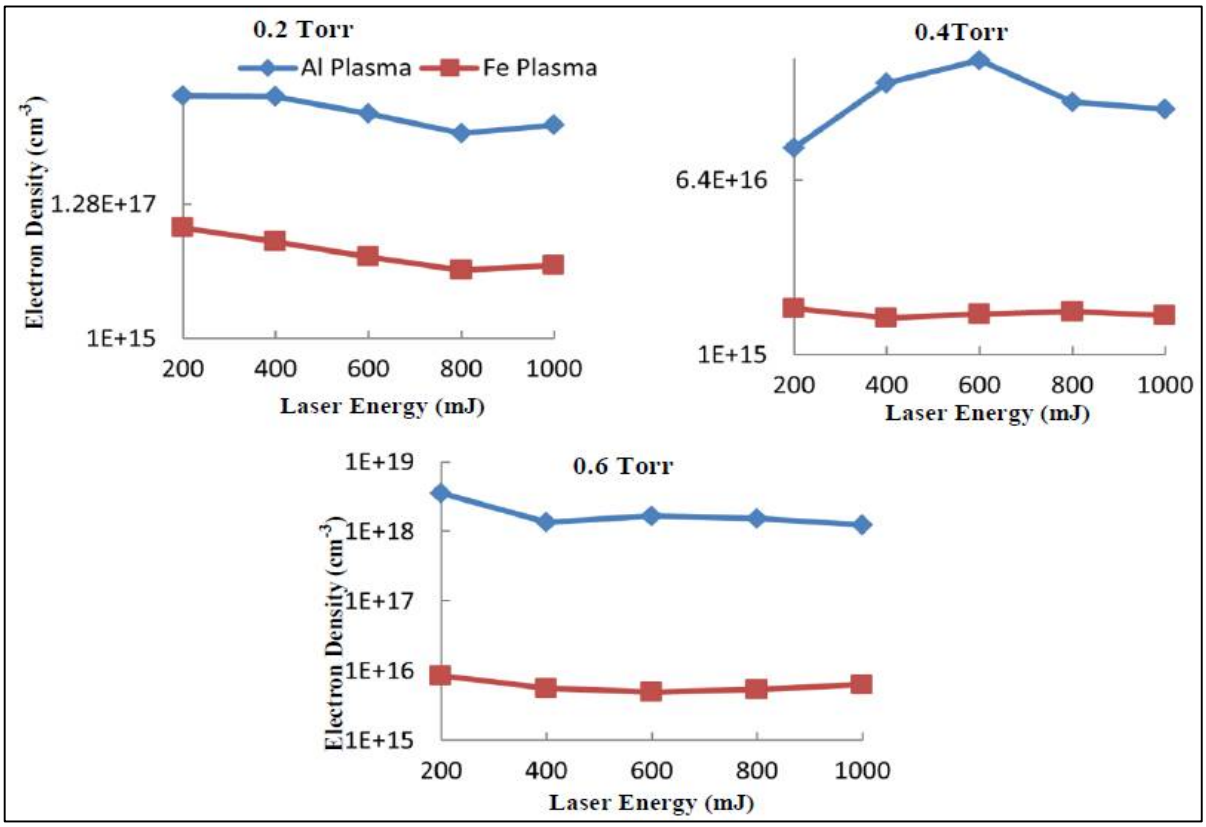

Figure (7): The variation of electron density with pulse laser energy for Al and Fe plasmas at different pressure.

Indian Journal of Natural Sciences www.tnsroindia.org.in ©IJONS

Vol.9 /Issue 51 / December / 2018 *International Bimonthly* *ISSN: 0976 – 0997*

RESEARCH ARTICLE

Elastic Electron-Selenium Scattering

Altaf A. Al- Rahmani* and Sarah.Sh.Mutar

Department of Physics, College of Science for Women, University of Baghdad, Baghdad, Iraq.

Received: 24 Aug 2018 Revised: 26 Sep 2018 Accepted: 01 Nov 2018

***Address for Correspondence**

Altaf A. Al- Rahmani

Department of Physics,
College of Science for Women,
University of Baghdad,
Baghdad, Iraq.
Email:mutar.s41@yahoo.com

ABSTRACT

The charge momentum distributions (CMD) and the elastic electron scattering form factors F(q) of the ground state for some medium mass nuclei in the fp shell such as ^{74}Se, ^{76}Se, ^{78}Se, ^{80}Se and ^{82}Se are presented and offered the usageof the Coherent Density Fluctuation Model (CDFM) and expressed in terms of the fluctuation function (weight function) $|F(x)|^2$. The fluctuation function has been associated with thecharge density distribution (CDD) of the nuclei and determined from the theory and experiment.The difference of the CDDfor the isotope pair (^{80}Se -^{78}Se) has been also calculated to demonstrate the affect of the extra two neutrons on the CDD. The property of the long-tail behavior at high momentum region of the charge momentum distribution has been obtained by both the theoretical and experimental fluctuation functions. The calculated form factors F(q) on Z=34 isotopicare compared to available experimental data.

Keywords: difference of the CDD($\Delta\rho$);Chargemomentum distributions; Longitudinal charge Form Factors;Coherent Density Fluctuation Model (CDFM); Weight function $|f(x)|^2$.

INTRODUCTION

Electron scattering off nuclei is a powerful tool for studies of nuclear structure and spectroscopy [1-11]. It allows to determine the charge distribution of nuclear ground states, as well as of the transition charge and current densities from the state to excited states. More global properties can be extracted from a detailed knowledge of charge distribution, like charge radii. Parameters characterizing the extension and surface thickness of the nuclear density can also be derived[12, 13]. As nuclear studies extend beyond the stability valley and far into the unstable region, nuclear physicists found it necessary to extend the studies of nuclear properties using electron scattering to unstable nuclei. Using the radioactive-isotope techniques [14,15], a next-generation electron-nucleus collider, part of the

MUSES project[16], has been designed and the construction is now in progress at RIKEN in Japan. The new collider is for the structure study of unstable nuclei by electron scattering. It is necessary that the relevant theoretical research on electron scattering off unstable nuclei. Antonov et al.[17] calculation of form factors for unstable neutron-rich isotopes of light, medium and heavy nuclei(He, Li, Ni, Kr, Sn) are presented and compared to those of stable isotopes in the same isotopic chain. For He and Li the proton and neutron densities are obtained within a microscopic large scale shell model, while for Ni, Kr and Sn the densities are calculated in deformed self consistent mean field Skyrme HF+BCE method. Calculation carried out both in plan wave Born approximation and in distorted wave Born approximation. Karataglids et al.[18] the elastic and inelastic electron scattering form factors for several neutron-rich exotic nuclei (He, Li, B) are presented.

The results have been obtained using large space no core shell model. While the elastic scattering form factors are insensitive to the details of the neutron density, it is found that inelastic scattering may be influenced be extensive neutron distributions. Wang et al.[19] have calculated the charge form factors of elastic electron scattering on light proton rich nuclei on the N=8, 10, 20 and 28 isotonic chain using the relativistic eikonal approximation with the charge densities generated by the RMF model. The results show that the occupation of the$2s_{1/2}$ state by protons has a great influence on the charge density distribution and consequently on the charge form factors. Gaidarov[20] was investigated the charge form factors, charge and matter densities and the corresponding ems radii for even-even isotopes of Ni, Kr, and Sn in the framework of deformed self consistent mean field SkyrmeDDHf+CS method.The nucleon momentum distributions for the same isotopic chain of neutron-rich nuclei are studied in the framework of the same mean field method, as well as of theoretical correlation methods on light-front dynamics and local density approximation.Al-Rahmani and Hussein[21] have studied the charge density distributions CDD and elastic electron scattering form factors of some $2s-1d$ shell nuclei utilizing the PWBA and illustrated that the inclusion of the higher $1f-2p$ shell in the calculations leads to produce a good results in comparison with those of the experimental data.

AL-Rahmani A.A.[22] has been studied the nucleon momentum distributions and elastic electron scattering form factor of the G.S for^{19}F,^{25}Mg,^{27}Al and ^{29}Si nuclei in the framework of the coherent density fluctuation model and expressed in terms of weight function$|f(x)|^2$. The experimental form factors for elastic electron scattering from ^{19}F and^{29}Si nuclei are well reproduced by the monopole form factors. It is found that the contribution of the quadrupole form factors in^{25}Mg and ^{27}Al nuclei which are describe by theunder formed 2S-1d shell nuclei, was essential for obtained a notable accordance the experimental and theoretical form factors.Al-Rahmani and Faris[23] have calculated the EES and PMD of the ground state for Ge isotopes by using the Coherent Density Fluctuation Model and expressed in terms of the fluctuation function (weight function). In addition, through her study the calculated the difference of the CDD of Ge isotopes to illustrate the influence of the extra two neutrons on the CDD.we give in this paper detailed formulae derived for the calculation of densities, momentum distributions and form factors.Sara and Al-Rahmani [24]calculated the ground state proton momentum distributions and elastic charge form factors for ^{88}Sr and ^{89}Y nuclei have been derived and studied using the Coherent Density Fluctuation Model and formulated by means of the fluctuation functionweight function$|f(x)|^2$. Illustrative applications to the even-mass $^{74-82}Se$ have permitted to analyses the main features of our method. Firstly we derived a theoretical form for CDD based on the use of the single particle (HO) wave functionand the occupation numbers of the state. The derived form of the CDD is employed in determining the theoretical weight function which is used in the CDFM to study the CMD and the elastic longitudinal form factors.

Theory

The charge density distribution of one –body operator can be written respectively, as [22]

$$\rho_c(r)=\frac{1}{4\pi}\sum_{nl}\eta_{nl}\,2(2l+1)\left|R_{nl}(r)\right|^2 \qquad (1)$$

where $\rho_c(r)$ is the charge density distribution of nuclei, η_{nl} is the proton occupation probability of the state nl (η_{nl} = 0 or 1 for closed shell nuclei and 0 < η_{nl} < 1 for open shell nuclei) and $R_{nl}(r)$ is the radial part of the single-particle harmonic oscillator wave function. To derive an explicit form for the CDD of fp shell nuclei, it is assumed that there is a core of filled $1s$ and $1p$ and 1d shells and the proton occupation numbers in $2s, 1f$, $2p$ and 1g shells are equal to $(2-\delta_{1g})$, $(Z-20-\lambda_{2p}), (\lambda_{2p})$ and δ_{1g} respectively, for consider nuclei, instead of 2, $(Z-20)$,0 and 0 as in the simple shell model. Using this assumption in equation (1), we obtain form for the ground state CDD in $2p-1g$ shell nuclei as

$$\rho_c(r)=\frac{1}{4\pi}\left\{\begin{array}{l}2|R_{10}(r)|^2+6|R_{11}(r)|^2+(2-\delta_{1g})|R_{20}|^2+10|R_{12}(r)|^2\\+(Z-20-\lambda_{2p})|R_{13}|^2+\lambda_{2p}|R_{21}|^2+\delta_{1g}|R_{14}|^2\end{array}\right\} \quad (2)$$

where Z is the atomic number of nuclei, the parameter δ_{1g} characterizes the deviation of the proton occupation numbers from the prediction of the simple shell model ($\delta_{1g}=0$), the parameter λ_{2p} is assumed as a free parameter to be adjusted in order to obtain the agreement with the experimental charge density distribution. After introducing the form of $R_{nl}(r)$ with a harmonic oscillator size parameter b in Eq.(2), an analytical form for the ground state CDD of the $2p-1g$ shell nuclei is expressed as

$$\rho_c(r)=\frac{e^{-r^2/b^2}}{\pi^{3/2}b^3}\{(5-\frac{3}{2}\delta_{1g})+[2\delta_{1g}+\frac{5}{3}\lambda_{2p}](\frac{r}{b})^2+[4-\frac{2}{3}\delta_{1g}-\frac{4}{3}\lambda_{2p}](\frac{r}{b})^4 +[\frac{8Z}{105}-\frac{160}{105}+\frac{20\lambda_{2p}}{105}(\frac{r}{b})^6+[\frac{16}{945}\delta_{1g}](\frac{r}{b})^8\} \quad (3)$$

The mean square charge radius (MSR) of the considered 2p-1g shell nuclei can be written as : [2,3]

$$\langle r^2\rangle=\frac{4\pi}{Z}\int_0^\infty \rho_c(r)r^4dr \quad (4)$$

The normalization condition of the $\rho_c(r)$ is given by [2,3]

$$Z=4\pi\int_0^\infty \rho_c(r)r^2dr \quad (5)$$

And the corresponding MSR is

$$\langle r^2\rangle=\frac{b^2}{Z}\{-30+\frac{37}{2}\delta_{1g}-\frac{9}{2}Z\} \quad (6)$$

The central $\rho_c(r=0)$ is obtained from Eq. (3) as

$$\rho_c(0)=\frac{1}{\pi^{3/2}b^3}\left\{5-\frac{3}{2}\delta_{1g}\right\} \quad (7)$$

The parameter δ_{1g} can be determined from the central CDD of Eq. (6) as

$$\delta_{1g} = \frac{2}{3}\left\{5 - \pi^{3/2} b^3 \rho_c(0)\right\} \quad (8)$$

In Eq. (8), the values of the central density, $\rho_c(0)$, are taken from the experiments while the harmonic oscillator size parameter b is chosen in away so that to reproduce the experimental root mean square charge radii $\left\langle r^2 \right\rangle_{\exp}^{1/2}$ of the considered nuclei.

The experimental charge density distribution of the 2PF is given by [11].

$$\rho(r) = \rho_0 /(1 + \exp((r-c)/z)) \quad (9)$$

The momentum distribution is a single particle observable and thus allows only an indirect measurement of correlation effects. In particular the uncertainties in the determination of an optimal one-body Hamiltonian lead to uncertainties in the analysis of the momentum distribution with respect to correlation effect. Nevertheless, a carful analysis of the momentum distribution may give some indications of the importance of correlation effects. The CMD $n(k)$, for the $2p-1g$ shell nuclei is studied by using two distinct methods. In the first method, it is determined by the shell model using the single-particle harmonic oscillator wave functions in momentum representation and expressed as:

$$n(k) = \frac{b^3 e^{-x^2/b^2}}{\pi^{3/2}} \left[\begin{array}{l} 5 - \frac{3}{2}\delta_{1g} + \{2\delta_{1g} + \frac{5}{3}\lambda_{2p}\](bk)^2 \\ + \{\frac{12}{3} - \frac{2}{3}\delta_{1g} - \frac{4}{3}\lambda_{2p}\}(bk)^4 \\ + \{\frac{8Z}{105} - \frac{160}{105} + \frac{20\lambda_{2p}}{105}\}(bk)^6 + \{\frac{16}{945}\delta_{1g}\}(bk)^8 \end{array} \right] \quad (10)$$

while in the second method, the $n(k)$ can be determined by the CDFM, where the mixed density is given by [2,3]

$$\rho(\vec{r},\vec{r}') = \int_0^\infty |f(x)|^2 \rho_x(\vec{r},\vec{r}')dx \quad (11)$$

since

$$\rho_x(\vec{r},\vec{r}') = 3\rho_0(x)\frac{j_1(k_F(x)|\vec{r}-\vec{r}'|)}{k_F(x)|\vec{r}-\vec{r}'|} \times \theta\left(\vec{x} - \frac{|\vec{r}+\vec{r}'|}{2}\right) \quad (12)$$

is the density matrix for Z protons uniformly distributed in the sphere with radius x and density

$\rho_0(x) = 3Z/4\pi x^3$. The Fermi momentum is defined as [2,3]

$$k_F(x) = \left(\frac{3\pi^2}{2}\rho_0(x)\right)^{1/3} \equiv \frac{V}{x}; \qquad V = \left(\frac{9\pi}{8}Z\right)^{1/3} \quad (13)$$

and the step function θ, in Eq. (12), is defined by

$$\theta(y)=\begin{cases}1, & y\geq 0\\ 0, & y<0\end{cases} \quad (14)$$

According to the density matrix definition of Eq.(11), one-particle density $\rho(r)$ is given by its diagonal element as [21,22]

$$\rho_c(r)=\rho_c(r,r')\,|_{r=r'}=\int_0^{\infty}|f(x)|^2\rho_x(r)dx \quad (15)$$

In Eq. (15), $\rho_x(r)$ and $|f(x)|^2$ have the following forms [2,3]

$$\rho_x(r)=\rho_0(x)\theta\left(x-|\vec{r}|\right) \quad (16)$$

$$|f(x)|^2=\frac{-1}{\rho_0(x)}\frac{d\rho_c(r)}{dr}|_{r=x} \quad (17)$$

The weight function $|f(x)|^2$ of Eq. (17), determined in terms of the ground state $\rho_c(r)$,satisfies the following normalization condition [2,3]

$$\int_0^{\infty}|f(x)|^2dx=1 \quad (18)$$

and holds only for monotonically decreasing $\rho_c(r)$, i.e. $\frac{d\rho_c(r)}{dr}<0.$

On the basis of Eq. (15), the CMD $n(k)$, is given by [2,3]

$$n(k)=\int_0^{\infty}|f(x)|^2 n_x(k)dx, \quad (19)$$

where

$$n_x(k)=\frac{4}{3}\pi x^3\theta\left(k_F(x)-|\vec{k}|\right) \quad (20)$$

is the Fermi-momentum distribution of the system with density $\rho_0(x)$. By means of Eqs. (17), (19) and (20), an explicit form for the CMD is expressed in terms of $\rho_c(r)$ [2,3] as

$$n^{CDFM}(k:[\rho_c])=\left(\frac{4\pi}{3}\right)^2\frac{4}{Z}\times\left[6\int_0^{V/k}\rho_c(x)x^5dx-\left(\frac{V}{k}\right)^6\rho_c\left(\frac{V}{k}\right)\right] \quad (21)$$

with normalization condition

$$Z = \int n^{CDFM}(k)\frac{d^3k}{(2\pi)^3} \quad (22)$$

While the experimental weight functions for considered nuclei determined the two- parameter Fermi (2PF)

$$|f(x)|^2_{2pF} = \frac{4\pi x^3 \rho_0}{3A_z}\left(1+e^{\frac{x-c}{z}}\right)^{-2}\exp\left(\frac{x-c}{z}\right) \quad (23)$$

Where the values of parameters c and z in above equation are taken from experimental data [11] while the constant ρ_0 is determined from the normalization of Eq. (5),

The elastic monopole charge form factors $F_{co}(q)$ of the target nucleus are also expressed in the CDFM as [2,3]:

$$F_{Co}(q) = \frac{1}{Z}\int_0^\infty |f(x)|^2 F(q,x)dx \quad (24)$$

Where the form factor of uniform charge density distribution is given by [2,3]

$$F_{Co}(q) = \frac{3Z}{(qx)^2}\left[\frac{\sin(qx)}{(qx)} - \cos(qx)\right] \quad (25)$$

Inclusion of the correction due to the finite nucleon size $f_{fs}(q)$ and the center of mass correction $f_{cm}(q)$ in the calculation requires multiplying the form factor of Eq. (24) by these corrections

Here, $f_{fs}(q)$ is considered as free nucleon form factor which is assumed to be the same for protons and neutrons [25]

$$f_{fs}(q) = e^{-0.43q^2/4} \quad (26)$$

The correction $f_{cm}(q)$ remove the spurious state arising from the motion of the center of mass when shell model wave function is used and is given by [25]

$$f_{cm}(q) = e^{q^2b^2/4A} \quad (27)$$

Multiplying the right hand side of Eq. (25) by these corrections yields:

$$F_{Co}(q) = \frac{1}{Z}\int_0^\infty |f(x)|^2 F(q,x)dx\ f_{fs}(q)\, f_{cm}(q) \quad (28)$$

It is important to point out that all physical quantities studied above in the framework of the CDFM such as $n(k)$ and $F_{Co}(q)$, are expressed in terms of the weight function $|f(x)|^2$. In the previous work [2,3], the weight function was obtained from the NDD, extracted by analyzing elastic electron-nuclei scattering experiments. In the present work, the theoretical weight function $|f(x)|^2$ is expressed, by introducing the derived CDD of Eq. (3) in to Eq. (17), as

$$|f(x)|^2 = \frac{8\pi x^4}{3Zb^2}\rho_c(x) - \frac{16x^4 e^{-x^2/b^2}}{3Zb^5\pi^{1/2}}\left[\begin{array}{l}\{\delta_{1g}+\frac{5}{2}\lambda_{2p}\}+\{\frac{12}{3}-\frac{2}{3}\delta_{1g}-\frac{4}{3}\lambda_{2p}\}(\frac{x}{b})^2 \\ +\{\frac{12Z}{105}-\frac{240}{105}+\frac{30\lambda_{2p}}{105}\}(\frac{x}{b})^4 \\ +\{\frac{32}{945}\delta_{1g}\}(\frac{x}{b})^6\end{array}\right] \quad (29)$$

RESULTS AND DISCUSSION

In this study, the charge momentum distribution $n(k)$ and elastic electron scattering form factors, F(q) are calculated by using CDFM, for some even 2p-1g shell nuclei, (such as: ^{74}Se, ^{76}Se, ^{78}Se, ^{80}Se and ^{82}Se) isotopes. The distribution $n^{CDFM}(k)$ of Eq. (21) was calculated by means of the CDD which was obtained firstly from theoretical consideration, like in Eq. (3). And then secondly from experimental data [11]. The size parameters b is choice in such a way so as to imitate the experimental root mean square (rms) charge radii of nuclei. The values of δ are determined by Eq.(8). The values of b and $(\lambda_{2p}, \delta_{1g})$ simultaneously with value of the central densities $p_{ex}(0)$ and the root mean square charge radii $\langle r^2\rangle^{1/2}_{\exp}$ for considered nuclei are present in Table1 and Table2.

In Fig. 1, explore the dependence of the CDD (in fm^{-3}) on r (in fm) for ^{74}Se [Fig. 1(a)], ^{76}Se [Fig. 1(b)], ^{78}Se [Fig. 1(c), ^{80}Se [Fig. 1(d)] and ^{82}Se [Fig.1(e)] nuclei. The solid and dotted curves are the measured charge density distributions of the treated nuclei by using Eq. (3) when $\delta_{1g} \neq 0$ and $\delta_{1g} = 0$, respectively while the solid circles correspond to the experimental data [11]. It is noticeable that the dotted curves distribution are poor agreement with the experimental data, particular for small r. Introducing the parameters δ_{1g} and λ_{2p} (i.e., taking into account the higher orbital) into our calculations leads to a good agreement with the experimental data as demorated by the solid curves. In Fig. 2, shows the difference of the charge density distributions (CDD) of the (^{80}Se-^{78}Se) isotopes. The shaded area represents the experimental data with its error bar [28], the dotted curve is the calculated difference of the CDD with $(\lambda_{2p}, \delta_{1g} \neq 0)$, and the solid curve is the calculated difference of CDD by hatree-fock method with a Skyrme potential [11].Its clear from this figure that our calculated result(blue curve) is better representing the data, especially at (r≤3.5 fm) than H.F calculation (red curve). It is seen that the addition two of neutrons to the ^{78}Se nucleus leads to change slightly the distribution of the protons in the shells due to the nuclear interactions that will be happen between these addition neutrons and protons. These interactions lead to some dwindling in the CDD particularly at the central regions of these nuclei, i.e. the additive neutrons leads to increase the probability of transferring the protons from the central region of the nucleus towards its surface.

In Fig. 3, we display the dependence of the $n(k)$ (in fm^3) on k (in fm^{-1}) for ^{74}Se [Fig. 2(a)], ^{76}Se [Fig. 2(b)], ^{78}Se [Fig. 2(c)], ^{80}Se [Fig. 2(d)], ^{82}Se [Fig. 2(e)] nuclei. The long-dashed curves correspond to the CMD's of Eq. (10) evaluated by the shell model calculation used the single particle harmonic-oscillator wave function in the momentum space.The solid circles symbols and solid curves correspond to the CMD's obtained by CDFM of Eq. (21) employing the experimental and theoretical CDD, respectively. It is evident that the behavior of the dash distribution curves estimated by the shell model is in contrast with distributions imitated by the CDFM. The significant property of the long-dashed distribution is the steep slope mode, when k is increases. This behavior is in disagreement with our studies [2,3,26,27] and it is attributed to the fact that the ground state shell model wave function given in terms of

Slater determinant does not take into account the major effect of the short range dynamical correlation functions. Hence, the short range repulsive features of the nucleon-nucleon force are responsible for the high momentum behavior of the CMD [26,7]. The property of long-tail behavior obtained by the CDFM, which is in agreement with the studies [2,3,26,27], is connected to the presence of high densities $\rho_x(r)$ in the decomposition of Eq. (15), though their fluctuation functions $|f(x)|^2$ are small. The CMD of (^{74}Se, ^{76}Se and ^{78}Se) nuclei present in Figs.3 (a), 3 (b) and 3 (c) respectively, show quite well agreement between the calculated data (the solid curve) and the experimental data (solid circles) up to k $\geq$ 2.1 *fm*$^{-1}$, for ^{74}Se nucleus, k $\geq$ 2.3 *fm*$^{-1}$ for ^{76}Se nucleus and k $\geq$ 2.5 *fm*$^{-1}$ for ^{78}Se nucleus while beyond this region they shows an explicit deviation between them. The CMD of ^{80}Se nucleus present in Figs.3 (d) shows a good agreement between the experimental data and calculated data , but there is a deviation between them in two region at (1.9 *fm*$^{-1} \leq k \leq 2.1\, fm^{-1}$) and k$\geq$ 2.5 *fm*$^{-1}$, respectively. The CMD of ^{82}Se nucleus present in Figs.3 (e) shows a goodagreement between the experimental data and calculated data , but there is a deviation between them in two region at (1.9 *fm*$^{-1} \leq k \leq 2.3\, fm^{-1}$) and k$\geq$ 2.4 *fm*$^{-1}$ Besides, This deviation in CMD at large k may be interpreted by the deviation between the calculated charge density distribution and those of the experimental two parameters Fermi by used the charge density equation: $\rho(r) = \rho_0 /(1+\exp((r-c)/z))$ where their parameter is listed in Table1 [11]. Since this deviation affect greatly the PMD's due to the dependence of the CMD on the employed CDD.

The elastic electron scattering charge form factors for the considered nuclei are calculated in the framework of the (CDFM) through introducing the theoretical weight functions $|f(x)|^2$ of Eq. (29) into Eq. (28). In Fig. 4, we present the dependence of the form factors F(q) on the momentum transfer q (in *fm*$^{-1}$) for ^{74}Se [Fig. 4(a)], ^{76}Se [Fig. 4(b)], ^{78}Se [Fig. 4(c)], ^{80}Se [Fig. 4(d)] and ^{82}Se [Fig. 4(e)] nuclei. where the circles are representing experimental data [10]. This figure shows that the diffraction minima and maxima of the considered nuclei are reproduced in the correct places. In all these Fig. 4, Both the behavior and the magnitudes of the calculated form factors of these nuclei are in reasonable agreement with those of the experimental data.

CONCLUSIONS

The (CMD) and elastic electron scattering form factors, calculated in the framework of the (CDFM), are expressed by means of the weight function $|f(x)|^2$. The weight function, which is connected with the local density $\rho(r)$, was determined from experiment and from theory. If neutrons has been added to the nucleus, it may be explained by the proton redistribution due to the nuclear interaction between those additional neutrons and the protons as indicated by the change of the parameters ($\lambda_{2p}, \delta_{1g}$) and (b). The feature of the long-tail behavior of the (CMD) is obtained by both theoretical and experimental weight functions, which is in agreement with the other studies [2,3, 26, 27] and is related to the existence of high densities $\rho_x(r)$ in the decomposition of Eq. (15), though their weight functions are small. The experimental form factors for elastic electron scattering from (^{74}Se, ^{76}Se, ^{78}Se, ^{80}Se and^{82}Se) isotopes are well reproduced by the monopole form factors. It is noted that the theoretical (CDD) of Eq.(3) employed in the determination of the theoretical weight function of Eq.(29) is capable of reproducing information about the *(*PMD) and elastic form factors.

REFERENCES

1. R. Hofstadter,lectron Scattering and Nuclear Structure Rev. Mod. Phys. 28, (1956) 214.
2. A. N. Antonov, P. E. Hodgson and I. ZhPetkov.,Nucleon Momentum and Density Distribution in Nuclei. Clarendon Press, Oxford,(1988)1-165.
3. A. N. Antonov, V. A. Nikolaevand I. Zh. Petkov.,Physik, A297, (1980), 257-260.
4. J Heisenberg and H P Blok Ann., Rev. Nucl., Part. Sci. 33 (1983) 569.
5. H. De Vries, C.W. De Jager, and C.De.Vrise, Nuclear charge density distribution parameters from elastic electron scattering, Atomic Data and Nuclear Data Tables, 36, (1987), 495.
6. B. Frois and C. N. Papanicolas. Ann. Rev. Nucl. Part. Sci, 37, (1987), 133.
7. M. Traini and G. Orlandini,Physik Z., A321, (1985) pp. 479-484.
8. P. E. Hodgson, Hyperfine Interactions,74 (1992), 75.
9. J. D. Walecka, Electron Scattering for Nuclear and nucleon Structure, (Cambridge University Press, Cambridge, 2004)
10. A. A. Khomich, N. G. Shevchenko,E.O. Babichev, A. Yu. Buki, V. N. polishchuk, B. V. Mazanko, and V.P. Sergienko, "Elastic scattering of 225-MeV electrons on ^{74,76,78,80,82}Se" Sov. J. Nucl. Phys. 47(2), 1988.
11. G.Fricke, C. Bernhardt, , K. Heiling, L. A. Schaller, L. Schellenberg, , E.B. Shera, and C. W. Jager , "Nuclear ground state charge radii from electromagnetic interactions",Nucl. Data Table, (1995) 60 -177
12. J Friedrich and N. Voegler, Nucl. Phys. A459, (1982), 192.
13. J Friedrich, N. Voegler and P. G. Reinhard, Nucl. Phys. A459, (1986), 10.
14. I. Tanihata, Prog. Part. Nucl.Phys. 35, (1995), 505.
15. A. Mueller, ProgPart. Nucl.Phys. 46, (2001), 359.
16. T. Suda, M.Wakaugi, Prog Part. Nucl.Phys. 55, (2005), 417.
17. Antonov,A.N., Kadrev,D.N., Gaidarov,M.K., De Guerra,E.M., Udias,J.M., Lukyanov V. K., Zemlyanaya E. V., And Krumova G. Z., Phys. Rev. C72, (2005) 44307.
18. S Karataglidis and K.Amos, AIP Conference Proceeding 1013, (2008), 328.
19. Zaijun Wang,Zhongzhon Ren, Nuclear Physics A 794, (2007), 47.
20. M K. Gaidarov, Journal of Physics: conference Series 381, (2012), 12112
21. A.Al-RahmaiBaghdad Science Journal, 7(2) (2010) 1028; A. Al-Rahmani and H. Husse, Iraqi J. Sci. 55 4B(2014) 1868
22. A. A. AL-Rahmani, International Journal Of Science and Research ; IJSR, 5, 1, (2016)741./A. A. AL-Rahmani, Indian J. Phys. (2016).
23. A. A. Al-Rahmani and F.F. Kaddoori, "Elastic electron scattering from some even-even Ge-isotopes", International journal of science and research, 6, 2, (2017).
24. Sara Shaker Mutor and Altaf Abdul Majeed Al-Rahmani,"Elastic Electron Scattering from ^{88}Sr and ^{89}Y Nuclei",American Journal of Physics and Applications,5(6), (2017), 113
25. V. V. Burov andV. K. Lukyanov 1977 JINR preprint, Dubna R4-11098: V. V. Burov, D. N. Kadrev, V. K. Lukyanov and Yu. S. POl 1998 Phys. At. Nucl.61 525.
26. H.C Moustakidis, and S.E. Massen, .Phys. Rev., C(62). pp: 34318-1 -(2000) 34318-7.
27. M. Dal RI, S. Stringariand O. Bohigas.Nucl. Phys., , A376, (1982) p:81.
28. A. A. Khomich, N. G. Shevchenko, V. N. polishchuk, T. S. Nazarova, B. V. Mazanko, V. I. Kuprikov, and Yu. N. Ranyuk, "Elastic scattering of electrons with energy 225 MeV by the nuclei$^{78-80}$Se", Sov. J. Nucl. Phys. 43(6), (1986).

Table 1: Parameters used in the present calculations forCDD of (^{74}Se, ^{76}Se, ^{78}Se, ^{80}Se and ^{82}Se) nuclei

Nucleus	Type of PDD[25]	$P_{exp}(0)(fm^{-3})$[25] P W eq.(7)	$< r^2 >^{1/2}_{exp}$ (fm)[25]	C(fm)[25]	Z(fm)[25]
^{74}Se	2PF	0.08072234	4.07(2)	4.387(22)	0.6078(7)
^{76}Se	2PF	0.0760315	4.162(10)	4.471(11)	0.6208(39)
^{78}Se	2PF	0.07308028	4.138(14)	4.581(18)	0.5729(41)
^{80}Se	2PF	0.07067005	4.124(10)	4.667(10)	0.5339(42)
^{82}Se	2PF	0.06925115	4.118(11)	4.718(11)	0.5102(49)

Table 2: Calculated parameters used in Eq. (3), to calculate CDD and occupation number in 2p-1g for (^{74}Se, ^{76}Se, ^{78}Se, ^{80}Se and ^{82}Se) nuclei and the calculated $< r^2 >^{1/2}_{cal}$

Nucleus	b	λ_{2p}	$< r^2 >^{1/2}_{cal}$ eq.(6)	Occupation No. of 2s $(2-\delta_{1g})$	Occupation No. of 1f $(Z-20-\lambda_{2p})$	Occupation No. of 2p λ_{2p}	Occupation No. of 1g δ_{1g}
^{74}Se	2.137	2.356	4.07826	1.59286	11.644	2.356	0.40714
^{76}Se	2.161	2.100	4.15845	1.52475	11.900	2.100	0.47526
^{78}Se	2.166	1.910	4.13683	1.42515	12.090	1.910	0.57484
^{80}Se	2.179	1.810	4.12315	1.38620	12.190	1.810	0.61379
^{82}Se	2.192	1.779	4.11681	1.37588	12.221	1.779	0.62411

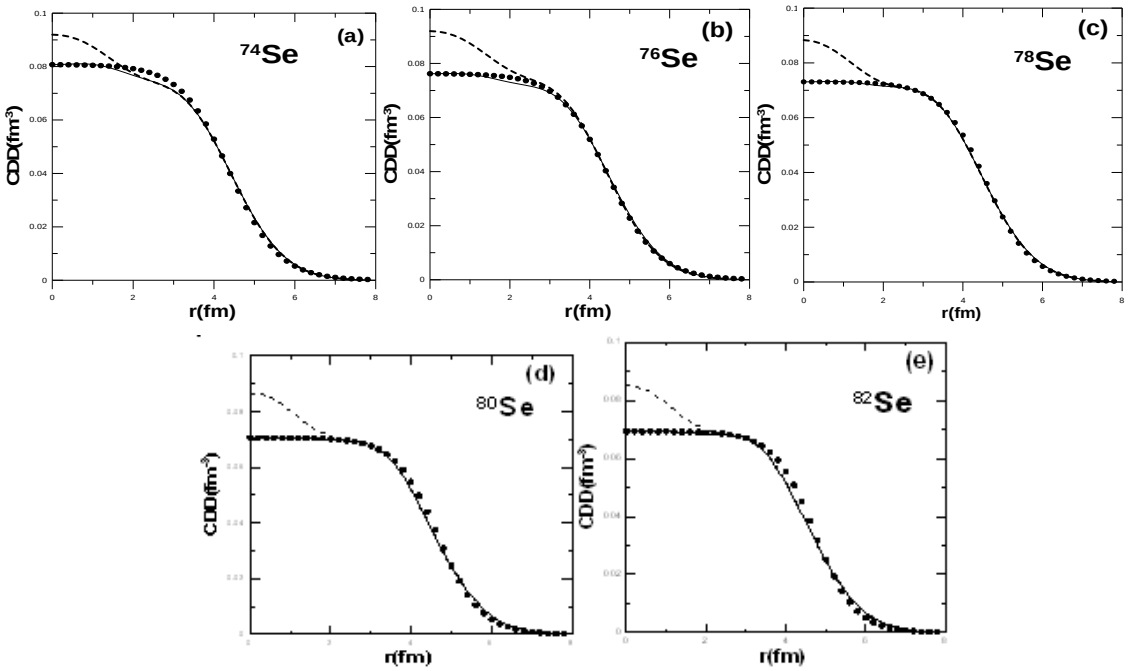

Figure 1.The ground state charge density distribution as a function of r(fm) for (a)^{74}Se, (b)^{76}Se (c)^{78}Se, (d)^{80}Se and (e)^{82}Se nuclei. the solid and dotted curves are the calculated CDD of the treated nuclei by using Eq. (3) when $(\lambda_{2p}, \delta_{1g} \neq 0)$ and $(\lambda_{2p}, \delta_{1g} = 0)$, respectively whereas the solid circles are those fitted to the experimental data of Two Parameter Fermi (2PF) CDD [11].

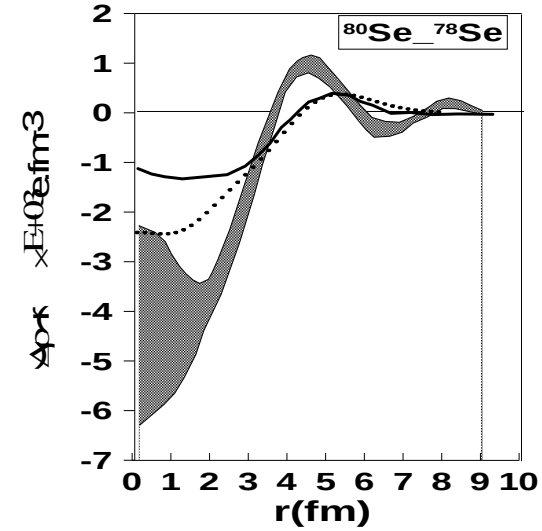

Figure 2.Dependence of the difference of the CDDfor the isotope pair (^{80}Se-^{78}Se) $\Delta\rho(r)$ on (r). The dotted curve is the calculated difference of the *CDD* with $(\lambda_{2p}, \delta_{1g} \neq 0)$. The solid curve is the calculated difference of CDD by Hartree-Fock [28], The shaded area represented the experimental data plotted with the error bands [28].

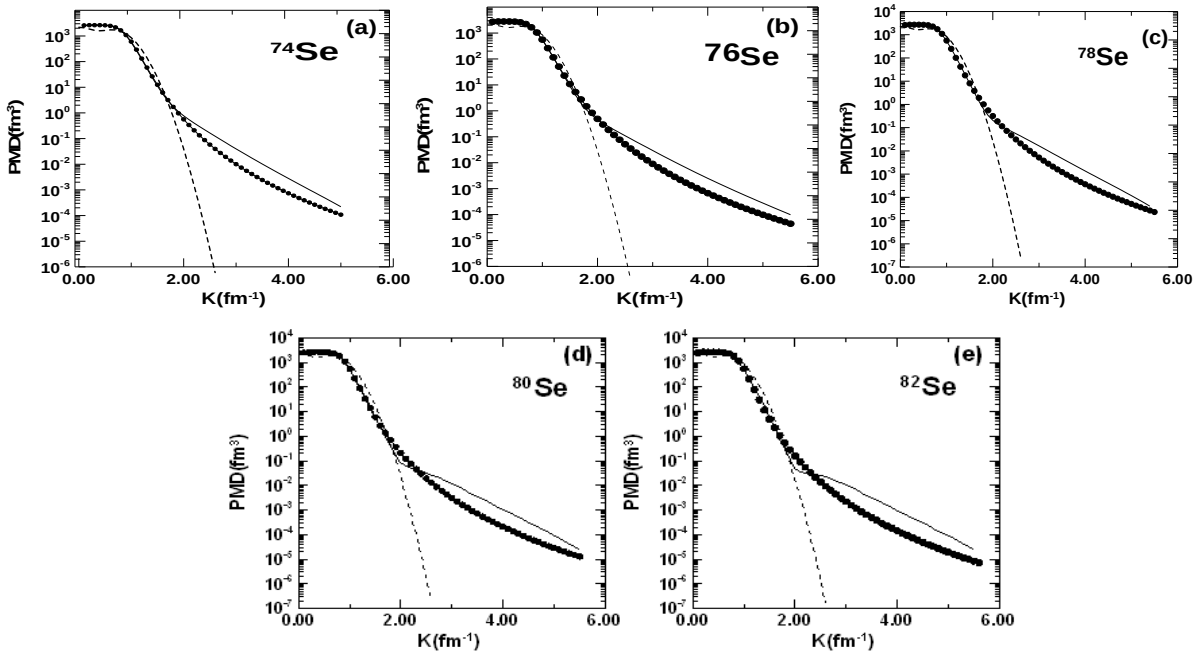

Figure 3.Proton Momentum distribution as a function of k(fm^{-1}) for (a)^{74}Se, (b)^{76}Se (c)^{78}Se, (d)^{80}Se and (e)^{82}Se nuclei. The long-dashed curves are the calculated PMD of Eq. (10) obtained by the shell model calculation using the single particle harmonic oscillator wave functions in momentum representation.The solid circles symbols and solid curves distributions are the calculated PMD obtained in terms of the CDFM.

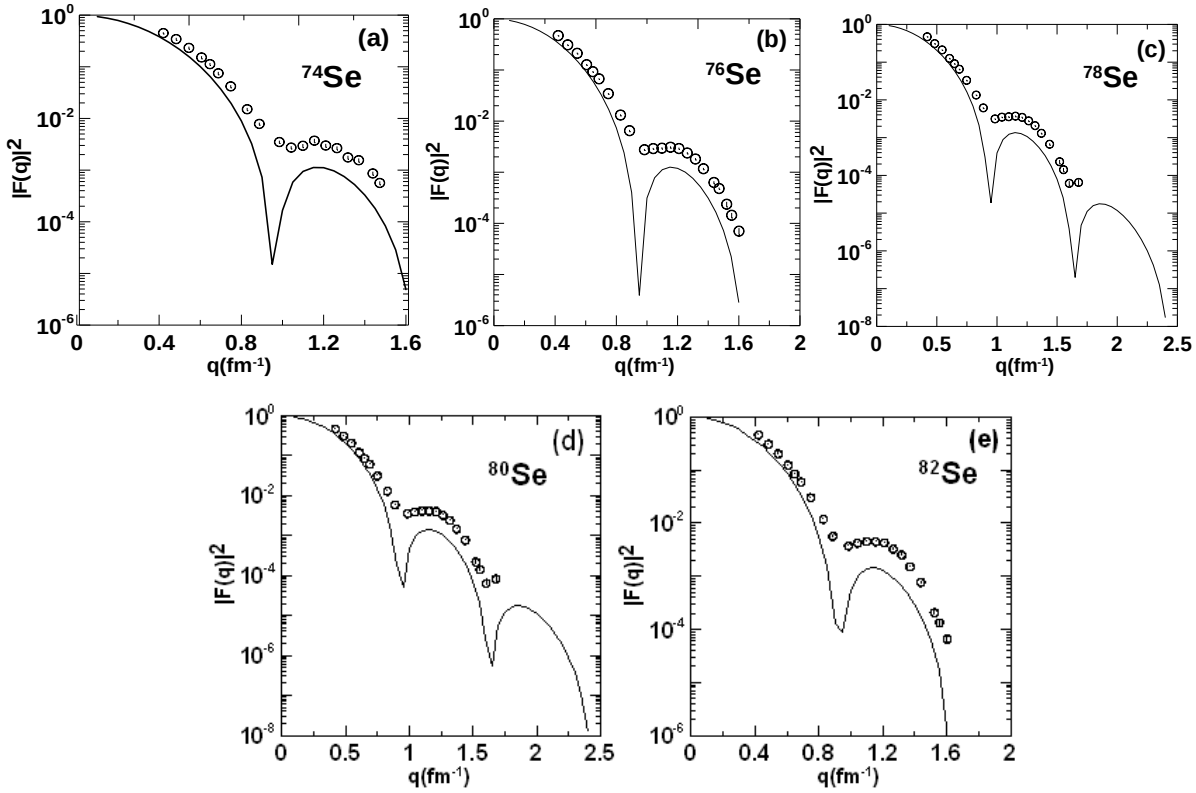

Figure 4.LongitudinalCharge Form Factors for elastic scattering as a function of q(fm^{-1}) for ground state of (a)^{74}Se, (b)^{76}Se (c)^{78}Se, (d)^{80}Se and (e)^{82}Se nuclei. The solid curve is the calculated F(q) of the Eq. (28). The circle symbols are the experimental data, taken from Ref.[10].

Indian Journal of Natural Sciences www.tnsroindia.org.in ©IJONS

Vol.9 /Issue 51 / December / 2018 *International Bimonthly* *ISSN: 0976 – 0997*

RESEARCH ARTICLE

Antimicrobial Properties of *Thymus vulgaris* and *Citrullus colocynthis* against *E. coli* and *Staphylococcus aureus* Isolated From Ground Meat in Hilla City

Mohammed KadhumWali*

Veterinary Public Health, College of Veterinary Medicine, University of AlQasim Green, Iraq.

Received: 21 Jul 2018 Revised: 24 Aug 2018 Accepted: 27 Sep 2018

***Address for Correspondence**
Mohammed KadhumWali
Veterinary Public Health,
College of Veterinary Medicine,
University of AlQasim Green, Iraq.
Email: mohammed.altae87@gmail.com

ABSTRACT

The present study is planned on antimicrobial effects of thymus *vulgaris* and colocynth against *E. coli* and *Staphylococcus aureus* isolated from ground meat. Forty ground meat samples were collected randomly from Al –Hilla city (5 samples /weekly). Our study showed that 13 (32.5%) positive culture of *Staphylococcus aureus* isolates and 8 (20%) positive cultures of *E. coli* was isolation from ground meat.

The recent study showed that the antimicrobial effect of thymus *vulgaris* and colocynth against *E. coli* and *Staphylococcus aureus*was determined by cork borer of 8.0mm diameter. It was found high significance ($p<0.05$) at different concentration (2.5%, 5%, 10% and 15%) between thymus *vulgaris* and colocynth against *E. coli* and *Staphylococcus aureus* against bacterial isolates. The minimum of inhibition zone (mean ±SE) to thymus vulgaris (15.75±0.75 and 8.50±1.32) at concentration 2.5%. While the maximum of inhibition zone (mean ±SE) to thymus vulgaris (25.25±1.25 and 19.50±0.95) at concentration 15% against *E. coli* and *Staphylococcus aureus* respectively. Conclusion, essential oil (thymus) uses antimicrobial effect due to prevent pathogenic bacteria and natural preservation of foods from microbial spoilages.

Key words: ground meat, thymus *vulgaris,* colocynth E. coli and *Staphylococcus aureus*.

INTRODUCTION

Minced meat isa rich medium in the growth ofpathogenic bacteria (Norman and Gravani, 2006).Hygiene of meat determined bybacterial quality.Unhygienic food handling due to contamination of foodwithbacteria (Tachbele,*et al*. 2006).Pathogenic bacteria enter from environmental exposure, tools, loss ofsanitation in slaughtering premises,operators and hands contaminate the meat product(Sachindra,*et al.* 2005 andKozačinski,*et al.* 2006).

Staphylococcus aureus is a pathogenicbacteria commonly responsible for meat and meat productcontamination (De Boer, *et al*., 2009 andOliveira, *et al.,* 2010); and produce the enterotoxins (Pu, *et al.,* 2009). Toxigenic *S. aureus*in meat results in a health hazard to consumers (Zouharova and Rysanek, 2008). Contamination of food by *Staphylococcal* enterotoxinsmay result directly from infected food-producing animals or may occur frompoor hygiene during retail andproduction process or foods storage. *Escherichia coli* is a food-illness pathogen,the commonmodes of transmission are due to consuming contaminated beef and beef products (Baran and Gulmez, 2000).Some of *E. coli*is harmless toconsumers, and othertypes of *E. coli* causes diseases; *E.coli* is the common virulent pathogenic that ability to cause severe disease and may be death (Mohawk, *et al.* 2010). Essential oils were an antimicrobial has been proceeded to increase the shelf life, safety and sensory quality of food production (Bajpai, *et al.,* 2012). Essential oil uses have been described with the phenol coefficients of a variety of essential oils (Ayah and Saad, 2016).Itssources of antimicrobial compounds, especiallyfor pathogenic bacterial (Lodhia*, et al.,* 2009). Essentialoils accumulate in the cytoplasmic membrane and cause damage such as loss of function of selective barrier (Millezi, *et al.,* 2012). Recently, it has been elucidated that thyme oil showed a significant activity against some Gram-positive and Gram-negative bacteria(Cruz, *et al*.,1993).It contains compounds important in anti-microbial and antioxidant compounds;also other compounds such as Phenols,Caffeic acid Tannins, Flavones and Linalool (Sajid, *et al.,* 2013).

CitrulluscolocynthisSchrad (colocynth) is a medicinal plant belonging to the Cucurbitaceae family. It is called bitter apple (Kim, *et al.,* 2015).Traditionally, it hasused for the treatment of pathogenic bacteria, urinary disease, diabetes, ulcer, inflammation and jaundice in Asian and African countries (Rajamanickan,*et al.,* 2010). Objects of the study antimicrobial properties of thymus vulgaris and Citrulluscolocynthis against *E. coli* and*Staphylococcus aureus* isolated from ground meat in Hilla city.

MATERIALS AND METHODS

Sample collection

Forty ground meat samples were collected randomly from Hillacity using a sterile aseptic glass jar and cool transported using ice and ice box tolaboratory examination in al Qasim University /Veterinary medicine. Even grams of ground meat were added to sterile peptone water in a flask and shaken well to make 10^{-1} dilution. Further dilutions were prepared in sterile distilled peptone water. Prepared samples were serially diluted (10^{-1} to 10^{-6}) in sterile water and used to enumerated bacteria in the specific culture mediumUsing pour plate, themedia for isolation were poured onto each plate. Thesewere incubated at 37^{o}C for 24hrs.

Detection of *Staphylococcus spp*

For the enumeration of coagulase positive Staphylococcus (*Staphylococcus aureus*), the mannitol salt agar was used for confirmation and incubated at37C° for 24 - 48 hours (Tijani,*et al.,* 2017).

Detection of *Escherichia coli*

For the enumeration of (*Escherichia coli*), Macconkey agar was used for confirmation and incubated at 37C° for 24 - 48 hours, developed colonies were counted, Suspected colonies were confirmed by EMB and insole, methyl red, Voges-Proskauer, citrate (IMViC) tests**(**Jamshidi,*et al*., 2008).

Extraction of thyme and colocynth

The plant extracts were studied in a sterilization method (Majid and Mahmoud, 1988). Ten gram of each studied plant powder was taken and placed in 100 ml of distilled water for 2 hours. At the same time, it was also stirred for

24 hours and the solids were disposed by filtration of plant extracts through filter paper then centrifuge using a device at 3000 RPM for ten minutes. Take the leachate and dry in the incubator and will work different concentrations.

The antimicrobial efficiency of thyme andcolocynth

On Muller Hinton agar Media 0.1mlofbacterial culture was spared andthen leave the agar dishes in the center of wells at room temperature for 15 minutes for the purpose of absorbing the vaccine.Five wells were made in each plate using 8.0mm diameter, then filled with various 100µl volume of each concentrations of thyme and colocynth (2.5%, 5%, 10% and 15%) inMueller Hinton agar.And then incubate the dishes at a temperature of 37 ° C for (18 hours).The zone of inhibition measured by mm after 24 hours of incubation (Al-Azzawi, 2011).

Statistical analysis

The experiment was performed using a complete randomized design with four replicates per treatment and then the mean was compared using the least significant difference test (LSD).

RESULTS AND DISCUSSION

Isolation bacteria

Forty ground meat samples were collected randomly from Al –Hilla city (5 samples / weekly) and transport to laboratory in ice pox for analyzer in the College of Veterinary Medicine \ University Al Qasim Green. Isolation and identification of *E. coli* and *Staphylococcus aureus* were confirmed based on biochemical test (motility test, in dole, vote's procure and Citrate utilization), Eosin methylene blue and manitol salt agar. *E. coli* was appearing green metallic sheen on Eosin methylene blue agar and positive to motility and indole while negative to vote's proskaure and Citrate utilization (Tijani, *et al.,* 2017). *Staphylococcus aureus* was appear golden- yellow on manitol salt agar and positive to vote's proskaure and Citrate utilization and negative to motility and indole(Cheesbrough2006).13 (32.5%) positive culture of *Staphylococcus aureus* isolates from ground meat.

This study similar to (Kelman, *et al.*,2011) found that 29% of ground beef samples were contaminated with *S. aureus.* (Özdemir and Keyvan, 2016) reported that 75 (14.6%) and 75(30.6%) of meat sheep and beef contaminated with *Staphylococcus aureus.*(Bhargava,*et al*.,2011and Pesavento, *et al.*,2007)reported levels of *S. aureus* at 23.8% and 22.5% of raw meat samples.8 (20%) positive cultures of *E. coli*was isolated from ground meat. (De Giusti,*et al.,* 2011) report that 94 (30.32%) of *E. coli*isolates from ground meat in Iran.(Sheikh, *et al.,*2013) who found that three (38%) isolate *E. coli*from ground beef. Beef plays animportant role in the epidemiology of human infections and regard reservoirs of *E. coli O157:H7 (*Bai,*et al.,* 2010; Olesen and Jespersen, 2010*)*

Antibacterial effect of essential oil on bacteria

The recent study showed that the antimicrobial effect of thymus *vulgaris* and colocynth against *E. coli* and *Staphylococcus aureus*was determined bycork borer of 8.0mm diameter. It was found high significance ($p<0.05$) at different concentration (2.5%, 5%, 10% and 15%) between thymus vulgaris and colocynth against *E. coli* and *Staphylococcus aureus* against bacterial isolates. The minimum of inhibition zone (mean ±SE) to thymus vulgaris (15.75±0.75 and 8.50±1.32) at concentration 2.5%. While the maximum of inhibition zone (mean ±SE) to thymus vulgaris (25.25±1.25 and 19.50±0.95) at concentration 15% against *E. coli* and *Staphylococcus aureus* respectively. Also the minimum of inhibition zone to *Citrullus colocynthis* (10.75±4.15 and 9.50±3.57) at concentration 2.5%, the maximum of inhibition zone to to *Citrullus colocynthis* (21.50±2.17 and 18.75±1.49) at concentration 15% respectively

against *E. coli* and *Staphylococcus aureus.*These results have in disagreement with those found by (Majed and Shatti, 2002) Concentrations (2.5 % and5 %) of the *Citrullus colocynthis* extract no effect on the *Staphylococcus aureus* and *E. coli* while the concentration of (10%) is effective. Also, disagreement with (Bnyan, *et al.,* 2013) water extracts of *Citrullus colocynthis* no effect in all bacterial species(*Proteus mirabilis*, *Staphylococcus aureus*, *Streptococcus pneumoniae*and *Klebsiella pneumonia*).(Muhammad Sajid ,*et al*., 2013) who study soil bacterium used Colocynth (*Citrullus colocynthis*) extract with concentration 10 % was effective.(Alkamel,2005)found that the in hibitory effect of C. colocynthis fruit aqueous extract may attributed to active compounds present in the extract.Confirmed the results of studies by (Gurudeeban,*et al.,*2010)the water extract of *C. colocynthis* plant has a high activity against bacteria*E.coli and Staphylococcus aureus.*This results disagreement with (Millezi, *et al.,* 2012)the minimum inhibitory concentrations of thymus vulgaris against *Staphylococcus aureus* at 0.5% but 50% against *E. coli.* .**(**Al.Maqtari,*et al.,* 2011)how found that thyme oil high sensitive against *E. coli* and *Staphyococcus aureus* and showed a significant bactericidal effect. (Al-Saimary,*et al.,* 2006) all essential oil extractsare more effective against Gram positive bacteria than Gram negative bacteria, due to the nature of bacterial cell structures. (Marino, *et al.,* 1999) detected that thyme use as an antibiotic. Also thymol is25 times as effective as phenol, but less toxic. Other work suggests that the in vitro the antibacterial activity of thyme preparations are due to the presence ofpolymethoxy flavones (Al-Saimary,*et al.,* 2006).

CONCLUSION

Essential oil (thymus) uses antimicrobial effect due to prevent pathogenic bacteria and natural preservation of foods from microbial spoilages.

REFERENCES

1. Al.Maqtari, M.A.A.; Alghalibi, S.M. and Alhamzy, E.H.(2011). Chemical composition and antimicrobial activity of essential oil of *Thymus vulgaris* from Yemen.Turk. J. Biochem., 36 (4), 342–349.
2. Al-Azzawi, H. Z. (2011). Comparison of the effect of plant extract and some antibiotics on Staphylococcus bacteriaGold isolated from gingivitis. Diyala Journal of Agricultural Sciences, 3(2), 3600 - 592:
3. Alkame, L.M.(2005). Antimicrobial activity of aqueous extract of CitrulluscolocynthisL.fruit.TikritJournql of Pharmaceutical Scinences,1(2):9- I 5.
4. Al-Saimary,L; Bakr,S.; Khudaier,S. andAbass,Y. (2006). Efficiency of antibacterial agents extracted from Thymus vulgaris l. (lamiaceae).The Internet Journal of Nutrition and Wellness. Vol 4 (1)**.**
5. Ayah, B. A-S and Saad, M.F.(2016). Influence of selected essential oils on some pathogenic microorganisms in white soft cheese**.**International Journal of ChemTech Research, 9 (12): 214-220.
6. Bai, J.; Shi, X.; Nagaraja, T. G. (2010). A multiplex PCR procedure for the detection of six major virulence genes in *Escherichia coli O157:H7*. J. Micro. Methods, 82:85-89.
7. Bajpai, V.K.; Baek, H.K. and Kang, S.C. (2012). Control of Salmonella in foods by using essential oils: A review. *Food Res. Int.*45: 722–734.
8. Baran, F. and Gulmez , M.(2000) . The Occurence of *Escherichia coli O157:H7* in the Ground Beef and Chicken Drumsticks.Internet Journal of Food Safety, V.2, 13-15.
9. Bhargava, K.; Wang, X. and Donabedian, S. (2011).Methicillin-resistant *Staphylococcus aureus* in retail meat, Detroit, MI, USA.Emerg. Infect Dis, 17, 1135-1137.
10. Bnyan,I.; Hamid Hasan, H.; Ewadh, M.(2013). Antibacterial Activity of CitrullusColocynthis against different types of bacteria.Advances in Life Science and Technology, Vol 7.
11. Cheesbrough, M. (2006).Microbiological tests. In: District laboratory practice in tropical countries, 2nd ed. The Anglo Egyptian bookshop.Part 2, Chapt. 7: 64-67 and 135-142.
12. Cruz , U.; Cabo, M.M.; Castillo, M.J.; Jimenez, J.; Ruiz, C. and Ramos-Cormenzana, A. (1993). Chemical composition and anti-microbial activity of the essential oils of different samples of *Thymus baeticus*Boiss.*Phytotherapy* ,7, 92-94.

13. De Boer, E.; Zwartkruis-Nahuis, J.T.M.; Wit, B.; Huijsdens, X.W.; De Neeling, A.J.; Bosch, T.; van Oosteron, R.A.A.; Vila, A. and Heuvelink, A.E. (2009). Prevalence of methicillinresistant *Staphylococcus aureus* in meat. Int. J. Food Microbial., 134: 52–56.
14. De Giusti, M.; Tufi, D.; Caterina, Aurigemma ,A.; Cimmuto D.; Trinti, F.; Mannocci, A. and Boccia, A. (2011). Detection of *Escherichia coli* O157 in raw and cooked meat: comparison of conventional direct culture method and Enzyme Linked Fluorescent Assay (ELFA).IJPH - Year 9, Volume 8, Number 1.
15. Gurudeeban, S.; Satyavani, K. and Ramanathan, T. (2010): Bitter Apple (*Citrulluscolocynthis*) An Overview chemical composition and Biomedical Potentials. *Asian Journal of Plant Sciences*, Vol. 9(7): Pp. 394 – 401.
16. Jamshidi, A. ;Bassami, M. R. and Rasooli, M. (2008)**.**Isolation of *Escherichia coli* O157:H7 from ground beef samples collected from beef markets, using conventional culture and polymerase chain reaction in Mashhad, northeastern Iran. Iranian Journal of Veterinary Research, Shiraz University, Vol. 9, No. 1, Ser. No. 22.
17. Kelman , A.; Soong, Y. A. and Dupuy, N. (2011). Antimicrobial susceptibility of *Staphylococcus aureus* from retail ground meats. J Food Prot. 74, 1625-1629.
18. Kim, W.; Lee, W. B. ; Lee, J.; Min, B. I. ; Lee, H. and Cho, S. H. (2015). Traditional herbalmedicine as adjunctive therapy for nasopharyngeal cancer: asystematic review and meta-analysis, Integr. Cancer Ther. 14:212-220.
19. Kozačinski*,* L.*;* Hadžiosmanović*,* M. and Zdolec*,* N. (2006)**.**Microbiological quality of poultry meat on the Croatian market. Vet. Arhiv.76(4), 305– 313.
20. Lodhia, M. H.; Bhatt,K. R. and Thaker,V. S.(2009).Antibacterial activity of essential oils fromPalmarosa, evening primrose, lavender and tuberose. 71 (2): 134-136.
21. MacRae, M.; Rebate,T.;. Johnson, M. and Ogden, I. D.(1997). The sensitivity of *Escherichia coli O157* to some antimicrobials by conventional and conductance assays. Lett.Appl. Micro. 25:135-137.
22. Majid, S. H. and Mahmoud, M. J. (1988).Plants and herbs among Iraqi folk medicine and scientific research.First Edition.Dar al-Thawra for Printing and Publishing, Baghdad.
23. Majid,R. G and Habib, M.S. (2002). Effect of antimicrobial activity of some plant extracts on some microbial growth. J.Vet. Sci, 8(2):75-68.
24. Marino, M. L.;Bersani, C. and Comi, G. (1999).Antimicrobial activity of the essential oils of Thymusvulgaris L. measured using a bioimpedometric method. J.Food. Prot., 62(9): 1017-1023.
25. MilleziA. F.; Caixeta, C.A.; Rossoni, D.F.;Cardoso, M.D. and piccolo, R.H.(2012).In vitro antimicrobial properties of plant essential oils *thymus vulgaris, cymbopogoncitratus*and *laurusnobilis*against five important foodborne pathogens.Ciência e Tecnologia de Alimentos,32(1): 167-172.
26. Millezi, A. F.; Caixeta, D. S.; Rossoni, D. F.; Cardoso, M. D. G., and Piccoli, R. H. (2012). In vitro antimicrobial properties of plant essential oils Thymus vulgaris, Cymbopogoncitratus and Laurusnobilis against five important foodborne pathogens. *Food Science and Technology (Campinas)*, *32*(1), 167-172.
27. Mohawk, K. L.; Melton-Celsa, A. R.; Zangari, T. ; Carroll, E. E. and O'Brien, A. D. (2010). Pathogenesis of Escherichia coli O157:H7 strain 86-24 following oral infection of BALB/c mice with an intact commensal flora, Micro. Path. 48,131-142 .
28. Norman, G. M. and Gravani, R. B. (2006).Principles of Food Sanitation. 5th Edition, Springer, USA.
29. Olesen, I. and Jespersen, L. (2010). Relative gene transcription and pathogenicity of enterohemorrhagic *Escherichia coli* after long-term adaptation to acid and salt s
30. Özdemir, H. and Keyvan, E. (2016). Isolation and characterization of *Staphylococcus aureus* strains isolated from beef, sheep and chicken meat. Ankara Üniv Vet FakDerg, 63, 333-338.
31. Pesavento, G.; Ducci, B. and Comodo, N. (2007). Antimicrobial resistance profile of *Staphylococcus aureus* isolated from raw meat: A research for methicilin resistant *Staphylococcus aureus (MRSA).* Food Control, 18, 196-200.
32. Pu, S.; Han, F. and Ge, B. (2009).Isolation and characterization of methicillin-resistant *Staphylococcus aureus* strains from Louisiana retail meats.Appl Environ Microbiol, **75**, 265-267.
33. Ragamanickam, E, Gurudeeben, S, Ramanathan, T., Satyavani, K. (2010).Evaluation of anti-inflammatory activity of citrulluscolocynthesis. Int. J. Cur. Res. 2:067-069.
34. Sachindra, N. M.; Sakhare, P.Z.; Yashoda ,K. P. and Rao, D. N. (2005).Microbial profile of buffalo sausage during processing and storage. Food Control, 16, 31–35.

35. Sajid, H. ;Sahebkar, A. and Iranshahi, M. (2013*). ZatariamultifloraBoiss.*An ancient condiment with modern pharmaceutical uses .journal of Ethno pharmacology volume 145, Issue 3, 13 p 686-698.
36. Tachbele, E.; Erku, W.; Gebre-Michael, T. and Ashenafi, M. (2006). Cockroachassociated food-borne bacterial pathogens from some hospitals and restaurants in Addi Ababa, Ethiopia: Distribution and antibiograms. J. Rural Trop Public Health, 5, 34–41.
37. Tijani, A. A.; Famotemi, A. C.; Orji, F. A.; Abimbola F. B.; Adams, F. M. and Aba, E. (2017).Antimicrobial susceptibility of bacteria isolated from abattoir, eatery and hospital effluents. Int. J. Adv. Res. Biol. Sci. 4(1): 142-156.
38. Tijani, A. A.; Famotemi, A. C.; Orji, F. A.; Abimbola F. B.; Adams, F. M. and Aba, E.(2017).Antimicrobial susceptibility of bacteria isolated from abattoir, eatery and hospital effluents. International Journal of Advanced Research in Biological Sciences. 4(1): 142-156.
39. Zouharova, M. and Rysanek, D. (2008). Identification of *S. aureus*enterotoxigenic strains from bulk tank milk. J. Zoonosis public health. 55 (6):313-319.

Table 1: The Minimum Inhibitory Concentrations of the *Thymus vulgaris* against *E. coli and staphylococcus aureus*.

Treatment / Isolates	Mean ±SE	Mean ±SE	Mean ±SE	Mean ±SE	LSD
	2.5%	5%	10%	15%	
E. coli	15.75±0.75 Da	18.75±2.17 Ca	21.75±1.37 Ba	25.25±1.25 Aa	2.03
Staphylococcus aureus	8.50±1.32 Bb	8.75±0.47 Bb	18.50±0.65 Ab	19.50±0.95 Ab	

Table 3: The Minimum Inhibitory Concentrations of the *Citrullus colocynthis* against *E. coli and staphylococcus aureus*

Treatment / Isolates	Mean ±SE	Mean ±SE	Mean ±SE	Mean ±SE	LSD
	2.5%	**5%**	**10%**	**15%**	
E. coli	10.75±4.15 Cc	15.75±1.54 Bb	20.25±1.31 Aa	21.50±2.17 Aa	**3.65**
Staphylococcus aureus	9.50±3.57 Cc	7.75±2.65 Cc	14.00±1.47 Bb	18.75±1.49 Aa	

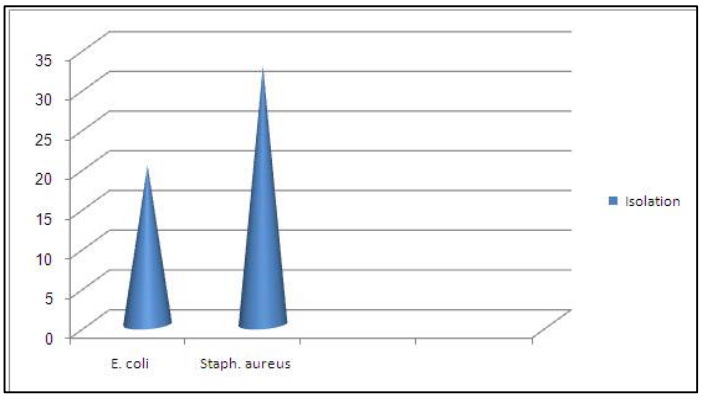

Fig.1.Isolation bacteria

Indian Journal of Natural Sciences www.tnsroindia.org.in ©IJONS

Vol.9 /Issue 51 / December / 2018 *International Bimonthly* *ISSN: 0976 – 0997*

RESEARCH ARTICLE

Anti Adhesive Activity of Biosurfactant Produced by *P. aeruginosa* Isolated from Rhizosphere Wheat Root from Iraqi Soil against Some UTI Bacteria

Sarah K.Suleman* and Amel H.Mussa

Department of Microbiology, College of Science, Al-Mustansiriyah University, Iraq.

Received: 02 Sep 2018 Revised: 04 Oct 2018 Accepted: 06 Nov 2018

***Address for Correspondence**
Sarah K.Suleman
Department of Microbiology,
College of Science,
Al-Mustansiriyah University, Iraq.

ABSTRACT

This study including extraction and purification of active compound biosurfactant produce from *P. aeruginosa* and purified by acid precipitation, using HPLC surface activity of crude biosurfactant were studied, antibacterial, antiadhesion activities were evaluated against some urinary tract infection, including *Escherichia coli, Klebsiella pneumonia*,*Morganella morganii, Proteus mirrabilis, Enterobacter cloacae, Pseudomonas aeruginosa , Serratia marcescens* and *Staphylococcus aureus* isolated from Iraqi women suffering from UTI. Crude biosurfactant showed that the surface activity was higher than purified biosurfactant.Both crude and purified biosurfactant showed inhibitory effect against UTI isolates and the higher activity wasagainst*K .pneumoniaand E. cloacae*which were 18 ,17mm respectively.For crude and for purified biosurfactent the highly effects was shown against *K .pneumonia* (16 mm) and *E. cloacae*(15).Antadhesive activity of biosurfactent wasdistinguished and the results revealedthat the highly activity of crude biosurfactent with *P. mirrabilis*35% then *K. pneumonia* 29% , whereas purified biosurfactant obtained antiadhesive activity against *p. mirrabilis* (34.9%) then *K. pneumonia* ,*S marcescens* 30% .

Keywords: Biosurfactant produce, *P. aeruginosa*, *K. pneumonia*, *S marcescens.*

INTRODUCTION

Soil colonized by various species of microorganisms,like bacillus and *pseudomonas* had the ability to produced numerous type of antimicrobial compounds (Abdu-Allah and Mussa .,2015) ,(Mussa and Baqer .,2017).Srfactant is biological surface active substance secret by living cells, mainly by a different type of microorganism, such as bacteria, mold and yeasts (Płaza*et al*., 2014).They have Many Application of biological surfactant compared with Artificial substance; involvement in biodegradability because their simple chemical structure, environmental affinity ,

decrease toxicity, which let usage in the cosmetic, pharmaceutical and food industry, high selectivity since to presence of specific functional groups, allowing specificity in the remove toxin of specific pollutants, and activity under circumastance of extreme temperatures- pH and salinity (Johny, 2013; Silva *et al*.,2014).,surfactant make decrease surface and interfacial tensions (Fanun, 2014).Biosurfactants can be classified into two major group beloing to their chemical structure and microbial origin,that is high molecular weight, such as polymeric and particulate surfactants low molecular weight molecules,including glycolipids, lipopeptids and phospholipids(Singh, 2012).The aim of this study was to distinguished the antibacterial and anti adhesive activity of biosurfactent produced from *P. aeruginosa* isolated from soil on some urinary tract infection (UTI) isolates .

MATERIALS AND METHODS

Microorganism

The soil samples were taken from rhizosphere reign from wheat root in order toisolation and identification of *P.aeruginosa* isolates (Omolola 2007).Soil isolates were subjected to numerous cultural and biochemical tests for identification as mentioned by Collee et al., (1996) and Brown, (2005).Isolation and Identification of UTI isolates were collected from urine specimen ofIraqi women in Baghdad hospitals. Theidentification of isolates was doneto confirm the identification of the isolates VITEK 2 system. The primary screening for *P. aeruginosa* isolate that have antimicrobial activity were done by inoculating in 100 ml of King -B- medium and incubated at (30)ºC for 72 hours in Shaker incubator(150) rpm., centrifuged the culture in (6000)rpm for 15 min filtered the supernatant with Millipore paper o.22 mm, using agar diffusion method to distinguished the antimicrobial activity against UTI isolates , incubated at 37 ºC for 24 hours . The inhibitory zone were measured in mm .(Thavasi*et al*., 2011).

Detection of Biosurfactant

Oil spreading test

P.aeruginosa isolates SA4, SA7, SA9 were cultured in flasks containing King-B-liquid at (30 ºC,) in incubator shaker 120 rpmfor48 (hours, centrifuged at (6,000×g for 20 min) at 4 ºCand the supernatant filter collected and sterilized with filter paper . Surface activity test was measured by the oil spreading method(Fracchia*et al*., 2010) by using(20 µL) of Motor oil dropped on to the surface of 20 µL of distilled water in a plate (90 mm in diameter) to form a thin layer. 20 µL of bacterial supernatant was softly put onto the center of the oil membrane. Measured of diameters to the oil displaced circle that forming.

Emulsification activity

The emulsifying ability was done by an emulsification index (E24). The E24 of culture isolate was specific by adding (2 ml) of Motor oil and (2 ml) of the bacterial filter in a test tube after the centrifugation of isolate incubated in 37 ºC for 24 hours , mixed with vortexes at high speed for 5 min and let to stand for 24hours. The emulsion activity was investigated after 24 hours. Theratio of emulsification index counted by using the following equal, The results were compared with phosphate buffer saline(PBS)as negative control. Das *et al*., (2009).E24=top of emulsion layer (cm)\top of the total mixture (cm)*100%

Purification of biosurfactant

The method recorded by Sorensen *et al* .,(2001)was used to purified biosurfactant as follows, the isolates were culture on King's -B- liquid plates in darkness at 28 ºC for 1 day, before being transferred to (20 ºC) and incubated for another 3 days. Colony material was suspended in demineralized water and mixing by shaking. Separated of the cell and

supernatant twice by centrifugation at (4,700 rpm) for 20 min at 4 ºC. The supernatant was sour to pH 2.0 with 1 M HCl and keep overnight in ice for a precipitate .The precipitate was centrifuged in sterile centrifuge tubes for (27 min) at (7,000 rpm) and (4 ºC). The supernatant was ignored, and the precipitate was rinsed twice with water at pH 2.0.The precipitate was dissolved in acidified water, and pH was fixed to 8.0 with 1 M Na -OH to complete dissolve the precipitate.The Solution was drying, and the Purity of thebiosurfactant preparations was qualitatively analyzed by high-performance liquid chromatography(HPLC). (Thomson *et al*.,1995 ; Sørensen*et al*., 2001).

High-performance liquid chromatography

High-performance liquid chromatography (HPLC) analysis of the lipopeptides followed the protocol by(Nielsen and Sørensen 2003) with minor modifications. Briefly, a Hypersil BDS C18 column (100×4.6 mm and 3 μm particle size) .was used for separation of the lipopeptides. Solvents were HPLC-grade acetonitrile (solvent A)and 0.1 % o-phosphoric acid(solventB), mixed in a linear gradient of 15 to 100 % solvent A from 0 to 40 min, and of 100 to 15 % solvent A between 40 and 44 min. The flow rate was 1 ml/min, and the column temperature was 40 ºC. The injected sample volume was 10 μl. monitored at wavelengths of 190 to 250 nm.

Antimicrobial activity of biosurfactant (crude and purified)

Agar well diffusion method used to distinguished the action of biosurfactant produced from *P. aeruginosa*isolates SA4 against uropathogenic bacteria,by spreading (0.1ml) of isolates *E.coli* ,*P. mirabilis* ,*M. morganii* ,*P.aeruginosa* ,*K. pneumoinae* ,*E.cloacae* ,*S. marcescence* and ,*S. aureus* on the Muller Hinton Agar. Wells of (5mm) width were punched in the agar with Cork borer filled with (100µl) of biosurfactant,incubated in 37 ºC for 24hours.The resulting of inhibition region was measured in millimeter (mm).

Anti adhesive activity

The anti adhesive activity of the crude and purified biosurfactantproduced from *P. aeruginosa* againsturo pathogenic isolates were quantified by co-incubation test according to the procedure described by Ali (2012). All of UTI causative bacterial suspensions in brain heart infusion with(2%) glucose(100 μl) were lodded to (96-well) flat-bottomed tissue culture plates with with (100 μl) of the crude and partial purified biosurfactant (singly). Control hole contained (180 μl) of brain heart infusion with (2%) glucose and (20μl of bacterial suspensions, The enveloped microtiter plate was closed with Parafilm incubation at (37 ºC) for 24hours. Unattached bacterial cells were removed by rinse the holes with physiological Normal Saline (pH 7.2). After drying at room temperature for15 min., (200 μl) of crystal violet (1%) was lodded to the holes for (20 min). The dye attached bacterial cells were rinsed with physiological Normal Saline (pH 7.2). let to dry at room temperature for (15 min), and extracted two time with (200 μl) of (95%)ethanol, and the absorbance of all holes was measured at (630nm) by using Enzyme Linked Immuunosorbent Assay (ELISA) Reader.

Inhibition of adhesion = [1-(A/A0)] x 100 %

A:- refer to the absorbance of the holes with a biosurfactant

A0:-refer to the absorbance of the control holes.

RESULTS AND DISCUSSION

The 3 isolates of *P. Aeruginosa* were showed higher activity aginest UTI isolates were subjected to detection of biosurfactant using Oil spreading test,the result appeared that the isolate SA4 ,SA7,SA9 had the ability to produce biosurfactant with diameter (7 mm,2mm ,3mm) lighted zone formed as a result of contact of oil-water interface surface this result were agreement with many report which showed that many strains of bacteria could produce biosurfactant and using oil spreading test to detect the production .(Brozozowski*et al*., 2011).

Emulsification activity

The three isolates of *P. aeruginosa* were tested for Emulsification index and the result obtained were summarized in Table (1).The result appeared the isolates SA4 having E57,1%,While SA4 and SA7 and SA9 were EA=55,5%. And 55.1%. Emulsification index has been reported to be proportional to the surfactant concentration (Das *et al*., 2009). For another studies *P .aeruginosa*formed good emulsifying ability (Brozozowski*et al*., 2011), while Techaoei*et al*.(,2007) showed that the E24 emulsification index of bacteria isolated from soil range from 7.8-63.3%. andJaysree*et al*., (2011) observed that the biosurfactants produced by *B. subtilis* had an emulsification capacity (E24) of 20% and 15%, and that by *B. cereus* was 30% and 20% for diesel and engine oil respectively .

Purified Biosurfactant with (HPLC)

purified biosurfactant compound produced freom SA4 isolate were investigated on preparative HPLC Column , the result obtained shown there were several peaks in different RT(Retention Time is a measure of the time taken for a solute to pass through a chromatography column.ItCalculated as the time from injection to detection) .fig (1)
The peaks in RT between (14 to 40 min) ,these peaks was identical to the result obtained from others researchers when using the same condition and solvent , Nielsen *et al* .,(2002) in his research pointed the purification of biosurfactant from *Pseudomonas spp*the peakshe obtained was in RT(27-37)min when using the same solvent as used in current study . the chemical structure of the biosurfactent could be lipopeptide according to RT as mentioned by Bak*et al*., (2013) in his report that the lipopeptide he could obtained from strain of *P. flourescence*produced several types of lipopeptide (viscosin ,massetotolid A and putisolvin) they were all characterized by RT dominant peaks 20 to 35 consummates by other minor peaks found before or after the major peaks .

Antimicrobial activity of crude and purified Biosurfactants against uropathogenic Bacteria

The antibacterial activity of the crude and biosurfactant (acid-precipitated fraction) was determined some bacteria causing UTI the results summarized in table (2).. The results observed that highest activity of crude biosurfactant appeared on isolates *K .pneumoniae*was(18mm) and the lowest activity was on*E.coli* and *S. aureu*s was (16mm).While purified biosurfactant appear higher activity on bacteria *P. mirabili*s and*E.cloacae*was(14)mm. It is worthy to note that the crude and partial purified biosurfactant produced by *P. aeruginosa* had a good activity against bacteria causing UTI. Several biosurfactants that exhibit antimicrobial activity have been previously described. Salman *et al*., (2013) show in his reporte that the crude biosurfactant isolated from *S. thermophilus* showed inhibitory effect against *Klebsiellaspp.* and *P. aeruginosa*.

Antiadhesive Activity

The antiadhesive activity of crude and purified biosurfactant was evaluated against uropathogenic bacteria. The crude biosurfactant showed antiadhesive activity against bacteria, the highest antiadhesive ratio was pointed for *P. mirrabilis* (43.5.%). Table(3), whereas purified biosurfactant obtained antiadhesive activity against *p.mirrabilis (34.9%)* ,Table(4).the results were agreement with others researched,Gudina*et al*., (2010) showed that the highest antiadhesive ratio were obtained for *S. aureus, S. epidermidis and S. agalactiae* for a biosurfactant isolated from *L. paracasei,* and a low activity was appeared for *P. aeruginosa* and *E. coli*. Biosurfactants produce by *Lactobacillus* had inhibition activity on biofilm formation for *E. coli, S. aureus, Salmonella arizonae*and *Listeria monocytogen* (Fracchia*et al*., 2010). (Ali, 2012)was demonstrated that the biosurfactant isolated from *L.acidophilus*inhibit biofilm produce by *P. mirabilis.* Positive ratio refer to the in bacterial adhesion ,when compared to the control, while negative ratio refer to the lower bacterial attachment One mechanism that could explain this global inhibition of pathogenic adherence by biosurfactants, the Biosurfactants are amphipathic molecules that have different purposes, such as attachment to surfaces [Spurbeck&Arvidson, 2010].[Rodrigues *et al*.,2006] showed that the main aim of biosurfactant is to modify the

physicochemical properties of the surface, in order to the force of attraction between microorganisms and the surface of the biomaterial.

REFERENCES

1. Abdu-Allah ,S.N. and Mussa ,A.H.(2015).Study the inhibitory effects of *Bacillus subtilis*filtrates isolated from Iraqi soil in combination with MIC of ciprofloxacin and imipimenon *Acinetobacterbumannii* isolated from wounds and burns.World Journal of Pharmaceutical Research,Vol 4, Issue 09, 2015.
2. Mussa A. H., Baqer M. S.(2017) The antimicrobial effect of Bacillus spp filtrates and extracted compound in some pathogenic agent.journal of the college of basic education,,(23 99) 121-128
3. Płaza, G. H.; Chojniak, J. and Banat, I. M. (2014). Biosurfactant mediated biosynthesis of selected metallic nanoparticles. International Journal of Molecular Sciences.15,13720-13737.
4. Silva , R. C. F. S.; Almeida , D. G.; Rufino , R. D.; Luna ,J. M.; Santos , V. A.; and Sarubbo, L. A. (2014). Applications of Biosurfactants in the Petroleum Industry and the Remediation of Oil Spills.International Journal of Molecular Sciences.15, 12523-12542.
5. Johny ,J. M. (2013). Inhibitory effect of biosurfactant purified from probiotic yeast against biofilm producers.Journal Of Environmental Science, Toxicology And Food Technology. 6(1):51-55.
6. Singh ,V. (2012). Biosurfactant–Isolation, Production, Purification & Significance.International Journal of Scientific and Research Publications.2, 7.
7. Fanun, M. (2014).The role of colloidal system in environmental protection.AlQudisuniversity , East Jerusalem. Palstine.
8. Omolola O.(2007) Isolation of *Pseudomonas aeruginosa*from septic sore using some biological tests .International Journal of food Safety .13:188-190
9. Ali,O.A.(2012).prevention of *Proteus mirabilis* Biofilmby Surfactant Solution.Egypt.Acadmic.Journal.Biology.Sciences.,4(1):1-8.
10. Brzozowski, B., Bednarski, W. and Gol´ek, P. (2011).The Adhesive Capability of Two Lactobacillus Strains and Physicochemical Properties of Their Synthesized Biosurfactants. Food Technol. Biotechnol., 49 (2):177–186.
11. Das , P.; Mukherjee, S. and Sen, R. (2008). Antimicrobial potential of a lipopeptidebiosurfactant derived from a marine Bacillus circulans. Journal ofApplied Microbiology 104:1675–1684.
12. Gudina, E.J., Teixeira, J.A. and Rodrigues, L.R. (2010). Isolation and functional characterization ofbiosurfactant produced by Lactobacillus paracasei. Colloids and Surfaces B: Biointerfaces., 76: 298–304.
13. Rodrigues , L.; Banat, I. M.; Teixeira, J. and Oliveira, R. (2006). Biosurfactants: potential applications in medicine. Journal of Antimicrobial Chemotherapy 57:609–618.
14. Salman, J.A.S,Khalaf ,K.J. and AL-Marjani, M.F.(2013).Study of inhibitory agents produce by *Streptococcus thermophiles* on growth and biofilm formation for some pathogenic bacteria .Journal of biotechnology research center .,7(2):24-31.
15. Spurbeck, R.R. and Arvidson, C.G. (2010).*Lactobacillus jensenii* Surface-Associated Proteins Inhibit Neisseria gonorrhoeae Adherence to Epithelial Cells. Infect Immun., 78(7): 3103–3111.
16. Fracchia, L., Cavallo,M., Allegrone, G. and Martinotti, M.G.(2010). A Lactobacillus – derived biosurfactant inhibits biofilm formation of human pathogenic candida albicans biofilm producers. Current Research, Technology and Education Topics in Applied Microbiology and Microbial Biotechnology., 827-837.
17. Sørensen D, Nielsen TH, Christophersen C, Sørensen J, Gajhede M. (2001). Cyclic lipoundecapeptideamphisin from Pseudomonas sp. strain DSS73. ActaCrystallogr C C57:1123–1124.
18. Thomson IP, Lilley AK, Ellis RJ, Bramwell PA, Bailey M.J.(1995). Survival, colonization and dispersal of genetically modified Pseudomonas fluorescens SBW25 in the phytosphere of fieldgrown sugar beet. Biogeosciences 13:1493–1497.

Table (1)The Percentage of Emulsification activity of filtrate biosurfactant .

Isolates	Emulsification activity
SA4	55,5%
SA9	57,1%
SA7	55,5%

Table (2) Antimicrobial activity of crude and purified biosurfactant on the Uropathogenic bacterial

Isolates	Crude biosurfactant	Purified biosurfactant
E. coli	16mm	12mm
K. pneumoniae	18mm	16mm
P. mirabilis	10mm	14mm
P. aeruginosa	0	12mm
M. morganii	0	0
S. marcescens	12mm	13mm
E. cloacae	17mm	15mm
S. aureus	16mm	0

Table(3):-Antiadhesive percentage of crude of biosurfactant produced from *P. aeruginosa*(SA4).

Isolates	O.D of Crude biosurfactant	O.D of Control	Antiadhesive percentage %
P. mirabilis	0.467	0.717	34,9 %
M. morganii	0.561	0.415	-35 %
E. coli	0.589	0.652	9,7 %
P. aeruginosa	0.459	0.486	5,6 %
E.cloacae	O.502	0.481	-4,3 %
S. aureus	0.576	0.515	-11,8 %
S. marcescens	0.542	0.288	-88 %
K. pneumonia	0.368	0.511	28 %

Table(4):- Antiadhesive percentage of purified of biosurfactant produced from *P. aeruginosa*(SA4).

Isolates	O.D of purified biosurfactant	O.D of Contrrol	Antiadhesive percentage %
P. mirabilis	0.368	0.617	43.5
M. morganii	0.840	0.826	-1.6
E. coli	0.386	0.585	34
P. aeruginosa	0.504	1.449	-12,2
S. marcescens	0,503	0.720	30
S. aureus	0,421	0.601	30
E.cloacae	0.513	0.377	-36
K. pneumonia	0.576	0.854	32.6

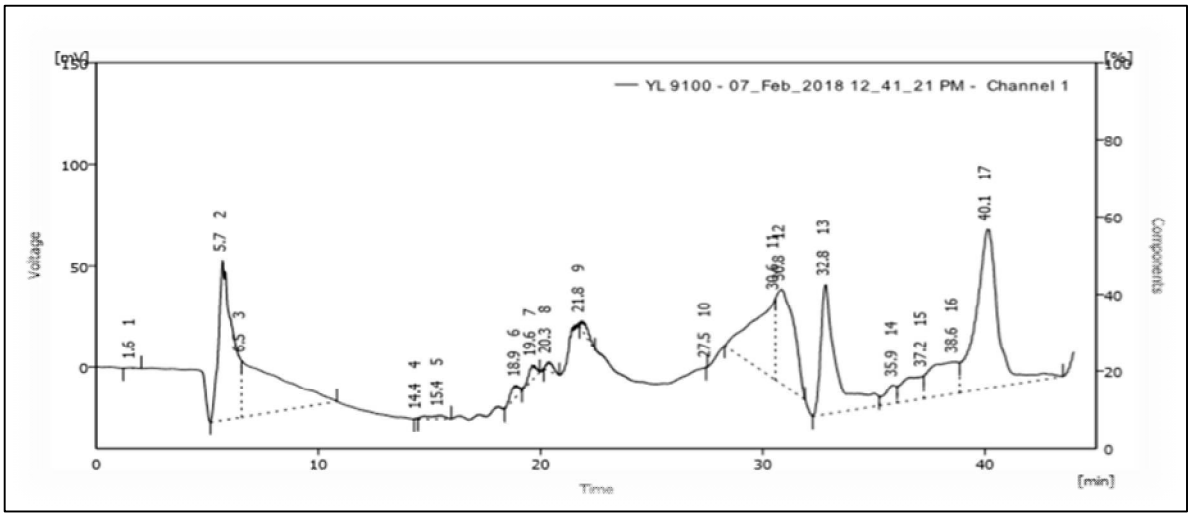

Fig (1) HPLC chromatogram for purified biosurfactant showed several peaks in different RT(14-40 min) produce by *P. aeruginosa* (SA4) isolated from soil rhizosphere.

Indian Journal of Natural Sciences www.tnsroindia.org.in ©IJONS

Vol.9 /Issue 51 / December / 2018 *International Bimonthly* *ISSN: 0976 – 0997*

RESEARCH ARTICLE

Effect of Clove Bud Oleoresin and Turmeric Oleoresin on Quality of Functional Chicken Cutlet

Christina Paulose[1]*, Renuka Nayar[2], Kavitha Rajagopal[2], Lijin James[1], Sunanda C[3] and Magna Thomas[4]

[1]MVSc Scholar, Department of Livestock Products Technology, College of Veterinary and Animal Sciences, Kerala Veterinary and Animal Sciences University, Pookode, Wayanad. Kerala - 673 576, India
[2]Assistant Professor, Department of Livestock Products Technology, College of Veterinary and Animal Sciences, Kerala Veterinary and Animal Sciences University, Pookode, Wayanad. Kerala - 673 576, India.
[3]Assistant Professor, Dept. of Statistics, College of Veterinary & Animal Sciences, Pookode, Wayanad, Kerala– 673 576, India.
[4]Assistant Professor, Dept. of Dairy Science, College of Veterinary & Animal Sciences, Pookode, Wayanad, Kerala– 673 576, India.

Received: 23 Sep 2018 Revised: 25 Oct 2018 Accepted: 27 Nov 2018

***Address for Correspondence**
Christina Paulose
MVSc Scholar,
Department of Livestock Products Technology,
College of Veterinary and Animal Sciences,
Kerala Veterinary and Animal Sciences University,
Pookode, Wayanad.
Kerala - 673 576, India
Email: christy04.mtdy@gmail.com

ABSTRACT

The present study was conducted in the Department of Livestock Products Technology, CVAS, Pookode to study the effect of clove bud oleoresin and turmeric oleoresin on the quality of chicken cutlet incorporated with elephant foot yam (*Amorphophallus paeoniifolius)* and stored in freezer (-18± 2^{0}C).Both oleoresins at 0.5% level was added to the treatment cutlets (T) and was compared with control cutlets (C) for physico-chemical, microbiological and sensory characteristics on days 0,30,60,75 and 90. C had higher pH on days 30 and 60 but there was no significant difference on day 0, 75 and 90. TBARS and tyrosine values of T were significantly lower than C and tyrosine values increased upon storage for both. Total phenolic content of T was higher than C on all days of storage and DPPH values of both oleoresins was evaluated for their antioxidant potential. Texture parameters did not show significant difference except cohesiveness which significantly decreased for T on days 75 and 90. There was no significant difference in moisture, protein and ash contents between C and T, however T had higher fat content. T had better redness and yellowness colour values than C but the values significantly reduced on storage. Aerobic plate, yeast and mould and psychrotrophic counts were significantly lower for T than C and they

significantly increased on storage for both. Both C and T showed 'moderately' to 'very' acceptable scores for all sensory attributes. Thus clove bud oleoresin and turmeric oleoresin at 0.5% level can effectively be incorporated in chicken cutlets for increasing freezer shelf life without affecting the sensory attributes.

Keywords: Chicken cutlet, Elephant foot yam, Clove bud oleoresin, Turmeric oleoresin, Freezer storage.

INTRODUCTION

Meat and meat products are widely consumed owing to their high protein content and nutritive value. Poultry meat is widely accepted without any religious taboo and also has additional benefits like low total fat content than other meats and more monounsaturated (MUFA) and polyunsaturated fatty acids (PUFA). Processing adds to the variety of meat, convenience, nutritive and functional properties of meat. Comminuted meat products contain mixture of meat and non meat ingredients. Elephant foot yam (*Amorphophallus paeoniifolius)* is widely grown tuber crop in India and can act as good binder in comminuted meat products. In addition, it has anti inflammatory, anti tumor, analgesic, gastro protective and antibacterial properties and contains dietary fibre. The phytochemicals present in yam like polyphenols and flavanoids have good antioxidant activity and can be used to prevent lipid oxidation in meat products.

Spices add to the flavour and aroma of foods and have good preservative, antioxidant and antimicrobial activity. Crude extracts from spices like oleoresins are preferred over whole spices due to easy handling and more concentration of phytochemicals rendering preservative action. Clove (*Syzygium aromaticum)* and turmeric (*Curcuma longa*) are two spices commonly used in Indian cuisine. The antimicrobial and antioxidant properties of the above spices may contribute to extend the shelf life of meat and meat products, at the same time adding to the flavour of the products. Extracts of clove had high antioxidant activity mainly due to presence of eugenol and the activity was higher than many synthetic antioxidants (Babuskin *et al*., 2014). Akram *et al*. (2010) stated that the major phenolic compound in turmeric was curcumin and it had potent antioxidant, anti-inflammatory and anti-carcinogenic effects. Hence the present study was conducted to develop chicken cutlets incorporating elephant foot yam along with clove (*Syzygium aromaticum)* and turmeric (*Curcuma longa)* oleoresins and to study effect of turmeric and clove oleoresins in extending shelf life of chicken cutlets.

MATERIALS AND METHODS

Preparation of chicken cutlets

Broiler chickens were procured from the local market, scientifically slaughtered and carcasses were chilled overnight. The carcasses were pressure cooked for 15 min, allowed to drain, deboned and the meat was chopped finely. Yam after peeling of skin was washed, cut into large pieces, pressure cooked for 15 min and mashed. Finely chopped condiments and well ground spice mix were sauted in oil for 15 min. Mashed yam, salt, sauted condiments and spice mix were added to meat. The final mix was divided into 2 equal parts: C - Control with no oleoresins, T - Treatment with 0.5 per cent clove bud oleoresin and 0.5per cent turmeric oleoresin. From each mix oval shaped cutlets (35 g) were moulded, dipped in whole egg and enrobed with rusk powder. The cutlets were subjected to aerobic packaging using high density polyethylene (HDPE) pouches, sealed and were stored at-18±2° C in a freezer. The cutlets were subjected to evaluation of physico-chemical, microbiological and sensory quality characteristics on days 0, 30, 60, 75 and 90.

Physicochemical characters

pH of the samples was measured by using a digital pH meter as per the method described by AOAC (2012). TBARS numbers of control and treatment samples were determined as per Witte *et al*. (1970). Tyrosine values of samples were estimated as per the method described by Pearson (1968). The concentration of total phenolics in acetone extract of the cutlet was determined by the Folin-Ciocalteus (F-C) assay (Escarpa and Gonzalez, 2001) and expressed as µg tannic acid equivalent /g of sample. 2,2'-diphenyl-1-picrylhydrazyl (DPPH) assay was done to evaluate the radical scavenging activity of the oleoresins by the method of Singh *et al*. (2002). Colour of the control and treatment cutlets was determined objectively as per Page *et al*. (2001) using Hunter Lab Mini Scan XE Plus Spectrophotometer (Hunter Lab, Virginia, USA) with diffuse illumination. The textural properties of the control and treatment cutlets were evaluated as per Bourne (1978) using a Universal Testing Machine (TRAPEZIUM EZ-SX, Shimadzu, Japan). Proximate principles were estimated as per AOAC (2012).

Microbiological characteristics

Aerobic plate count (APC) was evaluated as per the procedure of Morton (2001). Psychrotrophic count was analysed as per the procedure of Cousin *et al.* (2001) and yeast and mould count as per the procedure of Beuchat and Cousin (2001).

Sensory characteristics

Sensory evaluation of chicken cutlets was conducted by a semi–trained panel consisting of seven panelists from the Department of Livestock Products Technology, College of Veterinary and Animal Sciences, Pookode using an eight-point Hedonic scale.

Statistical analysis

The data obtained were statistically analyzed by one-way ANOVA, repeated measures ANOVA, Kruskal- Wallis test, rank Wilcoxon signed test, Friedman test, Mann Whitney test using SPSS software (VERSION 21) as per Snedecor and Cochran (1994).

RESULTS AND DISCUSSION

Physicochemical characters

There was no significant difference in pH between C and T on days 0, 75 and 90. But the pH was significantly low for T on days 30 and 60. pH values of both C and T increased during storage period and increase was significantly ($p < 0.01$) evident from 60th day of storage. There was a significant ($p<0.01$) decrease in TBARS values in control as well as treatment cutlets on day 30, followed by an increase up to day 75 and a highly significant ($p<0.01$) reduction on day 90 of storage. But on all days T had significantly lower TBARS values than C indicating the ability of oleoresins to reduce oxidative rancidity in the product. Sun *et al*. (2018) observed low TBARS values in dry sausages treated with spice extracts than control sausages and attributed it to the polyphenol compounds in spice extracts. Shan *et al*. (2005) observed that clove bud had the highest antioxidant activity, polyphenol content and gallic acid equivalent than 26 other spices when quantified by high performance liquid chromatography. Curcuminoids which are the major components of turmeric had unique conjugated molecular structures which gave them a better oxygen radical trapping ability (Metzler *et al*., 2013).

Tyrosine values of T were significantly lower than C on all days and the values increased subsequently on storage for all samples. Lower tyrosine values of T could be attributed to the antimicrobial and anti-proteolytic activities of spice oleoresins in the cutlets. Control cutlets had significantly ($p<0.01$) lower phenolic content than T on all days. The mean phenolic values of C and T were 19.77 ± 0.50 and 65.89 ± 3.18 (µg TAE /g of sample), respectively. Total polyphenol content of 13 spices were analysed and highest value of 79.5 mg GAE/ g was obtained for clove (Kong *et al*., 2010). Fresh yam (*Amorphophallus paeoniifolius)* showed a DPPH radical scavenging activity of 87.83 ± 0.89 %. DPPH radical scavenging activity of clove oleoresin containing 25µg of phenolics as tannic acid equivalents was found to be 56.19 ± 0.23% and turmeric oleoresin containing 25µg of phenolics as tannic acid equivalents was 69.14 ± 1.31%.

There was significant ($p<0.01$) difference in 'L' values of samples on all days of storage, with T showing the lowest values. This could be attributed to the yellowish tinge in cutlets treated with turmeric oleoresin. There was significant ($p<0.01$) increase in 'L' values of all the samples on storage. T had significantly higher 'a' and 'b' values than C and all values decreased on storage. Addition of rosemary and Chinese mahogany extracts significantly decreased the lightness values and increased the redness (a) values in chicken sausages (Liu *et al.,* 2009).Texture parameters did not show significant difference except cohesiveness which decreased for T on days 75 and 90.

Proximate analysis

Samples were evaluated for moisture, fat, protein and ash. Energy and carbohydrate values of samples were obtained by calculation. There was no significant difference in moisture, protein, ash and carbohydrate contents between C and T on any day of storage. But T had significantly ($p<0.01$) higher fat content and subsequently higher energy value than C and this might be due to the oil content in oleoresin. Dietary fibre content of yam incorporated cutlets ranged from 1.56 to 7.92 %. This might be due to different varieties of yam and stage of harvest. According to Yadav and Singh (2016) the crude fibre content of *Amorphophallus paeoniifolius* varied between different varieties and was 2.69% for NDA-5 variety and 3.20% for NDA-9 variety.

Microbiological characteristics

There was significant ($p<0.01$) difference in aerobic plate counts between control and treatment on all days of storage. Treatment had significantly ($p<0.01$) lower aerobic plate counts than C. The antimicrobial activity of essential oils when used in combination could lead to additive, synergestic or antagonistic effect which was in turn affected by intrinsic and extrinsic parameters and essential oils containing aldehydes or phenols as major components had the highest antimicrobial activity than others (Bassole and Juliani, 2012). Psychrotrophs were detected from 0^{th} day onwards. Control cutlets had significantly higher psychrotrophic count than treatments on all days except day 0. There was significant increase in psychrotrophic counts from day 60 onwards. Yeast and mould count also differed significantly ($p<0.01$) between samples except on 90^{th} day; C having significantly ($p<0.01$) higher counts when compared to T. The better microbiological quality of T could be due to the antimicrobial effect of clove and turmeric oleoresins. Hu *et al*. (2017) opined that antifungal activity of turmeric essential oil was by membrane disruption of fungal cell along with mitochondrial dysfunction and hence it could be used as a potent fungicide in food. Rana *et al*. (2011) studied the activity of clove oil against different stages of fungus and reported that eugenol in clove was responsible for antifungal activity and acted by the lysis of micelle and spores. All the microbial counts increased significantly across storage.

Sensory attributes

Sensory evaluation was done by semi trained panelists for various attributes like colour/appearance, flavour, texture, juiciness, aftertaste and overall acceptability. The colour/appearance scores of samples did not vary significantly

except on 90th day of storage in which oleoresin incorporated cutlets had significantly lower scores. Control showed a significant ($p<0.05$) lowering of flavour scores on storage. There was no significant difference in texture between samples and across storage period. Significant ($p<0.05$) difference was observed in aftertaste scores from day 60 of storage, with comparatively lower scores for oleoresin treated cutlets. Overall acceptability scores of all samples significantly ($p<0.05$) decreased along storage but both C and T showed 'moderately' to 'very' acceptable scores for overall acceptability on all days of storage. The cost of production of C and T were calculated and there was negligible difference between both and incorporation of oleoresin was economically feasible. Shelf life of C was130 days and that of T was 165 days indicating that oleoresins of turmeric and clove could extend the shelf life of chicken cutlet under freezer condition.Thus the study showed that incorporation of clove bud and turmeric oleoresins at 0.5% in chicken cutlets reduced the lipid oxidation, proteolysis, microbial growth and had better phenolics and radical scavenging activity. Incorporation of oleoresins in cutlets as functional ingredients can effectively preserve the product, extending the shelf life under freezer condition with negligible increase in cost of production and without affecting the organoleptic attributes of the product.

ACKNOWLEDGMENTS

The authors would like to thank Dean, CVAS, Pookode and faculty and staff of Dept of LPT for the facilities offered. The first author also acknowledges Kerala Veterinary and Animal Sciences University for providing funds for conducting the research work.

REFERENCES

1. Babuskin, S., Babu, P.A.S., Sasikala, M., Sabina, K., Archana, G., Sivarajan, M. and Sukumar, M. Antimicrobial and antioxidant effects of spice extracts on the shelf life extension of raw chicken meat. Int. J. Food Microbiol.2014; **171**:32-40.

2. Akram, M., Shahab-Uddin, A.A., Usmanghani, K., Hannan, A., Mohiuddin, E. and Asif, M. Curcuma longa and curcumin: a review article. Rom J Biol Plant Biol.2010;**55**(2): 65-70.

3. AOAC. 2012. Meat and meat products. *In Official Methods of Analysis of Analytical Chemists*. (19th Ed.)Association of Official Analytical Chemists. Inc., Arlington, Virginia. pp. 931-948.

4. Witte, V.C., Krause, G.F. and Bailey, M.E. A new extraction method for determining 2-thiobarbituric acid values of pork and beef during storage.J. Food Sci. 1970; **35**: 582-585.

5. Pearson, D. Application of chemical method for assessment of beef quality. In Methods related to protein breakdown. J. Sci. Food Agric.1968;**19**:364-366.

6. Escarpa, A. and Gonzalez, M. C. Approach to the content of total extractable phenolic compounds from different food samples by comparison of chromatographic and spectrophotometric methods. Anal. Chim. Acta.2001;**427**:119–127

7. Singh, R. P., Murthy, K.N.C. and Jayaprakasha, G.K. Studies on the antioxidant activity of pomegranate (*Punica granatum*) peel and seed extracts using in-vitro models. J. Agric. Food chem.2002;**50**:81-86.

8. Page, J.K., Wulf, D.M. and Schwotzer, T.R.. A survey of beef muscle colour and pH. J. Anim.Sci.2001;**79**:678-687.

9. Bourne, M. C. Texture profile analysis. Food Technol. 1978; **32**:62–66.

10. Morton, R.D.. Aerobic plate count. In: Downes, F.P., and Ito, K (ed.), *Compendium of Methods for the Microbiological Examination of Foods*. (4th Ed.). APHA, Washington, D.C. 2001;pp: 63-67.

11. Cousin, M.A., Jay, J.M. and Vasavada, P.C.. Psychrotrophic microorganisms. In: Downes, F.P., and Ito, K (ed.), *Compendium of Methods for the Microbiological Examination of Foods*. (4th Ed.). APHA, Washington, D.C.2001; pp.159-166.

12. Beuchat, L.R. and Cousin, M.A. 2001. Yeast and Molds. In: Downes, F.P., and Ito, K(ed.), *Compendium of Methods for the Microbiological Examination of Foods*. (4th Ed.). APHA, Washington, D.C. pp. 209-213.

13. Snedecor, G.W. and Cochran, W.G. 1994. *Statistical Methods*. (8th Ed.) The Iowa State University, Ames, Iowa, 313p.

14. Sun, Q., Zhao, X., Chen, H., Zhang, C. and Kong, B. Impact of spice extracts on the formation of biogenic amines and the physicochemical, microbiological and sensory quality of dry sausage. Food Control. 2018;**92**: 190-200.
15. Shan, B., Cai, Y.Z., Sun, M. and Corke, H. Antioxidant capacity of 26 spice extracts and characterization of their phenolic constituents. J.Agric Food Chem. 2005; **53**(20): 7749-7759.
16. Metzler, M., Pfeiffer, E., Schulz, S.I. and Dempe, J.S. Curcumin uptake and metabolism. Biofactors.2013; **39**:14–20.
17. Kong, B., Zhang, H. and Xiong, Y.L. Antioxidant activity of spice extracts in a liposome system and in cooked pork patties and the possible mode of action. Meat Sci. 2010; **85**(4): 772-778.
18. Liu, D.C., Tsau, R.T., Lin, Y.C., Jan, S.S. and Tan, F.J.Effect of various levels of rosemary or Chinese mahogany on the quality of fresh chicken sausage during refrigerated storage. Food Chem. 2009; **117**(1): 106-113.
19. Yadav, A. and Singh, S. Physicochemical Properties of Selected Varieties of Elephant Foot Yam (*Amorphophallus paeoniifolius*). Int. J. Home Sci.2016; **2**(3): 353-357.
20. Bassolé, I.H.N. and Juliani, H.R. Essential oils in combination and their antimicrobial properties. Molecules.2012; **17**(4): 3989-4006.
21. Hu, Y., Zhang, J., Kong, W., Zhao, G. and Yang, M. Mechanisms of antifungal and anti-aflatoxigenic properties of essential oil derived from turmeric (*Curcuma longa* L.) on *Aspergillus flavus*. Food Chem.2017; **220**: 1-8.
22. Rana, I.S., Rana, A.S. and Rajak, R.C.. Evaluation of antifungal activity in essential oil of the *Syzygium aromaticum* (L.) by extraction, purification and analysis of its main component eugenol. Brazilian J. Microbiol. 2011; **42**(4): 1269-1277.

Table 1. Aerobic Plate Counts (log $_{10}$ cfu/g sample) of control and treatment cutlets on different storage days

Treatment	Mean ± SE					F-value (p-value)
	Day 0	Day 30	Day 60	Day 75	Day 90	
C	4.82 ^{aE} ± 0.03	4.90 ^{aD} ±0.02	5.12 ^{aC} ± 0.06	5.70 ^{aB} ± 0.04	6.02 ^{aA} ±0.06	144.118** (<0.001)
T	4.69 ^{bE} ± 0.02	4.73 ^{bD} ±0.02	4.84 ^{bC} ± 0.02	5.06 ^{bB} ± 0.04	5.28 ^{bA} ±0.06	46.117** (<0.001)
F-value	14.474*	54.781**	24.196**	123.600**	83.125**	
p-value	0.003	< 0.001	< 0.001	< 0.001	< 0.001	

** Significant at 0.01 level; * significant at 0.05 level
Means having different small letter as super script are significantly different (p<0.05) within a column
Means having different capital letter as super script are significantly different (p<0.05) within a row

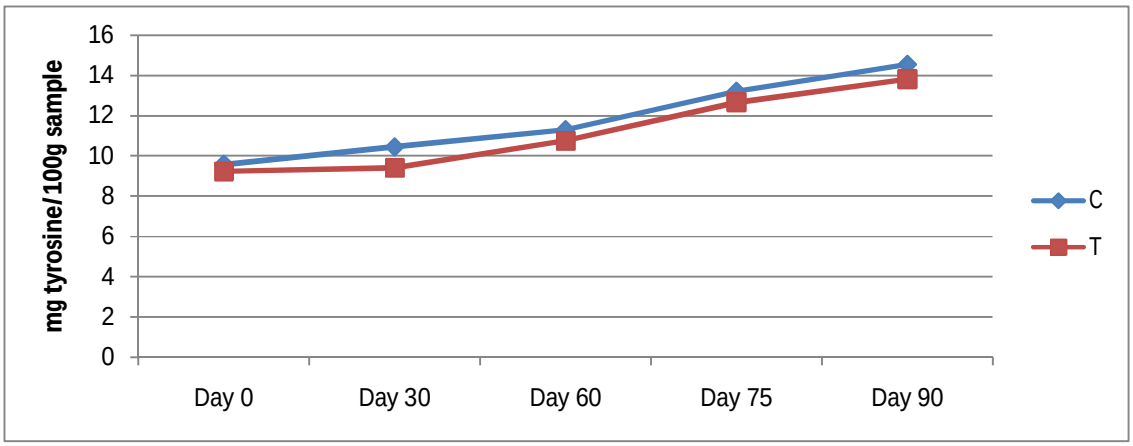

Fig 1: Tyrosine values (mg/100g sample) of control and treatment cutlets on different storage days

Indian Journal of Natural Sciences www.tnsroindia.org.in ©IJONS

Vol.9 /Issue 51 / December / 2018 *International Bimonthly* *ISSN: 0976 – 0997*

RESEARCH ARTICLE

Spectral Analysis of Water Reflectance for AL-Hammar Marshes, South of Iraq Using Remote Sensing Techniques

Tabarak S. Hashesh[1]* and Bushra A. Ahmed[2]

[1]Physics Department, College of Science, University of Baghdad, Iraq.
[2]Remote Sensing and GIS Department, College of Science, University of Baghdad, Iraq.

Received: 01 Sep 2018 Revised: 04 Oct 2018 Accepted: 07 Nov 2018

***Address for Correspondence**
Tabarak S. Hashesh
Physics Department,
College of Science,
University of Baghdad,Iraq.
Email : tabark.sami1994@gmail.com

ABSTRACT

The marshes are the largest ecosystem in the Middle East and West Asia, with its fresh water surface extending over three Iraqi provinces in the south of Iraq: Maysan, DhiQar and Basra, between the Tigris and Euphrates rivers on an area of about 16,000 km^2. This paper aimed to analyze the reflectance of locational variance, analyze seasonal difference for satellite images, find the long-term changes of water quality assessment for Al_Hammar marshes in the south of Iraq through measuring the changes of Iraqi marshland's area as well as the changes in the spectral reflectivity water quality using Geographic Information Systems (GIS) and remote sensing techniques. Temperature and Electrical conductivity (EC) as physical and chemical characteristics of water, Chlorophyll-a (*Chl-a*) and Secchi depth (SD) were studied for Al_Hammar marshes. In addition, the seasonal variation of all the parameters was covered through this paper, the obtained results showed some fluctuation during different seasons for different locations of the areas marshland. There were distinctive reflectance differences among the marshes areas in the south of Iraq using remote sensing techniques.This technique utilizes for generating thematic map of each seasons to assessment water quality in the studied marshes.

Keywords: Landsat, spectral reflectivity**,** water quality, remote sensing, IDW interpolation.

INTRODUCTION

The ecosystem contains many compounds and the important and abundant of them is water, which has ability to melt different organic and inorganic compounds. Wetland ecosystems have unique freshwater as in the Iraqi marshes which are one of the largest wetlands in the Middle East and Western Eurasia [1]. The Mesopotamian marshlands (hereafter "the Marshes") are home to ancient communities rooted in the dawn of human history. These marshes

were once the largest wetlands in Southwest Asia and covered more than 15,000 km^2.Originally covering considerable parts of the Mesopotamian Plain, which developed along the Euphrates and Tigris Rivers, Iraqi marshes are important as they have economic, social, and biodiversity value. They support coastal fisheries, which endow them with a truly global dimension, and they represent a permanent habitat for many unique species of plants, fish, invertebrate, and birds, and a flyway for millions of birds migrating between Siberia and Africa [2].The Marsh Arabs livelihood was tuned to the flood environment and consisted of a combination of fishing and rice cultivation mixed with livestock breeding of buffalos. Swamp reed was used to build houses and for centuries this self-sufficient way of life hardly changed. Both the Euphrates and Tigris rise in the Anatolian mountains in Turkey and snowfall there is the major precipitation source. Hence, the rivers gather their water resources in climates rich in precipitation and traverse hundreds of kilometers through arid lands where they are the main source of livelihood. Consequently, changes in the water flow upstream can have profound effects on the marshes. Conflicts over Euphrates and Tigris have been common for centuries Iraq, Syria, Iran, and Turkey share the waters of the Tigris and Euphrates, and Iraq and Syria especially are highly dependent on the water due to their arid climates and policies of food self-sufficiency [3]. In Mesopotamia, the drainage and diversion of water are the most serious threats, as typically supply for agricultural use, recently, for military reasons [1]. Physical and chemical properties play a big role to determine quality of water and to compare with the standard values. Water quality is represented in terms of restoration southern Iraqi marshes [4]. Different harmful contaminants beyond to increase human population, industrialization, fertilizers and man-made activity pollute water. Qualitative and quantitative measurements are useful to monitor water quality of various supplying sources. Water quality indices are tools to determine water condition[1].

MATERIALS AND METHODS

Description of a studied area

Al-Hammar marshes site in the space between Nasiriyah, Basrah, and Qurnah.Assessments of this marsh area domain from (2,800) km²of close permanent marsh and lake, extending to a total area of over (4,500) km² during periods of seasonal and temporary immersion. The high depth at low water levels is (1.8) m and about three meters at high water mark. During summer, large parts of the shore zone dry out, and banks and islands emerge in many places. Fed primarily by the Euphrates River and a considered amount of water from the Tigris River, overflowing from the central marshes, nourishes the Al-Hammar marshes. The coordinates of Al-Hammar marsh are (30° 35′ to 31° 00′ N), (46° 25′ to 47° 45′ E), and its altitude mostly ranges between (4.5 and 9m.) above sea level [5]. Al-Hammar marsh location and its selected points for study are clarified in figure (1) and table (1), respectively.

Define Parameters

Water Temperature (WT)

Water temperature is one of the most important parameters for water quality and ecosystem studies. Temperature can influence many chemical and biological processes and therefore impacts on the living conditions and distribution of aquatic ecosystems [6].

Electrical conductivity (EC):

Electrical conductivity represent the ability of current conduction and in water case it is an estimator of the total dissolved salts or ions amount in water, water conductivity may be fixed by different factors like watershed geology, the watershed's size in relation to lake size, wastewater from point sources, runoff from non-point sources, atmospheric inputs, evaporation rates, some types of bacterial metabolism etc. Is generally measured in (μs/cm) [7].

Image Classification

Satellite remote sensing technique which is applied to interpret the observed data and classify features combines to the approach of photointerpretation, and quantitative analysis that uses computer to label each pixel to particular spectral classes (known as classification), is usually used. Quantitative analysis preforms true multispectral analysis, allow using already brightness levels and getting high quantitative accuracy. This technique has two classification procedures: supervised classification and unsupervised classification.First one represents the fundamental tool that apply for extracting quantitative information from remotely sensed image data, and a maximum likelihood classification (MLC) is type of the supervised classification that is commonly used, it suggests that a multivariate normal distribution can be achieved to represent each spectral class [8], this procedure is shown in Figure (2).

Interpolation Methods

This method is defined asthe process of predicting a definite interested variable at unsampled locations beyond to measured values for selected points within the interest area and it covers two division deterministic and geostatistical technique. Deterministic interpolation techniques contain mathematical functions that use to calculate the values at nameless locations founded either on the similaritydegree (e.g. IDW) or the smoothingdegree (e.g. RBF) in relation with neighboring points. While geostatisticaltechniques contain mathematical and statistical functions to portend nameless locations values and to provide probabilistic estimates of the interpolation quality founded on the spatial autocorrelation between points. In addition, interpolation processes distinguish into two groups: local and global. First one operates within areas smaller than of the required area surround the position of the estimated point (neighborhood) [9].Some local deterministic methods are local polynomial Inverse Distance Weighting (IDW), and radial basis functions (RBF). On the other hand, the first one deals with all ready sample points to generate estimations for the whole area. These techniques may be applied to evaluate and remove global variations happened by physical trends in the data. Also, interpolation techniques may be divided into inexact and exact interpolations. Exact interpolators predict values corresponding to the measurements at sampled locations [9].The IDW method has been adopted.

Inverse Distance Weighted (IDW)

It is an exact local deterministic interpolation technique. This technique proposes that the unsampled location value is a distance-weighted average of values at sampled points through a specified neighborhood surrounding the unsampled point [9]. In other words, IDW suggests that closer points to the portending sites will have effect on the predicted value than points sited further away [10]:
IDW utilizes

$$z(s_o) = \sum_{i=1}^{N} \lambda_i . z(s_i) \quad ----------1$$

Where:

$z(s_o)$is a portended value at the unsampled site (s_o).
N is a calculated sample point's number within the determined neighborhood for s_0.
λ_i is related distance-dependent weights with each sample point.
$z(s_i)$is *the* observed value at site s_i.
$\lambda_i$is given by:

$$\lambda_i = \frac{d_{io}^{-p}}{\sum_{i=1}^{N} d_{io}^{-p}} ----------- 2$$

$$\sum_{i=1}^{N} \lambda_i = 1 ----------- 3$$

Where:
$d_{i0}$is the portending site $s_0$and the measured site location s_i distance.
P is the power parameter that set the reduction rate of the weights as distance increases.
IDW is controlled to be an exact interpolator to avoid the division by zero that occurs when d_{i0}= 0 at the sampled points [9, 10].

RESULTS AND DISCUSSION

Seasonal change of reflectance values

For analyzing the seasonal change of reflectance values, data were gathered into four seasons of 2017: winter (December, January and February), spring (March, April and May), summer (June, July and August) and autumn (September, October and November). Landsat 8 satellite images [11] were used for AL-Hammar Marshes and 10 sites were identified using GIS (Geographic Information System), the spectral reflectivity for water sites created by the Erdas imagines. Figure (3) shows the spectral reflectivity of water for 10 sites (p1- p10) in each season and for four bands (Blue, Green, Red and NIR). From the figures above, it can be seen that the highest values shown in spring and summer. It is found that the values of spectral reflectivity in all used ranges were the lowest values in winter and autumn due to the increased turbidity in both seasons.The reflectances of all seasons is quite identical in the blue and green bands. In the red band the values were equal as in the previous bands, but differences at point 7 and high reflectivity values during spring and summer seasons. In the NIR band, there was an increase in reflectivity values in the spring and summer seasons as well as in autumn, while the lowest reflectivity values were recorded during the winter season.

Results of the Physical and Chemical Characteristics of Water

The Landsat 8 satellite images were utilized for AL_Hammar Marshes located in the province of DhiQar (Lat 30 N/ Long 46, 47 E) and 10 sites were specified using GIS (Geographic Information System), as shown in the table (3-1). The physical and chemical characteristics of water such as temperature (whichcan influence many chemical and biological processes and then water quality) and Electrical conductivity (EC) (which is an estimator of the total dissolved salts or ions amount in water) were studied as shown below;

Water Temperature (WT)

From our results, the water temperature ranged between 11 and 32 during the 2017. The values showed that the highest value is in summer and spring and the value decreases gradually in autumn after then in winter. Statistical results of WT water in AL_Hammar Marshes are seen in Tables (2, 3, 4 and 5) and figure (6), the figure below shows the measurement of parameters for four seasons of the Marshes.
IDWinterpolation ofparameter WT in the fourseasons:

Electrical Conductivity (EC)

Results clarify that the electrical conductivity ranged between 5140 and 37700 during the 2017. The values showed that the highest value is in summer and autumn and the value decreases gradually in winter after then in spring. Statistical results of EC water in AL_Hammar Marshes are seen in Tables (2, 3, 4 and 5) and figure (6).Figure (5) illustrates the spatial distribution of EC in marshes.
IDWinterpolation ofparameter EC in the fourseasons:
The tables below show the minimum, maximum, scale and means with the standard deviation of the parameters during the seasons (spring, winter, summer and autumn) in 2017 for the AL_Hammar marshes.

Modeling Chlorophyll-a Quantities and Secchi Depths

Chlorophyll-a (*Chl-a*) and Secchi depth (SD) are used to essess the changes over season for 10 sites in section (4.1) of water in AL-Hammar marshes [12]:

$$Chl_{-a}\left(\frac{\mu g}{L}\right) = -46.51 + 105.30\left(\frac{G}{B}\right) - 40.39\left(\frac{R}{B}\right) - - - - - - - - - - (4)$$

$$SD(m) = 26.07 - 23.26\left(\frac{G}{B}\right) - 17.19\left(\frac{R}{B}\right) - - - - - - - - - - - - - - (5)$$

Where are represented by B, G and R the blue, green and red band reflectance values, respectively.
Figure (4) and (5) show the changes of estimated quantities. In general, the models show decrease in trends of chlorophyll-a quantitiesand an increasing of Secchi disk depth. In the sample from points P8 to P10 in winter, the chlorophyll-a decreases and the Secchi disk depths decrease too due to the lack of rain in this year.
The reflectance of water changes with the chlorophyll concentration is involved. Whereas, chlorophyll concentration increasing lead to increase reflectance green wavelengths (sample points P4 and P7 in green band in summer).)
(In general one can consider that the decreasing of chlorophyll values increase Secchi disk depth, the opposite results as shown in Figures (7,8) can be related to the dissolved organic compounds that change water color and non-algal particulates such as clay or sand [13].

Water Quality MappingofReflectance Values

The obtained results of the seasonal change for reflectance values analysis (value per sampling point) were then used as input data in ArcGIS 10.2. The sampling locations are integrated with the water datafor the generation of spatial distribution maps. The present study uses the Inverse Distance Weighted (IDW) method for spatial interpolation of water reflectance in AL-Hammar marshes of seasonal change in 2017as clarified in figures (9, 10, 11, and 12).
IDW interpolation in Spring season2017:

CONCLUSIONS

After analyzing the obtained results, we conclude important points as below

1. The reflectance values are significantly linked with seasons and they are lower in winter and autumn for all bands in compare to the rest of the seasons but for pring they have higher value.
2. The value of Water Temperature (WT) in the AL Hammar Marshes showed high seasonal variations and ranged from 11 to 32 °C.The highest values were recorded in the summer season and lowest during the winter months.

3. The value of Electrical Conductivity (EC) ranged from 5140 and 37700 in Hor Al-Hammar, higher EC were observed during summer and autumn than in winter and spring (Tables 2-5). Low values of conductivity could be attributed to the dilution of salts due to rainfalls. It could be concluded that the value of conductivity is within the productive range and the marshes of southern Iraq could be considered as a productive water body.
4. The modeling of chlorophyll-a values and Secchi disk depth in section 4.2 implied water clarity and chlorophyll-a values that both of them have decreased over the season. The water clarity decreasing beyond to many reasons as dissolved organic compounds that change water color and non-algal particulates like clay or sand. Further research may explain the reason for water clarity decreases in the best way;
5. The results of the interpolation for a water quality seasonally in all bands (Figs 9-12) showed that there is approximately a good adaption between selected points in AL-Hammar Marshes, South of Iraq to estimate far away point of the selected area.

REFERENCES

1. Talib, A. H., somelimnological features of AL-Hammar marshes south of iraqafter restoration. Iraqi Journal of Agricultural Sciences, 48(5), 1356-1363,2017.
2. Al-Gburi, H. F. A., Al-Tawash, B. S., & Al-Lafta, H. S. , "Environmental assessment of Al-Hammar Marsh, Southern Iraq", *Heliyon*, *3*(2), e00256, 2017.
3. Adriansen, H. K. ," The Iraqi Marshlands: Is Environmental Rehabilitation Possible", In Papers and Proceedings of Applied Geography Conferences, Vol. 29, 2006, pp. 214-223.
4. Al-Mosewi, T. J. K., Water Quality of Al-Hammar Marsh South Iraq. Journal of Engineering, 15(3), 3999-4008,2009.
5. Bedair, H. M., Al Saad, H. T., & Salman, N. A., Iraq's Southern Marshes Something Special To Be Conserved; A Case Study. Marsh Bulletin, 1(2), 99-126,2006.
6. Varol, M., Gökot, B., Bekleyen, A., &Şen, B., Water quality assessment and apportionment of pollution sources of Tigris River (Turkey) using multivariate statistical techniques—a case study. *River research and applications*, *28*(9), 1428-1438,2012.
7. Pal, M., Samal, N. R., Roy, P. K., & Roy, M. B. Electrical Conductivity of Lake Water as Environmental Monitoring–A Case Study of Rudrasagar Lake.
8. Xiong, L., Supervised Classification and Unsupervised Classification. ATS.1-12, 2005.
9. Peter, A. B. and Rachael, A. M., Principles of Geographical Information Systems. Oxford University Press Inc., New York, 17-34,1998.
10. Johnston, K., VerHoef, J. M.,Krivoruchko, K., and Lucas, N., Using ArcGIS geostatistical analyst (380). Redlands: Esri,2001.
11. https://earthexplorer.usgs.gov
12. Seong, J. C., Hwang, C. S., Gibbs, R., Roh, K., Mehdi, M. R., Oh, C., &Jeong, J. J. 2017. Landsat Big Data Analysis for Detecting Long-Term Water Quality Changes: a Case Study in the Han River, South Korea. ISPRS Annals of the Photogrammetry, Remote Sensing and Spatial Information Sciences, 4: 83-89.
13. Lakewatch, F., A Beginner's Guide to Water Management: Lake Morphometry. University of Florida Cooperative Extension Service, Institute of Food and Agricultural Sciences, EDIS: 1-32.2001.

Table 1: Shows the location of selected points AL_Hammar Marshes

X_coordinate	Y_coordinate
650349	3417505
691726	3420844
678659	3420338
659794	3411700
665800	3413954
640774	3427433
637228	3411997
656581	3420686
653435	3409801
653035	3409755

(Unite: meter in WGS_1984_UTM_Zone_38N)

Table 2:The minimum, maximum, scale and means with the standard deviation of parameters (WT and EC) for ALHammar marshes during Winter.

Parameters	Minimum	Maximum	Range	Means	Std. Deviation
WT (C°)	11	13	2	11.8	0.63246
EC(s/cm)	5140	22989	17849	10101	6223.801

Table 3:The minimum, maximum, scale and means with the standard deviation of parameters (WT and EC) for ALHammar marshes during Spring.

Parameters	Minimum	Maximum	Range	Means	Std. Deviation
WT (C°)	29	31	2	29.6	0.699206
EC(s/cm)	6845	13478	6633	9981	2543.648

Table 4:The minimum, maximum, scale and means with the standard deviation of parameters (WT and EC) for ALHammar marshes during Summer.

Parameters	Minimum	Maximum	Range	Means	Std. Deviation
WT (C°)	30	32	2	30.8	0.632456
EC(s/cm)	8099	37700	29601	14943.2	10013.755

Table 5:The minimum, maximum, scale and means with the standard deviation of parameters (WT and EC) for ALHammar marshes during Autumn.

Parameters	Minimum	Maximum	Range	Means	Std. Deviation
WT (C°)	27	30	3	28.8	1.032796
EC(s/cm)	8237	37140	28903	12209.5	8790.891

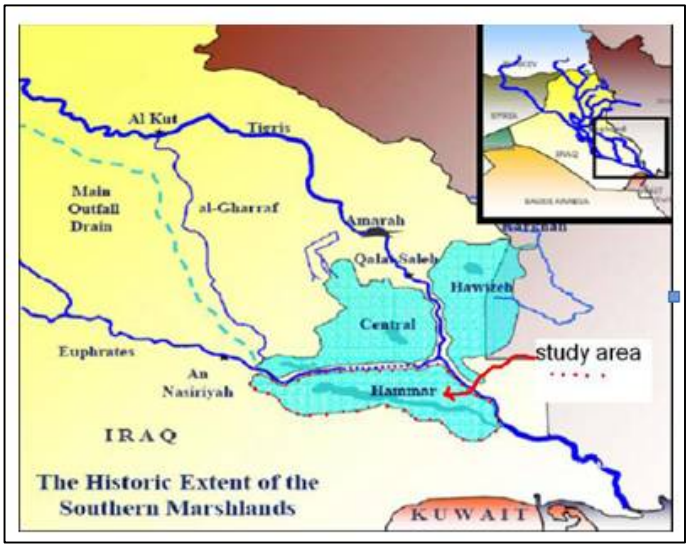

Figure 3: Map of southern Iraq, AL-Hammar marshes [5].

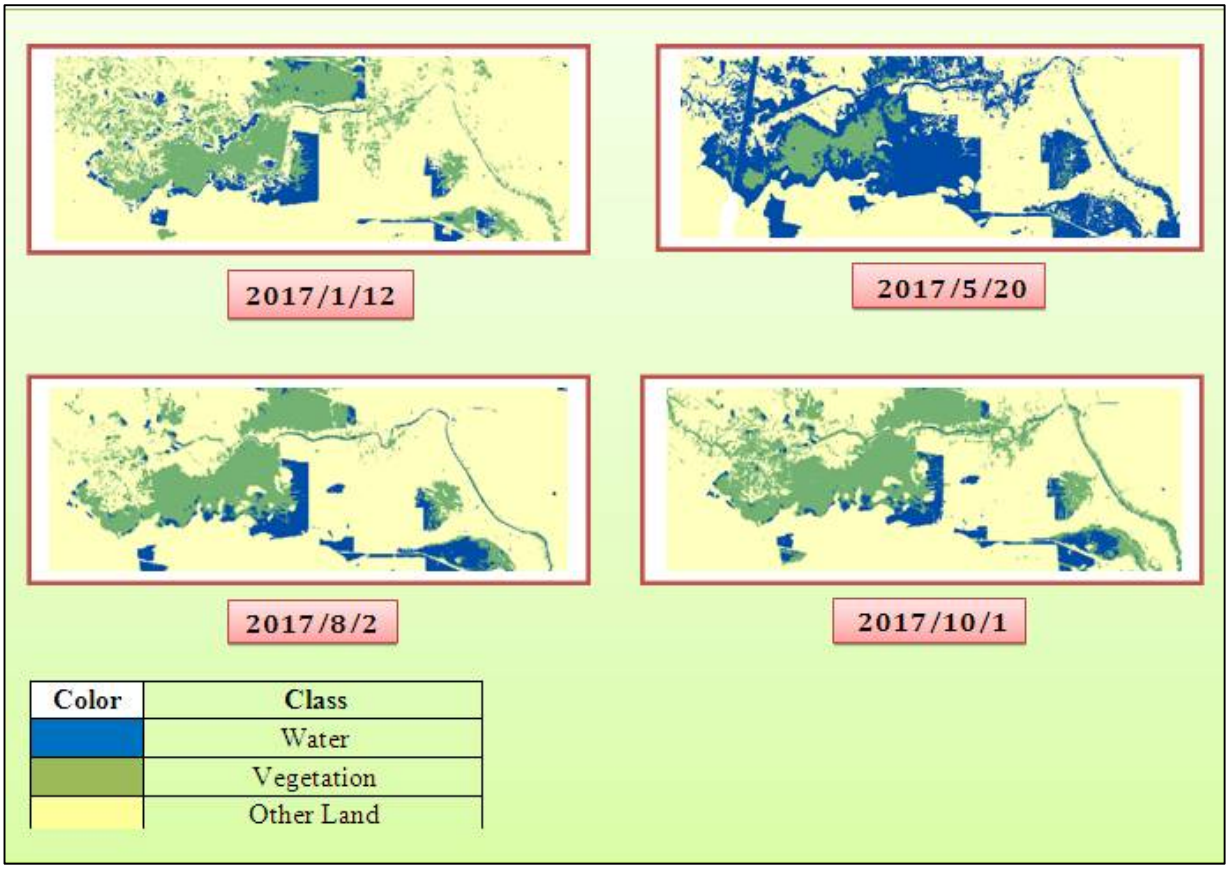

Figure 2:Supervise Classification of AL-Hammar for 2017.

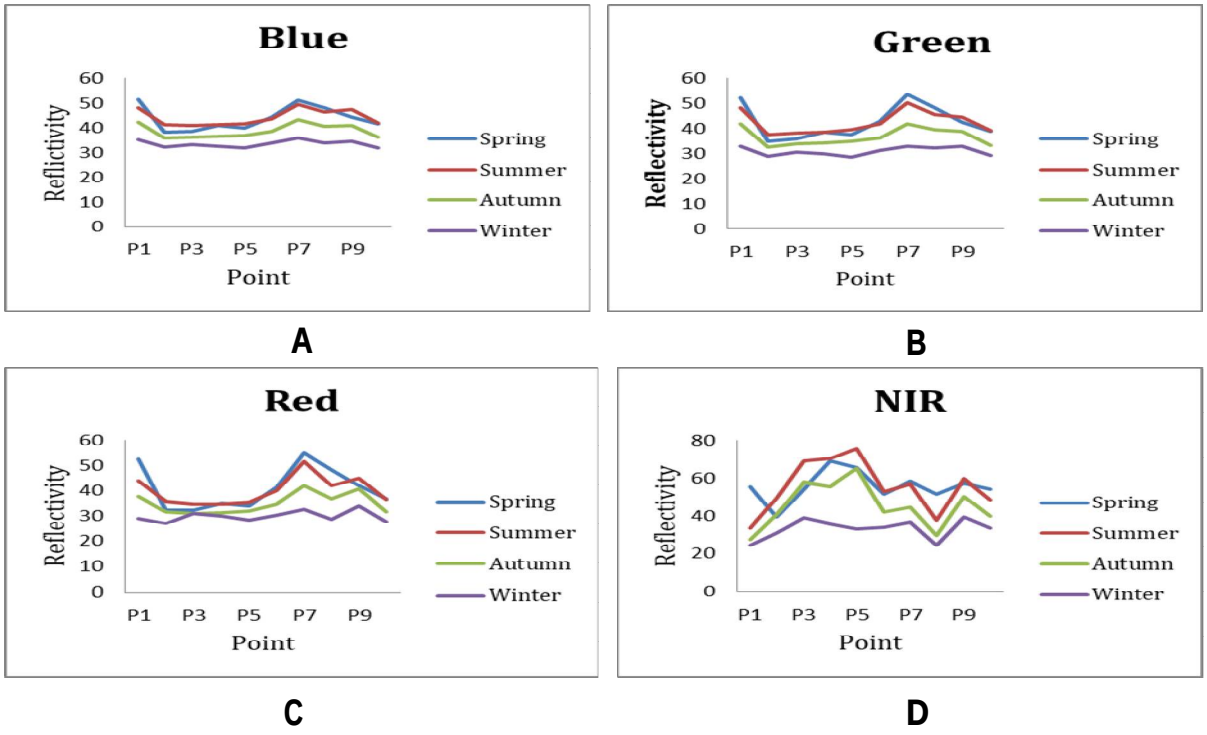

Figure 3: reflectance values at the sample points P1 through P10were inAL-Hammar marshes in2017.

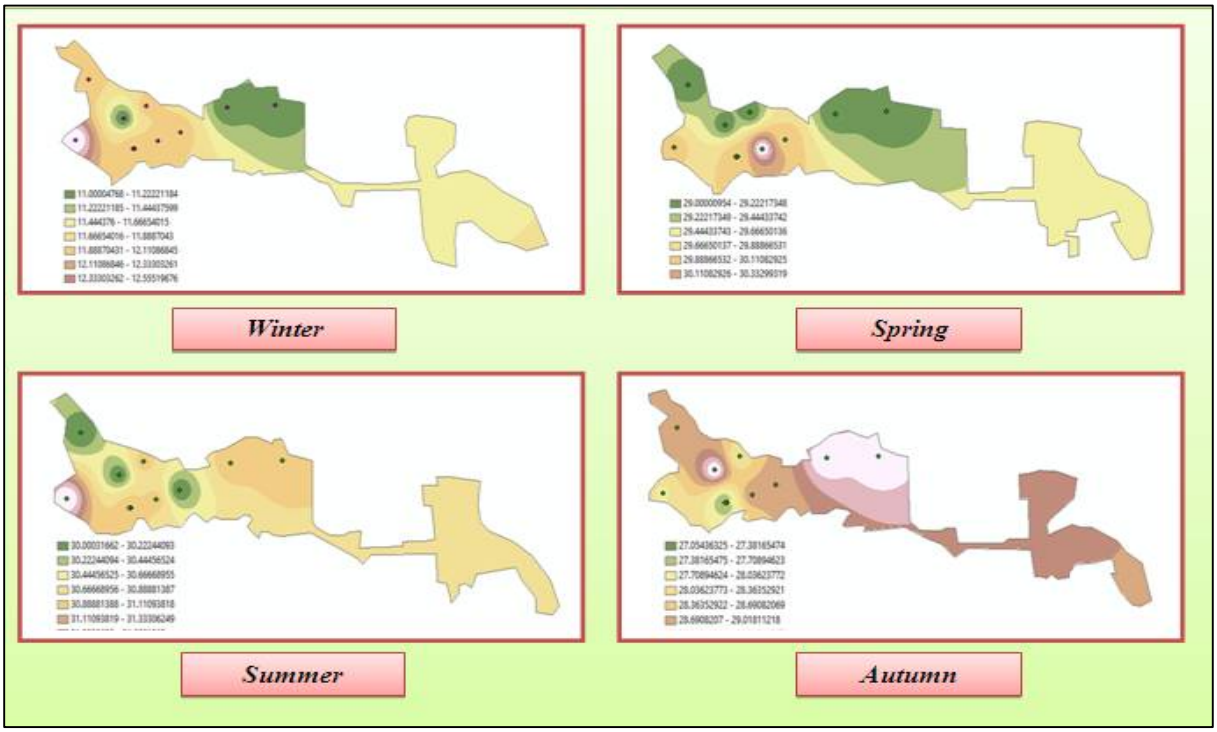

Figure 4: The spatial distribution of WT in seasons (winter, spring, summer and autumn) for Al_Hammar marshes

Figure 4: The spatial distribution of EC in seasons (winter, spring, summer and autumn) for Al_Hammar marshes

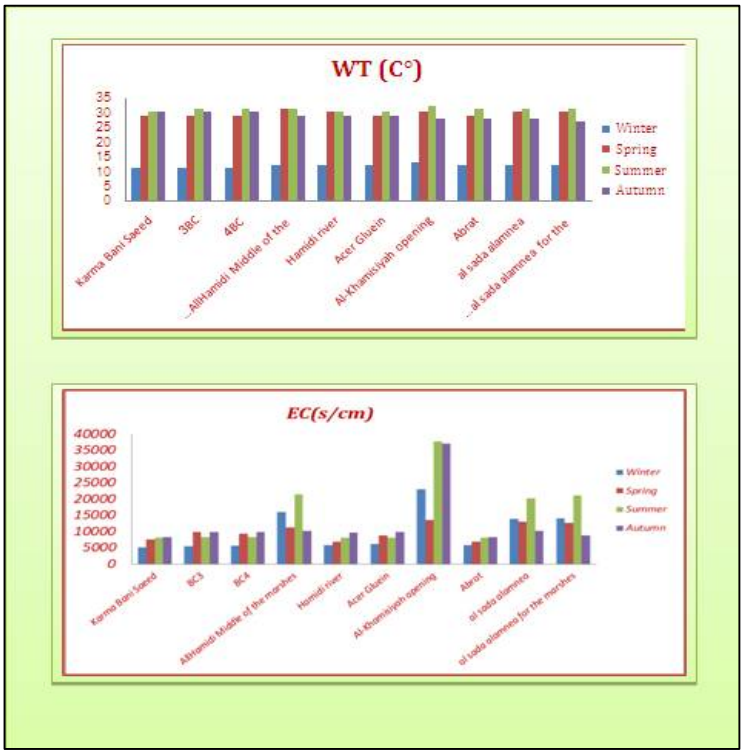

Figure 6:Results of water parameters (WT and EC)in the all season

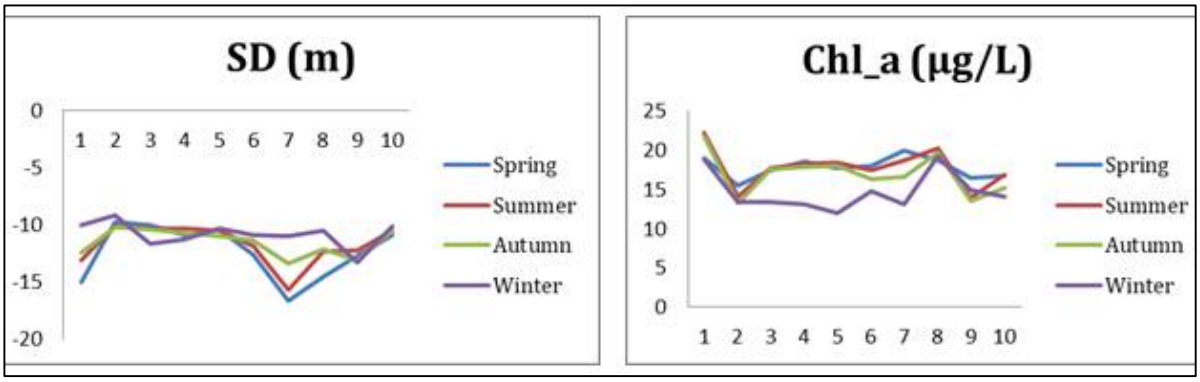

Figure (7): Shows the depth of water during the season for selected sites

Figure (8): Shows the value of chlorophyll of selected sites for each season

Figure 9: The interpolated data of the reflectance value of the water quality in Spring 2017 by using IDW interpolation over the AL-Hammar Marshes, South of Iraq.

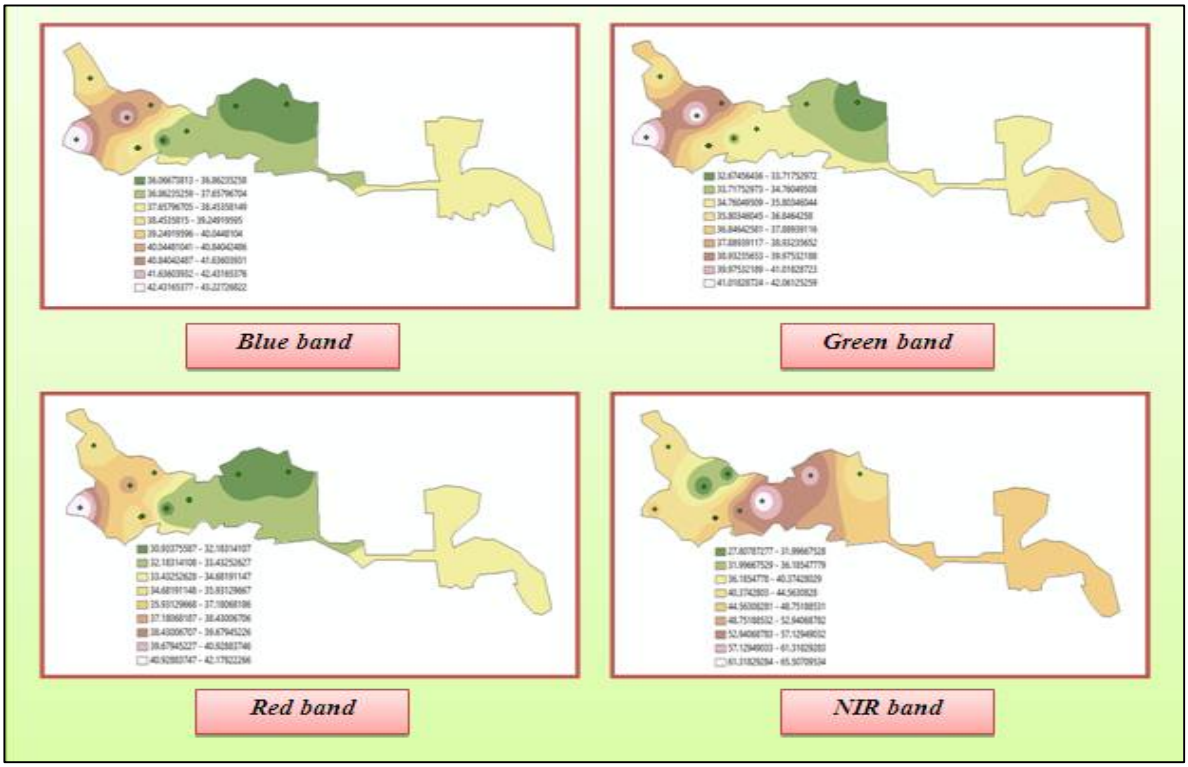

Figure 11: The interpolated data of the reflectance value of the water quality in Autumn 2017 by using IDW interpolation over the AL-Hammar Marshes, South of Iraq.

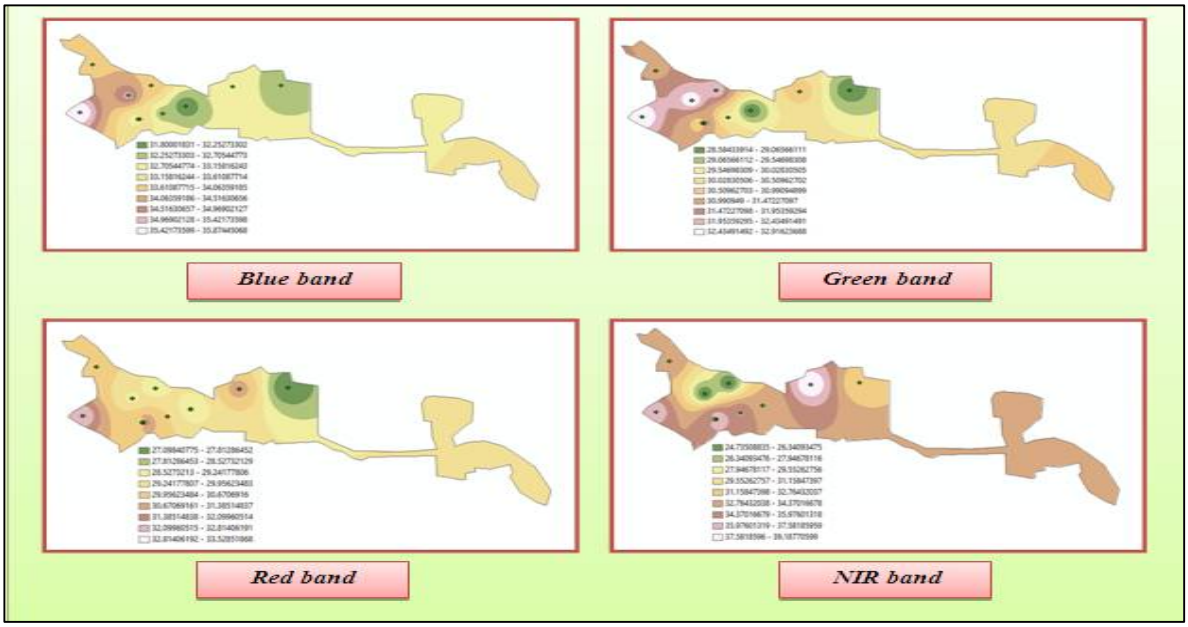

Figure 12: The interpolated data of the reflectance value of the water quality in Winter 2017 by using IDW interpolation over the AL-Hammar Marshes, South of Iraq.

Indian Journal of Natural Sciences www.tnsroindia.org.in ©IJONS

Vol.9 /Issue 51 / December / 2018 *International Bimonthly* *ISSN: 0976 – 0997*

RESEARCH ARTICLE

Omentin-1 and Irisin Levels in Obese Subjects with and without Metabolic Syndrome

Mays s. Al-Nawar[1], Namir I. A. Haddad[1*] and Essam Nori[2]

[1]Department of Chemistry, College of Science, University of Baghdad, Baghdad, Iraq.
[2]National Diabetes Center for Treatment and Research, Al-Mustansiriya University, Baghdad, Iraq.

Received: 01 Sep 2018 Revised: 04 Oct 2018 Accepted: 07 Nov 2018

***Address for Correspondence**
Namir I. A. Haddad
Department of Chemistry,
College of Science,
University of Baghdad,
Baghdad, Iraq.
Email:namir.haddad@gmail.com.

ABSTRACT

Adipose tissue and skeletal muscle have been identified as an organ of endocrine that is hypothesized to play role in the regulation of metabolism. Omentin-1 is identified as a good adipokine secreted by visceral adipose tissue and Irisin, which is a myokine secreted by skeletal muscle. The aim of the current study is to evaluate the serum omentin-1 and irisin levels and determine the correlations between them and with other biochemical parameters in Metabolic Syndrome(MetS) patients and obese patients without MetS. Our study consisted of eighty-six individuals who were classified into three groups (36 MetS patients, 28 obese patients, and 22 healthy individuals). The anthropometric measurements and biochemical parameters were measured for all subjects. Serum levels of omentin-1 and irisin were measured by enzyme-linked immunosorbent assay (ELISA) technique. The collected data were analyzed using ANOVA test and Pearson correlation coefficient from SPSS software. Fasting serum insulin and HOMA2-IR% levels in MetS and obese patients were showed a significant difference in comparison with the control group. Serum omentin-1 and irisin concentrations in obese and MetS groups were significantly lowerthan of the healthy individuals [mean omentin-1 levels, 19113.3 &24424.4 vs. 36816.4pg/ml, p=0.000; mean irisin levels, 32.63 &30.99 vs. 52.17 ng/ml, p=0.001, respectively). There is no statistical correlationobserved between serum levels of omentin-1 and irisin. Also, we found that irisin correlated significantly with some biochemical parameters. From our result in the current study, we conclude that omentin-1 and irisin could be used as indicators for obesity development, and to prevent the complication that lead to the risk of metabolic syndrome.

Keywords: Omentin-1,Irisin, Obesity, Insulin Resistance, Metabolic Syndrome.

INTRODUCTION

The Metabolic Syndrome (MetS) or 'syndrome X' the term coined by Reaven since 1988, represents a group of interrelated biochemical, clinical, physiological and metabolic risk factors including a hyperglycemia, dyslipidemia, hypertension, central obesity, the pro-thrombotic and pro-inflammatory states, which reflects insulin resistance[1, 2]. MetSis now taken into consideration from a major common health problem because it's quickly increasing spread worldwide and its association with cardiovascular disease and type2 diabetes[3]. MetSis linked with redundant aggregation of fat in the adipose tissue of the abdominal region. Adipose tissue has a role in energy storage, in recent years considered to be the greatest endocrine organ inside the body [4]. Adipokines are small protein secreted by adipose tissue including adiponectin, leptin, resistin glycolipids, tumor necrosis factor, retinol binding protein, visfatin, interleukin-6 and omentin [5]. Adipokines have wide effects on pathophysiological and physiological processes inside the body including lipid and carbohydrate metabolism, and an important role in the evolution of insulin resistance (IR) to diabetes and atherosclerosis. However, in metabolism, a few of these adipokines have a role in enhancing good health [6].

Omentin is a lately identified as a novel member of good adipokine group. Circulating omentin level is significantly lower in patients with obesity, insulin resistance and diabetes that subscribe to the main components of the metabolic syndrome and other conditions of illness like coronary artery disease (CAD), heart failure and atherosclerosis, etc. [7, 8]. Omentin which is also named intestinal lactoferrin receptor and intelectin-1 [9, 10], is a hydrophilic protein with 313 amino acids and 35 kDa of molecular weight. Gene expression of omentin is mainly occurring in stromal vascular cells of visceral adipose tissue (VAT) than in subcutaneous adipose tissue (SAT) [11]. In other tissues, omentin is also expressed, such as epicardial fat, reticulocytes, thymus, colon, small intestine, ovary, placenta and lungs [11, 12]. The omentinhas two isoforms, omentin-1, and omentin-2, its genes are located adjacent to each other in the 1q22-q23 chromosomal region, which hasbeen formerly linked to Type 2 Diabetes Mellitus in many populations [8, 13, 14].

Bostrom, *et al.*[15] reported that exercise and physical activity induce skeletal muscle on the liberation of peroxisome proliferator-activated receptor-coactivator 1-α (PGC-1α). PGC-1α is one of the nuclear receptor proteins that work as a regulator of the gene expression [16]. PGC-1α plays an essential role in the regulation of metabolism [17] and stimulates the expression and synthesis of fibronectin type III domain-containing protein 5 (FNDC5). FNDC5 is a transmembrane protein which cleavage by an unknown protease and synthesis new protein called "irisin" [15]. Irisin, a myokineinduces "browning" of white adipose tissue then stimulating UCP1 expression in white adipose tissue and promoting thermogenesisthereby the total energy expenditure increase and obesity decrease [15]. The first goal of our study is the estimation of serum omentin-1 and irisin levels in obese patients with and without MetS. The second goals are: 1) find out whether there is a correlation of omentin-1 with irisin levels and 2) find out whether there are correlations of omentin-1 and irisin levels with the anthropometric and other biochemical parameters in study groups.

MATERIALS AND METHODS

Study population

This study was conducted on eighty-eight individuals (44 male, 44 female) with age range of 27-74 years, during the period from October 2017 to February 2018. The subjects were attended to Al-ShuhadaModel Health Center / Baghdad Health Directorate - Al-Karkh and the National Diabetes Center for Treatment and Research at Al-Mustansiriya University, Baghdad, Iraq. All subjects completed a uniform questionnaire including name, age, gender, number of sample, anthropometric measurements, biochemical parameters, histories of past and present

illnesses and medication. Subjects were divided into three groups (obese without MetS, MetS and control group). If subject has central obesity (waist circumference (WC) ≥102 cm in male and ≥88 cm in female) and two or more of the risk factors for MetS according to the definition of the National Heart, Lung, and Blood Institute/American Heart Association criteria [18]:1) High fasting serum glucose: >100 mg/dl or history of diabetes mellitus or taking anti-diabetic medications; 2) High blood pressure: (BP) >130/85 mmHg or antihypertensive therapy; 3) Hypertriglyceridemia: TG ≥150 mg/dl or specific medication for this lipid abnormality and 4) Low HDL-C: HDL-C<40 mg/dl in male and <50 mg/dl in female or specific medication for this lipid abnormality, theindividual has MetS[18]. Subjects with T1DM, T2DM using insulin injection therapy, pregnant, alcohol consumption, acromegaly, anorexia nervosa patients, and kidney diseases were excluded.

Collection of blood samples

After overnight fasting (10-12h), five milliliters of blood were collected by vein puncture. The blood was placed in biochemistry tube containing gel separator, then it was centrifuged at 4000 x g for 8 min for separating the serum from cellular elements. In the same day, a fasting serum glucose test was carried out. Remaining of the serum was separated into portions (250-500 µl) in Eppendorftubes stored at -20°C until irisin, omentin-1, insulin hormone, and other biochemical analyses were determined.

Anthropometric measurements and laboratory assays

The body weight of the subject was measured to the near 0.5 kg after removal of heavy clothing and shoes using a digital scale of weighing. The height was measured to the nearest 1 cm using a ruler measuring. The WC dimension was made minimally to the nearest 1 cm, midway between the iliac crest and the last rib [19, 20]. Body Mass index (BMI),Waist-to-Hip Ratio (WHR), Waist-to-Height Ratio(WHtR) and Body Fat Percentage (BF %) indices were determined after getting on age, gender, body weight, height and WC indices for all subjects. BMI was calculated by dividing the weight of the person in (Kg) to square his length in (m^2) [21]. BF% was calculated from the following equation.

BF % = (1.20 * BMI) + (0.23 * age) - (10.8 * sex (male =1, female =0)-5.4[22]

Routine biochemistry analyses (fasting serum glucose (FSG), triglycerides (TG), total cholesterol (TC) and high-density lipoprotein cholesterol (HDL-C)) were performed using enzymatic standard methods. Then, by using the Friedewald formula, Low-density lipoprotein cholesterol (LDL-C) was calculated [23]. Insulin, irisin and omentin-1 hormones concentrations were measured by using (ELISA) technique. Fasting insulin level was measured by using reagents kit from (Monobind Inc., U.S.A) while fasting irisin and omentin-1 levels were determined by using kits from (MyBioSource Company, U.S.A). Insulin resistance was calculated by homeostasis model assessment (HOMA-IR) from the equation: [fasting serum glucose (FSG) (mg/dl) × fasting serum insulin (µU/ml)] / 405.

Statistical analysis for data

SPSS (statistical package for social sciences) Ver.20 was used to process the data. The mean and standard deviation of parameters for each group were found by using descriptive analysis. One-way analysis of variance (ANOVA) test was used to show the variances between parameters for more than two groups. The difference significance between the mean values of the two groups was predestined by (ANOVA) test else. The probability "P < 0.05" is significant, "P < 0.01" is a highly significant and "P> 0.05" is non-significant. The linear relationship between variables was estimated by using the Pearson correlation test (r). The closer (r) is to (+1.00), the correlation is strongly positive and the closer (r) is to (-1.00), the correlation is a strong negative.

RESULTS

All anthropometric measurements and biochemical analysis results of the eighty-six subjects were presented in Table (1). Waist, BMI, WHR, WHtR, BF%, and SBP showed a higher significantly increase in obese and MetS groups compared to healthy subjects (control group) (at $P < 0.01$). DBP was significantly higher ($P = 0.001$) in MetS group as compared to control group (87.03 vs. 74.05 mmHg), while it didn't appear any statistical difference between obese and control groups (81.50 vs. 74.05 mmHg) ($P = 0.110$). High significant differences in MetS group were observed in FBS, TG, HDL-C, and VLDL levels when compared with obese and control groups at ($P < 0.01$). But, no significant differences among the three groups were found when comparing the levels of serum total cholesterol (TC) and (LDL-C). Mean levels of serum insulin and HOMA-IR % showed a highly significant increase in MetS group compared to healthy control group (19.44 vs. 12.19 µIU/ml) and (2.65 vs. 1.6) respectively at ($p=0.000$), also a significant increase in obese patients observed in comparison with control group (17.49 vs. 12.19 µIU/ml; at $p=0.010$) and (2.21 vs. 1.56; at $p=0.013$) respectively. Omentin-1 mean levels in obese and MetS groups observed a highly significant decrease as compared with the control group (19113.3 and 24424.4 vs. 36816.4 pg/ml) respectively at ($P <0.01$). There was a non-significantly difference between mean levels of omenin-1 in obese and metabolic patient groups, as shown in (Figure 1). Mean of serum irisin appeared highly significant variances in the comparison of obese and MetS patients with healthy individuals (32.63 and 30.99 vs. 52.17ng/ml) respectively (at $P < 0.01$), but no significant difference was observed between Mets and obese groups, (Figure 5).

Bivariate correlation analysis was achieved to determine the correlations of serum omentin-1 and irisin levels with anthropometric and biochemical parameters in obese and MetS patients, as shown in Table 2 and Table 3. In obese group, the WC and TC were positively correlated with omentin-1 level ($r=0.405$, $p=0.026$) and ($r=0.408$, $p=0.025$) respectively, while in MetS group, serum omentin-1 levels did not show any correlation with anthropometric measurements and biochemical parameters. Serum irisin level did not show any correlation with other parameters in the obese group. While irisin mean levels in MetS patients was negatively correlated with insulin ($r = -0.359$, $p= 0.037$) and positively correlated with TG($r=0.414$, $p=0.012$), TC($r=0.379$, $p=0.022$) and VLDL-C($r=0.34$, $p= 0.041$).

DISCUSSION

Obesity is a common disease at the present time and a risk indicator for metabolic syndrome (MetS) development, type 2 diabetes mellitus (DMT2) and cardiovascular disease [24-27]. Many studies showed that insulin resistance, hyperglycemia, hypertension, and dyslipidemia are strongly linked with visceral obesity [28, 29]. Our study has been conducted to estimate levels of serum omentin-1 and irisin in metabolic syndrome patients and obese without MetS patients, and to study the correlation between these two hormones. In this regard, Barth *et al*. [30], showed that gene expression on omentin-1 and plasma omentin-1 level in visceral adipose tissue reduced in obese patients. Zhang *et al*. [31], found that the reduced omentin-1 levels may contribute to the development of insulin resistance and T2DM in Chinese adults. These studies are in agreement with the findings of our research underline that levels of omentin-1 are decreased in obese patients as shown in Table1. Omentin-1 level in the obese group did not appear any correlation with the anthropometric and biochemical parameters. De Souza Batista *et al.*[32], they revealed that circulating omentin-1 levels were negatively correlated with indicators of obesity, such as BMI and waist circumference. Although, another studies reported that the omentin-1 levels were not showed any correlation with WC in obese patients [33, 34]. So, the relationship between the omentin-1 levels and waist circumference (WC) remains in controversy and the need for many studies to prove the nature of this relationship.In MetS group, serum omentin-1 levels were decreased in comparison with healthy individuals and this finding is consistent with Auguet *et al.*[35] and Jialal*et al.*[36]. Our findings showed that MetS subjects had higher levels of serum omentin-1 than obese subjects but the differences were not significant. The anthropometric parameters and metabolic parameters were not correlated with omentin-1 levels. In contrast to the present study, Kilic*et al.* reported that the plasma omentin-1 levels were correlated with two parameters from metabolic syndrome (high TG and low HDL-C levels), so the omentin-1

levels were similar in MetS non-diabetic patients and healthy group [37]. In recent years, many human studies have an attempting to the possible evaluation of the relationship between irisin levels with clinical and metabolic parameters in obesity, diabetic and coronary artery disease (CAD) [38, 39], however, the role important of irisin in the clinical state is still vague. The result of the present study showed that serum irisin levels in obese non-metabolic patients were lower in comparison with control subjects, figure (2). These results are compatible with that of Moreno-Navarrete *et al.*[40], who reported that circulating irisin decreased in obese patients.In contrast to our study, Stengel *et al.* [41] and Pardo *et al.*[42], found that serum irisin levels in obese patients were a highercompared to normal weight and anorexia nervosa patients. In our study, serum irisin levels were not shown any correlation with the anthropometric and biochemical parameters in the obese group. Conversely,studies by Stengel, *et al.* and Pardo, *et al.* reported that Irisin levels showed a positive correlation with BMI, body weight [41, 42] and fat mass [42]. Another study by Sanchis-Gomar, *et al.* found that serum irisin levels were not shown any correlation with BMI [43].

Irisin levels in metabolic patients were significantly lower than in healthy control subjects. These results were compatible with the findings of Yan et al. [44], who found that serum irisin levels are significantly reduced in MetS subjects than control. In contrast to the present study, the findings ofHee*et al.* [16], who reported that baseline irisin levels are higher significantly in MetS patients than subjects without MetS. Our study showed a negative correlation between serum irisin and fasting serum insulin. On the contrary, the results of Reinehr*et al.*[45] showed that serum irisin levels had a positive correlation with fasting insulin. Also, we found that the serum irisin levels were positively correlated with TC and TG in MetS group, as shown in Table 3. This is in agreement with Hee Park *et al.*[46]and De la Iglesia *et al.*[47] as they found that serum irisin levels had a positive correlation with lipid profile(TC and TG). As well, we found that irisin levels are positively correlated with VLDL,while other studieshave reported that there were no correlations between serum irisin levels and lipid profile [40, 44, 48].

CONCLUSION

From our results, we conclude that:

- The obese without MetS and metabolic Iraqi patients have significantly lower serum omentin-1 levels compared to healthy control.
- The serum irisin levels were significantly lower in MetS patients and obese patients compared to normal weight control subjects.
- Omentin-1 and irisin could be used as indicators for obesity development, and to prevent the complication that lead to the risk of metabolic syndrome.

ACKNOWLEDGEMENTS

A very special gratitude goes out to all staff of laboratory in Al-Shohadaa Model Health Center / Baghdad Health Directorate - Al-Karkh for their help in the collection of samples.

REFERENCES

1. Reaven GM. Banting lecture 1988: role of insulin resistance in human disease. Nutrition. 1997;13(1):64.
2. Alberti K, Eckel RH, Grundy SM, Zimmet PZ, Cleeman JI, Donato KA, et al. Harmonizing the metabolic syndrome: a joint interim statement of the international diabetes federation task force on epidemiology and prevention; national heart, lung, and blood institute; American heart association; world heart federation; international atherosclerosis society; and international association for the study of obesity. Circulation. 2009;120(16):1640-5.

3. Collaborators GO. Health effects of overweight and obesity in 195 countries over 25 years. N Engl J Med. 2017;377(1):13-27.
4. Ahima RS. Adipose tissue as an endocrine organ. Obesity. 2006;14(S8):242S-9S.
5. Koleva DI, Orbetzova MM and Atanassova PK. Adipose Tissue Hormones and Appetite and Body Weight Regulators an Insulin Resistance. Folia medica. 2013;55(1):25-32.
6. Rabe K, Lehrke M, Parhofer KG and Broedl UC. Adipokines and insulin resistance. Mol Med. 2008;14(11-12):741.
7. Jaikanth C, Gurumurthy P, Cherian K and Indhumathi T. Emergence of omentin as a pleiotropic adipocytokine. Exp Clin Endocrinol Diabetes 2013;121(07):377-83.
8. Elbein SC, Hoffman MD, Teng K, Leppert MF and Hasstedt SJ. A genome-wide search for type 2 diabetes susceptibility genes in Utah Caucasians. Diabetes. 1999;48(5):1175-82.
9. Komiya T, Tanigawa Y and Hirohashi S. Cloning of the novel gene intelectin, which is expressed in intestinal paneth cells in mice. Biochem Biophys Res Commun. 1998;251(3):759-62.
10. Lee J-K, Schnee J, Pang M, Wolfert M, Baum LG, Moremen KW, et al. Human homologs of the Xenopus oocyte cortical granule lectin XL35. Glycobiology. 2001;11(1):65-73.
11. Yang R-Z, Lee M-J, Hu H, Pray J, Wu H-B, Hansen BC, et al. Identification of omentin as a novel depot-specific adipokine in human adipose tissue: possible role in modulating insulin action. Am J Physiol Endocrinol Metab. 2006;290(6):E1253-E61.
12. Schäffler A, Neumeier M, Herfarth H, Fürst A, Schölmerich J and Büchler C. Genomic structure of human omentin, a new adipocytokine expressed in omental adipose tissue. Biochimica et Biophysica Acta (BBA)-Gene Structure and Expression. 2005;1732(1-3):96-102.
13. Fu M, Gong D-w, Damcott C, Sabra M, Yang R, Pollin TI, et al. Systematic analysis of omentin 1 and omentin 2 on 1q23 as candidate genes for type 2 diabetes in the Old Order Amish. Diabetes. 2004;53:A59.
14. Wiltshire S, Hattersley AT, Hitman GA, Walker M, Levy JC, Sampson M, et al. A genomewide scan for loci predisposing to type 2 diabetes in a UK population (the Diabetes UK Warren 2 Repository): analysis of 573 pedigrees provides independent replication of a susceptibility locus on chromosome 1q. Am J Hum Genet. 2001;69(3):553-69.
15. Boström P, Wu J, Jedrychowski MP, Korde A, Ye L, Lo JC, et al. A PGC1-α-dependent myokine that drives brown-fat-like development of white fat and thermogenesis. Nature. 2012;481(7382):463.
16. Michalik L, Auwerx J, Berger JP, Chatterjee VK, Glass CK, Gonzalez FJ, et al. International Union of Pharmacology. LXI. Peroxisome proliferator-activated receptors. Pharmacol Rev. 2006;58(4):726-41.
17. Dunning KR, Anastasi MR, Zhang VJ, Russell DL and Robker RL. Regulation of fatty acid oxidation in mouse cumulus-oocyte complexes during maturation and modulation by PPAR agonists. PLoS One. 2014;9(2):e87327.
18. Grundy SM, Cleeman JI, Daniels SR, Donato KA, Eckel RH, Franklin BA, et al. Diagnosis and management of the metabolic syndrome: an American Heart Association/National Heart, Lung, and Blood Institute scientific statement. Circulation. 2005;112(17):2735-52.
19. Pelletiet D. Anthropometric standardization reference manual: Abridged edition. Edited by TG Lohman, AF Roche, and R. Martorell. vi+ 90 pp. Champaign, IL: Human Kinetics Books. 1991. US $15.00, Canada $18.50. Wiley Online Library; 1992.
20. Frisancho AR. Anthropometric standards for the assessment of growth and nutritional status. University of Michigan Press; 1990. p.
21. Holman RR, Paul SK, Bethel MA, Matthews DR and Neil HAW. 10-year follow-up of intensive glucose control in type 2 diabetes. N Engl J Med. 2008;359(15):1577-89.
22. Deurenberg P, Weststrate JA and Seidell JC. Body mass index as a measure of body fatness: age-and sex-specific prediction formulas. Br J Nutr. 1991;65(2):105-14.
23. Friedewald WT, Levy RI and Fredrickson DS. Estimation of the concentration of low-density lipoprotein cholesterol in plasma, without use of the preparative ultracentrifuge. Clin Chem. 1972;18(6):499-502.
24. Kershaw EE and Flier JS. Adipose tissue as an endocrine organ. J Clin Endocrinol Metab. 2004;89(6):2548-56.
25. Sharma A. Adipose tissue: a mediator of cardiovascular risk. Int J Obes. 2002;26(S4):S5.
26. Felber J and Golay A. Pathways from obesity to diabetes. Int J Obes. 2002;26(S2):S39.

27. Mirzaei K, Hossein-nezhad A, Aslani S, Emamgholipour S, Karimi M and Keshavarz S. Energy expenditure regulation via macrophage migration inhibitory factor in obesity and in vitro anti-macrophage migration inhibitory factor effect of Alpinia officinarum hance extraction. Endocr Pract. 2011;18(1):39-48.
28. Björntorp P. Metabolic implications of body fat distribution. Diabetes Care. 1991;14(12):1132-43.
29. Lemieux S. Contribution of visceral obesity to the insulin resistance syndrome. Can J Appl Physiol. 2001;26(3):273-90.
30. Barth S, Klein P, Horbach T, Dötsch J, Rauh M, Rascher W, et al. Expression of neuropeptide Y, omentin and visfatin in visceral and subcutaneous adipose tissues in humans: relation to endocrine and clinical parameters. Obesity facts. 2010;3(4):245-51.
31. Zhang Q, Zhu L, Zheng M, Fan C, Li Y, Zhang D, et al., editors. Changes of serum omentin-1 levels in normal subjects, type 2 diabetes and type 2 diabetes with overweight and obesity in Chinese adults. Ann Endocrinol (Paris); 2014: Elsevier.
32. de Souza Batista CM, Yang R-Z, Lee M-J, Glynn NM, Yu D-Z, Pray J, et al. Omentin plasma levels and gene expression are decreased in obesity. Diabetes. 2007;56(6):1655-61.
33. Alissa EM, Maisa'a M, Alama NA and Ferns GA. Role of omentin-1 and C-reactive protein in obese subjects with subclinical inflammation. J Clin Transl Endocrinol. 2016;3:7-11.
34. Moreno-Navarrete JM, Catalán V, Ortega F, Gómez-Ambrosi J, Ricart W, Frühbeck G, et al. Circulating omentin concentration increases after weight loss. Nutr Metab. 2010;7(1):27.
35. Auguet T, Quintero Y, Riesco D, Morancho B, Terra X, Crescenti A, et al. New adipokines vaspin and omentin. Circulating levels and gene expression in adipose tissue from morbidly obese women. BMC Med Genet. 2011;12(1):60.
36. Jialal I. Adipose tissue dysfunction in nascent metabolic syndrome. J Obes. 2013;2013.
37. Kilic DC, Oguz A, Uzunlulu M, Celik S and Koroglu G. Plasma omentin-1 levels are similar in nondiabetic metabolic syndrome patients and healthy subjects. Journal of Endocrinology and Metabolism. 2011;1(4):182-7.
38. Huh JH, Ahn SV, Choi JH, Koh SB and Chung CH. High serum irisin level as an independent predictor of diabetes mellitus: a longitudinal population-based study. Medicine. 2016;95(23).
39. Lee MJ, Lee SA, Nam BY, Park S, Lee S-H, Ryu HJ, et al. Irisin, a novel myokine is an independent predictor for sarcopenia and carotid atherosclerosis in dialysis patients. Atherosclerosis. 2015;242(2):476-82.
40. Moreno-Navarrete JM, Ortega F, Serrano M, Guerra E, Pardo G, Tinahones F, et al. Irisin is expressed and produced by human muscle and adipose tissue in association with obesity and insulin resistance. The Journal of Clinical Endocrinology & Metabolism. 2013;98(4):E769-E78.
41. Stengel A, Hofmann T, Goebel-Stengel M, Elbelt U, Kobelt P and Klapp BF. Circulating levels of irisin in patients with anorexia nervosa and different stages of obesity–correlation with body mass index. Peptides. 2013;39:125-30.
42. Pardo M, Crujeiras AB, Amil M, Aguera Z, Jiménez-Murcia S, Baños R, et al. Association of irisin with fat mass, resting energy expenditure, and daily activity in conditions of extreme body mass index. Int J Endocrinol. 2014;2014.
43. Sanchis-Gomar F, Alis R, Pareja-Galeano H, Sola E, Victor VM, Rocha M, et al. Circulating irisin levels are not correlated with BMI, age, and other biological parameters in obese and diabetic patients. Endocrine. 2014;46(3):674-7.
44. Yan B, Shi X, Zhang H, Pan L, Ma Z, Liu S, et al. Association of serum irisin with metabolic syndrome in obese Chinese adults. PLoS One. 2014;9(4):e94235.
45. Reinehr T, Elfers C, Lass N and Roth CL. Irisin and its relation to insulin resistance and puberty in obese children: a longitudinal analysis. J Clin Endocrinol Metab. 2015;100(5):2123-30.
46. Hee Park K, Zaichenko L, Brinkoetter M, Thakkar B, Sahin-Efe A, Joung KE, et al. Circulating irisin in relation to insulin resistance and the metabolic syndrome. J Clin Endocrinol Metab. 2013;98(12):4899-907.
47. de la Iglesia R, Lopez-Legarrea P, Crujeiras AB, Pardo M, Casanueva FF, Zulet MA, et al. Plasma irisin depletion under energy restriction is associated with improvements in lipid profile in metabolic syndrome patients. Clin Endocrinol (Oxf). 2014;81(2):306-11.

48. Sesti G, Andreozzi F, Fiorentino T, Mannino G, Sciacqua A, Marini M, et al. High circulating irisin levels are associated with insulin resistance and vascular atherosclerosis in a cohort of nondiabetic adult subjects. Acta Diabetol. 2014;51(5):705-13.

Table 6: Anthropometric measurements and biochemical profiles for obese, MetS, and control subjects.

Groups / Parameters	Obese n = 28	MetS n = 36	Control n = 22	P_a	P_b	P_c	P_d
Gender M,F	14M ,16F	19M ,17F	11M ,11F	---	---	---	---
Age(Y)	44.13±8.43	48.89±11.73	38.59±12.26	0.170	0.002	0.186	0.003
W.C(cm)	108.10±9.62	112.33±13.03	84.45±7.92	0.000	0.000	0.390	0.000
BMI (kg/m^2)	35.09±4.62	33.68±6.05	23.69±2.26	0.000	0.000	0.472	0.000
WHR	0.96±0.06	0.98±0.06	0.87±0.07	0.000	0.000	0.080	0.000
WHtR	0.66±0.06	0.68±0.07	0.52±0.05	0.000	0.000	0.729	0.000
BF%	41.81±9.24	40.25±9.71	26.49±7.69	0.000	0.000	0.769	0.000
SBP (mmHg)	129.20±17.61	143.53±22.86	113.05±9.44	0.007	0.000	0.007	0.000
DBP (mmHg)	81.50±10.93	87.03±16.48	74.05±8.46	0.110	0.001	0.206	0.002
FSG(mg/dl)	89.43±9.86	128.17±41.03	89.04±12.55	0.999	0.000	0.000	0.000
Insulin (µIU/ml)	17.49±5.02	19.44±8.19	12.19±3.57	0.009	0.000	0.425	0.000
HOMA-IR%	2.21±0.62	2.65±1.01	1.56±0.45	0.013	0.000	0.083	0.000
TG (mg/dl)	81.53±33.93	144.51±79.31	65.60±34.77	0.585	0.000	0.000	0.000
TC (mg/dl)	161.40±41.22	178.00±65.57	161.81±32.57	1.000	0.474	0.392	0.338
HDL-C (mg/dl)	45.07±10.57	33.17±10.66	50.80±12.19	0.160	0.000	0.000	0.000
LDL-C (mg/dl)	103.88±37.11	121.33±64.29	100.66±29.89	0.970	0.268	0.323	0.109
VLDL-C (mg/dl)	16.27±6.61	30.49±18.89	13.30±6.83	0.701	0.000	0.000	0.000
Omentin1(pg/ml)	19113.3±6130.1	24424.4±7158.7	36816.4±15931.5	0.000	0.000	0.079	0.000
Irisin (ng/ml)	32.63±13.36	30.99±10.12	52.17±13.51	0.000	0.000	0.859	0.000

Results are presented as mean ± SD. (standard deviation); P_a, the comparison between obese and control; P_b, the comparison between MetS and control; P_c, the comparison between obese and MetS; P_d, the comparison among all groups. W.C: waist circumference, BMI: body mass index, WHR: waist to hip ratio, WHtR: waist to height ratio, BF%: body fat percent, SBP: systolic blood pressure, DBP: diastolic blood pressure, FSG: fasting serum glucose, TG: triglycerides, TC: total cholesterol, HDL-C: high density lipoprotein cholesterol, LDL-C: low-density lipoprotein cholesterol, VLDL-C: very low density lipoprotein cholesterol, HOMA-IR%: homeostasis model of assessment-insulin resistance%, non-significant at $p > 0.05$,significant at $p < 0.05$, highly significant at $p < 0.01$.

Table 7: Correlation between serum omentin-1 and irisin levels with anthropometric measurements and biochemical analysis results for the obese group (n=28).

Parameter / Obese	Omentin-1		Irisin	
	r value	P value	r value	P value
Gender M,F	-0.338	0.078	0.135	0.493
Age(Y)	0.110	0.577	-0.303	0.117
Waist (cm)	0.242	0.215	-0.030	0.878
BMI (kg/m^2)	-0.157	0.425	-0.060	0.762
WHR	0.241	0.216	0.172	0.380
WHtR	0.098	0.621	-0.038	0.847
BF%	-0.282	0.145	-0.021	0.916
SBP(mmHg)	0.160	0.417	-0.093	0.916
DBP (mmHg)	0.095	0.629	0.038	0.849
FSG(mg/dl)	0.022	0.911	-0.057	0.772
Insulin (µIU/ml)	0.307	0.112	-0.144	0.447
HOMA-IR%	0.298	0.123	-0.143	0.451
TG (mg/dl)	0.270	0.368	-0.218	0.265
TC (mg/dl)	0.087	0.659	-0.180	0.358
HDL-C (mg/dl)	-0.025	0.901	-0.167	0.397
LDL-C (mg/dl)	0.031	0.876	-0.068	0.731
VLDL-C (mg/dl)	0.339	0.077	0.164	0.404
Irisin (ng/ml)	-0.058	0.769	1.000	------
Omentin-1 (ng/ml)	1.000	------	-0.058	0.769

W.C: waist circumference, BMI: body mass index, WHR: waist to hip ratio, WHtR: waist to height ratio, BF%: body fat percent, SBP: systolic blood pressure, DBP: diastolic blood pressure, FSG: fasting serum glucose, TG: triglycerides, TC: total cholesterol, HDL-C: high density lipoprotein cholesterol, LDL-C: low-density lipoprotein cholesterol, VLDL-C: very low density lipoprotein cholesterol, HOMA-IR%: homeostasis model of assessment-insulin resistance%, non-significant at $p > 0.05$ andsignificant at $*p \leqslant 0.05$.

Table 8: Correlation between serum omentin-1 and irisin levels with anthropometric measurements and biochemical analysis results for MetS group (n=36).

Parameter / MetS	Omentin-1		Irisin	
	r value	P value	r value	P value
Gender M,F	-0.198	0.248	0.187	0.275
Age(Y)	-0.207	0.225	0.060	0.954
W.C (cm)	0.013	0.940	0.010	0.954
BMI (kg/m^2)	-0.078	0.650	0.038	0.825
WHR	0.060	0.729	-0.170	0.322
WHtR	-0.031	0.858	0.122	0.477
BF%	-0.189	0.268	0.211	0.216
SBP(mmHg)	-0.297	0.079	0.039	0.820
DBP (mmHg)	-0.160	0.352	0.311	0.065

FSG(mg/dl)	0.001	0.994	0.108	0.530
Insulin (µIU/ml)	0.211	0.218	-0.359	0.037*
HOMA-IR%	0.195	0.255	-0.328	0.051
TG (mg/dl)	0.082	0.633	0.414	0.012*
TC (mg/dl)	0.323	0.055	0.379	0.022*
HDL-C (mg/dl)	0.088	0.610	-0.015	0.932
LDL-C (mg/dl)	0.215	0.208	0.287	0.089
VLDL-C (mg/dl)	0.084	0.628	0.341	0.041*
Irisin (ng/ml)	0.132	0.443	1.000	-----
Omentin-1 (ng/ml)	1.000	-----	0.132	0.443

W.C: waist circumference, BMI: body mass index, WHR: waist to hip ratio, WHtR: waist to height ratio, BF%: body fat percent, SBP: systolic blood pressure, DBP: diastolic blood pressure, FSG: fasting serum glucose, TG: triglycerides, TC: total cholesterol, HDL-C: high density lipoprotein cholesterol, LDL-C: low-density lipoprotein cholesterol, VLDL-C: very low density lipoprotein cholesterol, HOMA-IR%: homeostasis model of assessment-insulin resistance%, non-significant at $p > 0.05$ andsignificant at $*p \leqslant 0.05$.

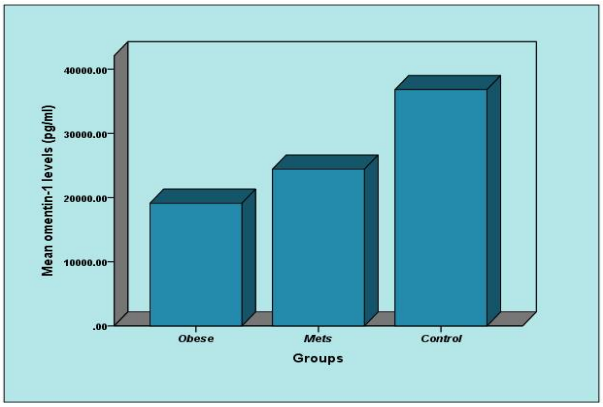

Figure 1: Serum omentin-1 levels in studied groups.

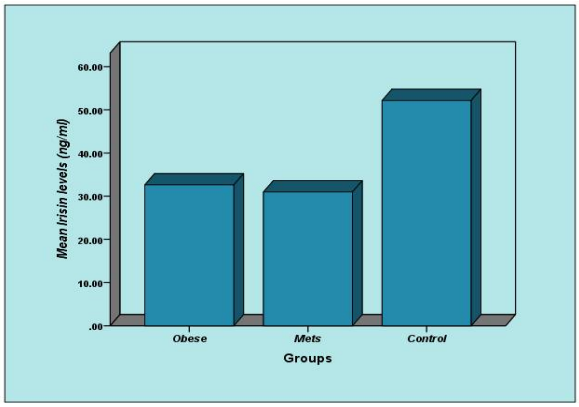

Figure 2: Serum irisin levels in studied groups

Indian Journal of Natural Sciences www.tnsroindia.org.in ©IJONS

Vol.9 /Issue 51 / December / 2018 *International Bimonthly* *ISSN: 0976 – 0997*

RESEARCH ARTICLE

Immunological, Bacteriology and Hematology Studies on Pneumonia in Camels in Al-Muthanna Province

Tareq Jaffaar Al-jindeel*, Ali Mosa Rashid Al-Yasari, and Nawar Alsalih

College of Veterinary Medicine, Al-Muthana University, Al-Muthana, Iraq.

Received: 04 Sep 2018 Revised: 06 Oct 2018 Accepted: 09 Nov 2018

***Address for Correspondence**
Tareq Jaffaar Al-jindeel
College of Veterinary Medicine,
Al-Muthana University,
Al-Muthana, Iraq.

ABSTRACT

The aim of this study was to isolated the main causative agent of pneumonia in camels have the clinical signs related to pneumonia from 18 November 2017 to 14 March 2018. A total of 53 samples of camels' lung tissue and blood were collected from massacres of Samawah and Rumathia cities at Muthanna province. Animals are of 8 months to 7 years old and of both sexes (35 males and 18 females).The lung tissue samples were transport directly by cooled box to the laboratory for bacteriological studies. The results of the current study revealed that A total of 53 samples were collected from lung tissue samples was reported 34 samples with *Klbesialla pneumonia* and 19 samples with *Streptococcus pneumonia* from the total samples collected from camels suffering from pneumonia.The results confirm by biochemical reaction were done by Api-20E system (Analytical profile index). Immunological studies on blood samples, the mean concentrations of total protein (g/l).Serum total protein concentration was significantly higher ($P<0.01$) in infected compared to healthy camels.The mean concentrations of γ-globulins were significantly higher ($P<0.01$) in infected camels compared to healthy camels. The mean AIG ratio were significantly higher ($P<0.01$) in infected camels compared to healthy camels. Hematologic studies on blood parameters in infected camels with pneumonia and control group were reported an increasing of ESR level and decrease of HB percentage.

Key Words: *Pneumonia,* camels, Animals, tissue, samples

INTRODUCTION

Streptococcus pneumoniae, pneumococcus, is an important pathogen that causes bothserious invasive infections, such as septicemia, meningitis and pneumonia, and mild upper respiratory infections. It belongs to the normal nasopharyngeal microbial flora that consists of bacteria with physiologic and genetic properties suitable for colonization and multiplication under certain conditions. These microbes are usually harmless and they even benefit

human health by preventing the growth of more pathogenic bacteria (1). Pneumococcus was described the first time over 130 years ago. In spite of the development of new possibilities to examine pneumococcus, the traditional phenotypic definition of *S. pneumoniae* has not changed. Pneumococcus is a gram-positive, α-hemolytic, bile-soluble and commonly capsulated streptococcus that is usually identified without problems. Identification is based on the bacterial colony morphology on a blood agar plate, optochin sensitivity, bile solubility and the presence of a capsule. So far, 90 different capsular serotypes have been identified (2). In addition, unencapsulated isolates are rather common in the nasopharynx (3). Molecular taxonomic studies have increased information on bacterial relationships, and during the last decades have brought changes to the classification of the genus *Streptococcus* (4),(5).

Al-muthanna city is one of the largest camel populated area in the world. The camels were, and still are, valued as riding, baggage, draught animals, hair hides and as well as the best food providers in the arid areas. Camel respiratory infection had received a little attention in the Iraq. There is no workers studied camel pneumonia in Irag. Their studies stated the seasonality in the occurrence of camel pneumonia and established the many etiological agents responsible for the condition such as *Staphyolcoccusspp, Corynebacterium. Spp, Streptococcus spp, Klebsiella pneumonae, Diplococcus pneumoniae, E .coli, Bacillusspp, Pasteurellaspp, Haemophilus somnus Micrococcus spp, Actinomycesspp and Mycobacterium spp.* In recent years, camel's research received good attention not only in Iraq but worldwide. This referred to the progressive importance of these animals uniquely adapted to harsh environmental conditions especially in the arid and semi-arid areas, in addition to their propagated role in the national income(6). Camels like other domestics animals are also exposed to various pathogenic, infectious agents and disease (7).

The study was started from 18 November 2017 to 14 March 2018. A total of 53 samples of camels' lung tissue and blood were collected from massacres of Samawah and Rumathia cities at Muthanna province. Animals are of 8 months to 7 years old and of both sexes (35 males and 18 females).The lung tissue samples were transport directly by cooled box to the laboratory for bacteriological studies. A clinical examination was performed on all camels. The examination includes general condition; body temperature and external shape such as the nature of the camels lint and weaknesses, respiratory rate, heart rate, and examination of superficial lymph nodes, as well as examination third eyelid. Samples were identified according to Bergeys manual using different morphologicand biochemical tests. First the samples were cattedand grown on brain heart infusion broth, incubated at 37 ˚ C for 24h. The growing bacteria on the medium were cultivated on MacConkey agar and Blood agar (aerobic and anaerobic) and incubated at 37 ˚C for 24h(8).

RESULTS

Culture of all the samples (swabs) was done on blood agar and MacConkey's agar and (Eiosine methylene blue) EMB using standard techniques. Culture plates were incubated at 37˚ C overnight. Next day, colonies obtained on the culture plates were further studied on the basis of colony morphology, and biochemical reactions, (9).Colonies of *Klebsiella pneumoniae* (mucoid or smooth) encapsulated bacterium ,on MacConkey agar the colonies appeared pink in color as a result of lactose fermentation ,fig. (2), on EMB mucoid colonies and violet in color, as shown in fig. (1) .

A total of 53 samples were collected from lung tissue samples was reported 34 samples with *Klbesialla pneumonia* and 19 samples with *Streptococcus pneumonia* from the total samples. The results shown in table (1). According this test (Api–20E system BioMerieux France was used forconfirm the biochemical diagnosis the bacterial isolates. This test have 25 strips, each strip contain 20 microtubes with contained dried material. According to the manufacture instructions, the following steps have been done. Hematologic studies on blood parameters in infected camels with pneumonia and control group were shown in table (2). Blood samples were taken from 20 camels. 5ml of blood was collected from the jugular vein and serum was separated from samples by centrifugation. Capillary electrophoresis of serum proteins identified six protein fractions in adult camels, includingalbumin, and gamma globulins, serum levels of these parameters were g/dl, g/l, respectively. the albumin/globulin (A/G) ratio was 1.238 ±0.14. The present the

results obtained were reported in table (3). *Streptococcus pneumonia* colonies on blood agar appear a wide zone of clear (beta-type) hemolysis, as shown in fig. (3).

DISCUSSION

The results were obtained in our studies agreed(10) whowere isolate and characterized the bacteria associated with pneumonia in Sudanese camels and isolated different bacteria included Str.pneumoniaeand *Staphylococcus spp, Corynebacterium spp, Pseudomonas spp, K.pneumoniae and E.coli Staphylococcus spp* in this study were isolated from all types of pathological lesions described and they were the most prevalent organisms (30.4%). In a similar study in camels, found 16.6% of his isolates to be Staphylococcus spp and found 27.9% of this organism(11).The Streptococcus spp. represented 17.6% of the isolates, while found them to be 5.33%, 7% and 19.3% of their isolates from camels(12). The A. pyogenes was also isolated from camels. The organism was not previously reported in camels as a respiratory tract pathogen. It caused supportive lesions and abscesses in various organs and tissues mainly lungs (13) .Hematological and biochemical analysis of blood often provides valuable information for diagnosis and surveillance of general health (14).

The result were concluded thatcamels play an important role in the epidemiology of pneumonia diseases under the three aspects of animal health, transmission to other livestock and zoonoses.serum protein electrophoresis and determination of absolute values of serum protein fractions in dromedary camels by cellulose acetate electrophoresis is very useful for clinicians to diagnose and evaluate various pathological conditions. The results presented in this study showed a significant effect of bacterial infection on the concentrations of some of the serum protein fractions in camels(8).results were obtained in our studies agreedwith(15) and. The present work reflects the current state of knowledge on the microbial causative agent and hematological parameter of pneumonia disease and serum protein electrophoresis and determination of absolute values of serum protein fractions and AIG ratio may be useful diagnostic tool in camels.in al-muthanna province camels.

REFERENCES

1. Aniasson G, Alm B, Andersson B, Larsson P, Nylén O, Peterson H, Rignér P, Svanborg M &Svanborg C (1992) Nasopharyngeal colonization during the first years of life. J Infect Dis 165: S38-42.
2. Henrichsen J (1995) Six newly recognised types of *Streptococcus pneumoniae*. J Clin Micro-biol 33: 2759-62.Appelbaum PC, Jacobs MR, Palko WM, Frauenhoffer EE &Duffett A (1986) Accuracy and reproducibility of the IDS rapID STR system for species identification of strepto-cocci. J ClinMicrobiol 23: 843-6.
3. Carvalho MG, Steigerwalt AG, Thompson T, Jackson D &Facklam RR (2003) Confirmation of nontypeable*Streptococcus pneumoniae*-like organisms isolated from outbreaks of epidemic conjunctivitis as Streptococcus pneumoniae. J ClinMicrobiol 41: 4415-7.
4. Van Belkum A, Struelens M, de Visser A, Verbrugh H &Tibayrenc M (2001) Role of ge-nomic typing in taxonomy, evolutionary genetics, and microbial epidemiology. ClinMicrobiol Rev 14: 547-60.
5. Facklam R (2002) What happened to the streptococci: overview of taxonomic and nomencla-ture changes. ClinMicrobiol Rev 15: 613-30.
6. Llull D, Lopez R & Garcia E (2006) Characteristic signatures of the lytA gene provide a basis for rapid and reliable diagnosis of *Streptococcus pneumoniae* infections. J ClinMi-crobiol 44: 1250-6.
7. Bekele, M. (2010). An Epidemiological Study on Major Camel Diseases in the Borana Lowland, Southern Ethiopia. DCG Report No. 58, Drylands Coordination Group, Oslo. pp. 67-98.
8. Shaaly A, Tellevik MG, Langeland N, Hoiby EA &Jureen R (2005) Comparison of serotyping, pulsed field gel electrophoresis and amplified fragment length polymorphism for typing of *Streptococcus pneumoniae*. J Med Microbiol 54: 467-72.

9. Herva E, Granat S, Mia Z, Ollgren J, Piirainen L &Makela PH (2006) Field evaluation of the chessboard modification for serotyping of *Streptococcus pneumoniae* in a small labo-ratory in Bangladesh. Am J Trop Med Hyg 74: 863-7.
10. Batt SL, Charalambous BM, McHugh TD, Martin S & Gillespie SH (2005) Novel PCR-restriction fragment length polymorphism method for determining serotypes or sero-groups of *Streptococcus pneumoniae* isolates. J ClinMicrobiol 43: 2656-61.
11. Bekele, M. (2010). An Epidemiological Study on Major Camel Diseases in the Borana Lowland, Southern Ethiopia. DCG Report No. 58, Drylands Coordination Group, Oslo. pp. 67-98.
12. Musher DM(1992) Infection caused by Streptococcus pneumonia:clinicalspectrum,pathogenesis ,immunity and treatment.Clinical Infect Dis 14:801-9.
13. Jedrzejas M.J (2004) .Extracellular virulence factors of streptococcus pneumonia.FrontBio_sci 9:891-914.
14. Tariq, A., Ijaz, A., Fatima, A., Qurat, U.I., Ansari, U. and Ahmed, A.(2016).Clinical analysis by microchip capillay electrophoresis. Clin. Chem. 52, 37-45.
15. O.Abdoslam et al.(2018) .Percentage and concentrations of six fractions of proteins and A/G ratio. http://www.openveterinaryjournal.com Open Veterinary Journal,Vol. 8(1): 1-4.

Table (1) show the percentage of streptococcus and KIbesialla pneumonia.

Patients No.	Proteus spp	
	Streptococcus pneumonia	***KIbesialla pneumonia***
53	**19**	**34**

Table (2) Blood parameters in infected camels with pneumonia and control group.

Parameters	Infected group Mean ±S.E
RBC ×10^6 µl	6.92 ±0.433 **
HB gm/100 ml	8.88 ± 1.44**
PCV %	25.62 ± 3.721**
MCV /fl	53.6 ±5. 664
MCHC gm/dl	28.0.± 2.553
ESR ml/20 mints	83.76 ± 5.321 **

Blood samples were taken from

Table (3) showed the the albumin/globulin (A/G) ratioin camels.

Index	Band	Ref. Area %	Conc. g/L mean ± SD	Normal Range g/L
1	Albumin	35.55 %	36.4±0.53	35.00-50.00
2	Gamma	25.12 %	29.4±0.33	7.00-15.55
A /GRatio		1.415		1.238±0.14

Fig. (1) EMB mucoid colonies and violet

Fig. (2): *K. pneumonia*on MacConkey agar

Fig. (3):*S. pneumonia* on bloodagar

Indian Journal of Natural Sciences www.tnsroindia.org.in ©IJONS

Vol.9 /Issue 51 / December / 2018 *International Bimonthly* *ISSN: 0976 – 0997*

RESEARCH ARTICLE

A Study of the Impact of Some Economic Factors on Farm Size for Cucumber Farmers (Al-Yousifiyah County Model)

Omer Khudhair Abbas Al-Hamadani[1]*and Afaf Saleh Hasan Al-Hani[2]

[1]Researcher, Ministry of Agriculture, Iraq.
[2]Professor, College of Agriculture Engineering Sciences, University of Baghdad, Iraq.

Received: 01 Sep 2018 Revised: 05 Oct 2018 Accepted: 10 Nov 2018

***Address for Correspondence**
Omer Khudhair Abbas Al-Hamadani
Researcher,
Ministry of Agriculture, Iraq.
Email:Omar_kd@yahoo.com

ABSTRACT

Identifying farm size is considered as on of the most challenges facing the farming product. This is due to the farm size importance in determining the typical agricultural areas available to maintain the highest possible income through diversity of crops cultivated. In order to meet the research requirements and objectives, the data were randomly collected from 45 farms of the Al-Youssifiyah district in Baghdad province for the 2016-2017 agricultural seasons. The study aimed to identify the most important economic variables affecting the determination the farm size, as well as identifying the relationship between the farm size and the productivity level of Crop cucumber in the study under discussion. The results showed that there was an inverse relationship between the productivity of a previous year and farm size, as well as the inverse relationship between farm size and each of the average cost variables, work resource price, and land resource price. At the same time, the results showed that there is a direct relationship between the farm size and the family members working, the Explanatory variables (60%) were taken to mean of fluctuations in the dependent variable through the value of the identifying factor (R^2).The study accomplished with a set of conclusions. The most important one is that the inverse relationship between farm size and productivity for the previous year was due to the security and environmental conditions of scarcity of water in the region during the period of study. The inverse relationship of the total average cost variable refers that the cultivated areas could be increased through managing the costs and the optimum use of production resources for the Crop cucumber. The study also concluded other recommendations, the most important one to highlight on modern agricultural means and methods that should move up Crop cucumber productivity and , as a result, promoting farmers to enlarge the cultivated areas.

Key words: farm size, productivity, family member working

INTRODUCTION

The Crop cucumber (*Cucumis sativus*) is an important summer crop plant in Iraq and worldwide. Its origin is India and Africa. References said that it has been cultivated in West Asia region some 3000 years ago (Matloob,1983,68).The Crop cucumber is belong to the sub- Cucarbitaceae family. Each (100) grams of Crop cucumber contains (95-96) g of humidity, (15) heat calories, (0.9 – 1) g of protein, (2-4.3) g of carbohydrate, (0.6) g of fiber and (0.5) g of ash. It also contains low nutrition elements and vitamins (A, B, D). The Crop cucumber used as a fresh plant in salads and could be cooked. It is also used in the vinegary process (Farhan, 2017, 71). In Asia, the Crop cucumber ranks the fourth crop in importance after tomatoes, cabbage, and onion (Alazawi and AlEbade, 2017. 127). The argument on farm size and its relation with productivity is considered as one of the important argument in the agricultural economic literature which attracting scholars up to date (Pillai, 2012,287). There are many attempts in economic literature which study the impact of economic size on different economic events but this did not provide adequate and accurate information on the economic efficiency impact level on different farm size.

However, some studies have concentrated, based on hypothesis, the impact of some variables of economic nature on farm size as far as productivity of area unit and benefit maintained. The income or work revenue level, land, and capital depend on the using of theses resources' services to produce goods that suit the desires of the consumer and suit his taste. At the same time, their prices depend upon that desire. If the revenues of the resources used are high, the income of the farms increases by increasing the size of demand on goods which is undoubtedly reflected on the increase use of resources. Therefore, the amount of profit achieved differences depend on the performance of size and capacity. Most farmers are classified of higher income categories if the area under exploitation is sufficient enough to use the capital. Very few farmers are within this classification, for those who have an area which is not capable to apply the modern technologies or can not bear the cost related due to the efficiency of the administration issue. Thus, choosing the optimum size farm is an important decision in agricultural planning. Its role and importance is not only to provide an adequate income for the farming family members, but also to develop the provincialism region by promoting farming growth.

The problem of research in the determination of farm size for farmers is the economic challenges regarded the high costs of acre for different crops. It is worth to mention that there are many external influences and determinants that prevent maintaining the desired levels of farm size. However, there is a need to study these determinants and identify the nature of their impact on the farm size. The research aims to identify the most important economic variables affecting the determination of the farm size, as well as the correlation between the farm size and the level of productivity of the plant under discussion (Crop cucumber). The data were hot from their primary and secondary data,The primary data were obtained from the survey form. The secondary data which include the time chronology were obtained from the related departments and ministries, planning and follow-up department, agricultural Statistics and Personnel office- Ministry of Agriculture, planning and follow-up department- Agricultural Statistics office Ministry of Planning and Development Co-operation.

MATERIALS AND METHODS

The farm is defined as an enterprise which performs producing and selling. The most familiar concept of the farm size is that it gives a scale for the productivity competence. There are many methods to measure the farm size. The most traditional one to measure the farm size is a spatial scale such as acre or hectare. It is a fact that one acre of the irrigated land differs than the one acre of a rained land. There is another common method to measure the farm size through the total value of sales or product. The total sales are a scale which depends on the acre output. This method provides some indicators that help to identify the productive of land capacity, and it is relatively easy to measure total sales, although it has changed upon conditions unrelated to farm size. Among these conditions are the weather fluctuations and its impact on crops or the annual fluctuations in agricultural commodity prices (Ahearn & Yee,

2004).The production activity is considered as the main support that a nation civilization depends on and represents its ability to grow on the social and economical level. It is the effective means to exploit the physical and human wealth so as to meet the growing citizen desires and needs for goods and services. The production activity is also the main source to provide employment through which individual could promote his economic, social and cultural level. Consequently, productivity has currently become one of the major issues to be put into consideration within the economic and international communities' challenges. Therefore, put it into high consideration, on improving and increasing its rate level as far as quality and quantity are concerned, would decrease costs and promote competence capability of organizations (Prokopenko, 1987, 6). One of the long-term problems in the agricultural production of developing countries is the inverse relationship between farm size and productivity. The production in each unit of land is higher in small farm than large farm. This inverse relationship between farm size and productivity was first discovered in Russian agriculture. (Chayanov 1926)

Interest in this issue intensified in the 1960s and 1970s (Sen. 1962; 1975; Bardhan, 1973). Since then, the inverse relationship between farm size and productivity has become a serious topic in discussion between economists in agriculture and in development (Carter 1984; Feder, 1985; Benjamin, 1992; Lamb, 2003) and has played an important role in planning agricultural policies and lands in developing countries. The inverse relationship of farm productivity is the main reason for the implementation of land reforms in many developing countries including India (Deininger 2003; Thapa2007, Ghatak and Roy, 2007). The argument is clear because small farms are more productive than large farms. The distribution of more lands from large farms to small farms would lead to increase productivity and economic growth (Feder1985) Econometric methods are a key tool that gives the economic theory the applied appearance which helps in evaluating its elements, testing their hypotheses, and making sure that they are correct in order to make them more logical and reasonable in evaluating the behavior of economic units (production, consumption...).To tackle the econometric model, the first step to categorize the model was identifying the variables involved.

The mathematical relationship between the variables was also formulated as a second step (Koutsoyannis, 1977, 16). The study under discussion i.e measuring and analyzing the impact of the relationship between farm size and productivity in addition to other variables (average total costs in the short term, labor resource price, the price of the land supplier, family members working in the farm, farming income, price of products, expertise in agriculture, farmers age, educational level, revenue...). However, the following variables were selected as being the most influential variables in the models adopted in estimating the size functions for different crops (the production of the acre in previous year, average short-term total costs, labor resource price, land resource price, farming income, family members working in farm, product price ...). The impact of these variables has been determined by previous studies and research that have been relied upon, as well as by the study of the reality of the area under consideration. The mathematical shape of the farm size has been formulated: $Y= f(X_1,X_2,X_3,X_4,X_5,X_6)$

The formulation of the relationship described in the standard format takes the following form:

$$Y = B_0 + B_1X_1 + B_2X_2 + B_3X_3 + B_4X_4 + B_5X_5 + B_6X_6 + Ui$$

Y = The dependent variable Dependent Variable represents the size of the total cultivated area of the crop (acre).
X_1 = one acre productivity of previous year (kg/acre)
X_2 = average total cost for acre and represent the total cost on the short term divided by the production quantity
X_3 = price resource agent (ID)
X_4 = land resource price represents the cash amount in ID Dinar to the land resource
X_5 = Farming family members
B's = sample parameters
Ui = error limits and absorb the affect of the eliminated variables.

After the characterization and formulation of the model and the use of Cross-Sectional data with standard methods to choose the appropriate relation between the size of the farm and the variables affecting it which were mentioned previously. The function has been estimated using the method of the Ordinary Least Square OLS to recognize the parameters of the model. This method is considered as one of the most applied method in estimating the econometric model relations because they have typical characteristics such as unbiased bias, minimum variance. In addition to the ease of calculations, and by using the statistical program SPSS (20) . EViews9, many function formulas gave been estimated (linear, logarithmic-double, half-logarithmic) and it was found that the half-logarithmic function is the most appropriate for the economic logic and the best for the statistical and standard tests.

RESULTS AND DISCUSSION

Through the results of the statistical analysis, the following estimated function has been obtained: It was clear that the half-logarithmic form is the most representative model of the relationship between the farm size and the Explanatory variables (the production of in previous year, average total costs, labor resource price, land resource price, family members working in farm).Through the results of the statistical analysis, the following estimated function has been obtained for the Crop cucumber as on Table (1):

$$y = 34.117 - 0.895 lnx_1 - 0.725 lnx_2 - 0.088 lnx_3 - 1.520 lnx_4 + 0.454 lnx_5$$

The slope model was estimated by using the Ordinary Least Square (OLS). The half-logarithmic function was adopted for being the most convenience model. The factor of the R^2 value was about (60%) which refers that 60% of fluctuation in the dependent variable was illustrated by the Explanatory variables included in the model. The F test proved a significance of the model with in total at high level. The Explanatory variables also showed high significance level except the labor source variable. The value of the productivity factor for the previous year showed a negative sign. This refers that the increasing of the productivity of the Crop cucumber in the open cultivation affects negatively on the increase in the area planted with the crop.

This was because there are other competent crops to be cultivated, which decreases the area under crop cultivation to maintain a stable production level and exploit those areas to cultivate other competent crops to maintain crop diversity in the farm and consequently diversify sources of income.The total average cost coefficient appeared with a negative sign of (0.725) and was identical to the economic theory logic. This indicates that the increase in average total costs automatically leads to a decrease in the cultivated area due to the fact that the farmer tries to reduce loss related to increased costs under the stability of the revenue. As for the labor resource variable price, it appeared with a negative sign identical to the economic theory logic but the variable is not significant. This refers that increasing the price of the labor resource, this leads to a decrease in the area cultivated with the crop and can be attributed to the high crop necessities of the labor in the harvest season and other agricultural processes.

The land resource variable price factor also indicates the inverse relationship between the increase in the land resource price and the farm size. Its value (-1.520) indicates that by increasing the land resource price, the area allocated to crop cultivation will decrease. This is due to the higher share cost of land resource than the total cost of producing the crop. So the increase in the price of a resource will increase the cost of producing the crop. Consequently, the farmer will decrease the areas cultivated with the crop.The variable coefficient of the family members working on the farm shows a positive sign and identical to the economic theory logic. Its value was (0.454), which indicates that by increasing the family members working on the farm give the farmer confidence to increase the cultivated areas in order to provide the labor required to cultivate the Crop cucumber. To ensure that the model is free of standard problems and to be acceptable and reliable, diagnostic tests have been applied to detect the existence of these problems and as follows:

Autocorrelation problem

The Durbin-Watson test was used to detect the presence of correlation problem. Through the D* value between ($d_u < d^* < 4-d_u$) i.e. (1.287<1.806<2.224) for significant level of a 5%, which means it is within the hypothesis of absence, which states that there is no autocorrelation between Explanatory variables. Thus the model does not have any autocorrelation problem.

Heteroscedasticity Problem

As long as our study based on cross- data, there should be an Inconsistency of Heteroscedasticity Problem, which often come with such data. Detecting this problem can be done by the (Breusch-Pagan-Godfrey) test. The following results were got:

(Multicollinearity)

Determining the Linear Duplex Problem is to detecting the degree of correlation and it is not to experience whether existed. The multicollinearity contains two Explanatory variables (Gujarat19i88). There are many ways to detect this phenomenon such as Farrer – Clouber, Klein or by the Variance Inflation-Factor (VIF) for each of the instructive variables. Last test was used to detect the multicollinearity problem. If the value of VIF > 10, it indicates that there is multicollinearity among the Explanatory variables. Table (3) shows that the value of (VIF) of the estimated parameters is less than 10 and this indicates that there is no risk from multicollinearity among the Explanatory variables.The study dealt with the size of possession and profits It divided the possession of farmers into four classes, The second classes (11-19) dunums recorded the highest profit rate of about (1.34) million dinars / dunum, which constitutes about (11.1%) of the sample size, while the third category recorded a loss of about (- 0.37) Million dinars / dunum, which constitutes about 15.6% of the sample size. That the rate of profit decreases by increasing possession due to the lack of water needed to water the crop and the security conditions and military operations in the sample study.

The study reached a number of conclusions, the most important of which is the negative relationship between the size of the farm and the productivity variable for the previous year. This is due to the lack of water needed to irrigate the crop, in addition to the military operations that took place in the study area. The negative relationship between the average total costs and the size of the farm suggests that it is possible to influence the size of the farm by reducing the average total costs using modern methods and techniques in agriculture that will provide the agricultural areas for the production of other crops. The study concludes that the low rate of profit by increasing possession is due to the fact that the cucumber crop is cultivated in the traditional way. This method has disadvantages such as large quantities of irrigation water and high crop cultivation costs.Based on previous conclusions, the study recommends that attention be given to modern agricultural methods and means that increase the productivity of agricultural crops and thus encourage farmers to increase cultivated areas. And the development of programs by agricultural specialists to exploit resources in a manner that saves or reduces waste in the quantities of resources used.

REFERENCES

1. Al-Azzawi, Omar Saeed, al-Abadi, Issam Mohamed, 2017, The Impact of Organic feeder, Humic and Chemical Fertilizer, on Leaves Content of the elements and the total yield of the Cucumis Sativus l plant. Journal of Iraqi Agricultural Sciences, 48 (3).
2. Ahearn, M. C. and Yee J. and, 2004, Alternative Measures of Farm Size: Trends and Determinants. Paper Prepared for Presentation at the Southern Agricultural Economics Association Meetings Tulsa, Oklahoma.

3. Bardhan, P. K. (1973). Size, productivity, and returns to scale: An analysis of farm-level data in Indian agriculture. The Journal of Political Economy.
4. Benjamin, D. (1992). Household Composition, Labor Markets, and Labor Demand: Testing for Separation in Agricultural Household Models, Econometrics, 60(2).
5. Carter, M. R. (1984). Identification of the inverse relationship between farm size and productivity: an empirical analysis of peasant agricultural production. Oxford Economic Papers.
6. Deininger, K. (2003). Land markets in developing and transition economies: Impact of liberalization and implications for future reform. American Journal of Agricultural Economics, 85(5).
7. Farhan, Mohammed Khalid Mohammed, 2017, Integration of Socio-Economic and Technical Methods to determine the motives of Agricultural Policy to Promote Sustainable use of Water and Lands (WLI project in Iraq-a case study), PhD thesis, College of Agriculture, University of Baghdad.
8. Feder, G.(1985), "The Farm Size and Farm Productivity: the Role of Family Labour, Supervision and Credit Constraints", Journal of Development Economics.
9. Ghatak, Maitreesh, and S. Roy (2007). Land Reform and Agricultural Productivity in India: A Review of the Evidence. Oxford Review of Economic Policy, 23(2).
10. Gujrati. N. D. 2004. Basic Econometrics.Mc-Graw Hill Co. Press. LTD
11. Koutsoyiannic, A. 1981. Theory Economics .second Edition Mc. Millan.
12. Lamb, R. L. (2003). Inverse productivity: land quality, labor markets, and measurement error. Journal of Development Economics, 71(1).
13. Matloob, Adnan Nassir, 1983, Vegetable Production in Adequate Environment, printing and publishing house, Ministry of Higher Education and Scientific Research, University of Mosul, Nineveh.
14. Pillai , Dr.Thirumagal , 2012 , Farm Size And PRODUCTIVITY RELATIONSHIP (An Empirical Investigation based on Cost of Cultivation Data). International Journal of Physical and Social Sciences
15. Prokopenko, Joseph, 1987, Productivity Management A practical handbook .
16. Sen, A. K. (1962). An Aspect of Indian Agriculture. Economic Weekly, 14, 243–266.
17. Srildhar Thapa, 2007, The relationship between farm size and productivity: empirical evidence from the Nepalese mid-hills. Contributed paper prepared for presentation at the 106th seminar of the EAAE Pro-poor development in low income countries: Food, agriculture, trade, and environment , Montpellier, France.

Table (1) the estimated factors of the farm size function for the Crop cucumber.

Variable	Coefficient	S.E	t.statistics	P.value
Constant	34.117	6.835	4.992	0.000
Lnx_1	-0.895	0.246	-3.643	0.001
Lnx_2	-0.727	0.112	-6.455	0.000
Lnx_3	-0.088	0.152	-0.578	0.566
Lnx_4	-1.520	0.560	-2.715	0.010
Lnx_5	0.454	0.164	2.765	0.009
D-W=1.806 F=11.862 n=45 0.60 R^{2}l=0.55 R^{2}=				

Source: Prepared by the researcher based on the results of the of the statistical Program analysis spss (20).

Table (2) : test of (Breusch-Pagan-Godfrey) for the model varianles

Heteroskedasticity Test: Breusch-Pagan-Godfrey

F-statistic	0.316993	Prob. F(5,39)	0.8998
Obs*R-squared	1.757384	Prob. Chi-Square(5)	0.8816
Scaled explained SS	1.590232	Prob. Chi-Square(5)	0.9024

Test Equation:
Dependent Variable: RESID^2
Method: Least Squares
Date: 10/10/18 Time: 13:54
Sample: 1 45
Included observations: 45

Variable	Coefficient	Std. Error	t-Statistic	Prob.
C	-0.273514	11.31012	-0.024183	0.9808
PR	0.016642	0.406908	0.040899	0.9676
AC	0.141340	0.185843	0.760533	0.4515
WORK	0.161875	0.252601	0.640834	0.5254
LAND	-0.138174	0.927065	-0.149044	0.8823
FARMWORK	-0.237097	0.271716	-0.872591	0.3882

R-squared	0.039053	Mean dependent var	1.180554
Adjusted R-squared	-0.084145	S.D. dependent var	1.853215
S.E. of regression	1.929610	Akaike info criterion	4.276079
Sum squared resid	145.2124	Schwarz criterion	4.516967
Log likelihood	-90.21177	Hannan-Quinn criter.	4.365879
F-statistic	0.316993	Durbin-Watson stat	1.764227
Prob(F-statistic)	0.899758		

Source: Prepared by the researcher based on the statistical program spss 20.

Table (3): VIF coefficient value of Explanatory variables.

Independents Variables	VIF
lnpr	**1.081**
lnATC	**1.055**
lnPWork	**1.077**
LnPLand	**1.053**
Lnfamily	**1.051**

Source: Prepared by the researcher based on analysis results using the statistical program SPSS (20).

Table 4. classes of possession and profit rate of the research sample.

n	classes	Rate of profit/million dinars	Number of farmers	Percentage%
1	10 - 2	0.82	20	44.4
2	19 – 11	1.34	5	11.1
3	28 -20	-0.37	7	15.6
4	29 more	-0.56	13	28.9
total		**0.29**	**45**	**100**

Source: Prepared by the researcher based on the questionnaire survey

Indian Journal of Natural Sciences www.tnsroindia.org.in ©IJONS

Vol.9 /Issue 51 / December / 2018 *International Bimonthly* *ISSN: 0976 – 0997*

RESEARCH ARTICLE

Phytochemical Screening and Antibacterial Effect of Abgaw (Lamiaceae: *Premna odorata* Blanco)

Honey Dawn T. Salvanera[2], Lilybeth F. Olowa[1]* and Mark Anthony I. Jose[1]

[1]Professor, Department of Biological Sciences, College of Science and Mathematics, Mindanao State University, Iligan Institute of Technology, Iligan City 9200, Mindanao, Philippines.
[2]Student, Department of Biological Sciences, College of Science and Mathematics, Mindanao State University, Iligan Institute of Technology, Iligan City 9200, Mindanao, Philippines

Received: 04 Sep 2018 Revised: 07 Oct 2018 Accepted: 10 Nov 2018

***Address for Correspondence**
Lilybeth F. Olowa
Professor, Department of Biological Sciences,
College of Science and Mathematics,
Mindanao State University,
Iligan Institute of Technology,
Iligan City 9200,
Mindanao, Philippines.
E.mail: lilybetholowa@gmail.com

ABSTRACT

The use of plants as an alternative medicine to treat various diseases gained much attention in recent years. *Premna odorata* Blanco (Alagaw) is among those plants which are being studied for their remarkable use in traditional system of medicine. The antibacterial effect of the ethanolic leaf extract of the plant was evaluated using Agar disc diffusion method. The selected pathogens were *Staphylococcus aureus* and *Bacillus subtilis* for the Gram-positive bacteria and *Escherichia coli* and *Pseudomonas aeruginosa* for the Gram-negative bacteria. Inhibitions were only observed at the highest concentration (20mg/ml) of the extract in which *S. aureus* and *B. subtilis* were susceptible with an average zone of 14.67 mm and 8 mm, respectively. Phytochemical screening showed presence of alkaloids, flavonoids, steroids, and tannins. The antibacterial effect of the plant might be due to these bioactive compounds. Thus, results may validate the ethnomedicinal uses of the plant.

Keywords: antibacterial, bioactive, ethanolic extract, pathogens, *Premna odorata*

INTRODUCTION

Considered to be one of the most biodiverse countries, the Philippines is home for various medicinal plants. For centuries now, many parts of the world have been using local medicinal plants in treating bacterial infections but

later commercially available antibiotics revolutionized the treatment of microbial infections. Unfortunately there has been an increasing case of drug resistances towards many antibiotics resulted from the indiscriminate use by the people. Due to this phenomenon there has been an increasing demand for the search of antimicrobial agents back again from natural sources. Recently, new sources of therapeutic agents were identified from the studies focusing on the investigations of traditional African, Caribbean and Indian medicinal plants [1].Despite the country's richness in medicinal plants, there are only ten (10) approved by the Department of health in spite the many works done by Guerrero (1921), Masulingan et al. (1955), Quisumbing (1978), Santos et al. (1981), de Padua et al. (1977, 1978, 1981, 1983), Manalo and Genetiano (1998) among others [2]. Although the Department of Science and Technology-Philippine Council for Health Research and Development and the National Research Council of the Philippines and other major academic institutions such as the University of the Philippines and University of Santo Tomas supported many studies on medicinal plants, only two plants recommended by the Philippine government are antibacterials, guava and ringworm bush (acapulco) [2].

The methanolic extract of Queen sago (*Cycas circinalis*) ovules was investigated for antibacterial activity against human pathogenic bacteria, *Bacillus cereus*, *Staphylococcus aureus* and E*scherichia coli* showed significantly higher inhibitory activity than the antibiotics tested [3]. Acetone extract of *Syzygium jambos*'s bark, leaf and seed were active against *S. aureus*, *E. coli*, *Salmonella typhi*, *Pseudomonas aeruginosa* and *Vibrio cholerae* [4]. These researches gained significance due to the resistance acquired by pathogens towards a number of widely-used drugs. This research focuses on the antibacterial effect of an endemic plant in the Philippines, *Premna odorata* Blanco or Alagaw (Tagalog name) and Abgaw (Cebuano Bisaya name) using ethanolic leaf extract. The plant is traditionally used in Albay Province, in southeastern Luzon, Philippines to treat tuberculosis [5]. Previous study by Pinzon et al. [6] on *P. odorata* Blco. Leaves revealed presence of diosmetin and acacetin which are antimicrobial, anti-inflammatory, and chemopreventive, however there are still remaining unidentified compounds in the other fractions that will be investigated in this research. Specifically, the study evaluates the antibacterial effect of the plant species against Gram-positive bacteria *S. aureus* and *Bacillus subtilis* and Gram-negative bacteria *E. coli* and *P. aeruginosa.* This study validates the medicinal uses of *P. odorata* through phytochemical analysis of the plants' bioactive compounds.

MATERIALS AND METHODS

Collection and Preparation of Plant Materials

Healthy mature leaves of *P. odorata* were harvested early in the morning from a single tree in Mahayag Zamboanga del Sur, Philippines. The plant was validated by a plant expert from the Department of Biological Sciences, Mindanao State University-Iligan Institute of Technology. The leaves were washed under running tap water and shade dried under room temperature for three to four weeks. Leaves were homogenized to fine powder using waring blender and stored in airtight container in a dark area. Exposure to direct sunlight was avoided to prevent the loss of active components.

Extraction of Plant Leaves

The fine powdered leaves, weighing 1000 g, were soaked in 95% ethanol for 72 h. The crude ethanolic leaf extract was filtered and concentrated with a rotary evaporator.

Phytochemical Screening

Phytochemical screening was conducted at the Chemistry Laboratory of the Department of Chemistry in MSU-IIT. The freshly prepared ethanolic leaf extract was subjected to phytochemical analysis using standard methods

described by Sazada et al. [7], Harborne [8], and Trease and Evans [9] to find the presence of the following phyto constituents: flavonoids, alkaloids, glycosides, tannins, anthraquinones, and steroids.

Test Microorganisms

The test microorganisms were purchased from the Philippine National Collection of Microorganisms, National Institute of Molecular Biology and Biotechnology, University of the Philippines Los Baños. Two Gram-positive bacteria: *S. aureus* and *B. subtilis* and two Gram-negative bacteria: *E. coli* and *P. aeruginosa* were used to test the extract.

Preparation of Inoculum

Stock cultures were maintained at 4°C on slopes of nutrient agar. Active cultures for experiments were prepared by transferring a loopful of cells from the stock cultures to test tubes of Mueller-Hinton broth (MHB) for bacteria and were incubated without agitation for 24 h at 37°C. To 10ml of MHB, a loopful of culture was inoculated and incubated until it reached the turbidity equal to that of the standard 0.5 McFarland solution at 600nm which is equivalent to 10^6–10^8 CFU/ml.

Preparation of Control

Tetracycline and chloramphenicol were used as positive controls. About 0.03 g of the antibiotics was dissolved in 10 ml sterile distilled water (Manual on Antimicrobial Susceptibility Testing).

Antibacterial Assay

The assay was performed using the modified Kirby-Bauer disc diffusion method with Muller Hinton Agar (MHA) plates following the method of Samie et al. [10]. The MHA plates were prepared by pouring 25ml of molten media into sterile Petri plates. Then, the plates were allowed to solidify for 10-15 min and 100 µl inoculum suspension was spread uniformly using sterile glass spreader and was allowed to dry for 10 min. The extracts were tested using 6mm sterile filter paper discs. *P. odorata* leaf extract was diluted to 20mg/ml, 15mg/ml and 10mg/ml respectively. Discs were impregnated with 10 µl of the different concentrations of the test sample, allowed to dry and placed onto inoculated plates and allowed to diffuse for 15 min. The plates were kept for incubation at 37°C for 24 h. The assay was performed in triplicate. At the end of incubation, inhibition zones formed around the disc were measured with a transparent ruler in millimeter.

Statistical Analysis

One way ANOVA was used to analyze the data (zones of inhibition in millimeter) in order to determine if the varied concentrations, including the control, has significantly different effects from each other following the method of Mengiste et al. [11].

RESULTS AND DISCUSSION

The phytochemicals isolated from the ethanolic leaf extract were alkaloids, tannins, flavonoids, steroids, anthraquinones, and cyanogenic glycosides (Table 1). Results showed that there is a heavy precipitate or very intense color of tannins, flavonoids, and steroids indicated by the three plus sign (+++) followed by moderate presence of alkaloids with two plus sign (++). Although anthraquinones and cyanogenic glycosides were below detection (-) it

does not mean that the compounds are totally absent in the plant extract. The amount present may not be enough for the compounds to be detected.

The results confirmed the presence of constituents found by the previous study of Pinzon et al. [6] which revealed presence of flavones: diosmetin and acacetin which are antimicrobial, anti-inflammatory and chemopreventive. The isolated compounds are known to exhibit medicinal as well as physiological activity [12]. Phytochemical constituents such as alkaloids, flavonoids, and tannins which are observed in the present study along with phenols, saponins, and several other aromatic compounds are secondary metabolites of plants that serve a defense mechanism against prediction by many microorganisms, insects and other herbivores. These bioactive compounds are known to act by different mechanism and exert antimicrobial action [13].

Previous study showed alkaloids and their derivatives have activities against *S. aureus* and methicillin-resistant *S. aureus* as reported by Chitemerere and Mukanganyama [14]. The mechanism of action of highly aromatic planar quaternary alkaloids is attributed to their ability to intercalate with DNA. Plants having alkaloids are used in medicines for reducing headache and fever [15]. Tannins are reported to bind to proline rich proteins and interfere with the protein synthesis. They are polymeric phenolic substances capable of tanning leather or precipitating gelatin from solution, a property known as astringency. They are used in pharmaceutical preparations because of their astringent action. Tannins are well known to possess general antimicrobial and antioxidant properties. At low concentration tannins can inhibit the growth of microorganisms, and act as an antifungal agent at higher concentration by coagulating the protoplasm of the microorganism. Aside from the use of tannins as antimicrobial agents or prevention of dental caries, they are now being used in the manufacture of plastics, paints, ceramics and water softening agents [16]. Flavonoids (a large group of naturally occurring plant phenolic compounds including flavones, flavonols, isoflavones, flavonones and chalcones) also known as nature's tender drugs, possess numerous biological/pharmacological activities. They are hydroxylated phenolic substance known to be synthesized by plants in response to microbial infection and it should not be surprising that they have been found *in vitro* to be effective antimicrobial substances against a wide array of microorganisms. Their activity is probably due to their ability to complex with extracellular and soluble proteins and to complex with bacterial cell walls [17]. Recent reports of antiviral,anti-fungal, antioxidant, anti-inflammatory, antiallergenic, antithrombic, anticarcinogenic, hepatoprotective, and cytotoxic activities of flavonoids have generated interest in studies of flavonoid-containing plants. Of these biological activities, the anti-inflammatory capacity of flavonoids has long been utilized in Chinese medicine and the cosmetic industry as a form of crude plant extracts.

Steroids have also been reported to have antibacterial properties, the correlation between membrane lipids and sensitivity for steroidal compound indicates the mechanism in which steroids specifically associate with membrane lipid and exerts its action by causing leakages from liposomes [13]. Steroids are plant compounds that may or may not act as weak hormones in the body. They are mainly used to treat reproductive complications such as treatment of venereal diseases, used during pregnancy to ensure an easy delivery, as well as to promote fertility in women and libido in men. They are also analgesic, anti-inflammatory, and of use in treating stomach ailments and in decreasing serum cholesterol levels [18]. Anthraquinones was reported to possess antiparasitic, bacteriostatic, antidepressant, and antimicrobial properties. Reports about the antibacterial and antifungal activities of anthraquinones isolated from the natural sources involved two types of anthraquinone, emodin and physcion isolated from *Ventilago madraspatana* which showed antibacterial activity against three *Bacillus* sp. [19]. Cyanogenic glycosides are inactive in themselves but break down (either spontaneously in acid conditions or in hydrolytic reactions catalysed by ß-glycosidases) to generate cyanide (CN^-). CN^- is a potent inhibitor of cytochrome oxidase that catalyses the final transfer of electrons to molecular oxygen in the mitochondrial respiratory (electron transport) chain. The best known cyanogenic glycosides are those occurring in plants of economic importance including: amygdalin from *Prunus amygdalis* (almond) (Rosaceae) seed; dhurrin from *Sorghum* species (Poaceae); linamarin (manihotoxine) from *Linum usitatissimum* (flax) (Linaceae) seedlings and in *Manihot esculentum* (cassava) (Euphorbiaceae); linustatin and neolinustatin from flax seeds; prunasin from bark of *Prunus* species (Rosaceae) [20]. There are still other numerous

plants that contain CN glycosides. Also the plants mentioned here may contain more than one type of cyanogenic glycoside [21].

The present study carried out on the plant sample revealed the presence of medicinally active constituents. These compounds detected in the ethanolic leaf extract of *P. odorata* supported the observed antibacterial property of the plant. Evaluation of antibacterial effect was performed by disc diffusion method. Diameter of the zone of inhibition (ZOI) was measured for the estimation of potency of the antibacterial substance. At 16 hours, both the gram-positive bacteria (*S. aureus* and *B. subtilis*) were inhibited by the ethanolic leaf extract with the highest concentration (20mg/ml). However, the gram-negative bacteria (*E.coli* and *P. aeruginosa*) were found to be resistant (Table 2). These observations are likely to be the result of the differences in cell wall structure between Gram-positive and Gram-negative bacteria, with the latter having an outer membrane that acts as a barrier to many environmental substances including antibiotics [22]. At 24 hours, the same results were obtained; however, there is a slight difference in the diameter of zones of inhibition in *S. aureus* (Table 3).

A decrease in the zones of inhibition on the Gram-positive *S. aureus* was observed in the leaf extract after 24 hours. This showed that the leaf extract has a bacteriostatic effect against the test organism.As for the reference antibiotics used in this study, tetracycline and chloramphenicol; all four bacterial species were found to be susceptible to tetracycline. For chloramphenicol, only three out of the four test bacteria showed susceptibility. The antibiotic had no effect on *P. aeruginosa*. Results showed that both drugs are bacteriostatic against the four test bacteria. Findings were in accordance with the results of Herman-Ackah [23] and Rahal and Simberkoff [24]. Only *E. coli* showed increase susceptibility after 24 hours for chloramphenicol. For tetracycline, *S. aureus* exhibited the largest zone of inhibition followed by *E. coli*, *B. subtilis* and *P. aeruginosa*. For chloramphenicol, only three out of the four test bacteria showed susceptibility. *B. subtilis* had the maximum zone of inhibition followed by *S. aureus* and *E. coli*. At 24 hours, *B. subtilis* and *E. coli* had the largest zone of inhibition in chloramphenicol. Furthermore, the inhibition zone (value) showed by the positive controls were significantly higher compared to those displayed by the ethanolic leaf extract.

The present study also reveals that the ethanolic leaf extract of *P. odorata* has a narrow spectrum of activity for it only inhibited the bacterial growth of the Gram-positive bacteria. These findings were in consonance with the previous investigation by Oboh et al. [25]. The high resistance of Gram-negative bacteria is attributed to their cell walls which have a more complicated structure than those of Gram-positive bacteria. Gram-negative bacteria offer a complex barrier system to biocides and antibiotics, regulating, and sometimes preventing, their passage to target regions [26]. The cell wall in Gram-negative bacteria contains much less peptidoglycan and is surrounded by an outer membrane. The outer membrane of Gram-negative bacteria is another lipid bilayer similar to the cytoplasmic membrane and contains lipids, proteins, and lipopolysaccharides (LPS). The outer membrane of Gram-negative bacteria acts as a molecular filter for hydrophilic compounds. The active components of these molecular sieving properties are a major class of proteins called porins [27, 28]. LPS, the major component of the outer membrane, confers a negative charge and also repels hydrophobic compounds including certain drugs and disinfectants that would otherwise kill the cell [29].

Figure 1 shows the comparison of the effect of the 20mg/ml ethanolic leaf extract of *P. odorata* against *S. aureus* and *B. subtilis*. Results showed that the extract is more effective against *S. aureus* than *B. subtilis* at a p-value of 0.007661. Results of Post-Hoc Tukey HSD test showed that there is a significant difference (p=0.007661) on the zones of inhibition between *S. aureus* and *B. subtilis* using the ethanolic leaf extract. Comparison of the zones of inhibition of the ethanolic leaf extract with the positive control, tetracycline, also showed a statistically significant difference for *S. aureus* (p=0.000257) and for *B. subtilis* (p=0.000227) (Table 4). Comparing the effects of the ethanolic leaf extract to the standard antibiotics, tetracycline and chloramphenicol, it is evident that the zones of inhibition for the reference antibiotics were all greater than those of the extract. This indicates that the leaf extract may not be as effective against the selected human pathogens as the commercially available antibacterial drugs used in the study.

S. aureus was the most susceptible bacterium, an observation that may be attributed to the presence of single membrane of the organism which makes it more accessible to permeation by active principles of the extract in consonance with the earlier reports of Samie et al. [10], Girish and Satish [30], Chitravadivu et al. [31] and Shihabudeen et al. [13]. *S. aureus* was found to be sensitive to five plant extracts wherein *Eugenia jambolana* (kernel) and *Cassia auriculata* (flowers) exhibited the highest antimicrobial activity at a minimum concentration. Ethanolic extracts of *Acalypha indica*, *Cassia auriculata*, *Eclipta alba* and *Phyllanthus niruri* also showed higher Relative magnitude of inhibition (RMI) against *S. aureus* as reported by Chitravadivu et al. [31]. In contrast, *P. aeruginosa* showed the greatest resistance. The bacterium was only inhibited by the positive control, tetracycline. This may be due to the fact that *P. aeruginosa* has intrinsic resistance from a restrictive outer membrane barrier and trans-envelope multidrug resistance pumps (MDRs) [30]. It is well known that *P. aeruginosa* is notorious for its resistance to antibiotics and is, therefore particularly dangerous and dreaded pathogen. Aside from being naturally resistance to many antibiotics due to the permeability barriers afforded by its outer membrane composed of lipopolysaccharide (LPS), also its tendency to colonize surfaces in a biofilm form makes the cells impervious to therapeutic concentrations of antibiotics [32].

The degrees of antibacterial effect of plant extracts are also affected by the solvent used in the extraction. The fact that the organic solvent extracts exhibited greater antimicrobial activity because the antimicrobial principles were either polar or non-polar and they were extracted only through the organic solvent medium. Ethanol will dissolve organic compounds better than aqueous extract and also liberate the active component required for antibacterial activity. Organic solvent extraction was suggested to be more suitable to verify the antimicrobial properties of medicinal plants as supported by the many investigators [10, 30, 31, 22, 13]. Other factors could have also affected to the efficacy of the plant extract against the selected pathogens such as the method of extraction, the bacterial strains used, and the environmental and climatic conditions of the plant being tested.

Generally, the results of this study revealed the presence of medicinally active constituents in the ethanolic leaf extract of *P. odorata*. The phytochemical compounds identified in this study have earlier been proved to be bioactive. The presence of some of these compounds have been confirmed by previous workers to have medicinal as well as physiological activity and therefore could be said to be responsible for the antibacterial effect of the plant and thus confirms and justifies the medicinal use of the plant in the treatment of some common ailments. The continued traditional medicinal use of the plant is therefore encouraged. While it is suggested that further work should be carried out using the decoctate of fresh leaves to compare its effectiveness with the results obtained from organic solvent extraction.

REFERENCES

1. Cock IE. Antimicrobial activity of Syzygium australe and Syzygium leuhmannii Leaf Methanolic Extracts. Pharmacongnosy Communications, 2012; 2(2).
2. Penecilla GL and Magno CP. Antibacterial activity of extracts of twelve common medicinal plants from the Philippines. Journal of Medicinal Plants Research, 2011; 5(16): 3975-3981.
3. Kalpashree MM and Raveesha KA. Antibacterial Activity of Cycas circinalis Ovules – A Naked Seeded Gymnosperm. International Journal of Herbal Medicine, 2013; 1 (3): 53-55.
4. Murugan S, Uma Devi P, Kannika Parameswari N, and Mani KR. Antimicrobial Activity of Syzygium jambos Against Selected Human Pathogens. International Journal of Pharmacy and Pharmaceutical Sciences, 2011; 3(2): 44-47.
5. Lirio SB, Macabeo AP, Paragas EM, Knorn M, Kohls P, Franzblau SG, Wang Y, and Aguinaldo MA. Antitubercular Constituents from Premna odorata Blanco. Journal of Ethnopharmacology, 2014; 154(2): 471-474.

6. Pinzon LC, Uy MM, Sze KH, Wang M, and Chu IK. Isolation and Charaterization of Antimicrobial, Anti-inflammatory and Chemopreventive Flavones from *Premna odorata* Blanco. J. Med. Plants Res., 2011; 5(13): 2729-2735.
7. Sazada S,Verma A, Rather AA, Jabeen F, and Meghvansi MK. Preliminary phytochemicals analysis of some important medicinal and aromatic plants. Adv. in Biol. Res., 2009; 3:188-195.
8. Harborne JB. Phytochemical Methods. Springer (India) Pvt. Ltd., New Delhi; 2005;17: 49-188.
9. Trease GE and Evans WC. Pharmacognosy. 13th ed. Bailliere Tindall, London; 1989; 176-180.
10. Samie A, Obi CL, Bessong PO, Namrita L. Activity profiles of fourteen selected medicinal plants from Rural Venda communities in South Africa against fifteen clinical bacterial species. African Journal of Biotechnology, 2005; 4(12): 1443-1451.
11. Mengiste B, Hagos Y, Moges F, Tassew H, Tadesse G, and Teklu A. In vitro Antibacterial Screening of Extracts from Selected Ethiopian Medicinal Plants. Momona Ethiopian Journal of Science, 2014; 6(1): 102-110.
12. 12. Njoku, OV and Obi C. Phytochemical constituents of some selected medicinal plants. African Journal of Pure and Applied Chemistry, 2009; 3(11): 228-233.
13. Shihabudeen MS, Hansi PD, Thirumurugan K. Antimicrobial activity and phytochemical analysis of selected Indian folk medicinal plants. International Journal of Pharma Sciences and Research, 2010; 1(10): 430-434.
14. Chitemerere TA and Mukanganyama S. In vitro Antibacterial Activity of Selected Medicinal Plants from Zimbabwe. The African Journal of Plants Science and Biotechnology, 2011; 5(1): 1-7.
15. Wadood A, Ghufran M, Jamal SB, Naeem M, Khan A, Ghaffar R. and Asnad. Phytochemical Analysis of Medicinal Plants Occurring in Local Area of Mardan. Biochem Anal Biochem, 2013; 2(4): 1-4.
16. Peteros NP and Uy MM. Antioxidant and cytotoxic activities and phytochemical screening of four Philippine medicinal plants. J. Med. Plants Res., 2010; 4(5): 407-414.
17. Manaharan T, Cheng M, Appleton DR, Hwee M, and Palanisamy UD. Flavonoids isolated from Syzygium aqueum leaf extract as potential antihyperglycaemic agents. Food Chemistry, 2012; 132(4): 1802-1807.
18. Njeru SN, Matasyoh J, Mwaniki CG, Mwendia CM, and Kobia G. A Review of some Phytochemicals commonly found in Medicinal Plants. International Journal of Medicinal Plants, 2013; 135-140.
19. Bezerra de Barros I, Feijo de Souza Daniel J, Pinto JP, Rezende MI, Filho RB, and Ferreira DT. Phytochemical and Antifungal Activity of Anthraquinones and Root and Leaf Extracts of Coccoloba mollis on Phytopathogens. Brazilian Archives of Biology and Technology, 2011; 54(3):535-541.
20. Polya G. Biochemical Targets of Plant Bioactive Compounds. South African Journal of Botany. Taylor & Francis Inc., New York, USA; CRC Press, 2003; 71(3).
21. Holstege CP, and Lawrence D. The Evaluation and Management of Acute Poisoning Emergencies. 4th Edition National Association of EMS PhyPrehospital Systems and Medical Oversight, 2009.
22. Bishnu J, Lekhak S, and Anuja S. Antibacterial Property of Different Medicinal Plants: Ocimum sanctum, Cinnamomum zeylanicum, Xanthoxylum armatum and Origanum majorana. Kathmandu University Journal of Science, Engineering and Technology, 2009; 5(1): 143- 150.
23. Heman-Ackah SM. Comparison of Tetracycline Action on Staphylococcus aureus and Escherichia coli by Microbial Kinetics. Antimicrobial Agents and Chemotherapy, 1976; 10(2): 223-228.
24. Rahal JJ JR. and Simberkoff MS. Bactericidal and Bacteriostatic Action of Chloramphenicol Against Meningeal Pathogens. Antimicrobial Agents and Chemotherapy, 1979; 16(1): 13-18.
25. Oboh G, Akinyemi AJ, and Ademiluyi AO. Antioxidant Properties and Inhibitory Effect of Ethanolic Extract of Struchium Sparganophora (Ewuro Odo) Leaf on α - Amylase and α - Glucosidase Activities. Afr J Tradit Complement Altern Med. 2012; 9(3): 342–349.
26. Denyer SP and Maillard JY. Cellular impermeability and uptake of biocides and antibiotics in Gram-negative bacteria. J Appl Microbiol, 2002; 92 Suppl:35S-45S.
27. Nakae T. Outer membrane of Salmonella. Isolation of protein complex that produces transmembrane channels. Journal of Biological Chemistry, 1976; 251: 2176-2178.
28. Benz R and Bauer K. Permeation of hydrophilic molecules through the outer membrane of gram-negative bacteria. European Journal of Biochemistry, 1988; 176: 1-19.

29. Paustian T. The cell wall surrounds and holds in the microbe. Through the Microscope: A Microbiology Textbook 5th ed., 2009; http://www.microbiologytext.com/5th_ed/.
30. Girish HV and Satish S. Antibacterial Activity of Important Medicinal Plants on Human Pathogenic Bacteria-a Comparative Analysis. World Applied Sciences Journal, 2008; 5 (3): 267-271.
31. Chitravadivu C, Manian S, and Kalaichelvi K. Antimicrobial Studies on Selected Medicinal Plants, Erode Region, Tamilnadu, India. Middle-East Journal of Scientific Research, 2009; 4 (3): 147-152.
32. Panghal M, Kaushal V, and Yadav JP. In vitro antimicrobial activity of ten medicinal plants against clinical isolates of oral cancer cases. Ann Clin Microbiol Antimicrob, 2011; 10(21): 1-11.

Table 1. Phytochemicals detected on the ethanolic leaf extract of *P. odorata*.

Bioactive Constituents	Observation
Alkaloids	++
Tannins	+++
Flavonoids	+++
Steroids	+++
Anthraquinones	-
Cyanogenic glycosides	-

+++ Heavy precipitate or very intense color, ++ Moderate, + Turbid only if precipitate or very light color, - Below detection

Table 2. Zone of inhibition on the different concentrations (mg/ml) of the ethanolic leaf extract of *P. odorata* against Gram-positive and Gram-negative bacteria after 16 hours at 37°C.

Test Organism	Zone of Inhibition (mm)				
	10mg/ml	15mg/ml	20mg/ml	Tetracycline (30mg/ml)	Chloramphenicol (30mg//ml)
Staphylococcus aureus	-	-	14.67	40	30
Bacillus subtilis	-	-	8	22.67	30.67
Pseudomonas aeruginosa	-	-	-	22	-
Escherichia coli	-	-	-	32.67	26.67

Note: Values are mean of three replicates.

Table 3. Zone of inhibition on the different concentrations (mg/ml) of the ethanolic leaf extract of *P. odorata* against Gram-positive and Gram-negative bacteria after 24 hours at 37°C.

Test Organism	Zone of Inhibition (mm)				
	10mg/ml	15mg/ml	20mg/ml	Tetracycline (30mg/ml)	Chloramphenicol (30mg//ml)
Staphylococcus aureus	-	-	14	38	27.33
Bacillus subtilis	-	-	8	21.33	28.67
Pseudomonas aeruginosa	-	-	-	22	-
Escherichia coli	-	-	-	30	28.67

Note: Values are mean of three replicates.

Table 4. Post-hoc Tukey HSD *p*-values in comparing the zones of inhibition of Gram-positive bacteria against the ethanolic leaf extract of *P. odorata* and the standard antibiotics.

Test Organism	C vs. T	C vs. E	E vs. T
Staphylococcus aureus	0.009003	0.001182	0.000257
Bacillus subtilis	0.000316	0.000227	0.000227

Note: C stands for chloramphenicol, T for tetracycline, and E for the ethanolic leaf extract

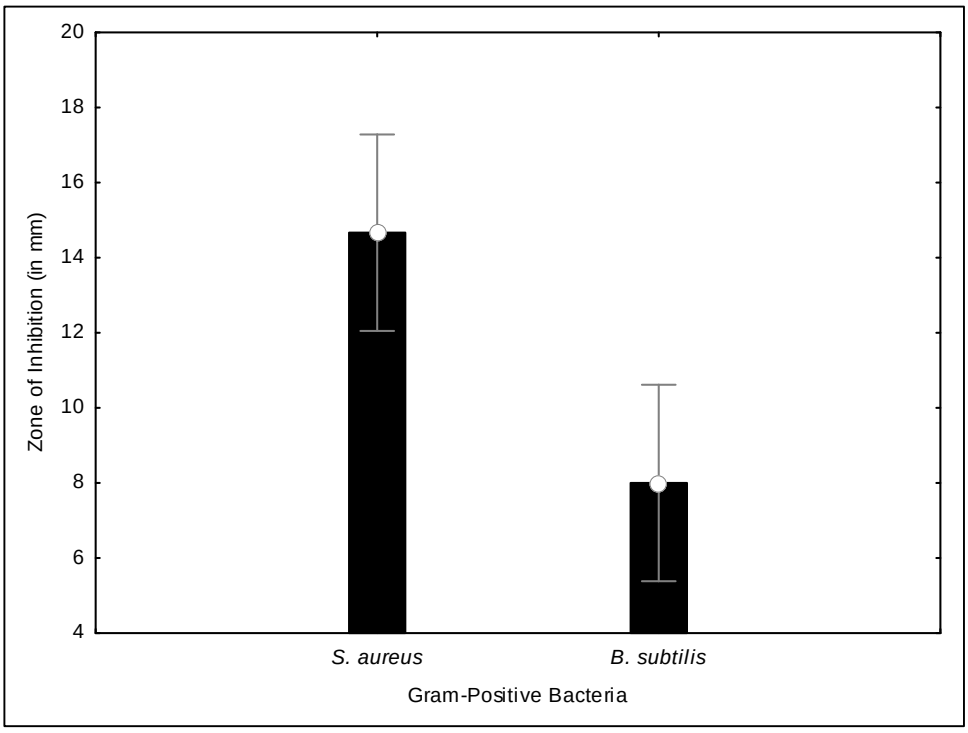

Figure 1. Comparison of the effect of the ethanolic leaf extract of *P. odorata* at 20 mg/ml on Gram-positive bacteria.

Indian Journal of Natural Sciences www.tnsroindia.org.in ©IJONS

Vol.9 /Issue 51 / December / 2018 *International Bimonthly* *ISSN: 0976 – 0997*

RESEARCH ARTICLE

The Activity of Aqueous and Alcoholic Extracts of *Curcuma longa* against Some Types of Bacteria

Ali H. Saliem*

Department of Physiology, Biochemistry and Pharmacology, College of Veterinary Medicine, University of Baghdad, Baghdad, Iraq.

Received: 06 Sep 2018 Revised: 08 Oct 2018 Accepted: 10 Nov 2018

***Address for Correspondence**
Ali H. Saliem
Department of Physiology,
Biochemistry and Pharmacology,
College of Veterinary Medicine,
University of Baghdad,
Baghdad, Iraq.
E-mail: alisaliem977@gmail.com

ABSTRACT

Activities of *Curcuma longa* aqueous and alcoholic extracts were studied against pathogenic *Escherichia coli*, *staphylococcus aureus* and *Streptococcus pyogens* bacterial strains and compared with ampicillin as reference antibacterial by utilizing the method ofwell diffusion in agar.The study reveals that the inhibition range varied with the extraction solvents. Plant extracts prepared in ethanol give more consistent activity comparing to aqueous extracts against bacterial strains. Active materials like curcumin, demethoxycurcum in, bisdemethoxycurcum in flavonoids, and alkaloids make ethanol extract more active against this types of bacteria.Gram negative bacteria and Gram positive bacteria were inhibited by all the extracts even in very little concentrations. Results of this study refers to ability of using active antibacterial ingredient from *Curcuma longa* extracts.

Key words: extracts, Curcuma longa, bacteria.

INTRODUCTION

The using of herbal medicines in the treatment of many disorders increased in general population.Also there is several drugs derived from plants directly or indirectly and used to reduce the hazards of developing microorganisms resistance[1].*Curcuma longa* is an erect perennial herb [1] with tuberous, pulpy, orange, roots have 2 feet in length [2] and belongs to the family Zingiberaceae withpungent and bitter rhizome and widely used in local medicine [3].The root and other parts contains curcumin as the active ingredient, which is a phenolic pigment with yellow color. In the crude extracts of C. longa there is 70 to 76 % curcumin, about 16% demethoxycurcumin and 8% bisdemethoxycurcumin[4] and others like alkaloids and flavonoids[20].It is useful for treating high cholesterol,

diabetes, abdominal pains, menstrual disorder, inflammations, wounds, eczema, jaundice[2].Researches have also investgated anti-inflammatory [5,6,7], antioxidant [8], antitumor [9,10], antibacterial [11], antifungal [12], antiviral [13], anti-spasmodic [14], immunomodulation [15] and hepatoprotective [16] activities. This study was aimed to evaluate the antibacterial properties of aqueous and alcoholic extracts of *Curcuma longa* against *Escherichia coli*, *staphylococcus aureus* and *Streptococcus pyogens.*

MATERIALS AND METHODS

Plants material and extraction

The dried curcuma rhizomes that collected from local markets in Baghdad were ground by electrical grinder to fine powder. This powder was stored in bottles to be used in various extraction procedures. After mixing 100g of the fine powder in one liter of distilled water for 48 hours at 50°C in magnetic stirrer, the solution was filtered by muslin cloth. This was then filtered with Whatman No. 1 to remove all un-extractable matter. The filtrate was concentrated on an incubator. All dried extract samples were stored at 4°C.

Bacterial Isolates

Activation of bacteria was by 10 ml of brain heart infusion agar slantsin screw capped tubes and incubated at 37^{o}C for24 hours, then the brain heart infusion agar were stored at 4^{o}C, and sub -cultured once every 14 daysfor further investigations[17].The strains of pathogenic bacteria obtained from the College of Veterinary Medicine**/** University of Baghdad.

Standard Suspension of Bacteria

The standard McFarland solution Number.0.5 used to determine the mean of the viable bacterial cell numbers/ ml of the stock suspensions by taking 1 milliliters from cultures (brain heart infusion broth) of bacterial suspension and mixed it with 9 ml of pepton water, then taking 1 ml of this suspension and serial ten-fold dilution was prepared [17].

Antibacterial and *Curcuma longa* extracts Concentrations

Ampicillin Stock solution was prepared by adding 0.1 gram to10 ml of distilled water (10mg/ml) and mixed gently, after that(0.2 µg/ µl) were calculated by mixing known amount of the stock solution with distilled water. In other time 0.1 gram with 10 ml of distilled water (10mg/ml), used to prepare stock solution of each extracts,then concentrations of (100, 200 and 300µg**/** µl) were prepared by adding known volume of stock solution with distilled water, bothextracts and antibacterial agent were used in followed steps to determine sensitivity of bacteria.

Sensitivity Test

Agar well diffusion method was used to evaluate the sensitivity of bacterial strains to the aqoues and ethanolic extract of *Curcuma longa* compared with reference agent adopted according to Kavanagh[18] and Perez,*et al.*,[19]. 0.5mlliliter of stock suspensions (1.5 ×10^{8} cfu/ml) of each strains of bacteria was add to 500 ml of sterile Mueller Hinton agar at 45 ^{o}C. Fifteen ml of the inoculated Mueller Hinton agars were put in sterile Petri dishes of each. The agars were left to set for ten minutes to allowagar solidifying and making 6 mm wells in these plates by sterile Pasteur pipette and the piece of agar were removed by sterile forceps, then the wells were filled with (55) microliter of each extracts concentrations (100, 200 and 300µg**/** µl) using micropipette. The plates of this test were then incubated at 37 ^{o}C**f**or (24) hours. The activity was dictated by measuring the diameter of inhibition zone around

wells by millimeter against *Escherichia coli*, *staphylococcus aureus* and *Streptococcus pyogens* at the same time. The observations and standard errors meanes values were tabulated.Ampicillin was the reference to investigate *Escherichia coli*, *staphylococcus aureus* and *Streptococcus pyogens*senstivity. The same procedure which was used for *Curcuma longa* extracts was used for determination the activity of reference agent with concentration (0.2 µg**/** µl).

RESULTS AND DISCUSSION

Curcuma longa aqueous and ethanolic extracts concentrations (100, 200,300µg/µl) and antibacterial (0.2 µg/µl) were used in the method of agar well diffusion, caused zones of inhibition in various degree against *Escherichia coli*, *staphylococcus aureus* and *Streptococcus pyogens*. The inhibition zones diameters were different according to the extracts concentration and antibacterial, the size of inhibition zone proportionally elevated with increasing of agents concentration, table (1) and figure(1). The results showed that *Escherichia coli*, *staphylococcus aureus* and *Streptococcus pyogens* were significantly ($P<0.05$) sensitive to ethanol extract more than aqueous extract in the concentrations (100µg/µl, 200 µg/ µl and 300 µg/ µl) utilized in this study. In this concentrations, there was a significant increase ($P<0.05$) in inhibition zone diameter in *Escherichia coli*, *staphylococcus aureus* and *Streptococcus pyogens* growth as compared with inhibition zones of aqueous extract. This referred to sensitivity of bacteria towards different tested extracts concentrations. Ethanolic, aqueous and antibacterial were appeared to be concentration dependent and this observed significantly in the concentrations 100, 200 and 300 µg/ µl.

Curcuma longa alcoholic and aqueous extracts activity against different bacterial types was demonstrated upongram-negative bacteria and gram-positive bacteria and this may be attributed to the presence of alkaloids and flavonoids [20].The variation in the observed activities of different extracts may be due to varying degrees of solubility of the active constituents in the solvent used and different solvents have different solubility for different phytoconstituents ·Previous studies have revealed that *curcuma* extracts are more affective against Gram positive bacteria than Gram negative in agreement with[21] and may be attributed to presence of lipopolysaccharides (LPS) in the Gram negative bacteria.

CONCLUSIONS

1. The extract of *Curcuma longa* extracts have antimicrobial activity against gram negativebacteria(*Escherichia coli*) andgram positive bacteria (*Streptococcus pyogens staphylococcus aureus*).
2. Antibacterial activity concluded that the alcoholic extracteffective for the three types ofbacteria when compared with aqueous extract and antibacterial reference.
3. Antibacterial activity of *Curcuma longa* extractswas concentration dependent.

Recommendations

1. Study the effect of extractson other bacterial types.
2. Study the effect of extract in animal model.
3. Use another types of extract.

REFERENCES

1. Gopinathan N, M Sai Harish Singh, Chitra K, Uma Maheswara Reddy C. In Vitro Antiplatlet Activity- Ethanolic Extract of Rhizome of Curcuma Longa Linn. Ijbr, 2011; 2 (2)138-142.
2. Sawant RS, Godghate AG. Qualitative Phytochemical Screening of Rhizomes of Curcuma Longa Linn. International Journal of Science, Environment and Technology, 2013; Vol. 2, No 4, 634 – 641

3. Aggarwal BB, Kumar A, Aggarwal MS, Shishodia S. In: Bagchi D, Preus HG. (Eds.) Phytopharmaceuticals in Cancer Chemoprevention,CRC Press: Boca Raton, FL, 2004; 349–387.
4. Cooper TH, Clark JG, Guzinski JA. In: Ho CT, Osawa T, Rosen T (Eds.) Food Phytochemicals for Cancer Prevention IIteas, spices &herbs.American Chemical Soeity: Washington DC, 1994; 23: 231-.
5. Arora RB, Kapoor V, Basu N, Jain AP. Ind. J. Med. Res, 1971; 59(8) :1289-1295.
6. Menon VP, Sudheer AR. AdvExp Med Biol, 2007; 595:105-25.
7. Jacob A, Wu R, Zhou M, Wang P. PPAR Res, 2007; 89369.
8. Adhikari S, Indira-Priyadarsini K, Mukherjee T.J. Clin. Biochem. Nutr, 2007; 40(3): 174–183.
9. 9.Kawamori T, Lubet R, Steele VE, KelloffGJ,Kaskey RB, Rao CV, Reddy BS. Cancer Res.,1999; 59:597-601
10. Bisht S, Feldmann G, Soni S, Ravi R, Karikar C, Maitra A, Maitra A. J. Nanobiotechnology,2007; 5: 3.
11. Negi PS, Jayaprakasha GK, Jagan Mohan Rao L, Sakkariah KK. J. Agric. Food Chem, 1999; 47:4297-4300
12. Apisariyakul A, Vanittanakom N, Budddhasukh D. J.Ethnopharmacol, 1995; 49:163-9
13. Bourne KZ, Bourne N, Reising SF, Stanberry LR. Antiviral Res, 1999; 42:219-226
14. Itthipanichpong C, Ruangrungsi N, Kemsri W, Sawasdipanich J. Med. Assoc. Thai, 2003; 86:299-309
15. Gautam SC, Gao X, Dulchavsky S. Adv. Exp. Med. Biol, 2007; 595:321-41.
16. Park EJ, Jeon CH, Ko G, Kim J, Sohn DH. J. Pharm. Pharmacol, 2000; 52:437-440.
17. Quinn, P.J.; Carter, M.E.; Markey, B. and.Carter, G.R. (2004). Clinical Veterinary Microbiology. Mosby. Edinburgh, London, New York, Oxford and Philadelphia (2nd Ed.),USA.Pp. 21-63.
18. Kavanagh, F. (1972). Analytical Microbiology. F. Kavanagh (ED), Vol:II, Academic press, New York, and London., Pp.11.
19. Perez, C.; Pauli, M. and Bazerque, P. (1990). An antibiotic assay by agar-well diffusion method. *ActaBiologiaeetMedecineExperimentaalis*, 15 (15): 113-115.
20. Ankur Gupta, Surabhi Mahajan and Rajendra Sharma (2015).Evaluation of antimicrobial activity of Curcuma longa rhizome extract against Staphylococcus aureus Biotechnology Reports.6(2015):51-55.
21. Shgufta N.,Sfia .,Saiqa I .F.M., Farah I. and Aamir A.(2010).Antibacterial activity of curcuma longa varieties against different strains of bacteriaPak. J. Bot., 42(1): 455-462, 2010.

Table (1): *Curcuma longa* extractsand reference antibiotic activityin different concentrations against different types of bacteria (diameter of inhibition zone in mm.)

Curcuma longa extract type	Concentration µg/µl	inhibitionZone (mm)		
		E. coli.	***Staph. aureus***	***Streptococcus pyogens***
Alcoholic	100	4.88±0.10 Dc	7.16±0.10 CDb	8.48±0.23 Da
	200	6.09±0.27 Cc	7.68±0.30 Cb	9.22±0.24 Ca
	300	7.12±0.14 Bc	8.90±0.16 Bb	10.70±0.33 Ba
Aqueous	100	4.62±0.21 Dc	5.28±0.18 Eb	6.98±0.08 Ea
	200	4.64±0.09 Dc	5.74±0.12 Eb	8.02±0.17 Da
	300	5.48±0.15 Dc	6.78±0.21 Db	9.12±0.19 Ca
Reference antibacterial	0.2	18.44±0.10 Ac	21.12±0.09 Ab	23.06±0.25 Aa

LSD= 0.61

The different capital letters refer to significant differences between different bacteria (column) at (P<0.05)

The different small letters refer to significant differences between different agents (row) at (P<0.05)

Figure (1):Correlation between concentrations of aqueous and alcoholic extract of curcuma longa and mean of inhibition zone diameters (mm.) against different types of bacteria.

Indian Journal of Natural Sciences www.tnsroindia.org.in ©IJONS

Vol.9 /Issue 51 / December / 2018 *International Bimonthly* *ISSN: 0976 – 0997*

RESEARCH ARTICLE

Geology and Structure Analysis of Shaqlawa – Merawa Area, Northern Iraq Using Remote Sensing, GIS and Field Observations

Mahmood Abdulameer Al-Sadi*, Mustafa Ali Hassan and Shatha Fathi Hassan

Department of Geology, College of Science, University of Baghdad, Iraq.

Received: 08 Sep 2018 Revised: 10 Oct 2018 Accepted: 12 Nov 2018

***Address for Correspondence**
Mahmood Abdulameer Al-Sadi
Department of Geology,
College of Science,
University of Baghdad, Iraq.

ABSTRACT

This study appears GIS techniqueand remote sensing data are matching with the field observation to identify the structural features such as fault segments in the urban area such as the Merawa and Shaqlawa Cities. The use of different types of data such as fault systems, drainage patterns (previously mapped), lineament, and lithological contacts with spatial resolution of 30m was combined through a process of integration and index overlay modeling technique for producing the susceptibility map of fault segments in the study area. GIS spatial overlay technique was used to determine the spatial relationships of all the criteria (factors) and subcriteria (classes) within layers (maps) to classify and map the potential area of geological outcrops and fault zones of the study area. The fault segments map appears that there is well correlation and distribution between fault segments and fault systems in the study area.There are dozens of fault segments which may represent new faults in the area being identified. The presence of these faults is not known from the literature. These fault systems could be active due to the convergent system of the closure of new Tethys and building of Zagros belt. Active or reactivated faults can cause enormous damage to settlement (houses or construction project) areas by rock mass movement along the fault surfaces or bedrock cracks, damage which refers to loss of life or injury, or damage to roads. Furthermore, updated the maps and old study create new ones using new data and techniques and advise the people about the proper sitting of houses and restricting settlement activities in danger areas. GIS models can then yield more accurate estimates of the fault mapping using more data such as geophysical data.

Key Words : Structure Analysis, Shaqlawa-Merawa, Remote Sensing, Field observations.

INTRODUCTION

Faults are represented weakness zones in the brittle rocks of the lithosphere; along the movement zones can take place in response to induced stresses. When faults undergo displacement, depending on the conditions of geology and structural features, strain markers can be formed on the fault surface (DehandSchutter, 2001). The presence of faults in any area is based on displacement of rock layers. But also, most of faults are represented by some geological features such as drainage patterns, lineaments (linear features), and lithological contacts between rock units within the rocks of the area. The presence of fault systems may be indicated by these geologicalfactors.The term lineament was first introduced by (Hobbs, 1904 and Hobbs,1911) who distinguished the existence of linear geomorphic features and interpreted them as surface deformations of zones of weakness or displacement of the earth's crust. Lineaments are linear features on the Earth's surface, usually related to the subsurface phenomena. Generally, lineaments are related to large fracture and fault systems where their directions and numbers give an idea of fracture pattern of rocks (Arlegui and Soriano, 1998). In the recent years, the lineaments have been defined as natural crustal structures that may represent a zone of structural weakness (Walker, 2006).

The drainage pattern, which develops the basin, is strictly dependent on the slope, the nature, and attitude of bedrock and on the regional and local fracture pattern (Travaglia and Dainelli, 2003). Most stream networks are adapted to regional slope and geological structures, picking out the main fractures in the underlying rocks (Morisawa, 1985).The contact between two lithologies can also appear as a linear feature. This contact may appear as a change in drainage pattern across the structural features (Brockmann et al. 1977] or the two units may have different spectral properties (Nguyen and Ho, 1988). Based on the definitions of lineaments, drainage patterns (including pattern the length, spatial distributions), and the lithological contacts between different rock types, the faults could be mapped in the study area. These geological features mostly resemble a fault lines in the area. The most important features in the studied area are the presence of drainage lines patternsand fractures. Lineaments, drainages, lithological contacts, and previous fault lines data are important data and used in this research for fault segments mapping using GIS technique.

With the advent of remote sensing and GIS technique in the geosciences, geological observation and interpretation have entered a new area. Remote sensing technology is very efficient for collecting data. The geographic information system (GIS), supplies a different method for data storage, integration, analysis, and display. The combination of remote sensing and GIS provides an optimum system for various geological observations such as fault systems mapping (Chen, 1992). The benefit of integrating different data and techniques in structural features such as faults identification and analysis made possible using remote sensing and GIS techniques is the ability to identify faults based on their characteristics. Creation and classification of various types of geological features can be carried based on the purpose of the study. Once the preparation, identification and processes of data are complete, geographic information systems (GIS) functionality, such as overlapping the vector and raster spatial analysis, can be employed for structural (fault systems) mapping and analysis using powerful software programs [Elias, 2003].

Generally, Shaqlawa and Merawa areas are located in the southwestern part of Arabian Peninsula, and Both E-W Taurus mountains and NW-SE Zagros Mountains trending in the north and northeastern of Iraq was formed by the closure of the Neo-Tethys and the continental collision of the Arabian Plate with the plates of Turkish and Iranian (Jassim and Goff, 2006). The study area takes a possession of changing in the fold axesdirection. These axes tend to be E-W trending in the north and northwestern part of the study area, while in the southern and southeastern part till the Greater Zab River it becomes corresponding with the NW-SE direction (Fouad,2014) see Figure (1). The High Folded Zone forming an arch shaped belt with different widths. It runs from the Turkish border in the NW Iraq to the Iranian border, in the SE (Al-Kadhimi et al., 1998). The previous works (data) such as geological and structural maps are very limited data, showing a few of fault lines in the study area. For this purpose, mapping of faults may lead to updating these data. In this paper, the using of remote sensing (data processing) and GIS (modeling)

techniques could be helpful tools for mapping of faults, where the different geological features (factors) are taken in the considerations. The aims of this study are to test the integration between the remote sensing and geographic information system (GIS) for detecting the fault segments (fault lines) over the study area and to investigate the ability of this method in giving real results compared to the previous data with respect to the field work.

MATERIALS AND METHODS

Various data were used for fault segment susceptibility mapping (potential fault zones mapping) in the study area. Various image processing and enhancement techniques were applied on different remote sensing data including theLandsat ETM-7 (EnhancedThematicMapper) satellite imagesand SRTM (The Shuttle Radar Topography Mission) to getmaximum information by using different approaches ofextraction methods. The other data used in this study weretopographic maps, geological maps, and field data.During conducting this study, many different softwarepackages were used since there was no single software thatwould process all steps in the analyses.Therefore, the diversesoftware used for the analysis in the current study is PCIGeomatica (version 9.1), ERDAS (version 8.4), and Ilwissoftware (version 3.3).

Geologic setting

The studied area is built up of sedimentary rocks ranging in age from Late Eocene – late miocene, beside various types of Quaternary sediments, the exposed formations are described briefly (from older to younger) (Fig.2):

Aqra-Bekhme Formation (Campanian-Maastrichtian)

This formation exposed at the body of Safin anticline core, its characterized by reef limestone, fore-reef, shoal limestone and associated facies. The formation consists mainly of limestone and dolomite beds at lower part, the limestone is grey and grayish brown in color, hard to very hard, well bedded to massive, the thickness of massive limestone exceeds 30 m the middle part of the formation, but the thickness of layer in well bedded limestone are range from (0.5-1.5 m) (Ismail, 2013). The dolomite is light yellowish brown and grayish brown color, very hard, very fine grained and rarely medium to coarse grain. The depositional environment of Aqra-Bekhme Formation is shallow tropical marine reef and fore reef (Jassim and Goff, 2006).

Shiranish Formation (Maastrichtian)

This formation exposed at the foot of the Safin mountain around the area, the formation consists of two part, the lower is limestone frequently marly or clayey, with gray color and well bedded. This limestone is partly fossilifirous, while other are micritic. Some joints and fractures are commonly seen, sometime filled by clayey or calcareous materials(Ismail, 2013).

Tanjero Formation (Late Maastrichtian)

The formation exposed at the trough of the syncline, the formation consists of clastic which dominate dark yellowish green and olive-green colors. Lithologically the formation is composed of sandstone, claystone, shale and conglomerate, the sandstone that the main constituent is either in form of beds or large concretion ball within claystone and shale, the grain size of the sandstone is medium to coarse (Ismail, 2013).

Kolosh Formation (Paleocene-Early Eocene)

This formation exposed at NW and northern part of Shaqlawa city, consist of clastic rocks which are dark gray to black in color, some rare brown or violet horizons also may occur. Lithologically the formation is composed of shale, claystone, sandstone and siltstone. The shale and claystone are soft papery and fragmented, the mainly thick black or gray clayey soil. The sandstone is dark in color fairly hard to friable, medium to coarse grained. The contact with the underlying formation is unconformable (angular unconformity).

Gercus Formation (Middle Late Eocene)

The formation consists of red clastic rock, which are mainly of claystone, siltstone and sandstone, with a different layer of conglomerate at upper part. The main rock type of this formation is the claystone which is reddish brown, brown in color, soft and fragmented to small chipsets, occasionally the claystone is silty and very rarely sand grains could be seen. The sandstone is less abundant than the claystone and occur at thin beds. The thickness of the formation is varying along Shaqlawa area, at Sork mountain is about 180 m.

Pila Spi Formation (Late Eocene)

The formation forms continuous high ridges with very common flat iron morphology, the formation consists mainly of limestone, which are crystalline, dolomitic and clayey or chalky, the color is white creamy, light gray and yellowish white, well bedded, the thickness of the individual bed ranges from less than 0.4 m to 1.5 m, hard to very hard occasionally the limestone is fossiliferous. Fossils are mainly Foraminifera and Gastropods. The thickness of the formation is about 90m, the lower contact is unconformable with Gercus Formation.

Injana Formation (Late Miocene)

Injanah Formation is exposed in a very small part within the eastern margin of the field area. It consists of alteration of claystone, siltstone and sandstone in coarsening upwards cycles; it reaches 160 m in thickness. The lower contact is not exposed, whereas the upper contact with Muqdadiyah Formation is conformable based on first appearance of pebbly sandstone.

Mukdadiyah Formation (Late Miocene – Pliocene)

Muqdadiyah Formation is exposed along the eastern half part of the Field area. It consists of alternation of sandstone, siltstone and claystone in fining upwards cycles; some of the sandstone layers are pebbly. The thickness of the formation is (500 – 600) m. The lower contact with Injana Formation is conformable based on the first pebbly sandstone bed.

Bai Hassan Formation (Pliocene – Pleistocene?)

Bai Hassan Formation is widely exposed and covers most of the west of field area. It consists of alternation of conglomerate, claystone and sandstone in fining upwards cycles. The thickness of the formation is 1200 m. The lower contact with Muqdadiyah Formation is conformable and marked at the base of the first conglomerate bed.

Quaternary Sediments

Quaternary deposit iron flat Questa-Hogback, ride, cliff and badland are the most dominant geomorphological erosion features, which mainly control by structural and lithological properties, parallel type of drainage pattern are very common. The Quaternary sediments include the following types:

Slope Sediments (Pleistocene – Holocene)

These are developed mainly in the western corner of the studied area in small patches. They usually consist of gravel, which are derived from Bai Hassan Formation. The thickness of these sediments varies from 20 cm to 1.5 m.

Residual Soil (Holocene)

It is developed in small part only and it is mainly of clayey and silty types. The thickness varies from 20 cm to 1.0 m.

Valley Fill Sediments (Holocene)

These sediments are developed in Safin syncline and surrounding valleys. They consist mainly of gravels of different sizes, sand and silt. The thickness ranges from less than one meter to 2 m.

Data Processing

According to this paper the linear featuresdelineation was based on decision of the most appropriatedata, such as drainage patterns, lineament, fault (previouslymapped), and lithological contact layers for mappingof fault segments using GIS.The previous data about the study area including geological, structural, and topographic maps are digitized. Toprepare these maps, first, themaps are converted into a digitalformat by using the scanner. There are some data which wereextracted from data in digital formats, such as Landsat ETMsatellite images and SRTM. Generally, four digital layers (maps) such as drainage patterns,fault (previously mapped), lineament, and lithological contact were prepared and converted into secondary datasuch as drainage buffer, fault buffer, lineament buffer, andlithological contacts buffer layers.These layers were converted into slicing layers with fiveclasses. Each class was determined as 30m. This is becausethese layers were generated fromdifferent data (ETM, SRTM,and previous maps) with different spatial resolutions andscales. Due to this, these layers should be enhanced andresampled (rescaled) to be suitable in resolution for GIS model.

The resolution was selected as 30m for this processbased on the ability of satellite image of 30m spatial resolutionto identify the geological features in the area. Then, slicing layers were converted into weight layers (thematiclayers). Arbitrary classifications are still common; however, themain classification approaches are ranking, natural breaks,equal interval classes, equal area classes, and mean valueand standard deviation intervals (Chung and Fabbri, 1999 andAyalew et al. 2004). Hence, theclassification determines the spatial distribution of bufferingzones or susceptibility (classifying susceptibility) based onequal area classes. Classes (five classes of each weight layer) and their weightvalues are given in Table 1. Each class has a weight to expressthe contribution to the occurrence of fault segments. Theweight value was assigned to be between 1 to 5 (Table 1). These weight layers (maps) were input into GIS model. The resultant map (susceptibility map) was classified into different zones, very low, low, moderate, high, and very high fault susceptibility zones or equal area classes using ranking approach.

Lineament Factor

Lineaments are related to large structuralfractures (Arlegui and Soriano, 1998) and it may represent zones of weakness (Bates and Jackson, 1987). Also, the presence of tectonic structures such as linearfeatures could be important factor in geological hazardoccurrences (Donati and Turrini, 2002).Filtering is useful in image enhancement. An edge enhancing filter can be used to highlight any changes ofgradient within the image features, such as structural lines [Ali and Pirasteh, 2004]. They generated lineament maps and determinedseveral significant structural features.In the recent years, the lineaments have been definedas natural crustal structures that may represent a zone ofstructural weakness (Masoud and Koike, 2006). Landsat ETM-7 satellite data wereused and the first step was to select the band that shouldbe used for lineament extraction (S¨uzen and Toprak, 1998). Visual inspection ofthe individual bands was carried out, based on the abilityto identify features, and band-5 (1.55–1.75 μm) (SWIR) wasselected as shown in Figure 4. And it was stretched linearlyto output range from 0 to 255 (Figure 5), because it is theleast affected band by the scattering, through the travel pathof the long wavelength in the atmosphere.Therefore, it showsa good contrast and better display of geological featurescompared to other bands.The second step was to select the filter type. For thispurpose, different types of filters are tested such as 3 by 3sobel kernel filter, 5 by 5 edge kernel filter, and 7 by 7 edgekernel filter. The 5 by 5 and 7 by 7 edge enhancement filtersgive thicker and less linear areas after threshold application;sobel results in thinner and more linear zones that give thebest result compared with other two filters.

The lineaments detected during the interpretation process were digitized directly on the image on the screen, and the final lineament map was recorded and stored in vector files (Figure 8). There are important points which need to be mentioned and should be followed in relation to the aboveprocedure forlineamentmapping. First, care is needed in the interpretationof the result of such analysis to exclude man-made features;therefore, the final map was screened to remove lineamentsrelated to cultural features such as roads, canals, and fieldplantation boundaries by comparing it with the topographicmaps and geological map of the area. All procedures mentionedabove have been followed during trace lineamentsfrom binary image. The lineament map was prepared and converted intolineament buffer layer and then converted into slicing layerwith five classes. Finally, this layer was converted into weightslayer (Fig.3). The weight value was assigned to be between1 and 5 (Table 2). And, this layer was ready to be input intoGIS modeling.Drainage Patterns Factor.The drainage patternsare apparently being controlled by structural and lithological features in the study area. The lithologic variation has given a rise to different drainage patterns. For example, radial and dendritic drainagepatterns are developed over sedimentary rocks. Moreover, the most important features in the studied area are the presence of drainage patterns and fault systems. It is clearly to see that there is a good relationship between these fault lines and drainage pattern system distribution especially with third and fourth river orders in the area.

Geological features are any alignment of features on satellite images such as the various types recognized including hills held, topographic, drainage, vegetative, and color alignments. Digital elevation models (DEMs) are very useful in aiding the classification of landforms for many purposes such as recognition of drainage patterns (Fig.4). This map was converted into vector layer. The drainage pattern layer (vector layer) was converted into drainage buffer layer and then converted into slicing layer with five classes. This map was converted into weights layer (Figure 4). Theweight valuewas assigned to be between 1 and 5 (Table 1). This layer was ready to be input into GIS modeling.Extraction of topographic feature information from DEMs has become increasingly popular in structural analysis (Ganas et al., 2005). Digital elevation models(DEMs) data were used to observed the trace tectonic features andmapping geologically and topographically defined structuresin many areas (Sarapirome et al., 2002). The Shuttle Radar Topography Mission(SRTM) data were also used to trace of hillshade and mapping of slope(Sarp and Toprak, 2007). The extraction ofnegative system lines (fault lines) from DEM data mostlyresembles drainage lines patterns (Anwar et al., 2010).SRTM radar images with 90m resolution were used toobtain contour line data. This contour data was used to createthe DEM with 30m resolution of the study area. The interpolationand resampling processing techniques were used toconvert the contour line data (polygon) into 30m grid layerand the gridlayerwas converted

into DEM with 30ms patial resolutions.The result of the hillshade and slope map using automatic extraction technique is shown in (Fig5a and b).This technique helps us to extract the drainage patterns over the settlement area, and the topographic maps were used as reference data.

Lithological Contact Factor

Lithological contacts were found in the field, such as bedding planes and lithological contacts between different rock types. The lithological contact layer of the study area (Fig.7) was digitized from the geological map of Shaqlawa area with scale 1 : 250,000. The lithological contact layer (vector layer) was converted into lithological buffer layer and then converted into slicing layer with five classes. And this map was converted into weights layer (Fig.4). The weight value was assigned to be between1 and 5 (Table 1). This map was ready to be input into GISmodeling. Geologic and structural data analysis of the Merawa and Shaqlawa anticlines are commonly adapted from field work and remote sensing measurement data. Inaccessible areas, consider handicap to measure the attitude of the observed formations (i.e., strike and dip). It made the reasons that may not give a good geometrical property of structural features. The study area characterizes by complex structural systems and some areas along the flanks of the anticlines are difficult access. After matching the remote sensing and GIS data with the field measurement data for selected area (A-B) with azimuth 202.73°(Fig.8), we can obtain a geological section of the most important sequences and rock changes, as shown in the figure below.

Evaluation of the Susceptibility Map

Theabove-mentionedtechnique was used to produce the fault segmentsusceptibilitymap from the different data.The result obtained fromthis techniqueneeds tobe evaluatedinsomemanner.Thefirstevaluation was made with respect to the fault map (previousfault map) using GIS overlay technique to determine wherethe fault segments and true faults arematched over the studyarea.During fieldwork, structural data (strike/dip of faults)were collected from 200 stations in the study area(Fig.9). Thesedata were used for the fault segment map evaluation.Thesestations were located in the fault segments map to makewhether there is any correlation between the fault segmentsand the faults collected from the field.

CONCLUSIONS

This study appears that GIS technique and remote sensing data are matching with the field observation to identify the structural features such as fault segments in the urban area such as the Merawa and Shaqlawa Cities. The use of different types of data such as drainage patterns, fault systems, lineament, and stratigraphic contacts with spatial resolution of 30m was combined through a process of integration and index overlay modeling technique for producing the susceptibility map of fault segments in the study area. GIS spatial overlay technique was used to determine the spatial relationships of all the criteria (factors) and subcriteria (classes) within layers (maps) to classify and map the potential area of geological outcrops and fault zonesof the study area. The fault segments map appears that there is well correlation and distribution between fault segments and fault types in the study area. There are dozens of fault segments whichmay represent new fault systems in the studied area being identified. The presence of these faults is not known from the literature. These faults could be active due to the convergent system of the closure of new Tethys and building of Zagros belt. Active or reactivated faults can cause enormous damage to settlement (houses or construction project) areas by rock mass movement along the fault surfaces or bedrock cracks, damage which refers to loss of life or injury, or damage to roads. Furthermore, updated the maps and old study create new ones using new data and techniques and advise the people about the proper sitting of houses and restricting settlement activities in danger areas. GIS models can then yield more accurate estimates of the fault mapping using more data such as geophysical data.

REFERENCES

1. Al-Kadhimi JAM, Sissakian VK, Fattah AS and Deikran DB (1996) Tectonic map of Iraq, 2nd edit., scale 1:1000 000. GEOSURV, Baghdad, Iraq
2. Arlegui L. E. and SorianoM. A.1998, "Characterizing lineaments from satellite images and field studies in the central Ebro basin (NE Spain)," International Journal of Remote Sensing, vol. 19, no.16, pp. 3169–3185.
3. Arlegui L. E. and Soriano, M. A.1998 "Characterizing lineaments from satellite images and field studies in the central Ebro basin (NE Spain)," International Journal of Remote Sensing, vol. 19, no.16, pp. 3169–3185.
4. Bates R. L. and JacksonJ. A.1987, Glossary of Geology, American Geological Institute, Alexandria, Va, USA.
5. Brockmann,C. E. Fernandez,A. BallonR., and Claure,I. I.,1977. "Analysis of geological structures based on landsat-1 images," in Remote Sensing Applications for Mineral Exploration, W.L. Smith, Ed., pp. 292–317, Dowden, Hutchinson and Ross, Strondsberg, Pa, USA.
6. ChenX. 1992, Application of remote sensing and GIS techniques for environmental geologic investigation, northeast Iowa [Ph.D. thesis], University of Iowa, Iowa, Iowa, USA.
7. Chung C. F. and Fabbri,A. G. 1999. "Probabilistic prediction models for landslide hazard mapping," Photogrammetric Engineering and Remote Sensing, vol. 65, no. 12, pp. 1389–1399.
8. Donati L. and Turrini,M. C. 2002 "An objective method to rank the importance of the factors predisposing to landslides with the GIS methodology: application to an area of the Apennines (Valnerina, Perugia, Italy)," Engineering Geology, vol. 63, no. 3-4, pp. 277–289.
9. EliasK. M. M.,2003. "Multiple data set integration for structural and stratigraphic analysis of Oil and Gas bearing formation using GIS," in Proceedings of the Map India Conference, Geology & Mineral Resource, 2003.
10. Fouad, S.F. (2014) Tectonic Map of Iraq, Scale 1 1000000. 3rd Edition, Iraq Geological Survey (GEOSURV) Publications, Baghdad.
11. Ganas,A. Pavlides,S. and Karastathis,V., 2005. "DEM-based morphometry of range-front escarpments in Attica, central Greece, and its relation to fault slip rates," Geomorphology, vol. 65, no. 3-4, pp. 301–319.
12. Hobbs, W. H. 1904 "Lineaments of the Atlantic Border region,"Geological Society, vol. 15, pp. 483–506,.
13. Hobbs, W. H. 1911 "Repeating patterns in the relief and in the structure of the land," Geological Society, vol. 22, pp. 123–176,.
14. Ismail S. O., 2013. Hydrogeology and Hydrochemistry of Shaqlawa Area, Erbil Governorate - Northern Iraq.Ph.D. thesis in College of Science, university of Baghdad.
15. Jassim S. Z. and Goff J. C. 2006. Geology of Iraq .Dolin, Prague and Moravian Museum, Brno. pp: 341.
16. Jassim SZ, Goff JC (2006) Geology of Iraq. Published by Dolin, Prague and Moravian Museum, Brno. 1–345.
17. Masoud A.and KoikeK. 2006, "Tectonic architecture through Landsat-7 ETM+/SRTM DEM-derived lineaments and relationship to the hydrogeologic setting in Siwaregion,NWEgypt," Journal of African Earth Sciences, vol. 45, no. 4-5, pp. 467–477, 2006.
18. Morisawa,M.1985. Rivers, Longman, New York, NY,USA,.
19. Nguyen P. T. and HoD.1988, "Multiple source data processing in remote sensing," in Digital Image Processing in Remote Sensing, J. P. Muller, Ed., pp. 153–176, Taylor and Francis, Philadelphia, Pa, USA.
20. S¨uzen M. L. and Toprak,V. 1998 "Filtering of satellite images in geological lineament analyses: an application to a fault zone in Central Turkey," International Journal of Remote Sensing, vol. 19, no. 6, pp. 1101–1114.
21. Sarapirome,S. Surinkum,A. and Saksutthipong,P., 2002. "Application of DEM data to geological interpretation: Thong PhaPhum area, Thailand," in Proceedings of the 23rd Asian Conference on Remote Sensing (ACRS '02), Kathmandu, Nepal.
22. Sarp G. and Toprak, V. 2007 "An Integrated Lineament Analysis from Satellite Images," in Proceedings of the 28th Asian Conference on Remote Sensing (ACRS '07), Kuala Lumpur, Malaysia.
23. Sissakian, V.K. and Deikran, D.B., 1998. Neotectonic Map of Iraq, scale 1: 1000 000, GEOSURV, Baghdad, Iraq.
24. Walker R. T., 2006 "A remote sensing study of active folding and faulting in southern Kerman province, southeast Iran," Journal of Structural Geology, vol. 28, no. 4, pp. 654

Table1:Parameters and the weight values are given to different factors in the study area.

Classes	Weightvalue
<30m	5
30–90m	4
90–150m	3
150–210m	2
>210 m	1

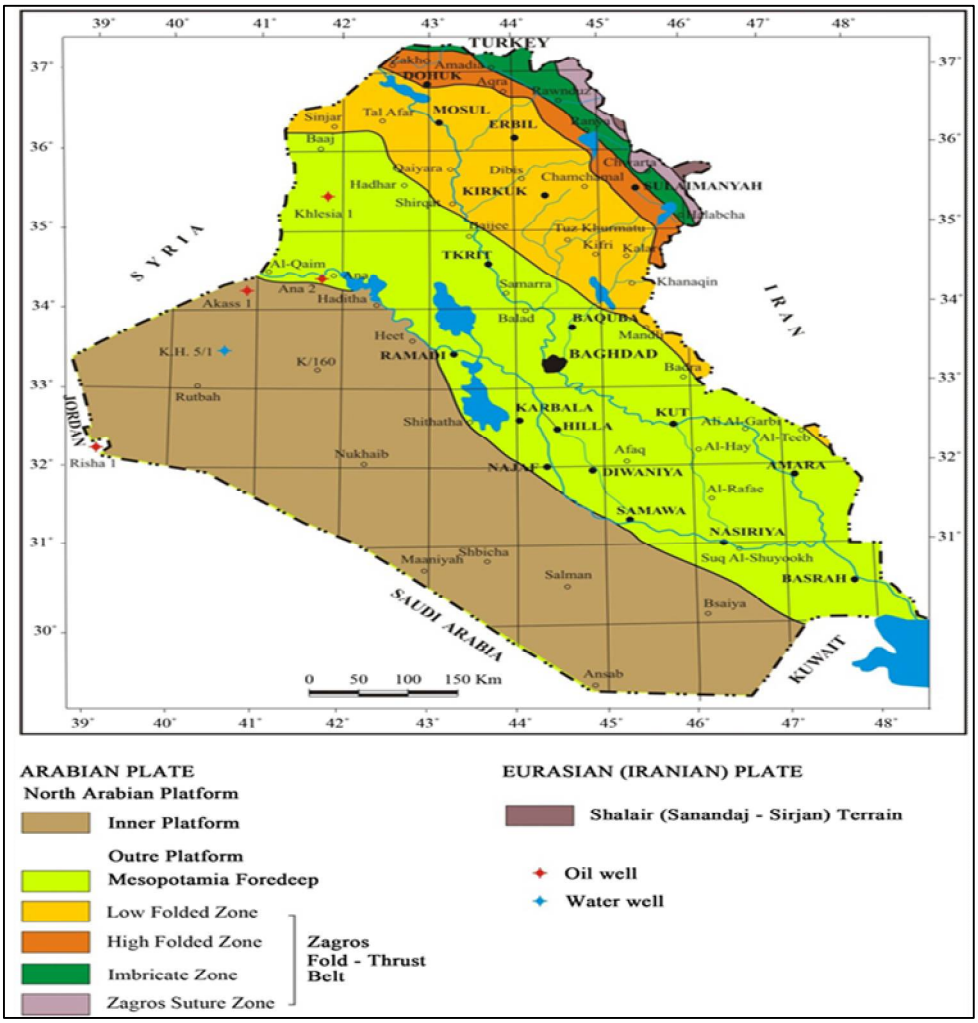

Figure (1) Tectonic Map of Iraq (Fouad, 2014)

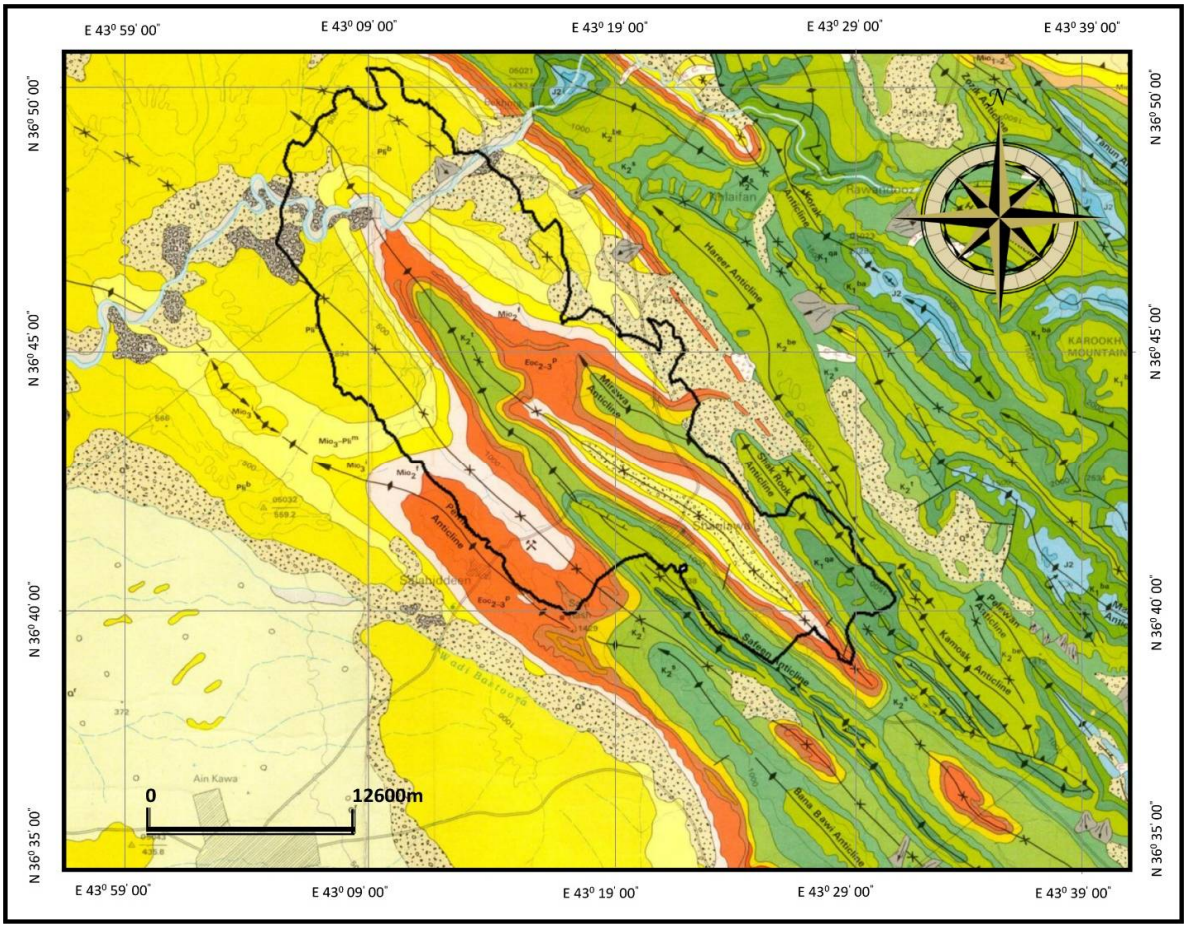

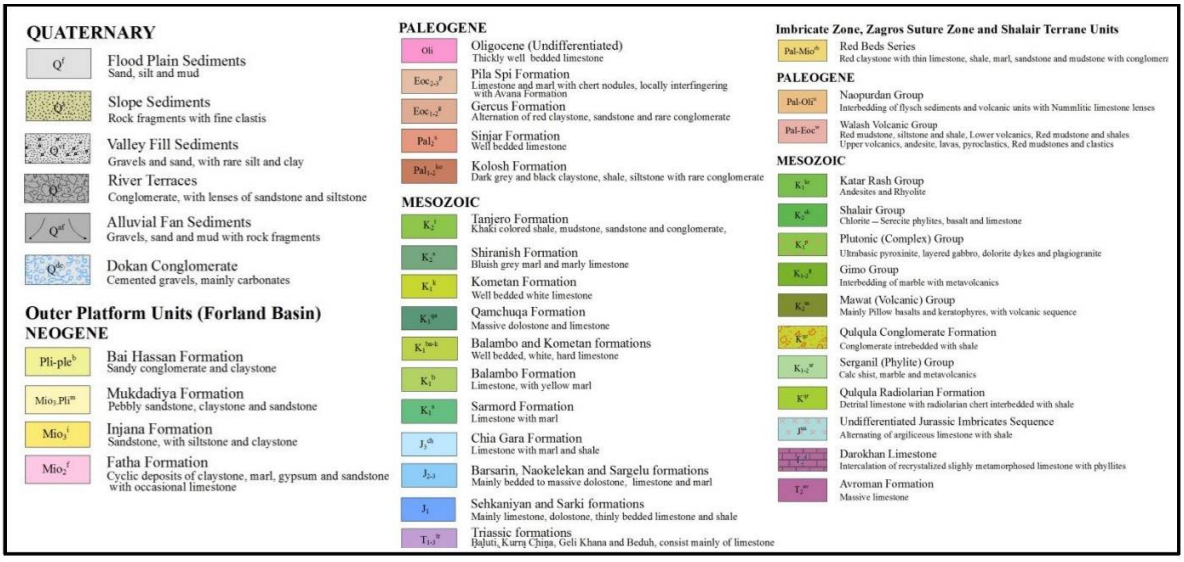

Fig.2.Location map of thestudy area and geologic map according to (Al-Kadhimi et al. 1996)

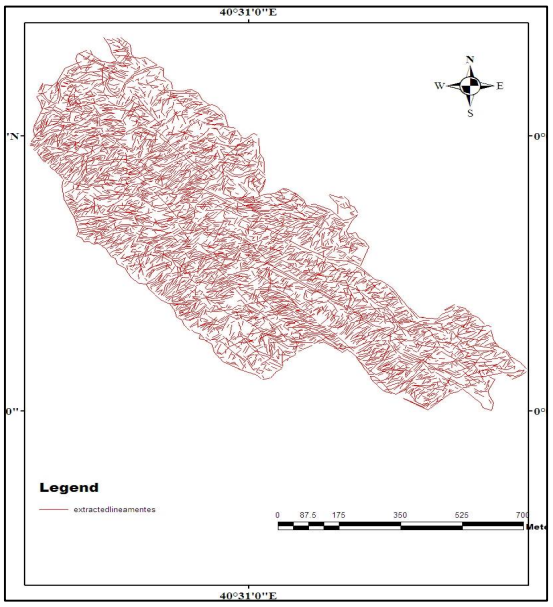

Figure (3) Lineaments extracted from lineament buffer layer and then converted into slicing layer with five classes.

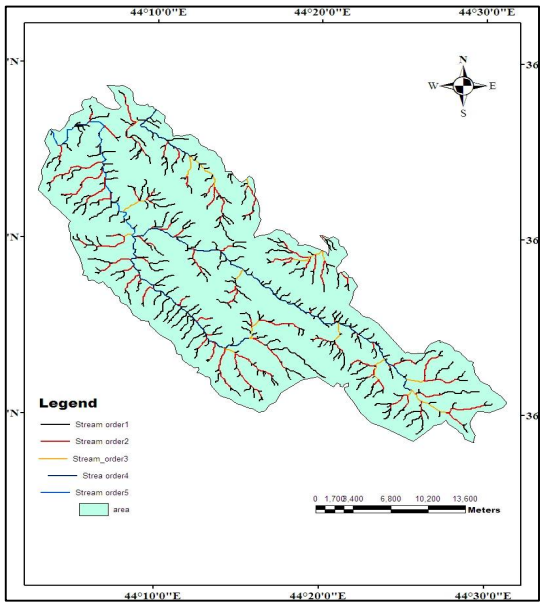

Figure (4) Drainage weight layer and order.

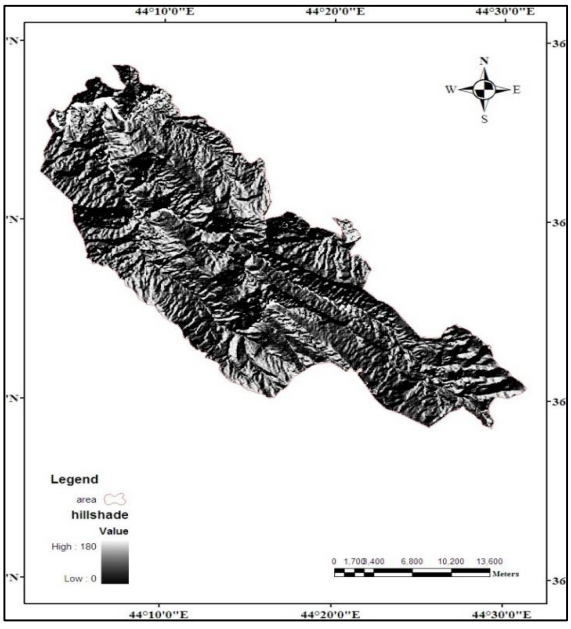

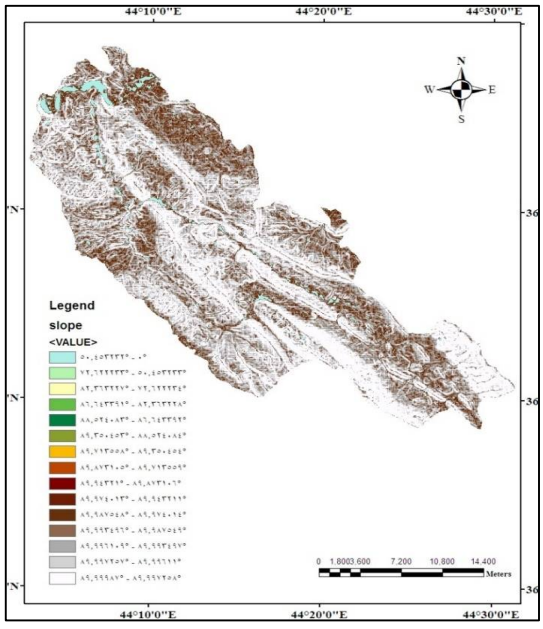

Figure (5):- A. Hillshade map and B. Slope map for the study area.

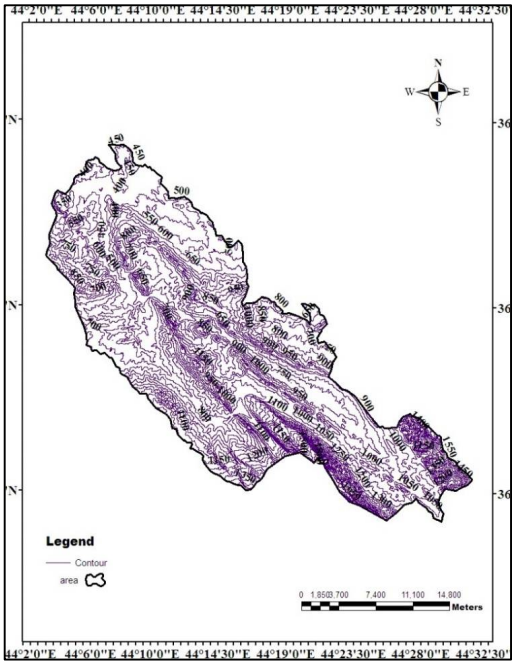

Figure (6):- Topographic map of the study area.

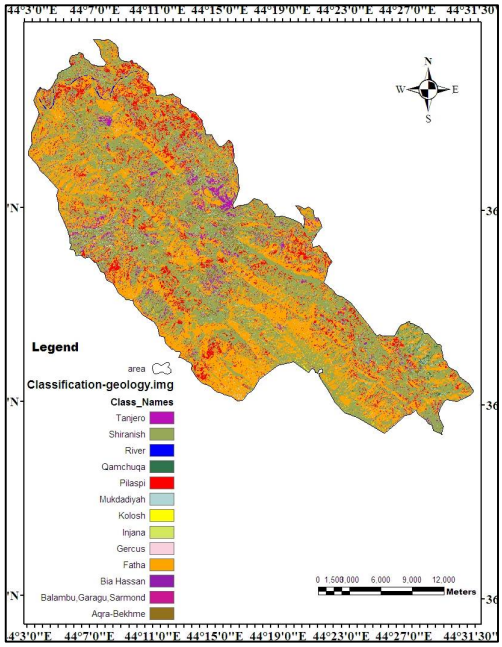

Figure (7):- approximated geological map by remote sensing technique for the study area, showing the checking section A-B.

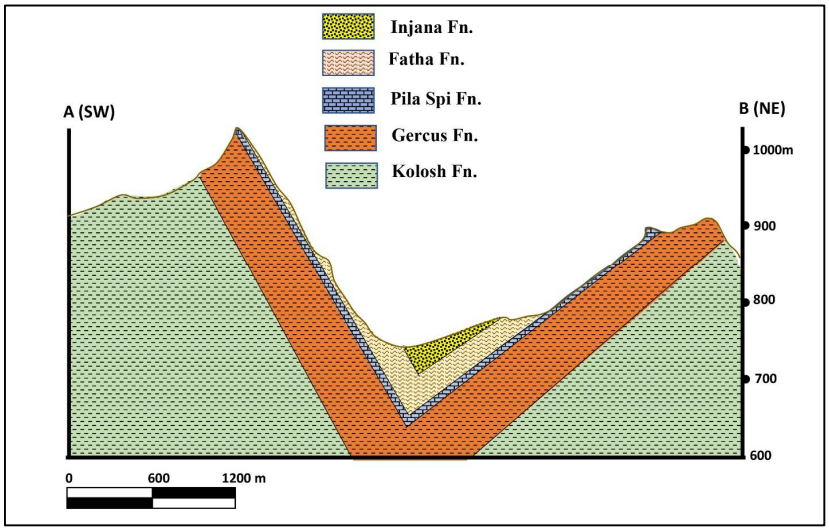

Figure (8):- geological cross section drawing with matching the field and remote sensing data.

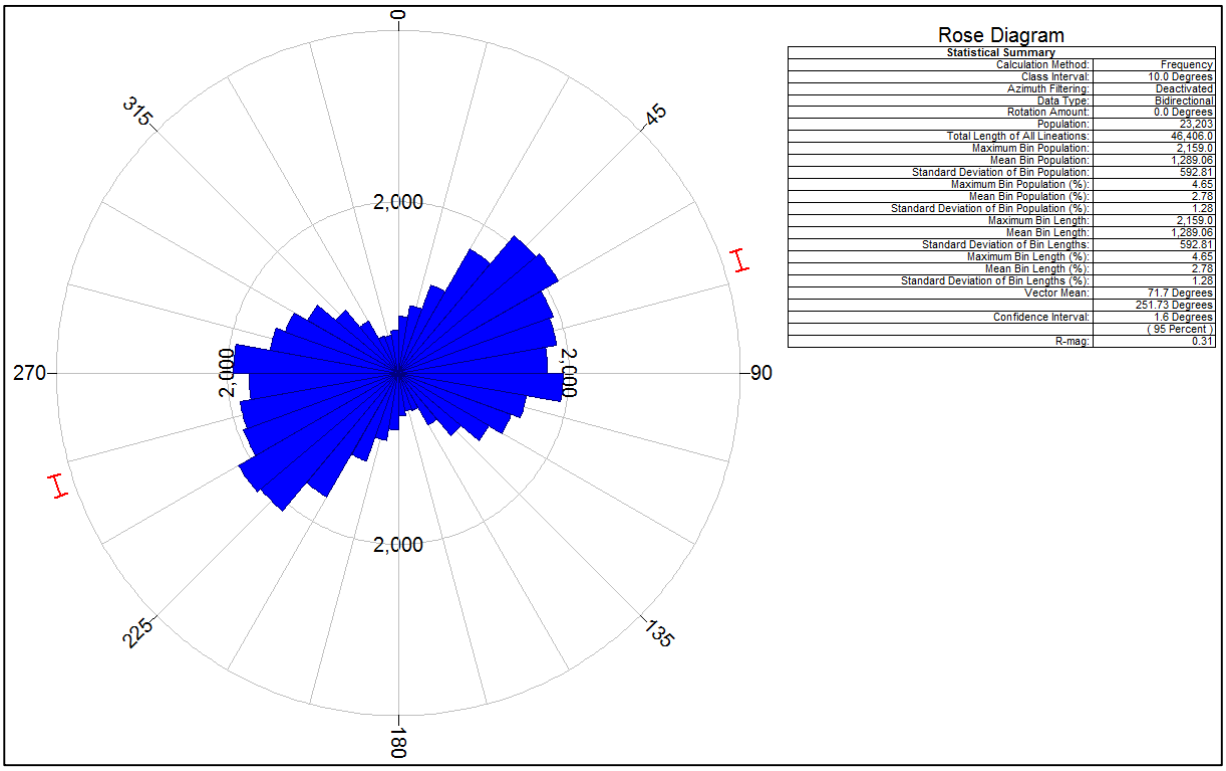

Figure (9):- Rose diagram shows the dip and strike values for the study area .

Indian Journal of Natural Sciences www.tnsroindia.org.in ©IJONS

Vol.9 /Issue 51 / December / 2018 *International Bimonthly* *ISSN: 0976 – 0997*

RESEARCH ARTICLE

Anatomical & Morphometrical Study of the Lacrimal Apparatus in Adult Iraqi Local Breed Cattle *(Bos taurus)*

Nabeel Abd Murad AL-Mamoori[1]*and Mahdi Abdul-Kareem Atyia[2]

[1]Department of Anatomy & Histology, College of Veterinary Medicine, University of Al-Qadisiyah, Iraq.
[2]Department of Anatomy & Histology, College of Veterinary Medicine, University of Baghdad, Iraq.

Received: 05 Sep 2018 Revised: 09 Oct 2018 Accepted: 12 Nov 2018

***Address for Correspondence**
Nabeel Abd Murad AL-Mamoori
Department of Anatomy & Histology,
College of Veterinary Medicine,
University of Al-Qadisiyah, Iraq.
Email: Nabeel.almamorri@qu.edu.iq

ABSTRACT

Used 10 fresh heads of cattle specimens were collected from AL-Diwaniyah abattoir directly after slaughter. The present study was found the lacrimal apparatus in the adult local breed of cattle *(Bos taurus)* consists of glandular part & ducts system convey the secretion. The glandular part was consisting of right & left lacrimal glands, while duct system consists of a number of canals started by an excretory duct, dorsal & ventral puncta, dorsal & ventral lacrimal canaliculi & finally the nasolacrimal duct. The lacrimal glands in was situated on the dorsolateral aspect of the eyeball, elongated, lobulated, flattened, brown in color. Each gland was consist of two parts main part (body) & accessory part (appendage (.The mean weight, length, width, thickness & volume of a body the right lacrimal gland was 4.055±0.197gm, 37.232±1.447mm, 23.112±0.966mm, 7.746±0.345mm & 4.083±0.153cm3 respectively, while the mean weight, length, width, thickness & volume of the body the left lacrimal gland was 4.358±0.222gm, 37.207±1.622mm, 24.053±0.523mm, 8.043±0.333mm & 4.166±0.247cm3 respectively. There were two puncta can be observed in the medial canthus of the eyeball. The two puncta lead into two cylinders, narrow & short canaliculi (dorsal & ventral). The lacrimal sac consists from joined the lacrimal canaliculi together in the distal end to form the small a dilated lacrimal sac.The nasolacrimal ducts in cattle represent last part of the lacrimal apparatus. It was started from the distal end of the lacrimal sac. The mean total length of the right & left nasolacrimal duct in cattle was 185.268±7.602mm & 190.008±5.731mm respectively.

Keywords: cattle, morphology, lacrimal apparatus, lacrimal gland, nasolacrimal duct.

INTRODUCTION

A cattle is most important types of ruminants, which provide meat, milk and leather. Many of them are spread in different region of the country (1). The eyes were the sensory organ responsible for eyesight. It is well protected from damage by the bone which formed the orbit. It has accessory structures important in the process of maintaining eye, including the lacrimal gland, 3rd eyelid gland (2(.The lacrimal apparatus group of structures that production & drain away tears. It consist of lacrimal gland, lacrimal puncta, lacrimal canaliculi, lacrimal sac, nasolacrimal duct & nasal punctum. The lacrimal gland is pink in color, lying on the dorsolateral aspect of eyeball. It releases seromucous secretions by a number of ducts onto the surface of the eyeball which are responsible for the protection the eye & conjunctiva from drying & also nourishes & lubricates. The duct system that conveys the lacrimal fluid after it has washed over the eye, into the nasal cavity (2; 3 & 4) In bovine, caprine, ovine, camel & equine except canine, swine, feline the lacrimal gland was situated within a special division of the periorbital between the dorsolateral part of the eyeball & the supraorbital process of the frontal bone and the frontal process of the zygomatic bone. The major part of the gland was covered by the supraorbital & frontal processes dorsally, whereas a small caudal part (about 1cm wide) was covered only by adipose tissue, fascia and skin in canine and feline the orbital cavity shallow due to the absence of frontal and zygomatic process (5 & 6). In most of the domestic mammalian the two lacrimal ducts beginning with a small dorsal & ventral openings, the lacrimal punctum located near to the medial canthus of the eyes. The puncta of the camel are absent (4;7; 8 & 9)

MATERIALS AND METHODS

Morphological and biometrical study

For anatomical & morphometric studies used 10 fresh heads specimens were collected from AL-Diwaniyah abattoir directly after slaughtering of the cattle by dislocation of heads from the carcasses at the level of atlanto-occipital joint. The first step clean the specimens by washed with tap water & kept in clean plastic containers. It was transported into the laboratory to record the required relationship of the apparatus & biometric measurement. The second step should be carefully dissecting the specimen by remove the skin, muscles & bone to exposure the lacrimal apparatus (lacrimal gland & duct system). For studying the lacrimal gland should be dissected the superior orbital skin, zygomatic process of the frontal bone & frontal processes of zygomatic bone. The periorbital connective tissues were carefully dissected & lastly the glands were carefully detached.

To study the duct system that consist of lacrimal duct, lacrimal sac & nasolacrimal duct should be dissected superior maxillary & incisive skin & muscle, & made longitudinal incision to divided the head into symmetrical parts. After that dissected to remove the nasal concha to exposure the course of nasolacrimal duct. Injected the nasolacrimal duct with the red colored latex substance (2 : 3 latex with ammonia mixed with carmine stain) to exposure the duct. We using blunt needle & syringe. Glacial acetic acid was used with cotton to prevent any leakage of latex from the damaged duct by pressing on the site of oozing. Then the specimens were immersed in 10% formalin for 24 hours to fixing the tissue & setting of the injected material Finally described the morphological features including the shape, location, relationship & color of the lacrimal apparatus. Record the measurements by using vernia, measurement tape, ruler & sensitive balance.

- Weight, length, width, thickness & volume of lacrimal gland.
- Length & diameter of nasolacrimal duct.

RESULTS

Anatomical study

The current study was found in the lacrimal apparatus in the adult local breed of cattle *(Bos taurus*) consists of glandular part & ducts system convey the secretion. The glandular part was consist of right & left lacrimal glands. The duct system consists of a number of canals started by an excretory duct, dorsal & ventral puncta, dorsal & ventral lacrimal canaliculi & finally the nasolacrimal duct.

Lacrimal glands

The lacrimal glands in was situated on the dorsolateral aspect of the eyeball. Where was above dorsal rectus muscle & extend on the lateral rectus muscle. It was extended caudally along the medial surface of the zygomatic process of the frontal bone & frontal process of the zygomatic bone & the gland confined between these two bones of the orbit & the eyeball. (Fig.1). The lacrimal glands were elongated, lobulated, flattened with an irregular outline. It had light brown in color, covered by a capsule & surrounded by adipose tissue. Each gland was consist of two parts main part (body) & accessory part (appendage). It has two surfaces (Dorsal & ventral), two extremities (cranial & caudal extremities) & two borders (medial & lateral borders). The dorsal surface was convex opposite the inner surface of the orbit so that it takes the shape of the inner surface of it. While the ventral surface was concave opposite the convexity of dorsal (upper) surface of the eyeball & take the fitting shape of it (Fig.1, 2 &3).

The body of lacrimal gland was flattened oval in shape & the cranial end narrowing than the caudal end (Fig.2 &3). The mean weight, length, width, thickness & volume of body the right lacrimal gland was 4.055±0.197gm, 37.232±1.447mm, 23.112±0.966mm, 7.746±0.345mm & 4.083±0.153cm^3 respectively, while the mean weight, length, width, thickness & volume of body the left lacrimal gland was 4.358±0.222gm, 37.207±1.622mm, 24.053±0.523mm, 8.043±0.333mm & 4.166±0.247cm^3 respectively (Table 1). The appendage of lacrimal gland was cylinder elongated shape with irregular outline & extend on the lateral rectus muscle. It has dorsal & ventral surfaces, medial & lateral borders & cranial & caudal extremities (Fig. 2&3). The mean weight, length, width, thickness & volume of appendage of the right lacrimal gland was 0.983±0.072gm, 35.108±1.699mm, 11.95±0.351mm, 4.53±0.303mm & 1.083±0.083cm^3 respectively, while the mean weight, length, width, thickness & volume of appendage the left lacrimal gland was 1.105±0.058gm, 35.377±2.392mm, 13.908±0.828mm, 4.098±0.333mm & 1.166±0.105cm^3 respectively (Table 2).

Excretory ducts in cattle

The main macroscopic excretory ducts origin from the lacrimal glands to convey the secretion into the superior conjunctival fornix in the lateral canthus of the eyeball. (Fig.4&5). In cattle, the excretory ducts origin from the lateral borders of the middle area of the body of lacrimal glands. The mean number of ducts were 6-7 take slit-like opening & it has the same color of the conjunctival mucosa (Fig.4&5).

Lacrimal puncta in cattle

The puncta were slit-like opening & take grayish black in color. There were two puncta can by observed in the medial canthus of the eyeball (Fig.6). In cattle the diameter & distance of punctum from medial canthus of right & left dorsal puncta were 2.3166±0.089mm, 2.163±0.090mm, 5.688±0.804mm & 5.828±0.626mm respectively, while the right & left ventral puncta were 2.246±0.089mm, 2.308±0.157mm, 6.23±0.626mm & 5.688±0.804mm respectively (Table 3).

Lacrimal ducts (canaliculi) in cattle

The lacrimal ducts were started from the lacrimal puncta in the medial canthus of the eyeball & reached into the lacrimal sac. The two puncta lead to two cylinder, narrow & short canaliculi (dorsal & ventral). The mean length of the right & left dorsal lacrimal canaliculi were 15.14±1.082mm & 14.55±1.849mm respectively, while the right & left ventral lacrimal canaliculi were 14.935±0.752mm & 14.773±1.321mm respectively (Table 3).

Lacrimal sac in cattle

In cattle the two lacrimal canaliculi were joined together in the distal end to formation the small a dilated lacrimal sac. It was located in the small depression the lacrimal fossa of the lacrimal bone. It was continous from the distal end with nasolacrimal duct. The mean length of right & left lacrimal sac were 23.603±2.985mm & 16.583±3.314mm respectively (Table 3).

Nasolacrimal ducts in cattle

The nasolacrimal ducts in cattle represent last part of the lacrimal apparatus. It was started from the distal end of the lacrimal sac. It runs dorsally & distally to lacrimal sac. It extends ventrally on the medial side of the lacrimal, maxillary & incisive bones. The nasolacrimal duct runs on the medial side of the lateral wall of the nasal cavity (Fig.7). The mean total length of the right & left nasolacrimal duct in cattle was 185.268±7.602mm & 190.008±5.731mm respectively. The nasolacrimal duct divided into three parts according to course of ducts (Fig.7). The proximal part pass through the osseous canal in the lacrimal & maxillary bone. It could be observed after removed the dorsal & ethmoid (middle) nasal concha. The mean length of the right and left the proximal part in cattle was 55.081±4.096mm & 52.806±3.264mm respectively. The middle part was consisting of only mucous membrane & extends into the junction with the skin of the vestibule of the nasal cavity. It passes ventrally to the ventral nasal concha & covered by it. It could seem after removed the ventral nasal concha. The mean length of the right & left the middle part in cattle was 95.008±2.122mm & 94.03±3.342mm respectively.

The distal part was referred to cutaneous part supported by nasal cartilage. It was shorter part of the nasolacrimal duct ended by the external orifice of the nasolacrimal duct. The mean length of the right & left the distal part in cattle was 41.28±3.208mm & 45.44±2.117mm respectively. In cattle, the external orifice of the nasolacrimal duct has oval shape & located ventral to the alar fold of the ventral nasal concha. The mean diameter was 2.47±0.154mm & 2.185±0.168mm, also the mean distance of nasolacrimal orifice from nostrils opening (external nasal opening) was 16.166±1.728mm, 15.395±1.066mm in right & left side respectively (Table 3).

DISCUSSION

In the current study show the lacrimal apparatus in the adult local breed of cattle consists of glandular part & ducts system. This finding agreement with (10). But disagreement with (11 & 12) described the lacrimal apparatus in one humped camel was consists lacrimal gland & excretory duct, lacrimal sac, nasolacrimal duct & lack the two punctum. The lacrimal glands in cattle situated on the dorsolateral aspect of the eyeball. Our results accordance with the findings (4;10;13; & 14) in buffalo, sheep & dog. The lacrimal glands in cattle take light brown in color, covered by a capsule & surrounded by adipose tissue. This results accordance with (6;15;16;17&18) in Zavot fetuses, Bactrian camels, camel, goat, donkey & Lori sheep. Whereas disagreement with (19) described the lacrimal gland in American bison and cattle were pale yellowish in color & (13) show the lacrimal gland of the Philippine water buffalo was pink to red in color. (20 &21) explain in buffalo was pale yellow. We believe the cause of discoloration of the lacrimal glands may be due to differing the species of animals & the amount of blood remaining in the blood vessels that supply the gland or delayed time took the samples for anatomical study after slaughtering the animal. The lacrimal

glands in cattle was elongated, lobulated, flattened oval in shape, while the appendage was cylinder elongated. It was consist of two parts main part. This results accordance with (4;8;9;15;16;19;22 &23). While disagreement with (24) the lacrimal gland in European bison was uniform & undivided. (25) explain the lacrimal gland in goat & sheep consist one compact part undivided. Also (26) described the lacrimal gland in alpaca was uniform & undivided gland. This difference due to species of animal.

The recent results in cattle revealed that the mean weight, length, width, thickness & volume of body the right lacrimal gland disagreement with (27) explain in bovine the mean width and length of the lacrimal gland was 35 & 65 mm respectively. The current results find the excretory ducts of lacrimal gland in cattle had a slit-like opening & take the same color of the conjunctival mucosa of upper eyelids. This finding agreement with (12 & 14). But the disagreement with (12 & 28) in camel found that the excretory ducts of lacrimal gland difficult to find but were detected by black color imparted to them by melanin. In the present study seen the mean number of ducts in cattle was 6-7 take slit-like opening. This results agreement with (29) found the excretory duct of the lacrimal gland in porcine was 7 main excretory ducts responsible for transporting tear to the eye surface. But disagreement with (6) reported the lacrimal gland in camel was possessed 3 excretory ducts origin from the ventral surface of the gland.
The current study finds that the puncta in cattle was two slit-like opening & takes grayish black in color. This result was compatible with (10;18;20; 21 & 25) show most mammals had two lacrimal puncta of upper & lower eyelids in the medial canthus of eyes & the colour of puncta differs. But disagreement with (9;11;12 & 30) explains the lacrimal puncta in camel was absent & the lacrimal ducts start blindly.

We found the mean diameter & distance of punctum from medial canthus nearly accordance in some measurements & differ in other with (25) reported that in goat the diameter & distance of punctum from medial canthus of right & left dorsal puncta were 1.21±0.13mm, 1.08±0.06mm, 4.94±0.22mm & 4.81±0.27mm respectively, while the right & left ventral puncta were 1.54±0.15mm, 1.50±0.14mm, 3.63±0.16mm & 3.75±0.16mm respectively. The lacrimal ducts in cattle were started from the lacrimal puncta in the medial canthus of the eyeball & reached into the lacrimal sac. This was similar to that explained by (18& 20) in buffalo & Lori sheep. Whereas disagreement with (9;11& 18) explain that most of the domestic mammals have two lacrimal ducts starts by a small upper & lower openings, but in camel, the lacrimal ducts start blindly. In the present study show in cattle the two lacrimal canaliculi joined together in the distal end to form the small a dilated lacrimal sac. This finding similar with (10;18;20;21&25) in goat, buffalo & Lori sheep. The nasolacrimal ducts in cattle represent last part of the lacrimal apparatus. It was started from the distal end of the lacrimal sac. This finding agreement with (4;8 & 21). The mean total length of the right & left nasolacrimal duct in cattle was 185.268±7.602mm & 190.008±5.731mm respectively this finding disagreement with (10) described the total length left & right nasolacrimal duct in buffalo was about 232 mm & 235 mm. (20) show the mean length of nasolacrimal 263mm.

REFERENCES

1. AL-Sadi, H I. Animal wealth in Iraq and means of improving it. University of Mosul press: 203-204, 1980.
2. Akers, R M and D M Denbow. Anatomy and physiology of domestic animals. 2nd Ed. Wiley Blackwell, 2013.
3. Pasquini, C, T Spurgean and S Pasquini. Anatomy of domestic animal. 7th Ed. SUDZ publishing, 1997.
4. Dyce, K M, W O Sack and C J G Wensing. Textbook of Veterinary 4th edition. Philadelphia. London. New: W.B. Saunders Company, 2010.
5. Bacha, W J and L M Bacha. Color atlas of veterinary histology. 2nd Ed. Maryland, USA: Lippincott Williams & Wilkins, 2000.
6. Alsafy, M A. "Comparative morphological studies on the lacrimal apparatus of one humped camel, goat and donkey." Journal of Biological Sciences 10(3) 2010: 224-230.
7. May, N D. The anatomy of the sheep. 3rd Ed. Australia: Brisbone Australia university of queens land press, 1970.

8. Sisson, S and J D Grossman. The anatomy of domestic animals. Philadelphia. London. Toronto: W.B. Saunders Company, 1975.
9. Saber, A S and F M Makady. "Anatomy and clinical studies on the lacrimal system in camel (Camelus dromedarius)." Assuit Veterinary Medical Journal 19 1987: 12-17.
10. Al-Bayati, Mustafa kamal. Aanatomical and histological study of the lacrimal gland and nasolacrimal apparatus in indigenous buffalo (bubalus bubalis). thesis: vet. Med. Baghdad university, 2015.
11. Abdalla, O, M F Fahmy and I Arnactovic. "Anatomical study of the lacrimal apparatus of the one-humped camel." Acta. Anat 75 1970: 638-650.
12. Elmahadi, Huyam Elmahadi Mustafa. Studies on morphological and histochemical seasonal changes on the lacrimal apparatus of the One-humpedcamel (Camelusdromedarius). Thesis: Vet Me Sudan University of Science and Technology, 2017.
13. Maala, Ceferino P, Ruth A Cartagena and Grace D Ocampo. "Macroscopic, histological and histochemical characterization of the lacrimal gland of the Philippine Water Buffalo (Bubalus bubalis)." Philipp. J. Vet. Med 2 44 2007: 69-75.
14. AL-Obeady, Walaa Fadil. Morphometrical and histochemical comparative study of lacrimal gland and conjunctival glands between dog (Canis familaris) and ram (Ovis aris). Thesis: Vet Med University of Baghdad, 2016.
15. Aslan, Kadir, et al. "Gross anatomy of the lacrimal gland (gllacrimalis) and its arterial vascularization in the fetus of zavot-bred cattle." Kafkas Univ. Vet. Med. J 1 11 2005: 47-49.
16. Ibrahim, Z H, A B Abdalla and D I Osman. "A gross anatomical study of the lacrimal apparatus of the camel (Camelus dromedarius)." Journal of Science and Technology 9 2006: 1-8.
17. Chengjuan, G, et al. "Anatomical and histochemical characteristics of the lacrimal glands in bactrian camels." Chinesejournalof Anatomy 2008.
18. Abbasi, Mohsen , Hamid Karimi and Ahmad Gharzi. "Preliminary anatomical and histological study of lacrimal gland in Lori sheep." Journal Veterinary Science & Technology 1 5 2014: 154-158.
19. Pinard, C L, et al. "Normal anatomical and histochemical characteristics of the lacrimal glands in the american bison and cattle." Anat. Histol. Embryol 32 2003: 257-262.
20. Ali, mohammad Abbas. Anatomical and histological study of local buffalos eye (Bubalus bubalis). thesis: Vet Med University of Basrah, 2009.
21. Shadkhast, M and A S Bigham. "A Histo-Anatomical study of dorsal lacrimal gland in iranian river buffalo." Iran Online Veterinary Journal 1 5 2010: 50.
22. Getty , R. The anatomy of domestic animals. Philadelphia. London. UK: W.B. Saunders Company, 1975.
23. Budras, K D, et al. The atlas of bovine anatomy. 2nd Ed. Schlutersche.Germany: Hans-BOckler Allee, 2011.
24. Kleckowska-Nawrot, Joanna, et al. "Histology, histochemistry and fine structure of the Harderian gland,lacrimal gland and superficial gland of the third eyelid of the Europeanbison, Bison bonasus bonasus (Artiodactyla: Bovidae)." Zoologia 5 32 2015: 380-394.
25. Daryuos, M M and N S Ahmed.Comparative morphological and morphometrical study of lacrimal apparatus of Awasi sheep and black goat." AL-Qadisiyah Journal of Veterinary Medicine Sciences 11 1 2012a: 123-133.
26. Klećkowska-Nawrot, J, et al. "Histological, histochemical and fine structure studies of the lacrimal gland and superficial gland of the third eyelid and their significance on the proper function of the eyeball in alpaca (Vicugna pacos)." Folia Morphol Via Medica 2 4 2015: 195-205.
27. Diesem, D V. "Gross anatomic structure of equine and bovine orbit and its contents." American Journal of Veterinary Research 29 1968: 505-510.
28. Ibrahim, Z H, A B Abdalla and D I Osama. "A gross anatomical study of the lacrimal apparatus of the camel (Camelus dromedarius)." Sudan Journal of science and technology 2006: 1-8.
29. Henker, R, et al. "Morphological features of the porcine lacrimal gland and its compatibility for human lacrimal gland xenografting." Journal pone 9 8 2013: 40-46.
30. Sadegh, Amin Bigham, et al. "Lacrimal apparatus system in One-humped camel of iran (Camelus dromedarius): Anatomical and radiological study." Iranian Journal Of Veterinary Surgery Vol.: 2 No.: 5 2007: 75-80.

Table 1. Macroscopic parameters of the body lacrimal gland in cattle (Mean ±SE).

Parameter	Side	Cattle
Weight	Right side	4.055±0.197gm
	Left side	4.358±0.222gm
Length	Right side	37.23±1.447mm
	Left side	37.21±1.622mm
Width	Right side	23.11±0.966mm
	Left side	24.05±0.523mm
Thickness	Right side	7.747±0.345mm
	Left side	8.044±0.333mm
Volume	Right side	4.083±0.153ml
	Left side	4.167±0.247ml

Table 2. Macroscopic parameters of the appendage part of lacrimal gland in cattle (Mean ±SE).

Parameter	Side	Cattle
Weight	Right side	0.983±0.072gm
	Left side	1.105±0.058gm
Length	Right side	35.108±1.699mm
	Left side	35.377±2.392mm
Width	Right side	11.950±0.351mm
	Left side	13.908±0.828mm
Thickness	Right side	4.53±0.303mm
	Left side	4.098±0.382mm
Volume	Right side	1.083±0.083ml
	Left side	1.166±0.105ml

Table 3. Macroscopic parameters of the duct system in cattle (Mean ±SE).

Parameter	Side	Cattle
Diameter of dorsal punctum.	Right side	2.317±0.089mm
	Left side	2.163±0.090mm
Diameter of ventral punctum.	Right side	2.247±0.089mm
	Left side	2.308±0.157mm
Distance of dorsal punctum to medial canthus.	Right side	5.828±0.626mm
	Left side	5.688±0.804mm
Distance of ventral punctum to medial canthus.	Right side	6.230±0.470mm
	Left side	5.576±0.509mm
Length of dorsal lacrimal canaliculi.	Right side	15.14±1.082mm
	Left side	14.55±1.849mm
Length of ventral lacrimal canaliculi.	Right side	14.94±0.752mm
	Left side	14.77±1.321mm
Length of lacrimal sac.	Right side	23.6±2.985mm
	Left side	16.58±3.314mm
Length of nasolacrimal duct.	Right side	185.3±7.60mm
	Left side	190.01±5.73mm
Length of proximal part of nasolacrimal	Right side	55.08±4.096mm

duct inside of bone canal.	Left side	52.807±3.26mm
Length of middle part of nasolacrimal duct (mucous part).	Right side	95.01±2.122mm
	Left side	94.03±3.342mm
Length of distal part of nasolacrimal duct from mucous part to nasolacrimal opening.	Right side	41.28±3.208mm
	Left side	45.44±2.11mm
Diameter of nasal punctum of nasolacrimal duct.	Right side	2.47±0.154mm
	Left side	2.185±0.16mm
Distance of nasal punctum from nostrils opening.	Right side	16.17±1.728mm
	Left side	15.398±1.06mm

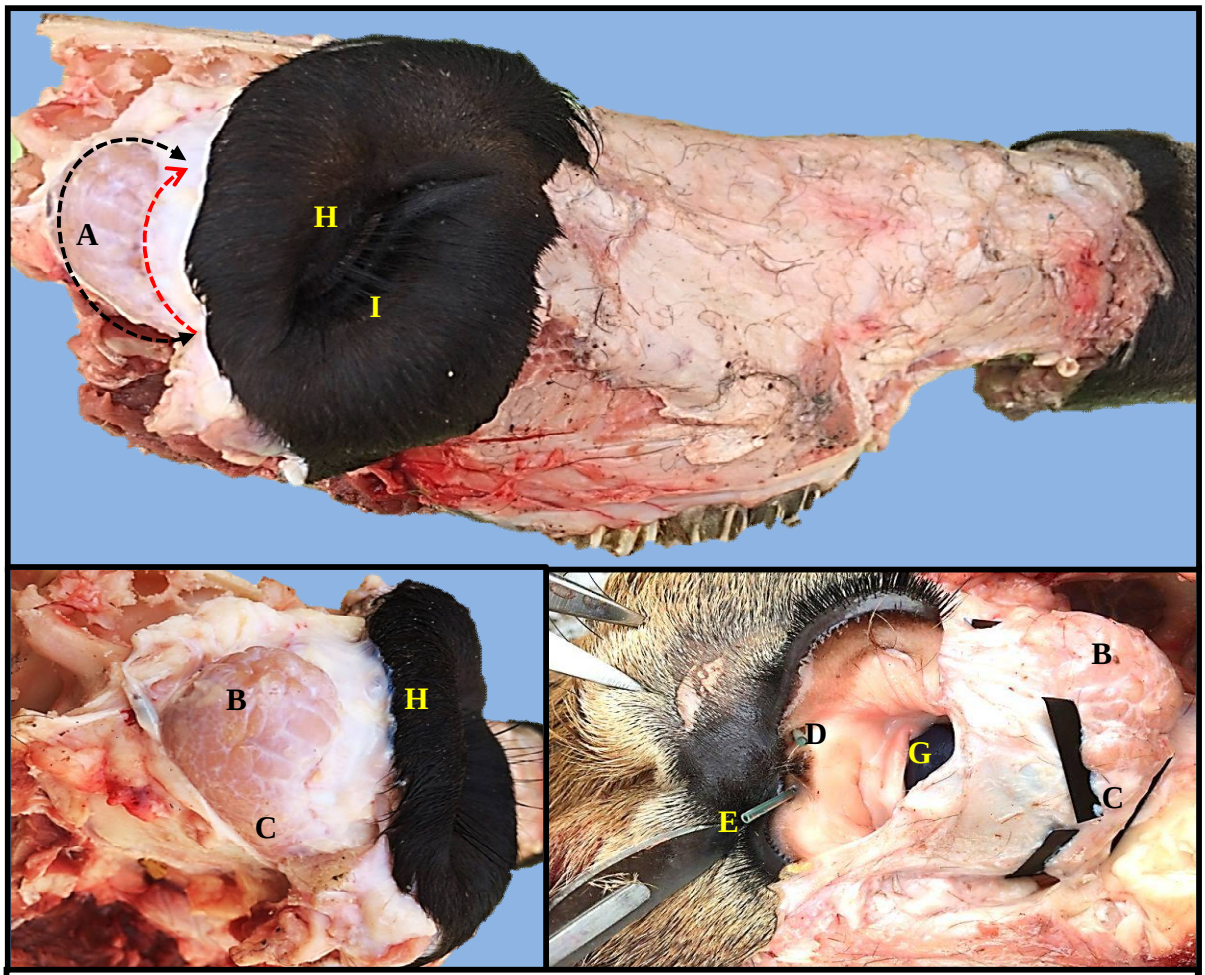

Fig.(1). Lacrimal gland in cattle Show: A- Lacrimal gland. B- Body of lacrimal gland. C-Appendage of lacrimal gland. D- Dorsal punctum. E- Ventral punctum. G- Eyeball. H- Upper eyelid. I- Lower eyelid.

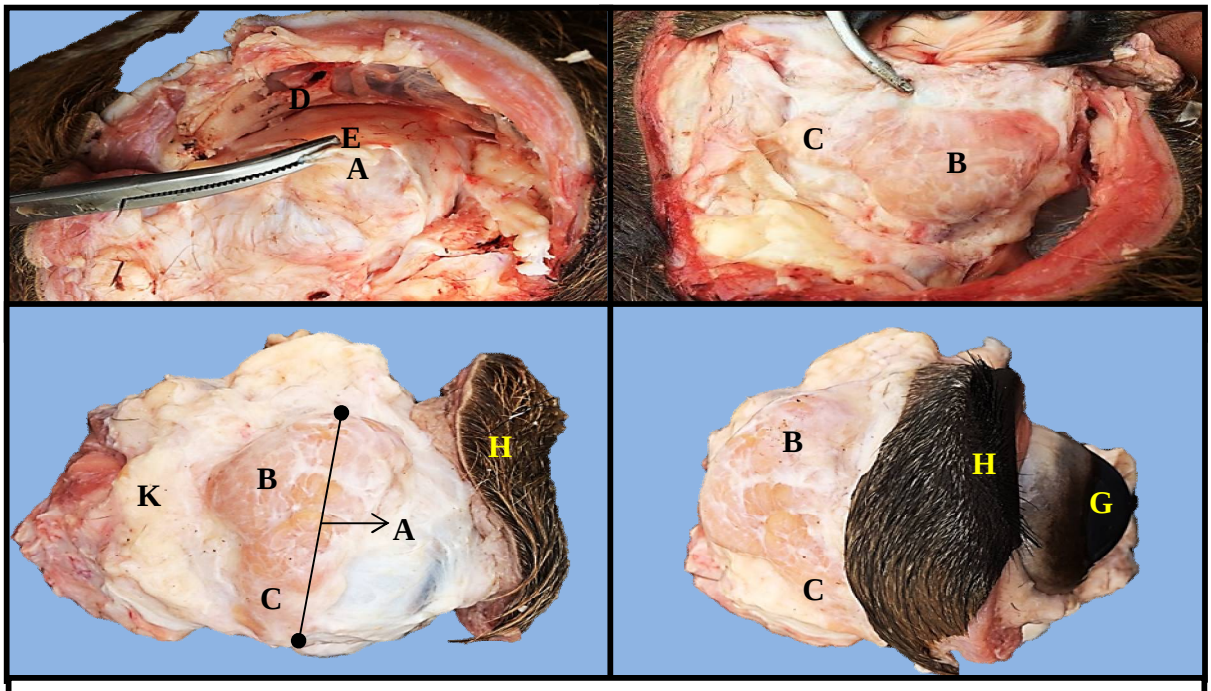

Fig.(2). Lacrimal gland in cattle Show: A- Lacrimal gland. B- Body of lacrimal gland. C-Appendage of lacrimal gland. D- Orbital cavity. E- Periorbital connective tissue. G- Eyeball. H- Upper eyelid. K-Adipose tissue.

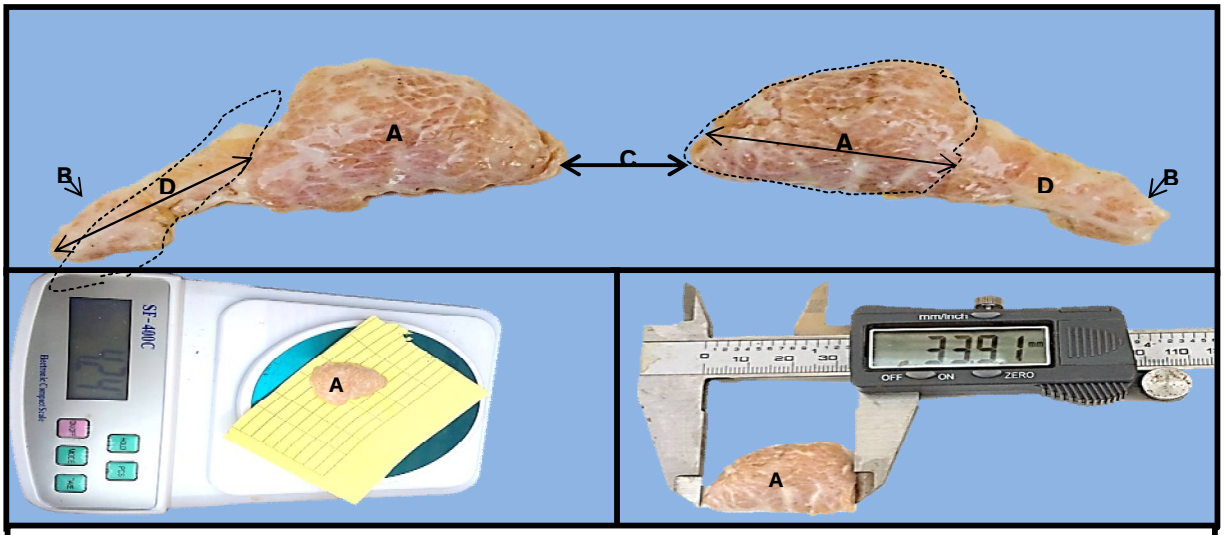

Fig.(3). Lacrimal gland in cattle Show: A- Body of lacrimal gland. B- Caudal end of lacrimal gland. C- Cranial end of lacrimal gland . D- Appendage of lacrimal gland.

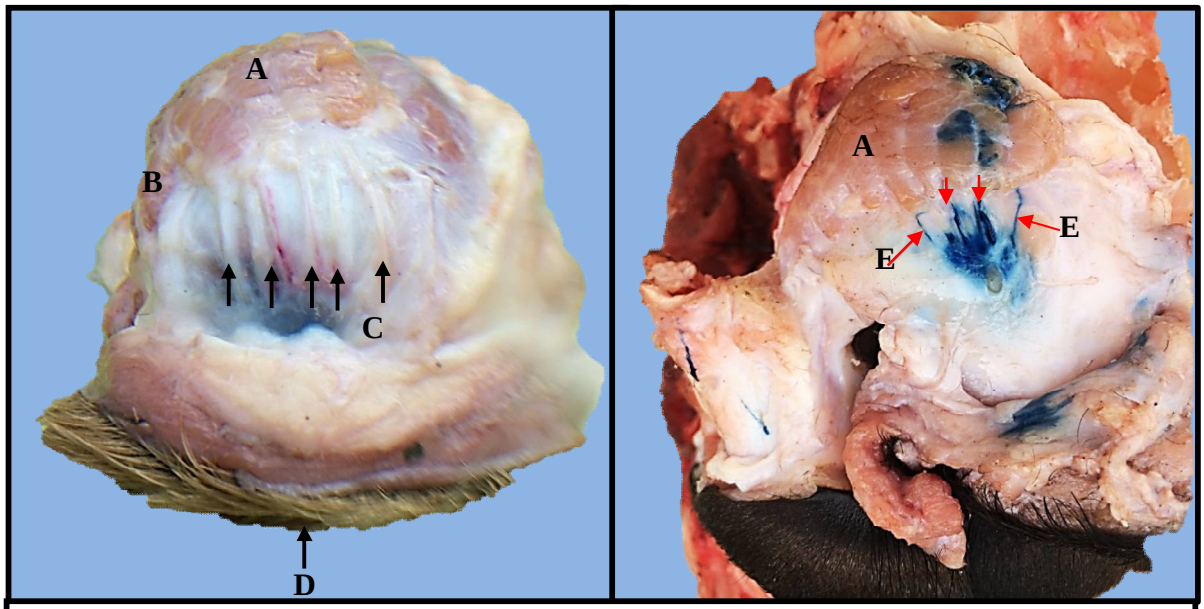

Fig.(4). Major excretory ducts of lacrimal gland in cattle show: A- Body of lacrimal gland. B- Appendage lacrimal gland. C- Major excretory duct of lacrimal gland (Black arrow). D- Upper eyelid. E- Major excretory duct injection with blue dye (Red arrow).

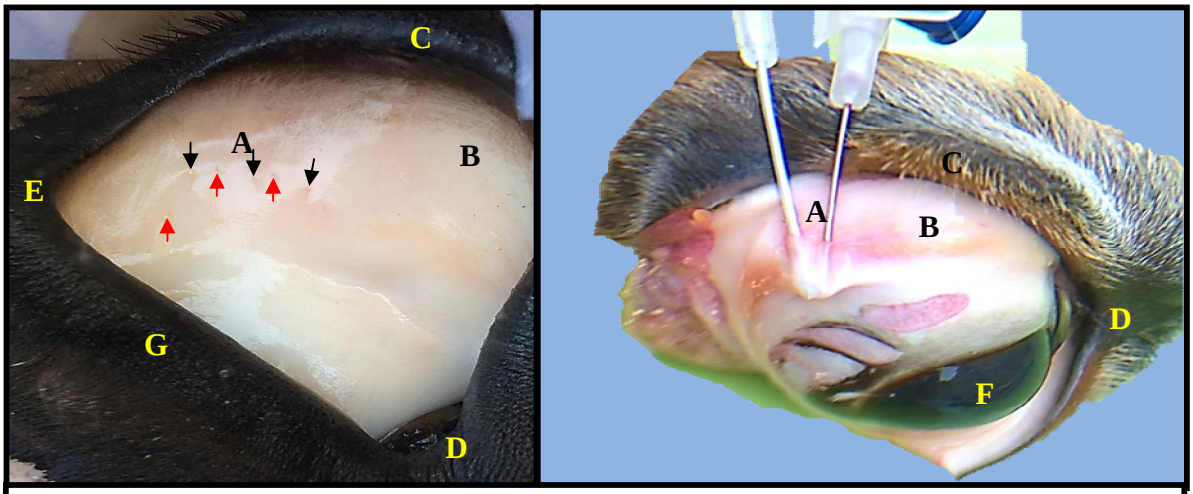

Fig.(5). Conjunctival surface of the upper eyelid in cattle Show: A- Major excretory duct of lacrimal gland (Black& red arrow). B- Conjunctival surface of upper eyelid (Fornix). C- Upper eyelid. D-Medial canthus. E- Lateral canthus. F- eyeball. G- Lower eyelid.

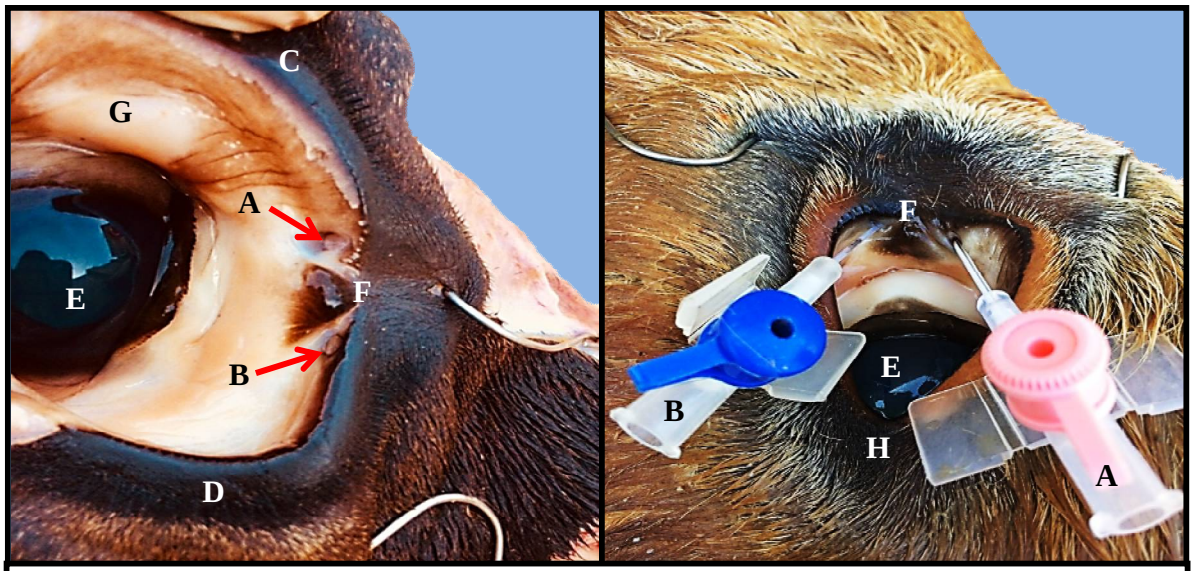

Fig.(6). Lateral view of the eye cattle Show: A- Dorsal punctum. B- Ventral punctum. C- Upper eyelid. D- Lower eyelid. E- Eyeball. F- Medial canthus. G- Conjunctival surface. H- Lateral canthus.

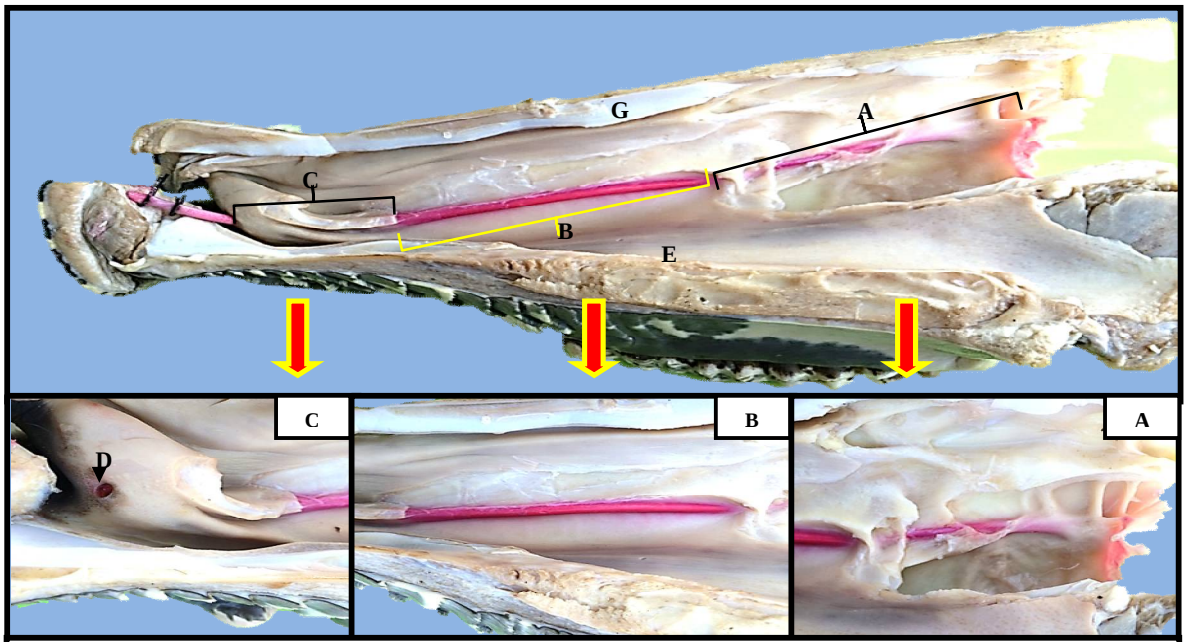

Fig.(7). Course of right side of nasolacrimal duct in cattle injected with latex & carmine Show: A- Proximal part(bony part). B- Middle part(Mucous part). C- Distal part(Cutaneous part). D- nasolacrimal opening. E- Floor nasal cavity. G- Roof nasal cavity.

Indian Journal of Natural Sciences www.tnsroindia.org.in ©IJONS

Vol.9 /Issue 51 / December / 2018 *International Bimonthly* *ISSN: 0976 – 0997*

RESEARCH ARTICLE

Petrophysical Analysis of Well Xin Oil Field Southern Iraq

Raghad Ahmed Naeem Al-Harethei* and Medhat E. Nasser

Department of Geology, College of Science, Baghdad University, Iraq.

Received: 16 Sep 2018 Revised: 19 Oct 2018 Accepted: 21 Nov 2018

***Address for Correspondence**
Raghad Ahmed Naeem Al-Harethei
Department of Geology,
College of Science,
Baghdad University, Iraq.
E-mail: roserrr@yahoh.com

ABSTRACT

Petrophysics analysis of well log dataits essential critical tool to identified and assessment the hydrocarbon bearing zones the purpose of this paper is to determine and evaluate the petrophysical properties of well x selected in oil field southrenIraq with a view to understand their effects properties on the reservoir. The evaluated properties include porosity, permeability ,fluid saturation, lithology ,net and cross pay were determined which are all inferred from well logs.The logs used are gamma ray, caliper log, spontaneous potential, resistivity, neutron log, density log and sonic log were analyzed for reservoir characterization. The analysis carried out involves lithology identification and determinations of petrophysical parameters. Well x was divided into 12 zones (Y1, Y1_top, Y3_top, Y3_base, Y4_top, Y4.2,Y4.3,Y4.4,Y4.5,Y4.6,Y5_top,andY5.2) were detected with their tops and bases at depth from 3605m to 3900.95 m. Computed petrophysical parameters across the reservoir gave porosity as ranging from 8 to 15% and average hydrocarbon saturation from 38-80.8 %. These results suggest high hydrocarbon production.

Keywords: petrophysical properties, residual hydrocarbon ,movable hydrocarbon and net pay.

INTRODUCTION

Petrophysics is the study of rock properties and their interactions with fluids in a porous medium. The petrophysical properties that effect of petroleum reservoirs are: porosity, permeability, Archie's parameters, mineralogy, water saturation, irreducible water saturation, hydrocarbon saturation, residual oil saturation, wettability, capillary pressure, pore size distribution and structure, net pay thickness and compressibility [2,6].The major objective of the present study is to evaluate the petrophysical characterization of the reservoir rocks including the porosity, permeability and fluid saturation of the selected well. Gamma ray (GR) used to calculated Vshale ,spontaneous potential (SP), caliper log, resistivity log (Rt), density log (RHOB) ,neutron log(NPHI),sonic log(DT) have been used to identified and detected the lithology and many calculated that related to evaluated petrophysical properties of the

reservoir, such as porosity,lithology,mineralogy, permeability, resistivity, water saturation and hydrocarbon saturation.The petrophysical properties that are determined from well log and discussed in this study include: Porosity(effective &total porosity), permeability, Water saturation ,Hydrocarbon saturation, Residual oil saturation, Net pay thickness ,lithology and Mineralogy.table (1)

Petrophysical analysis

Logs was the mirror that reflect the petrophysical properties of rocks so the petrophysical analysis based on logs (Gamma Ray,caliper, Neutron, Density, Sonic,Resistivity, and Spontaneouspotential) in this study. The analysis were made to calculate porosity, permeability, water saturation and hydrocarbon saturation by Techlog software. All of these parameters are very useful in investigating the reservoir characterization.

Shale volume calculation

The first step of interpretation was needed to Calculation of the gamma ray index to determine the volume of shalefrom a gamma ray log GR (VCLGR) is computed using the following equation

IGR = (GRlog-GRmin/GRmax-GRmin)----------(1)

Where:
IGR: Gamma ray index GRLog: Gamma ray reading GRmin: Minimum gamma ray reading GRmax: Maximum gamma ray reading Once the Igris calculated, the volume of shale (Vsh)is then determined from the following equation for older and consolidated rocks:

$Vsh = 0.33(2^{2 * IGR} - 1)$ ---------- (2)

Calculation Porosity from Density and Neutron log

After calculating the v shale volume .The combination of the neutron and density measurements is the most common of all porosity tool used to calculated the total porosity see figure (1) the total porosity (symbol Φt or PHIT) (interconnected and isolated pores) is defined as the ratio of total pore volume within a rock to the total bulk volume including voids. also "effective porosity" or "connected" pore space is commonly used to denote porosity that is most available for fluid flow (symbol Φ_E or PHIE). [5].was calculated.

Permeability (K)

In addition to being porous ,One of the most important criteria in defining the reservoir production is permeability. a reservoir rock must have the ability to allow petroleum fluids to flow through its interconnected pores. [5,9,10] define The rock's ability to conduct fluids is termed as permeability. There are many ways of estimating permeability from wireline tool, but the Timurand Schlumberger modelsis used to calculate the permeability.figure (1)

$K = 0.136\Phi^{4.4}/S^2_{wi}$----------(3)

Determined the lithology

The neutron-density cross plot is one of the oldest quantitative interpretation tools ,it was the principal method for determining the formation lithology. [3].this cross plot is considered most important and very frequently used to provided satisfactory resolution for quartz,calcite and dolomite .figure(2)showsthe points fall on the line of limestone with few points on dolomite and with some shale Another cross plot type that determined the lithology was sonic-neutron cross plot figure (3) also shows same systematic fall the points on line of limestone .

Calculated Water and hydrocarbon saturation from resistivity log

Porosity and fluid saturation are among the most important reservoir properties used in the reverse estimation oil and gas. Because of heterogeneity in most reservoir of these properties vs. depth is essential for accurate evaluation. [5].In log interpretation, the hydrocarbons, the rock, and the fresh water of the formation are all assumed to act as insulators and are, therefore, nonconductive (or at least very highly resistive) to electric current flow. Salt water, however, is a conductor and has a low resistivity. Resistivity is a basic measurement of a reservoir's fluid saturation and is a function of porosity, type of fluid (i.e. hydrocarbon, salt water, or fresh water),amount of fluid , and type of rock . because both the rock and hydrocarbons act as insulators but salt water is conductive, resistivity measurements made by logging tools can be used to detect hydrocarbons and estimate the porosity of a reservoir [2].. In this research, deep resistivity *Rt* ,shallow resistivity *Rmed* and micro resistivity *Rxo* were studied.

Deep resistivity is the resistivity recorded farther away from the inversion core created by the drilling mudwe can say that the resistivity of the formation R_t depends upon porosity Φ, water saturation S_w, and the resistivity of the formation water R_w. This resistivity is called the *true resistivity of the formation*. Shallow resistivity log is the resistivity recorded close to the oil well bore while the micro spherically focused log ,The resistivity of the formation in this zone depends upon the resistivity of the mud filtrate R_{mf}, the resistivity of any remaining formation water R_w, the saturation of the mud filtrate S_{xo}, the saturation of the remaining formation water S_w. A deep resistivity and shallow resistivity with low gamma ray log is indicative of hydrocarbon (HC) presence. Shales show low resistivity values with high gamma ray values. also by using the Density, Neutron and Resistivity logs we can identified fluid type and distribution. The water saturation in (flushed *Sxo*and uninvaded *Sw*)zones were determined from (micro*Rxo* and deep *Rt*)resistivity logs respectively based on keystone of log analysis Archie's equations.Subsequently we can estimate the residual and movable hydrocarbon as following equations. The saturation of flushed zone(*Sxo*) which is determined to estimate residual and movable hydrocarbon saturation ,calculated from following equations [7].

Sor={Φ*(1-Sxo)}----------(4)

Shr={Φ*(Sxo-Sw)}----------(5)

Where
Sor: residual oil saturation (fraction), Shr: movable hydrocarbon saturation (fraction)
The *Sw* and*Sxo* can be used to calculated the amount of movable hydrocarbon [8].

Movable hydrocarbon =Φsxo-Φsw----------(6)

water filled porosity in the invaded zone can be calculated by equation($B_{VWXO} = PHIE * S_{xo}$) and water filled porosity in the un-invaded zone by equation($B_{VW} = PHIE * S_W$).

Net and Gross pay

The most useful output of a petrophysical interpretation is a series of curves that show how porosity, water saturation, permeability and other properties vary along the well path.[4].So its calculated and displays in table (1)and figure(1)

RESULTS AND DISCUSSION

The final results of petrophysical representative well are shown in Fig.(1) These results are based on above method and current data available**.**Based on GR log, SP log and Caliper Log, marked reservoir zone. From the analysis, particularly the resistivity logs, all of these logs help to delineated reservoirs zones were identified as hydrocarbon bearing reservoir.Petrophysical parameters are estimate using empirical formulae .Shale volume , The effective and total porosities were calculated and its influence on hydrocarbon .The finalresults shown in below at Table (1) and figures of (1) .

CONCLUSIONS

A detailed petrophysical analysis have been carried out for reservoir characterization of well x in selected oilfield south Iraq, using well log data from well x in the field. The following conclusions can be drawn based on the above data analysis:

1. Lithological interpretation and effects of rock minerals and fluids have been assessed.
2. The reservoirs are mainly carbonate and clean with clay content as low as 10-18%. A wide range of variation is found in water saturation
3. The effective porosity is varying in the range of 8-15 %.
4. The cross plots (NPHI-RHOB) and (DT-NPHI) indicate that the main lithology of reservoir was limestone with some dolomite and little shale
5. Water saturation ,residual hydrocarbon and movable hydrocarbon were calculated and show were are increase in two unites reservoir and decrease in other .

REFRENCES

1. Asquith, G., and Gibson, C. “Basic Well Log Analysis for Geologists”, Methods in Exploration Series, AAPG, 1982.
2. Asquith, G., and Krygowski, D., 2004, Basic Well Log Analysis, 2nd.ed. Sections by Steven Henderson and Neil Hurleg. The American Association of Petroleum Geologist, Tulsa, Oklahoma. AAPG. Methods in Exploration series No.16, 244p.
3. Drawin V.E. and Singer , J.M.,2008 Well logging for earth scientist .2nd Edition .Springer. 692 p.
4. Kennedy .M,2015 Practical Petrophysics , UK, Elsevier ,P.403
5. Lucia F. J. ,2007 Carbonate Reservoir Characterization An integrated Approach ,Second Edition .Springer –Verlag Berlin ,Heidelberg .336 p.
6. Peters, E., J. (2006). *Petrophysics,* the University of Texas, Austin, Department of Petroleum and Geosystem Engineering UAS 78712 .
7. Serra O.,1986 "Fundamental of Well log Interpretation Volume the Acquisition of Logging Data" Development in petroleum science ,Elsevier ,Amsterdam.
8. Shulmberger,1989" Log Interpretation Principal /Application ",Hostanp.241.
9. Taib, D. and Donaldson, E.C. (2004). Petrophysics; *Theory and Practice of measuring Reservoir Rock and Transport Properties,* 2nd Edition, UK, Elsevier.

10. Tiab, D. and Donaldson, E.C.,2015, petrophysics theory and practice measuring reservoir rock and fluid transport properties ,4th edition, UK, Elsevier ,p 898.

Table 1. shows the results obtained by conventional logging of well x.

Zones	Top	Bottom	Gross	Net	Net to Gross	BVW	Shale Volume	Porosity	Water Saturation
Y1	3613	3643	30	9	0.3	0.082	0.199	0.147	0.062
Y1_top	3643	3663	20	18.15	0.908	0.251	0.137	0.08	0.172
Y3_top	3663	3688	25	20.95	0.838	0.301	0.141	0.136	0.106
Y3_base	3688	3690.14	2.14	0.65	0.304	0.015	0.103	0.095	0.249
Y4_top	3690.14	3706	15.86	1.15	0.073	0.048	0.048	0.103	0.408
Y4.2	3706	3721	15	3.5	0.233	0.134	0.108	0.096	0.398
Y4.3	3721	3740	19	5.25	0.276	0.312	0.108	0.142	0.419
Y4.4	3740	3752.5	12.5	6.45	0.516	0.288	0.105	0.112	0.397
Y4.5	3752.5	3783	30.5	6.75	0.221	0.352	0.143	0.127	0.412
Y4.6	3783	3806	23	9.45	0.411	0.272	0.145	0.15	0.192
Y5_top	3806	3824	18	6.9	0.383	0.346	0.187	0.123	0.407
Y5.2	3824	3900.9	0	0					

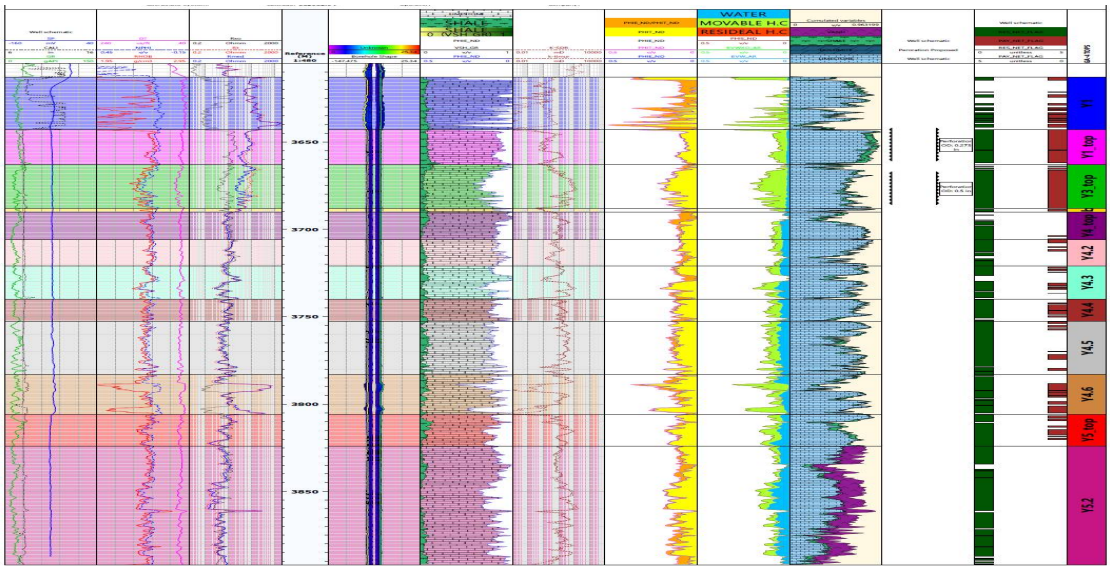

Figure 6 shows the computer process interpretation (CPI)of well-x

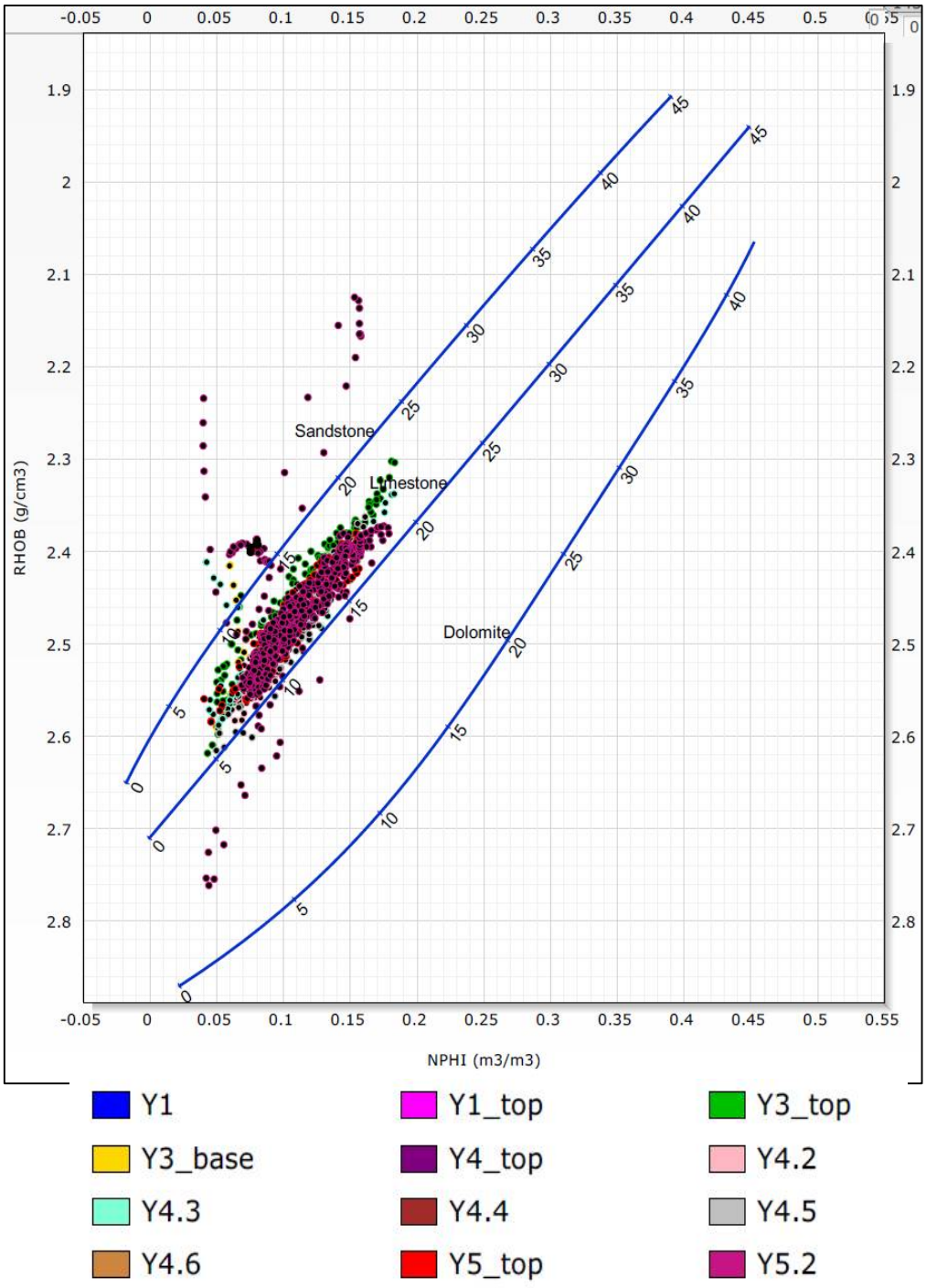

Figure 2 shows cross plot between NPHI and RHOB of well-x

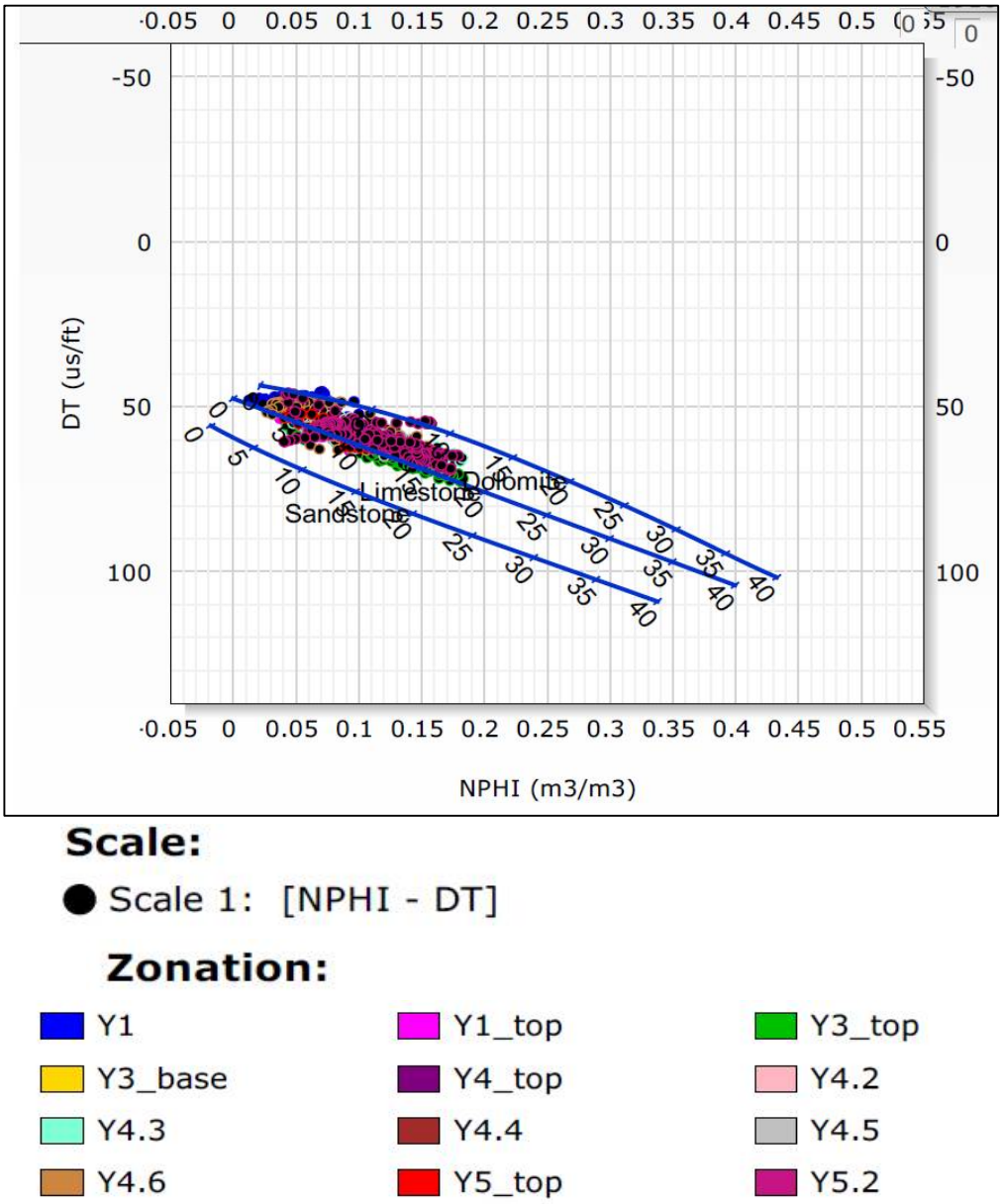

Figure 3 shows cross plot between NPHI and DT of well-x

Indian Journal of Natural Sciences www.tnsroindia.org.in ©IJONS

Vol.9 /Issue 51 / December / 2018 *International Bimonthly* *ISSN: 0976 – 0997*

RESEARCH ARTICLE

Effect of Different Molar Ratio and pH Reaction Solvent Tertiary Butanol (TBA) on the Hydrophobic and Structural Properties of Nanoporous Silica Cryogels

Mohammed Aziz Jadaa* and Wesam A A Twej

College of Science, University of Baghdad, Baghdad, Iraq.

Received: 14 Sep 2018 Revised: 18 Oct 2018 Accepted: 22 Nov 2018

***Address for Correspondence**
Mohammed Aziz Jadaa
College of Science,
University of Baghdad,
Baghdad, Iraq.
Email: mohammed_aziz80@yahoo.com

ABSTRACT

Nanoporous silica cryogels with a high specific surface area of 800 m^2g^{-1} were fabricated using freeze-drying method utilizing tertiary butanol as a reaction solvent. Alco-gels were synthesized through acid-base catalysis recipe using tetraethoxysilane as a silica precursor. Different of solvent/precursor molar ratio 7, 9, 11, 13 and 15 and different starting pH; 6, 7, 8 and 10 were employed in this work.The cryogels samples were examined by SEM, FTIR, nitrogenabsorption/desorption isotherms and hydrophobicity by contact angle measurements.We found that the best molar ratio was X=11, while the best sample at pH8. The modification process using TMCS enhanced the sample surface significantly and thecryogel was converted from a hydrophilic to hydrophobic.

Keywords: Vacuum freeze-drying; tertiary butanol; silica cryogels.

INTRODUCTION

Aerogel is defined as a gel comprised of a micro porous solid in which dispersed phase is a gas[1]. Aegerter et al. defined aerogels as gels that replaced their liquid with air, with little contraction in its network [2]. Aerogels are also known as frozen smoke because of its hazy blue appearanceor air-glass and are included of particles with sizes < 10 nm and pore sizes < 50 nm in diameters. Aerogels are micro- and mesoporous networks collected of randomly interlocking nano-scale filaments, It has more than 99% open pore space of its volume. This structure gives aerogels its exclusive physical properties.Among the more potentially useful properties of silica Aerogels exceptional properties, the low thermal conductivity (~0.01 W/m.K), high porosity (~99%), optical transmission in the visible region higher than 90%, high surface area (1000 m^2/g) low dielectric constant (~1.0-2.0), low refractive index (~1.05), and low sound velocity (100 m/s)[3-6]. Owing to these properties, aerogels find applications in a number of fields

such as capacitor electrodes, thermal insulation, catalysis, acoustic insulation, dielectrics, electronics, ultrafiltration membranes, controlled drug delivery and oil spill cleanup kits[7-19].Aerogels are usually produced by hydrolysis and the condensation of metal alkoxide, whoever they can also be produced from mineral salts.In freeze drying method the solvent was removed from the gel by lowering the gel temperature below solvent freezing temperature and reducing the pressure (sublimation). The product of this process is usually called a cryogel. In order to improve the physical and chemical stability of these systems water or solvent have to be removed. Freeze-drying is the most commonly used process in the pharmaceutical or food fields, which transforms the drying of solutions or pendants into stable materials for sufficient time to distribution and storage[20].

Freeze drying is an industrial process consisting of removing water or solvent from a frozen sample by sublimation by vacuum. Tertiary butanol (TBA) is among the best solvents tested for freeze-drying in recent years and has the greatest attention from researchers. This solvent is miscible with water at any ratio and at any temperature, it has low toxicity and appears suitable for freezing, including high melting temperature, high vapor pressure and low sublimation enthalpy. All TBAsolvent and water mixture synthesis share these desirable properties also and, consequently, they freeze under operating conditions for conventional commercial freeze-dryers and they sublime at a higher rate than neat water for similar process parameters.In this work, the effect molar ratio TEOS/TBA and pH value of the reaction solvent as well as the amount of surface modification on the properties of the prepared cryogels prepared were by a novel vacuum freeze drying were investigated.

MATERIALS AND METHODS

The chemicals used for the preparation of alcogels were tertiary butanol (TBA) (99%), tetraethoxysilane(TEOS, SiO_2> 28.5%), ammonia (NH_4OH, 28%) and hydrochloric acid (HCl, 36.5%). The double-distilled water (H_2O) was prepared in the authors' laboratory. Supplied company for all material sigma Aldrich.

Experiment

The wet gels were synthesized via acid-base catalysis sol-gel procedure. The molar ratio of tetraethoxysilane (TEOS), and tertiary butanol (TBA) were used as precursor and solvent, respectively.The concentration of catalyst of hydrochloric acid (HCl) and ammonia (NH_4OH) were fixed at 0.12 mol/L and 1.44 mol/L, respectively was added (HCl) to induce the hydrolysis of the precursor, and then the irreversible polycondensation reaction took place in the presence of a base catalyst (NH_4OH). Firstly, prepared a mixture of TBA/TEOS with molar ratios X = 7, 9, 11, 13 and 15. Then, added a diluted HCl (0.12 mol/L) to the mixture under continuous stirring for 30 min at 50 °C. Secondly, dilute NH_4OH (1.44 mol/L) was added as droplets under rapid stirring for 5 minutes, until the pH became about 8. The alcohols were then transferred to mould at room temperature, and gelled in 10-60 min. The molar ratio of TEOS: H_2O:HCl: NH_4OH was 1:3.7: 1.08×10^{-4}: 1.24×10^{-3}. Thirdly, the transparent alcogels were aged to strengthen the gel networks. for 24 h in a sealed cabin at room temperature. The alcogels were washed with TBA at 50 °C for each time per 8 h. The surface modification was carried out by immersing the gels in a mixture of TBA containing 5 % volume solution of Trimethylchlorosilane (TMCS) at 50 °C for ~24 h, the modification times were changed from 0 to 3 times.

Finally, the alcogels were dried by a vacuum freeze dryer using a special procedure, Alcogels were dried in a vacuum-freeze dryer (Homemade chamber) in two steps. Firstly, the alcogels were freeze to -30 ºC in the ice condenser chamber and kept there for 4 h. Secondly, the drying procedure started by vacuum the chamber. The temperature was increased from (-30 to 10) ºC at 10 ºC steps and a fixed pressure of 0.12 mbar and was kept for 1.5 h at every step. Then, it was increased from (10 to 25) ºC at 5 ºC steps and was kept for 15 min at a pressure of 0.63 mbar at every step. The temperature was raised with rate of 0.65 ºC min^{-1}. During this process, the frozen liquid was sublimed from solid to gas and removed using the vacuum pump. The obtained cryogels were very fragile, opaque powder. Then After choose any best molar ratio TEOS/TBA, here study, the effect of different pH value (6, 7, 8, 10) of

the reaction solvent tertiary butanol (TBA) on the properties of cryogels prepared, and the surface modification by Trimethylchlorosilane (TMCS) a novel vacuum freeze drying are investigated.

Characterization methods

The porosity properties of the cryogels were determined by nitrogen absorption/desorption measurements at 77.35 K using an ASAP2010 Micromeritics apparatus (USA). The pore size distribution and specific surface area were analyzed by the density functional theory (DFT) methods and Brunauer-Emmett-Teller (BET), respectively. The morphology was detected by Scanning Electron Microscopy (SEM, JSM-6330F, Japan).The Fourier Transform Infrared spectroscopy (FT-IR, Bruker TENSOR 27, Germany) and hydrophobicity of water and the surface modification of the cryogels were examined by measuring the contact angle by water dropped on the preforming cryogels.

RESULTS AND DISCUSSIONS

When taking a many with different molar ratio TBA/TEOS (7, 9, 11, 13 and 15) at fixed other parameters, as pH8 and temperature (-30) ºC of all the samples, we observed the density of all Cryogel samples without TMCS (hydrophilic) is less than the other samples with TMCS (hydrophobic). The best sample, which has the least density, at the molar ratio TBA/TEOS is 11 as shown in Figure 1. This means will give the largest specific surface area. Generally, high surface area cryogels has low density [21]. However, the density also depends on the pore size distribution and particle size. Figure 2 (A) and (B) show the variation of absorption/desorptionisotherm for N_2 gas by SiO_2 cryogels with the different molar ratio. The largest absorption molar ratio at X11.The porosity and the pore size distribution of silica cryogels was investigated by the N_2 absorption/desorption, the physic-sorption isotherm is of type IV, which is typical of mesoporous materials[22] as shown in Figure 3(A).The SiO_2 cryogels with X = 11 exhibit an extremely high specific surface area.Figure 3(B) show the pore size distribution and show a high density of micro- and mesopores. Large surface area and small pores that distribution in the sample can be attributed not only to the excellent dispersion function, but also to the smaller molecular size of the solvent used in this technique, which absorbs fluid easily and then make pores.

When select the best molar ratio (X11) and variation of pH, for pH6 and pH8 as shown in Figure 4 (A), the SiO_2 cryogels prepared of the pH8 exhibit an extremely high specific surface area of 800 m^2/g and Mean pore diameter 5.0818 (nm). Figure 4 (B) shows pore size distribution in the range of (0.3–19) nm with a high density of micro- and mesopores (0.37–8 nm). Decreasing the preparing pH to 6 leads to decrease the surface area to 769 m^2/g and mean pore diameter to 4.4492 (nm), while the pore size distribution increase in the range of (0.38–13) nm with a high density of micro- and mesopores (0.38–6 nm).Figure (5) shows the variation of density with pH for the best molar ratio (X11) at temperature (-30 °C). We observed that the best sample with least density at (pH8), this means this sample will give the largest specific surface area which is agree with the BET surface areas completely. Where generally, high surface area cryogels has low density[21]. However, the density also depends on the pore size distribution and particle size.

Figure 6 show surface profile and particle size of the samples cryogels prepared by different pH (6, 7, 8 and 10) represented images (A, B, C and D) respectively, of the reaction solvent tertiary butanol (TBA). From the scanning electron microscopy (SEM) images for the samples at 500 nano magnification (70 kx), micrograph study, it is observed that the effect of preparation pH values on the cryogel morphologies are very clear.The pH6 an pH7 image (A and B), reflects sticky and high aggregation between particles. So, the samples look like large smooth blocks with a few holes indicating high density.The pH8 and pH10images (C and D) seem with less aggregation, lower particles size and increase pore size. Increasing pH value leads to form silica clusters resulting in less cross linking between clusters and leading to change in the particle and pore sizes. The main particle size was 25 nm, having gaps estimated size to almost 100 nm. These gaps gave the lowest density of these samples compare with lower pH samples. Perhaps

the monolith consist of cluster-cluster and monomer-monomer network, leading to pour distribution irregular from region to another with this pH value, more and more -O-Si-$(CH_3)_3$ groups were attached to the already formed silica clusters.In case of pH10 sample the separation between particle and another is very clear, all particles have spherical shapes with diameter range (32-22) nm. There is aggregation in monolithic structure, pour size have diameter half range of particle size. Due to high homogeneity monitored through pH8 sample, in this work special attention have been done in SEM observation for this sample.Finally, from looking at image of pH10 sample, the aggregation in monolithic structure is very clear. Basically, under basic environment, the silica cross linking mechanism is followed this scenario; growth occurs primarily through the addition of monomers to the more highly condensed particles rather than by particle aggregation[23], so that the networks become more compact with small particle size and pore size. Therefore, the cryogels are mesoporous structure.

Figure 7 the surface modification was confirmed by FT-IR spectroscopy as shown in (E) without and (A, B, C, D) with three times surface modification using Trimethylchlorosilane (TMCS).Curves (A, B, C, D) show bonds at 3468 and 1600 cm^{-1} of O-H groups and the peaks of -CH_3located at 2960, 1380 and 860 cm^{-1}. We observe a clear change in the bonds between the non-modified sample and the improved ones. We note that there are no bonds belonging to C-H_3 in the non-modified sample, while they appear clearly in the other samples which indicates more -Si-$(CH_3)_3$ groups were attached to the silica networks and confirms the effect of surface modification on hydrophobicity.The hydrophobicity is due to the attachment of hydrolytically stable -Si-$(CH_3)_3$ groups by replacing surface H from -OH groups of silica surface leading to the hydrophobicity of the cryogels increases[24]. There was no significant change in the O-H and C-H_3 bonds energy in the modified samples by changing the pH value, except for a slight change in the intensity of the peaks at same locations. These changes suggest that the surface modification makes the cryogels more hydrophobic.The hydrophobicity of the cryogels was studied by measuring the contact angle of the water droplet on the cryogels surface as illustrated in Figure 8.The contact angle increased from 82.8º for one time modification to 151.5ºfor sample modified three times with TMCS as shown in table 1.

CONCLUSIONS

Hydrophobic silica cryogels were prepared by freeze-drying method using TBA as solvent by a locally manufactured low cost chamber. The technique has yielded good results for cryogels hydrophobicity, which are widely used in several applications. The silica cryogels obtained by this technique have an excellent porosity structure. The best ratio between TBA /TEOS is X=11with best surface area of the samples at pH8. The modification process using TMCS improved the sample surface significantly as the material was converted from a hydrophilic to hydrophobic.

REFERENCES

1. A. D. McNaught and A. Wilkinson, Compendium of Chemical Terminology, IUPACGoldbook, PAC, 2007, 791801, Blackwell Science, Oxford, Cambridge, UK, 2nd ed.
2. M. A. Aegerter, N. Leventis, and M. M. Koebel, Aerogels Handbook, Springer, New York, NY, USA, 2011.
3. Husing, N.; Schubert, U.; Aerogels - Airy Materials: Chemistry, Structure, and Properties, Angew. Chem. Int.Ed. 1998, 37 (1/2), 22–45
4. Fricke, J.; Aerogels - highly tenuous solids with fascinating properties, J. Non-Cryst. Solids 1988, 100,169–173
5. Pajonk, G. M., Transparent silica aerogels, J. Non-Cryst. Solids 1998, 225, 307–314
6. Kocon, L. ; Despetis, F. ; Phalippou, J., J., Ultralow density silica aerogels by alcohol supercritical drying, J. Non-Cryst. Solids 1998, 225, 96–100
7. Kistler SS (1932) Coherent expanded-aerogels. J PhysChem 36: 52–64
8. Kistler SS (1935) The relationship between heat conductivity and structure in silica aerogel. J PhysChem 39: 79–86
9. Kearby K, Kistler SS, Swann S Jr. (1938) Aerogel catalyst: conversion of alcohols to amines. IndEng Chem30: 1082–1086

10. Kistler SS, Fisher EA, Freeman IR (1943) Sorption and surface area in silica aerogel. J Am ChemSoc 65: 1909–1919
11. Gesser HD, Goswami PC (1989) Aerogels and related porous materials. Chem Rev 89: 765–788
12. Hench LL, West JK (1990) The sol-gel process. Chem Rev 90: 33–72
13. Pierre AC, Pajong GM (2002) Chemistry of aerogels and their applications. Chem Rev 102: 4243–4265
14. Hrubesh LW, Poco JF (1995) Thin aerogel films for optical, thermal, acoustic and electronic applications. J Non-Cryst Solids 188: 46–53
15. Schmidt M, Schwertfeger F (1998) Applications for silica aerogel products. J Non-Cryst Solids 225: 364–368
16. Fricke J, Emmerling A (1998) Aerogels-recent progress in production techniques and novel applications. J Sol-Gel Sci Tech 13: 299–303
17. Akimov YK (2002) Fields of application of aerogels (review). InstrumExp Tech 46: 287–299
18. Pajonk GM (2003) Some applications of silica aerogels. Colloid PolymSci 281: 637–651
19. Smirnova I, Suttiruengwong S, Arlt W (2004) Feasibility study of hydrophilic and hydrophobic silica aerogels as drug delivery systems. J Non-Cryst Solids 350: 54–60
20. Bhagat S D, Kim Y H, Moon M J, Ahh Y S and Yeo J G 2007 Solid State Sci. 9 628
21. L.C. Klein: Sol-Gel Technology for Thin Flims, Fibers, Performs, Electronic and Speciality Shapes (Noyes Publications, New Jersy, 1988).
22. F. Franks, Freeze-drying of bioproducts: putting principles into practice, Eur. J. Pharm. Biopharm. 45 (1998) 221 – 229.
23. M. A. Aegerter, N. Leventis, and M. Koebel, "Advances in sol–gel derived materials and technologies," ed: Springer, 2011.
24. J.L. Gurav, D.Y. Nadargi and A.V. Rao: Appl. Surf. Sci. Vol. 255 (2008), p. 3026.

Table (1): dependence of contact angle for TBA on surface modification times with TMCS

Modification times	one time	two time	Three time
Contact angle (degree)	82.8º	140.4º	151.5º

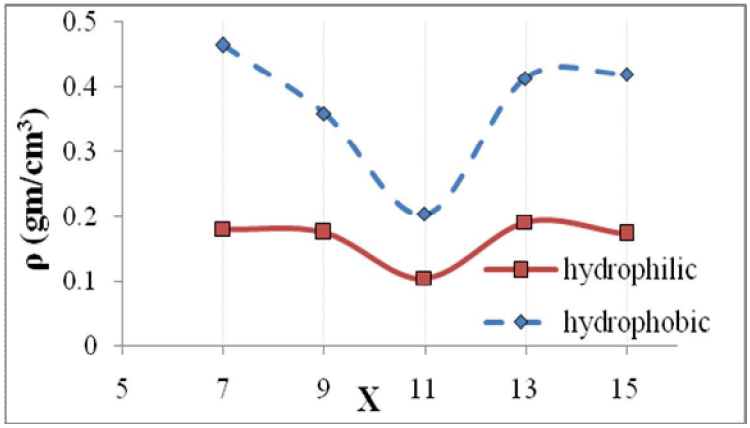

Figure (1): variation of cryogel density prepared with TMCS (hydrophobic) and without TMCS (hydrophilic) with different molar ratio TBA/TEOS

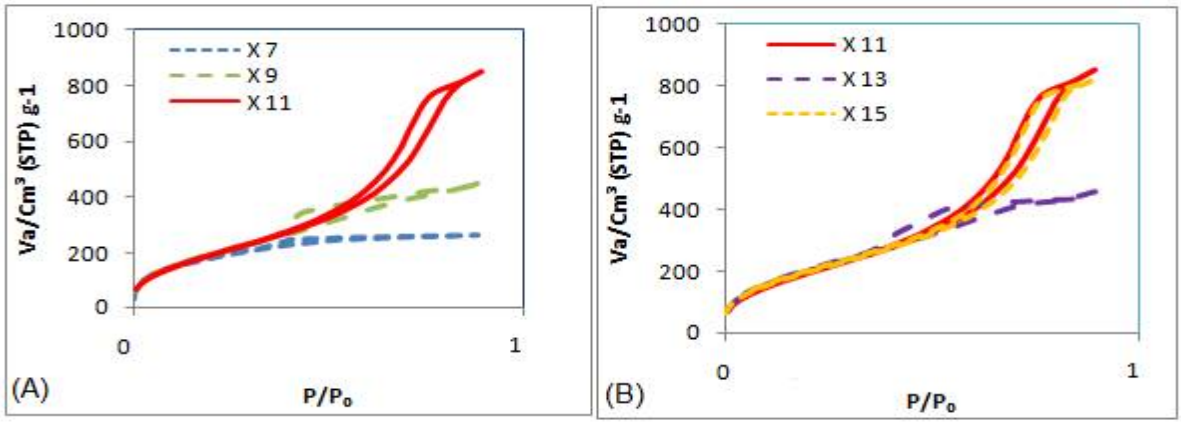

Figure (2): SiO_2 cryogels with different molar ratio by N_2 absorption/desorptionisotherm

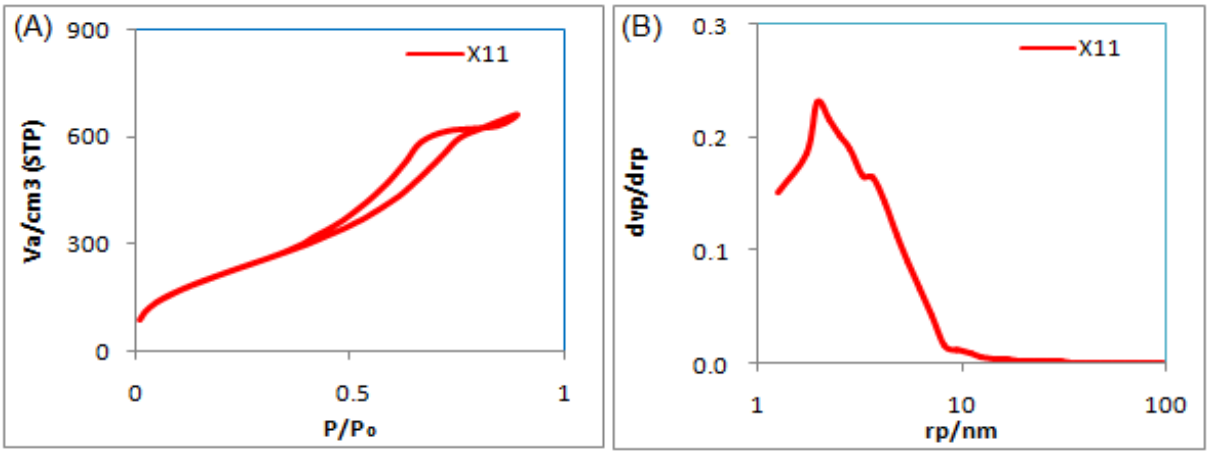

Figure (3): SiO_2cryogels with X = 11 : (A) N_2 absorption/desorptionisotherm and (B) pore size distributions obtained by the BJHmethod.

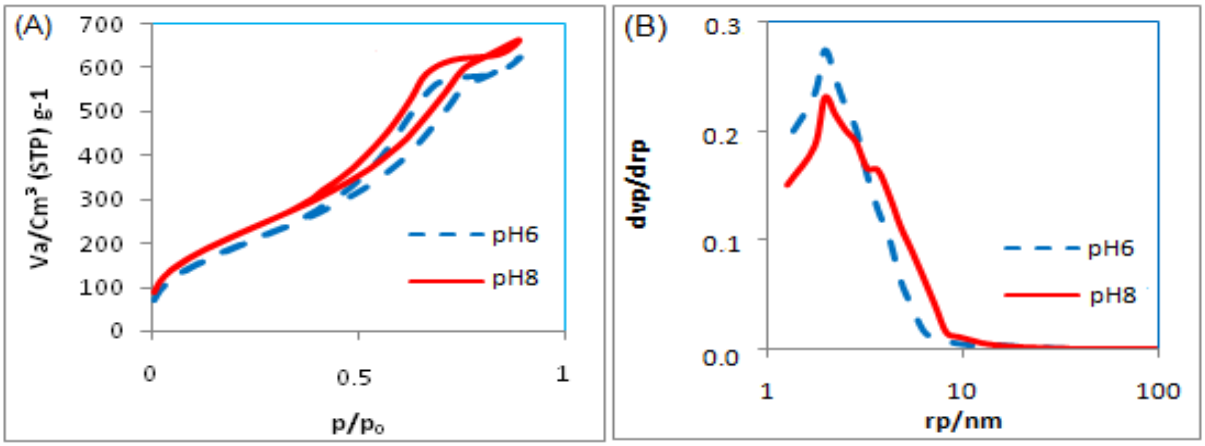

Figure (4): SiO_2 cryogels with X = 11 and temperature at -30 ºc prepared at different pH6 : (A) N_2 absorption/ desorptionisotherm and (B) pore size distributions obtained by the BJH method.

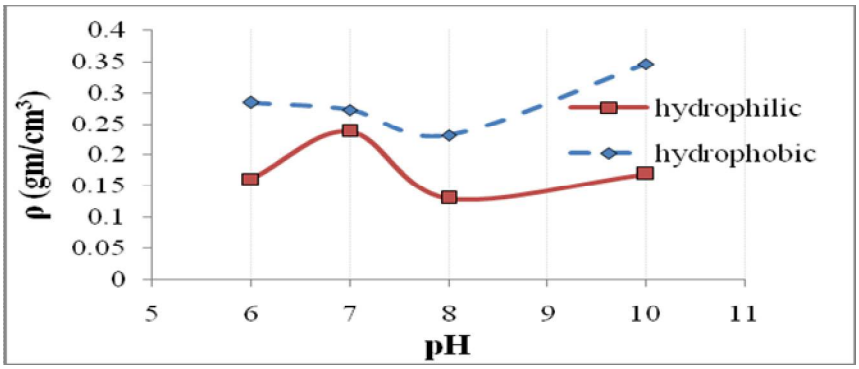

Figure (5): variation of cryogel density prepared with TMCS(hydrophobic) and without TMCS (hydrophilic) with different pH.

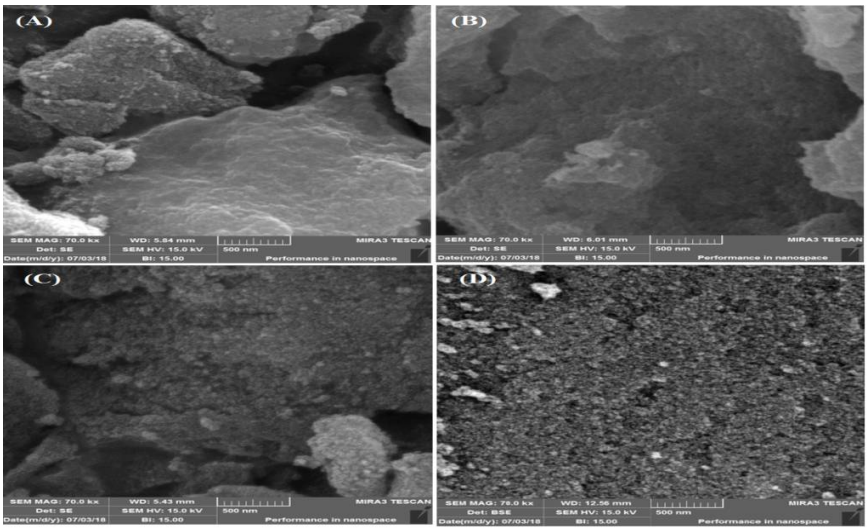

Figure (6): SEM of cryogel with different PH (6, 7, 8, 10) (A, B, C, D) respectively

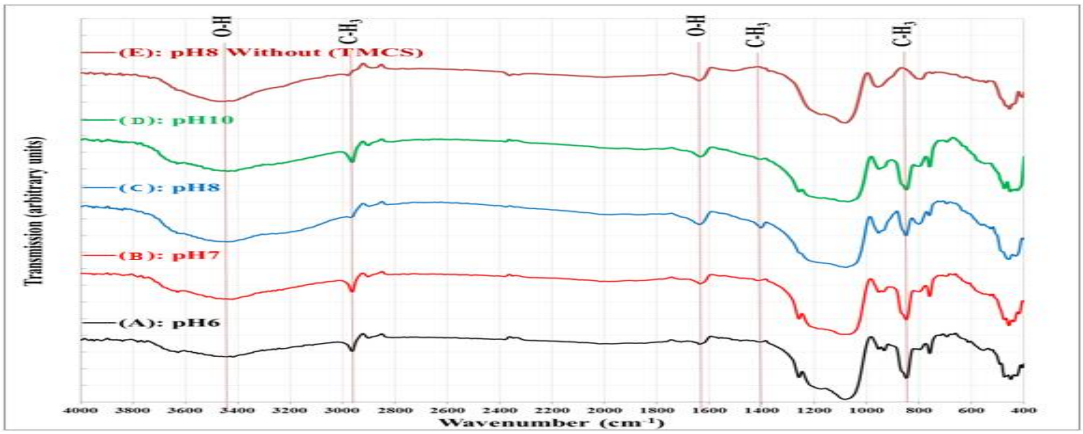

Figure (7): shown FT-IR spectroscopy for samples cryogel different PH (6, 7, 8, 10) with surface modification by (TMCS) and (E) PH8 without (TMCS)

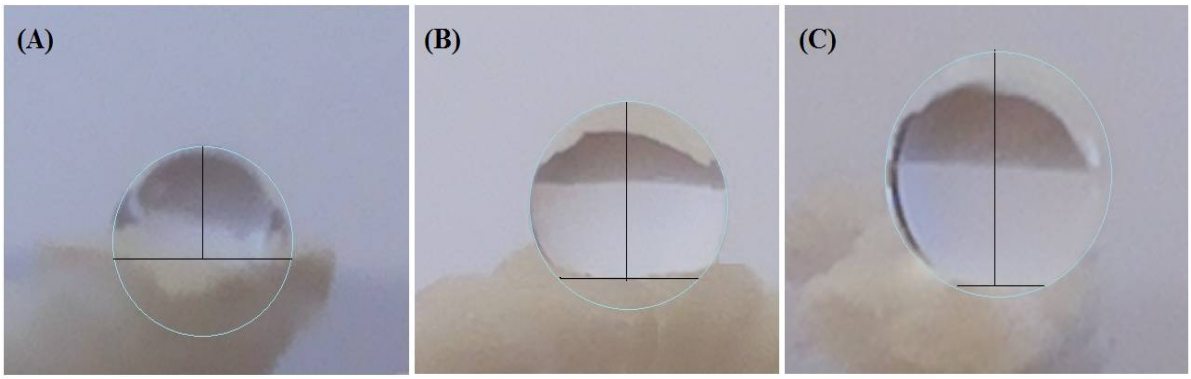

Figure (8): contact angle of the cryogels prepared with TBA: (A) one time modification (B) two time modification (C) three times surface modification with TMCS.

Indian Journal of Natural Sciences www.tnsroindia.org.in ©IJONS

Vol.9 /Issue 51 / December / 2018 *International Bimonthly* *ISSN: 0976 – 0997*

REVIEW ARTICLE

Review of the Secrets and Uses of Stem Cells

Wijdan Thamer Mahdi*

Department of Biology, College of Science, University of Al-Qadisiyah, Iraq

Received: 15 Sep 2018 Revised: 17 Oct 2018 Accepted: 22 Nov 2018

***Address for Correspondence**
Wijdan Thamer Mahdi
Department of Biology,
College of Science,
University of Al-Qadisiyah, Iraq
Email: Wejdan.thamer@qu.edu.iq

ABSTRACT

Stem cells are one of the most promising solutions that doctors and researchers study daily to treat many of the most intractable diseases. Stem cells are non-specialized cells that can differentiate to any type of cell in the body. Human, the cells that make up the embryo in its early stages, these cells have the ability to divide continuously in addition to their ability to differentiate. Stem cells are one of the medical discoveries that may change the entire medicine and ways to treat various diseases and intractable ones to scientists and doctors to the present time, and divide the stem cells into two sections embryonic stem cells and adult stem cells, and embryonic cells have the greatest ability to divide and differentiation of cells Adult cells are age-limited compared to fetuses, and fetal cells in embryos are in their early stages, while adult cells exist in both children and adults. . Muslim scientists have permitted the use and extraction of stem cells for scientific research and treatment if their source is permissible, such as adults after their consent and children with the consent of their parents and without harming them, placenta, umbilical cord, The parents have none of the past, and there are also some forbidden sources such as cloning or deliberately induced embryos.

Keywords: doctors, diseases, cells, embryos, treatment, Stem.

INTRODUCTION

Stem cells are defined as undifferentiated cells that may be subdivided into producing cells that continue as stem cells or become specialized cells. Stem cells are a constant source of the body's distinct cells responsible for forming tissues and organs not in the body. But also in plants [1].

Stem cell types

Stem cells are divided into four major types depending on their source and ability to differentiate: [2].

Embryonic Stem Cells

Embryonic stem cell (embryonic stem cell) is obtained from the internal cell mass of the embryo's erythema. Blastocyst, which is responsible for the production of more specialized cells, leads to the emergence of all cell types belonging to the different organs and tissues of the body. The internal cell mass can be extracted and developed in special laboratory conditions to maintain the characteristics of embryonic stem cells Where lies the importance of embryonic stem cells in that they were able to study the natural evolution, and the occurrence of diseases, as well as medications and other treatments tested [3].

Adult Stem Cells

Adult stem cells are also called tissue-specific stem cells and are capable of producing different types of tissue cells or organs in which they live, such as skin cells. Making it more specialized than embryonic stem cells. Hematopoietic stem cells, for example, are capable of generating red blood cells, white blood cells, and platelets, but they are not able to generate tissue cells and other organs, such as liver cells, Or Lung. It should be noted that there are types of adult stem cells found in some tissues and organs of the body, which are able to replace cells lost from the fabric in the normal daily life or when exposure to an injury, for example mesenchymal stem cells (Mesenchymal Stem Cells) They also have the term Stromal cells, which represent cells isolated from the connective tissue surrounding tissues and organs. Adult stem cells have been able to increase human knowledge of things related to natural development, changes in age, and what happens when a particular injury or disease occurs [4]. Multi-capacity induced stem cells represent multiple induced stem cells pluripotent stem cells) are engineered in the laboratory by converting adult stem cells into similar cells in their embryonic stem cell behavior, which may make them capable of generating all types of cells in the body. These cells have enabled scientists to become more familiar with natural development, the incidence and development of diseases, and the testing and development of drugs and other therapies [5].

Peripheral blood stem cells

Can be obtained through a blood sample. These cells can produce a large number of cells with different functions that make up the blood and the immune system, including Red blood cells, platelets, granulocytes, and lymphocytes [6].

Umbilical Cord Stem Cells

can be obtained from newborns. These cells are multi-capacity; That is, they are able to differentiate into a Conscious of certain cells and not all species, and this prompted doctors and scientists to store the umbilical cord blood at the birth of the child because of the likelihood of future use in the event of an individual need to stem cell therapy [7].

Stem cell benefits

Researchers and doctors have been interested in stem cell technology because of its many benefits, including the following:

1-Stem cells contribute to understanding and understanding how diseases occur and evolve by following the growth and development of stem cells in different organs and tissues of the body.
2-Some types of stem cells can be used to test the effectiveness and safety of new drugs. The efficacy of a new drug can be determined by testing its effect on a specific tissue.
3-Regenerative stem cells are used to generate healthy cells to replace diseased cells by directing stem cells to specialized cells that can be used to replace diseased or damaged tissues in the human body [8].

Stem cell-treated diseases

Immunotherapy is a promising hope for bronchitis in the treatment of various diseases such as Parkinson's disease and Alzheimer's, which are being researched using stem cells by producing new nerve stem cells and cardiovascular disease by repairing scars that occur in infected patients Stroke in the heart and blood vessels, in addition to diseases such as cerebral palsy, diabetes and even cancerous tumors, especially leukemia, as stem cells are drawn from the blood and bone marrow and then eliminate the cancer cells in the Blood completely, re-formation of blood using the extracted stem cells [9].Other diseases treated with stem cells are bone marrow failure, which is treated by matching stem cells in the patient, as well as diabetes, which is considered all existing drugs are drugs taken over the age to control it and not treat it completely, Stem cells can be used to treat deformities caused by burns. The skin has been implanted in people who have lost approximately 80% of their skin due to burns. These cells have grown in less than six months T remunerative than approximately 95% of these burns [10][11].

Constraints on the use of stem cells

There are several obstacles to the use of stem cells in the treatment of diseases, to this day, the use of stem cells as a method of treatment in a way that is approved only in the treatment of cancer and some diseases of blood and immunity in the blood. Many countries, such as the United States, some Western European countries, and Japan, still prohibit the use of stem cells for treatment outside specific diseases, partly because of the limited number of clinical studies under the laws of these countries that convince the authorities of the usefulness of using stem cells in specific diseases, The existence of large studies beyond its borders and the highest scientific and ethical standards. The lack of clinical studies in these countries is due to the lack of interest of manufacturers of drugs, which are usually conducted such studies, because such companies are not convinced of the economic feasibility of stem cell treatment because of the inability of these companies to produce stem cells in commercial quantities And the cost of stem cell therapy due to the high cost of the preparations and devices necessary for the separation and preparation of stem cells and the cost of imports, which are usually controlled by manufacturers of these substances under End devices and cosmetics research. In addition to these constraints, there is a lack of awareness among the various societies in different countries about stem cells and their different capacities to treat various diseases. Therefore, it is necessary to educate and educate the people about this new science, which will undoubtedly have the greatest impact in medicine and treatment. In the future [12][13].

Use caution of stem cells

The risks of stem cell therapy are concentrated in two things

Is related to the type of cells that are cultivated in the human body to be treated. The possible danger of the cells is determined depending on the type, the capacity and the source from which they were taken, as well as the factors that were exposed to the cells after taking them from the source and before planting them in the body. The safest cells are those taken from the same patient autologous, which is not rejected by the body and does not attack the body being part of it, but comes with this safety lack of ability of these cells to treatment, especially in the treatment of chronic diseases because the cells are the same age as the patient, The patient was a child or a young person. It is not harmful, but if the patient is ill, the ability of the cells to be treated and to become specialized cells decreases with age. The safest cells after autologous cells are umbilical cord cells because they are not known as cells that are alien to the body, and then come the less safe cells, the adult stem cells taken from another person where they can be rejected by the body being strange and there is a possibility that these cells stimulate an attack from a device Immunization of the person in which the organ is planted, and the cultivation of immature stem cells may contain immune cells that may attack the body and cause serious problems [14][15].

1-

It is related to the type of process performed for the patient to cultivate stem cells, as there are precautions and procedures are necessary as in the surgical procedures and any defect or neglect will lead to complications [16][17].

REFERENCES

1- Koch TG, Heerkens T, Thomsen PD, Betts DH. Isolation of mesenchymal stem cells from equine umbilical cord blood. BMC Biotechnol. 2007;7:26. doi: 10.1186/1472-6750-7-26.
2- Lanzoni G, Roda G, Belluzzi A, Roda E, Bagnara GP. Inflammatory bowel disease: Moving toward a stem cell-based therapy. World J Gastroenterol. 2008;14: 4616–4626. doi: 10.3748/wjg.14.4616.
3- Khan SN, Craig L, Wild R. Osteoporosis: therapeutic guidelines. Guidelines for practice management of osteoporosis. Clin Obstet Gynecol. 2013; 56(4):694–702. Epub 2013/11/02.
4- Tao H, Yang HY, Yu MC, Yang C, Zeng WQ, Duan FH, et al. Effects of systemic transplantation of allograft adipose-derived stem cells in glucocorticoid-induced osteoporosis rats. Acta Anatomica SinicaActa Anat Sin. 2011; 42(2):220–5.
5- degani FJ, Langroudi L, Arefian E, Shafiee A, Dinarvand P, Soleimani M. A comparison of pluripotency and differentiation status of four mesenchymal adult stem cells.
6- Al-Grawi, E.D.C., and G.R.L. Al-Awsi. 2018. "Expression of CDKN2A (P16/Ink4a) among Colorectal Cancer Patients: A Cohort Study." *Journal of Pharmaceutical Sciences and Research* 10 (5).
7- Ibraheen, Lujain Hussein and Abed, Salwan Ali (2017) Accumulation detection of some heavy metals in some types of fruits in the local market of Al-Diwaniyah City, Iraq. *Rasayan J. Chem*.10 (2), 339 -343. DOI: http://dx.doi.org/10.7324/RJC.2017.1021641.
8- Lateef, G., Al-Thahab, A., & Chalap Al- Grawi, E. (2018). Linkage between H. pylori Infection and TNF-α polymorphism in The Pregnant Women. *International Journal Of Research In Pharmaceutical Sciences, 9* (SPL1). doi:10.26452/ijrps.v9iSPL1.1298
9- Shamran, A. R, Shaker, Z. H, Al-Awsi, G. R. L, Khamis, A .S , Tolaifeh, Z. A. and Jameel, Z. I, 2018. RAPD-PCR IS A GOOD DNA FINGERPRINTING TECHNIQUE TO DETECT PHYLOGENETIC RELATIONSHIPS AMONG STAPHYLOCOCCUS AUREUS ISOLATED FROM DIFFERENT SOURCES IN HILLA CITY, IRAQ. Biochemical and Cellular Achieves. Vol. 18, Supplement 1, pp. 1157-1161.
10- Kolios G, Moodley Y. Introduction to stem cells and regenerative medicine. Respiration. 2013; 85:3–10. doi: 10.1159/000345615.
11- Singec I, Jandial R, Crain A, Nikkhah G, Snyder EY. The leading edge of stem cell therapeutics. Annu Rev Med. 2007; 58:313–328. doi: 10.1146/annurev.med.58.070605.115252.
12- Ma N, Stamm C, Kaminski A, Li W, Kleine HD, Müller-Hilke B, Zhang L, Ladilov Y, Egger D, Steinhoff G. Human cord blood cells induce angiogenesis following myocardial infarction in NOD/scid-mice. Cardiovasc Res. 2005;66: 45–54. doi: 10.1016/j.cardiores.2004.12.013.
13- Seghatoleslam M, Jalali M, Nikravesh MR, Hosseini M, Hamidi Alamdari D, Fazel A. Therapeutic benefit of intravenous administration of human umbilical cord blood- mononuclear cells following intracerebral hemorrhage in rat. Iran J Basic Med Sci. 2012; 15:860–872.
14- Alhadlaq A, Mao JJ. Mesenchymal stem cells: isolation and therapeutics. Stem CellsDev. 2004;13:436–448. doi: 10.1089/scd.2004.13.436.
15- Ji F, Wang Y, Sun H, Du J, Zhao H, Wang D, Xu Q, Duan D, Yang H. Human umbilical cord blood-derived non-hematopoietic stem cells suppress lymphocyte proliferation and CD4, CD8 expression. J Neuroimmunol. 2008;197:99–109. doi: 10.1016/j.jneuroim.2008.04.013.
16- Langer H, May AE, Daub K, Heinzmann U, Lang P, Schumm M, Vestweber D, Massberg S, Schönberger T, Pfisterer I, Hatzopoulos AK, Gawaz M. Adherent platelets recruit and induce differentiation of murine embryonic endothelial progenitor cells to mature endothelial cells in vitro. Circ Res. 2006;98: e2–e10.
17- Lanzoni G, Roda G, Belluzzi A, Roda E, Bagnara GP. Inflammatory bowel disease: Moving toward a stem cell-based therapy. World J Gastroenterol. 2008;14: 4616–4626. doi: 10.3748/wjg.14.4616.

Indian Journal of Natural Sciences www.tnsroindia.org.in ©IJONS

Vol.9 /Issue 51 / December / 2018 *International Bimonthly* *ISSN: 0976 – 0997*

RESEARCH ARTICLE

Effects of Q-Switched Nd:YAG Laser Surface Treatment on Some Properties of Zirconia-Porcelain Interface

Abdulsatar M.Abdulsatar, Basima M. A. Hussein* and Ali S. Mahmood

Institute of Laser for Postgraduate Studies, University of Baghdad, Iraq

Received: 21 Sep 2018 Revised: 25 Oct 2018 Accepted: 28 Nov 2018

***Address for Correspondence**
Basima M. A. Hussein
Institute of Laser for Postgraduate Studies,
University of Baghdad, Iraq
Email: basma.moh@ilps.uobaghdad.edu.iq

ABSTRACT

Background: Porcelain fuse to zirconia is one of the major restorations in dentistry. Various surface treatment methods have been suggested to obtain high bond strength between zirconia and porcelain such as sandblasting, chemical etching, grinding and laser surface treatments.Purpose: The aim of this study was to assess the effect of Q-switched Nd:YAGlaser on the shear bond strength of zirconia ceramic to porcelain.Materials and Methods: 30 zirconia specimens (9*4)mm were divided into three groups according to the type of zirconia : (a) Control group (n=10) samples were sintered and veneered with porcelain according to the manufacturer's instructions without surface treatment; (b) Q-switched Nd:YAG/Pre sintered zirconia group (n=10) samples were treated by laser(Energy density 30 J/cm^2 and frequency 10 Hz) then sintered and veneered with porcelain according to the manufacturer's instructions ; (c) Q-switched Nd:YAGSintered zirconia group(n=10) samples were sintered then treated with laser (Energy density 35 J/cm^2 and frequency 10 Hz) and veneered with porcelain according to the manufacturer's instructions. In this study, Surface morphology was examined using digitalmicroscope, surface roughness test was done by Atomical Force Microscope (AFM),and Shear Bond Strength test was done by a universal testing machine. After debonding, the zirconia surfaces were examined under a digital microscope to determine their fracture mode.Results: The Results of this study showed that the lowest SBS was recorded in control group, and the highest SBS recorded in the Q-switchedNd:YAG/ Pre sintered zirconia group, followed by Q-switchedNd:YAG/ sintered zirconia group, as well as improvement in surface roughness and positive change in the morphology and mode of failure in the experimental groups.Conclusion: This study shows that Fractional and Q switched Nd:YAGlaser treatment increase the bond strength higher than the untreated zirconia CO2 laser.

Key Words: Nd:YAG laser ; Zirconia ;Shea bond strength ; Surface treatment, porcelain.

INTRODUCTION

Zirconia has been used in dentistry due to its good mechanical properties, low degree of bacterial adhesion, biocompatibility and acceptable optical properties.[1]The development of computer-aided design/computer-aided manufacturing (CAD/CAM) technologies permitted the use of zirconia in a wide range of clinical applications. It is now used in single crown, fixed partial denture, and implants suprastructures.[2] Zirconia has three phases: 1. Monoclinic (m) below 1170°C, 2. Tetragonal (t) above 1170°C, 3.Cubic (c) above 2370°C. After firing, the tetragonal-monoclinical phase transformation take place during cooling, and the material changes from a tetragonal structure to a monoclinical, resulting in a volume increase of 3% to 5% and some fractures and cracks can form because of the compressive stresses in the lattice.[3] Zirconia is a material with a strengthened frame, and it must be sheltered with a semitransparent veneering porcelain to get an esthetic appearance.[4]

Effective bonding relies on the micro-mechanical interlocking between zirconia and the veneering porcelain, which is a very essential factor for the longevity of zirconia restorations. Unlike zirconia,a veneering porcelain does not have good mechanical properties, and the nonexistence of strong bonding at the interface between zirconia and the veneering porcelain may result in fractures in the dental restoration.[5]Factors affecting bond strength including mechanical and chemical bonding, residual stress, and wettability can affect the bonding between zirconia and porcelain.[67] Therefore, to increase the bond strengths of veneering porcelain, some surface treatment procedures on zirconia have been developed such as:application of the liners, mechanical surface roughening,silanisation, , tribochemistry , thermal spray, chloro-silane treatment with steam,fusion with glassy balls, selective infiltration etching which creates intergranular porosity, corrosion with hot solutions, complex primer that react with hydroxyl groups, laser treatments. [8]Previous studies employed different lasers such asCO_2, Nd;YAG and Er;YAG for surface treatment of zirconia and reported varying degree of success [9].Soltaninejad et al ,concluded that the surface treatment with Nd:YAG laser resulted in increased share bond strength and surface roughness [10],whileLiu L et al found that Nd:YAG laser cannot improve the surface roughness of zirconia[11].The aim of this study was to evaluate the effects of Q-switched Nd: YAGlaser for enhancing the bond strength between the veneering ceramics and zirconia.

MATERIALS AND METHODS

Fabrication of zirconia specimens

Forty three discs (9 mm diameter * 4mm thickness) were fabricated of Y-TZP zirconia block (Incoris TZI C /Sirona /Germany). First of all cylinder model was designed by Pc, then the data was exported to CAD/CAM system (Inlab CAD/CAM system / Sirona /Germany) for milling the zirconia block and producing the specimens .The bonding surface of zirconia specimens were then polished using with (800 ,1500 , 2000)-grit silicon carbide abrasive paper for 15 sec to obtain standardized surface roughness [12] .After that all specimens were cleaned ultrasonically using ultrasonic cleaner with distilled water for 10 minutes to remove any contaminants. The samples were divided to form three groups:

First group (Control group)

Eleven pre sintered zirconia specimens were left without laser surface treatment thenspecimens were sintered in a furnace (inFire HTC speed /Sirona / Germany) according to manufacture instructions and it is considered as a control group. One sample was tested by digital microscope for assessment of surface morphology followed by AFM test .Then the other samples (N=10) were prepared to Porcelain buildup for shear bond strength testing. First, each sample was attached to piece of sticky wax (5mm diameter * 3mm thickness) .After that the samples were placed in a rubber mold and the investment material was poured into the mold. Then wax elimination was done using hot steamer).Dental porcelain (VITA VM9 / VITAZAHNFABIRK /GERMANY) was applied on the mold after wax

elimination according to manufacture instructions and then placed in porcelain furnace (programate/ p500/ ivoclarvevadent / Germany After porcelain sintering the investment material was removed and porcelain fused to zirconia samples were produced .All samples were soaked into water bath with distilled water at 37^0 for 24 hours before shear bond strength test [13].Shear bond strength test of each sample was attached to the universal testing machine (INSTRON 1195 / England) and load was applied at 1 mm/ minwith blade tip perpendicular to zirconia porcelain interface [12]. Shear bond strength was calculated using the formula

Shear bond strength (MPa) =applied force (n) / area (mm^2)

Second group (Q-switchedNd:YAG/ Pre sintered zirconia)

Sixteen Pre sintered zirconia specimen surfaces were irradiated with Q Switched Nd: YAG laser(Daeshin enterprise/ Korea) with a 1064-nm wavelength by articulated arm transmission system. Pilot study was done to 5 samples, they were irradiated with an energy densityof 15, 20,25,30,35 J/cm^2, while the frequency was fixed to 10 Hz. Then the samples sintered and tested by light microscope and subjected to shear bond strength after porcelain build up.The digital microscopy and SBS test of the pilot study shows that (Energy density 30 J/cm^2 and frequency 10 Hz) is the best parameters with high SBS with no micro cracks. Ten samples were treated with these laser parameters and subjected to Shear bond strength test after sintering and porcelain build up over the zirconia samples. One sample was tested AFM test to assess the surface roughness.

Third group (Q-switchedNd:YAG/ sintered zirconia)

Sixteen sintered zirconia specimen surfaces were irradiated with Q Switched Nd:YAG laser(Daeshin enterprise/ Korea) with a 1064-nm wavelength by articulated arm transmission system. Pilot study was done to 5 samples, theywere irradiated with an energy density of 15, 20,25,30,35 J/cm^2, while the frequency was fixed to 10 Hz. Then the samples tested by digital microscope and subjected to shear bond strength after porcelain build up.The light microscopy and SBS test of the pilot study shows that (Energy density 35 J/cm^2 and frequency 10 Hz) is the best parameters with high SBS with no micro cracks. Ten samples were treated with these laser parameters and subjected to Shear bond strength test after porcelain build up over the zirconia samples. One sample was tested AFM test to assess the surface roughness.

Fracture mode

After SBS test the debonded surfaces of the zirconia was examined microscopically with (40 x) to determine the mode of fracture[14]where;

1. Adhesive failure: If less than 25% of the zirconia cylinder surface was covered with porcelain.
2. Cohesive failure: If less than 25 % of the zirconia cylinder surface was visible.
3. Mixed failure: for all other cases.

Statistical Analysis

StatisticalMethods were used in order to analyze and assess the result which includes:

A- Descriptive statistics: (mean and standard deviation).

B-Inferential statistics :(ANOVA test andDunnettT3 test was carried out) where p value less than 0.05 as a level of significance

RESULTS

Digital microscopic observations

The photographsshow the surface morphology of the zirconia specimens figure .The image of the untreated zirconia (A) appeared to be smoother than that of Nd: YAG Laser groups (B, C, D, E) and the surface texture of the laser treated zirconia consist of micro retentive pits with different degree of roughness between the two groups. There is no microcracks or defects appear in the microscopy images.

Shear bond strength

The means shear bond strength and standard deviations are shown in Table 1 and figure 2.In general, laser surface treatment increase SBS of zirconia to porcelain. The highest bond strength was obtained from the Q-switchedNd:YAG/ Pre sintered zirconiagroup (20.18). The lowest value was obtained from control group (7.397). The bond strength of the Q-switchedNd:YAG/ sintered zirconiagroup was lower than that of the Q-switchedNd:YAG/ Pre sintered zirconia.To test the significant difference between groups F test was used. (Table 2) shows high significant difference between the control and the experimentalgroups. DunnettT3 test between control and experimental groups in Table (3) shows that thereis a significant deference between the control and the experimental groups, butthere is non-significant difference between the two lasers treatedgroups.

Mode of failure

Failure types are shown in the table (4).The analysis of mode of failure after SBS test revealed that the adhesive failure was the predominantly mode in the control group. Regard of experimental groups, the mixed failure was the highest frequency in theQ switched Nd:YAG /pre sintered zirconia groups while inQ switched Nd:YAG / sintered zirconiagroup the mixed and cohesive mode of failure was the highest mode.

Surface roughness analysis

Surface roughness was evaluated by AFM .Table (5) displays surface roughness measurements of the different groups.The lowest Ra value was observed with the control specimen (12.9) followed by that Treated with Q switched Nd:YAG / sintered zirconiagroup (17.8) and the highest Ra value was shown with Q switched Nd:YAG /pre sintered zirconiagroup(21.6).

DISCUSSION

Laser was suggested by many authorsas an alternative surface treatment method to increase surface roughness of zirconia[15,16,17]. Therefore, the focus of the present study was to investigate the effect of Q switched Nd:YAG laser irradiation (at different intensities) on the bond strength of sintered and pre sintered Y-TZP to porcelain prior to sintering.Some studieshave evaluated the bond strength between the zirconia and veneering porcelain and the surface roughness after various surface treatments on zirconia[1819]. Effective bonding is essential to ensure longevity of the zirconia dental restoration; otherwise, there will be deboning of the porcelain. To remove this failure, researchers target to improve the bond strength by increasing the surface area of zirconia through different surface treatments.[20] Moon J et al, applied surface treatments on pre-sintered zirconia It was highlighted that pre sintered surface treatment had many benefits. Contrary to post-sintered surface treatment, micro cracks are not occurring[21].It has been reported that post sintering surface treatments increase the fracture risk by weakening the structure of zirconia and accelerating the tetragonal to monoclinical transformation .[22] In this study no microcracks were appeared which may related to the type of surface treatment laser. Shear stresses are thought to be major stresses leading to bonding

failure of restorative materials, and the shear bond strength tests are simple , quick and appropriate [11]. In this study, shear bond strength test was used to examine the bonding of zirconia ceramics to porcelain. The result of this study shows that using of Q switched Nd:YAG laser on the surface of zirconia resulted in significantly improved shear bond strengths compared to the control group , because of the increase of surface roughness on the zirconia surface that enhance the interlocking with the porcelain.This effect is related to the photomechanical effect (photo disruption) of laser. The nanosecond laser wave with high intensities lead to localized absorption of the high intensity beam and lead to cavity formation[23].

This result is in agreement withSoltanianijad et al.whom concluded that laser surface treatment on zirconia significantly increase shear bond strength because of surface roughness[10]. However the result disagrees with(Kirmali et al)Whom concluded that Nd;YAG lasers are not effective to increase the bond strength between zirconia and porcelain , this due to the fact that author in his study used different laser energy and different pulse duration[12].The morphology analysis in the present study was accomplished by digital microscope and showed increase in surface area of zirconia without any microcracks after laser irradiation. Thisfinding disagree with other studiesGorler et al and Akyil et al reporting cracks on zirconia surface after laser treatment[24,13]. This disagreement may be related to laser irradiation with different parameter. In this study the pulse duration was seated in nanosecond , while Gorler et al used microsecond laser.[13]So the shortest the pulse duration the minimum hazard affected zoon. In the study, it was observed that the number of adhesive failure types was less than mixed and cohesive failure type in laser treated groups because adhesive failure is related to low bond strength [25]. Laser surface treatment create some area for housing of porcelain as well as it helped by increase the surface area for improve the bonding between zirconia and porcelain.This finding in agreement withTsuo Y et al study in which the adhesive mode of failure is less in the laser treated group than the control group[18].(Cavalcani et al) examined the bond types after the surface treatments between ZrO2 and resin cement and found that the adhesive failure type was higher than the mixed failure type in all groups[26]. The reason may have been because the author used other type of laser(Er:YAG) .Differed laser produce different interaction with the material ,which is seem clearly between Er:YAG andQ switched Nd:YAGlaser. Within the limitations of this study, thefollowing conclusions are drawn:

- Laser parameters are a critical factor that effect on the surface treatment final result.
- Laser surface treatment can change the surface roughness, surface morphology of the zirconia and the fracture mode between zirconia and porcelain.
- Application of different laser improve SBS between ZrO_2 and porcelain.
- Both Q switched Nd:YAG laser/pre sintered zirconia and Q-switched Nd:YAG laser/ sintered zirconia demonstrated higher bond strength than untreated zirconia and there is no significant difference in SBS between the experimental groups.

ACKNOWLEDGEMENTS

Authors would like acknowledge all teaching staff at Institute of Laser for Postgraduate Studies –University of Baghdad

REFERENCES

1. Denry I, Kelly JR. State of the art of zirconia for dental applications. *Dent Mater*. 2008;24(3):299-307.
2. Wolfart M, Lehmann F, Wolfart S, Kern M. Durability of the resin bond strength to zirconia ceramic after using different surface conditioning methods. *Dent Mater*. 2007;23(1):45-50.
3. Piconi C, Maccauro G. Zirconia as a ceramic biomaterial. *Biomaterials*. 1999;20(1):1-25.
4. Sundh A, Molin M, Sjögren G. Fracture resistance of yttrium oxide partially-stabilized zirconia all-ceramic bridges after veneering and mechanical fatigue testing. *Dent Mater*. 2005;21(5):476-482.
5. Bona A Della, Pecho OE, Alessandretti R. Zirconia as a dental biomaterial. *Materials (Basel)*. 2015;8(8):4978-4991.

doi:10.3390/ma8084978.

6. Isgrò G, Pallav P, van der Zel JM, Feilzer AJ. The influence of the veneering porcelain and different surface treatments on the biaxial flexural strength of a heat-pressed ceramic. *J Prosthet Dent*. 2003;90(5):465-473.
7. De Jager N, Pallav P, Feilzer AJ. The influence of design parameters on the FEA-determined stress distribution in CAD–CAM produced all-ceramic dental crowns. *Dent Mater*. 2005;21(3):242-251.
8. Sato H, Yamada K, Pezzotti G, Nawa M, Ban S. Mechanical properties of dental zirconia ceramics changed with sandblasting and heat treatment. *Dent Mater J*. 2008;27(3):408-414.
9. Ahrari F, Boruziniat A, Mohammadipour HS, Alirezaei M. The effect of surface treatment with a fractional carbon dioxide laser on shear bond strength of resin cement to a lithium disilicate-based ceramic. *Dent Res J (Isfahan)*. 2017;14(3):195.
10. Soltaninejad F, Moezizadeh M, Khatiri M, Razaghi H, Namdari M, Nojehdehian H. Effect of Nd: YAG laser energy density on bond strength and phase transformation of zirconia. 2017.
11. Liu L, Liu S, Song X, Zhu Q, Zhang W. Effect of Nd: YAG laser irradiation on surface properties and bond strength of zirconia ceramics. *Lasers Med Sci*. 2015;30(2):627-634.
12. Kirmali O, Akin H, Ozdemir AK. Shear Bond Strength of Veneering Ceramic to Zirconia Core After Different Surface Treatments. *Photomed Laser Surg*. 2013;31(6):261-268. doi:10.1089/pho.2013.3487.
13. Gorler O, Ozdemir AK. Bonding Strength of Ceromer with Direct Laser Sintered, Ni-Cr-Based, and ZrO ₂ Metal Infrastructures After Er:YAG, Nd:YAG, and Ho:YAG Laser Surface Treatments—A Comparative *In Vitro* Study. *Photomed Laser Surg*. 2016;34(8):355-362. doi:10.1089/pho.2016.4129.
14. Tsuo Y, Yoshida K, Atsuta M. Effects of alumina-blasting and adhesive primers on bonding between resin luting agent and zirconia ceramics. *Dent Mater J*. 2006;25(4):669-674.
15. Li R, Ren Y, Han J. Effects of pulsed Nd: YAG laser irradiation on shear bond strength of composite resin bonded to porcelain. *Hua xi kou qiang yi xue za zhi= Huaxi kouqiang yixue zazhi= West China J Stomatol*. 2000;18(6):377-379.
16. Da Silveira BL, Paglia A, Burnett Jr LH, Arai Shinkai RS, Eduardo CDP, Spohr AM. Micro-tensile bond strength between a resin cement and an aluminous ceramic treated with Nd: YAG laser, Rocatec System, or aluminum oxide sandblasting. *Photomed Laser Surg*. 2005;23(6):543-548.
17. Spohr AM, Borges GA, Júnior LHB, Mota EG, Oshima HMS. Surface modification of In-Ceram Zirconia ceramic by Nd: YAG laser, Rocatec system, or aluminum oxide sandblasting and its bond strength to a resin cement. *Photomed Laser Surg*. 2008;26(3):203-208.
18. Cevik P, Cengiz D, Malkoc MA. Bond strength of veneering porcelain to zirconia after different surface treatments. *J Adhes Sci Technol*. 2016;30(22):2466-2476.
19. Kirmali O, Kapdan A, Kustarci A, Er K. Veneer Ceramic to Y-TZP Bonding: Comparison of Different Surface Treatments. *J Prosthodont*. 2016;25(4):324-329. doi:10.1111/jopr.12304.
20. Raigrodski AJ, Chiche GJ, Potiket N, et al. The efficacy of posterior three-unit zirconium-oxide–based ceramic fixed partial dental prostheses: A prospective clinical pilot study. *J Prosthet Dent*. 2006;96(4):237-244.
21. Moon J, Kim S, Lee J, Ha S, Choi Y. The effect of preparation order on the crystal structure of yttria-stabilized tetragonal zirconia polycrystal and the shear bond strength of dental resin cements. *Dent Mater*. 2011;27(7):651-663.
22. Guess PC, Zhang Y, Kim J-W, Rekow ED, Thompson VP. Damage and reliability of Y-TZP after cementation surface treatment. *J Dent Res*. 2010;89(6):592-596.
23. Meister J, Franzen R, Forner K, et al. Influence of the water content in dental enamel and dentin on ablation with erbium YAG and erbium YSGG lasers. *J Biomed Opt*. 2006;11(3):34030.
24. Akyıl MŞ, Uzun İH, Bayındır F. Bond Strength of Resin Cement to Yttrium-Stabilized Tetragonal Zirconia Ceramic Treated with Air Abrasion, Silica Coating, and Laser Irradiation. *Photomed Laser Surg*. 2010;28(6):801-808. doi:10.1089/pho.2009.2697.
25. Toledano M, Osorio R, Osorio E, et al. Durability of resin–dentin bonds: effects of direct/indirect exposure and storage media. *Dent Mater*. 2007;23(7):885-892.
26. Cavalcanti AN, Pilecki P, Foxton RM, et al. Evaluation of the surface roughness and morphologic features of Y-TZP ceramics after different surface treatments. *Photomed Laser Surg*. 2009;27(3):473-479.

Table (1):mean and S.D of the SBS (MPa) for the tested groups.

GROUPS	Mean (MPa)	SD ±
Control	7.397	2.288
Q-switched Nd:YAG/ Pre sintered zirconia	20.180	5.339
Q-switched Nd:YAG/sintered zirconia	19.876	2.307

Table (2): ANOVA test between SBSgroups

	Sum of squares	Df	Mean square	F	Sig
Between groups	1064.076	2	532.038	40.865	0.000
Within groups	351.523	27	13.019		
total	1415.600	29			

Table (3): DunnettT3 test between control and experimental groups

Groups		Mean difference	SIG
CONTROL	Q-switched Nd:YAG/ Pre sintered zirconia	-12.783	.000
	Q-switched Nd:YAG/ sintered zirconia	-12.479	.000
Q-switched Nd:YAG/ Pre sintered zirconia	Q-switched Nd:YAG/ sintered zirconia	.304	.998

Table (4): Mode of failure results of the tested groups.

Mode of failure	Control	Q switched Nd:YAG / pre sintered zirconia	Q switched Nd:YAG / sintered zirconia
Adhesive	6	2	2
cohesive	0	3	4
mixed	4	5	4

Table (5): surface roughness measurements by AFM test of the tested group

Control (nm)	Q switched Nd:YAG /pre sintered zirconia (nm)	Q switched Nd:YAG /sintered zirconia (nm)
12.9	21.6	17.8

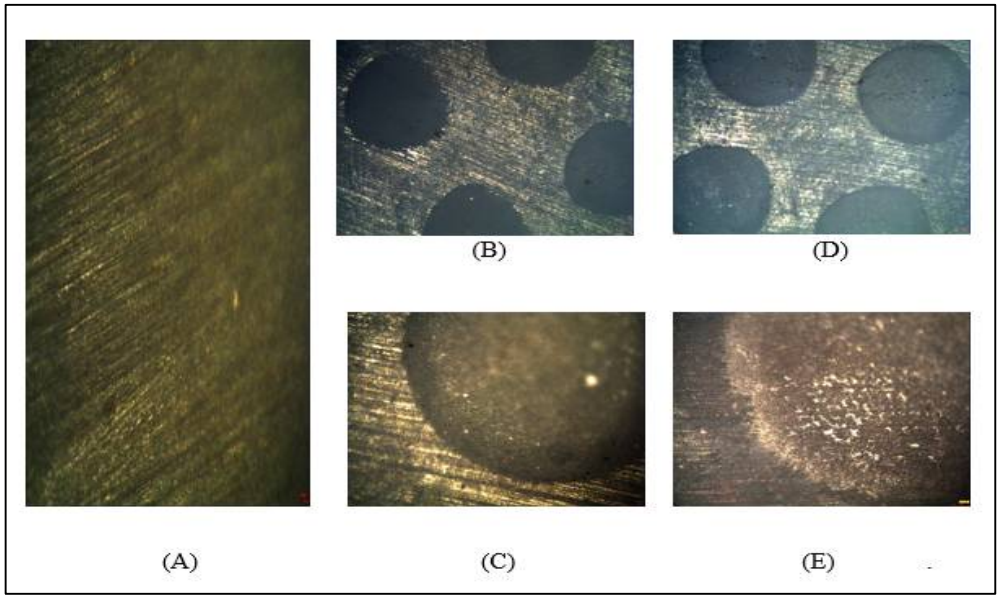

Figure (1): Digital microscopy pictures: A Control (100X), B.Q-switched Nd: YAG/ Pre sintered zirconia (40X). C.Q-switched Nd: YAG/ Pre sintered zirconia (100X).D.Q-switched Nd: YAG/ sintered zirconia (40X) E.Q-switched Nd: YAG/ sintered zirconia (100X)

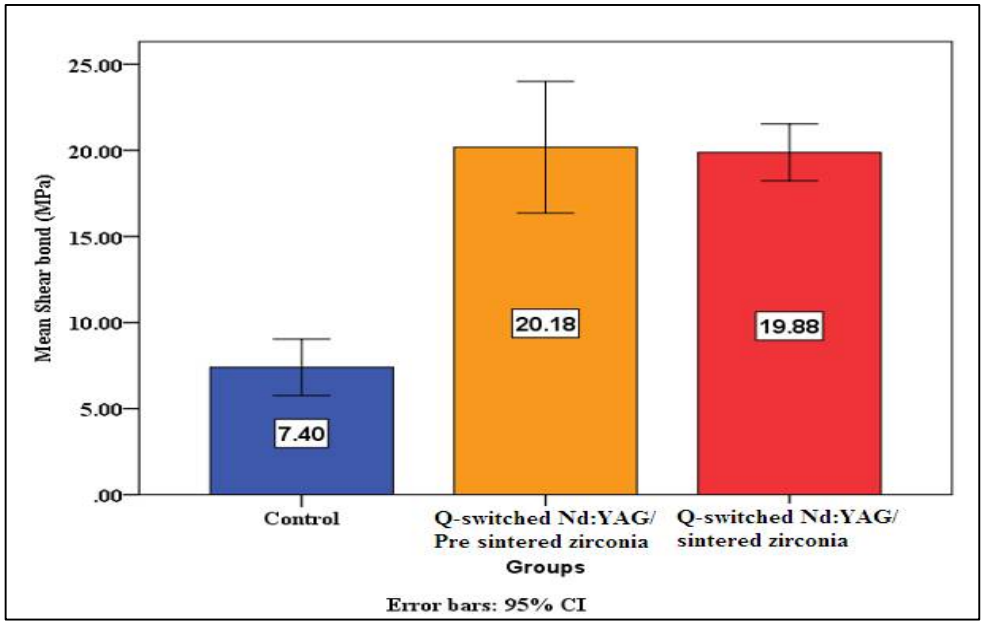

Figure (2) : Shear bond strength of the tested groups

Indian Journal of Natural Sciences www.tnsroindia.org.in ©IJONS

Vol.9 /Issue 51 / December / 2018 *International Bimonthly* *ISSN: 0976 – 0997*

RESEARCH ARTICLE

Absorption Enhancement of NiO Thin Film Prepared by SPT for Solar Absorber Application

Zaid L. Hadi[1]* and Bahaa T. Chiad[2]

[1]Ministry of Education, General Directorate of Education of Babylon, Iraq.
[2]Department of Physics, College of Science, University of Baghdad, Iraq.

Received: 20 Sep 2018 Revised: 23 Oct 2018 Accepted: 27 Nov 2018

***Address for Correspondence**
Zaid L. Hadi
Ministry of Education,
General Directorate of Education of Babylon, Iraq.
Email: zaid.altai@scbaghdad.edu.iq

ABSTRACT

Spray pyrolysis technique has been applied to deposit Nickel oxide thin films onto glass substrates, maintained at 350 °C. An aqueous solution of NiCl2.4[H2O] in 0.01 M was used for spraying process. Annealing was employed at 350 °C for 15 min. the annealing treatment was effected on the structural, optical, and morphological properties of the thin NiO films were examined. XRD endorses a polycrystalline cubic phase for both of deposit and annealed NiO films. A Polycrystalline nickel oxide was preferential growth along (111), (200), and (220) planes. XRD pattern has peak diffraction at 2θ = 37.28°, 43.29°, and 62.91°, respectively, for as-deposited and annealed. The FTIR investigation certified an enhanced in thin film absorbance after annealing. After the annealing process, an observable increase in the crystallite size was noted, where it measured using Scherrer's formula. The absorption spectroscopic study was recorded in the visible range of 350-750 nm. The surface morphology of deposit and annealed NiO films exposed a uniform coating on the substrate surface with a good distribution.

Keywords: NiO, Spray Pyrolysis, Solar Absorber, Annealing.

INTRODUCTION

Spray pyrolysis technique (SPT) can be classified as an inexpensive technique which simply fabricates a high-quality metal oxide thin films for different applications, for example, solar absorbers [1]. Nickelous oxide thin films were deposit using SPT. Whereas, NiO thin films could be deposit using several physical or chemical techniques [2]. Spray Pyrolysis is a thermally activated reaction between clusters of liquid or vapor atoms of different chemical species. In this process, the chemicals were fully dissolved within a carrier liquid which was sprayed onto the heated substrate in form of tiny droplets [3][4]. Among these, the SPT can be considered as a unique, safe, simple and cost-effective, where a subsequent annealing could possible just after the deposition process procedure done [5]. In addition, it has a wide renowned ability to deposit large area of layers [6]. Moreover, an allowance using important deposition

parameters such as substrate temperature, solution concentration, film thickness, etc. Where SPT was played a significant role in determining various properties of metal oxide thin films. SPT has been applied in last decades for solar cell production [7]. Many studies in scientific research have been dealt with for an over three decades on the SP for preparation of thin films [8]. It is noteworthy that, spray pyrolysis is a simple and inexpensive technique that based on a chemical vapor deposition process. In the present method, the precursor's solution was sprayed onto the preheated substrate using a compressed gas as a carrier [9]. In the present paper, NiO films were obtained by SPT from an aqueous solution of $NiCl_2.4H_2O$. Moreover, this study has dealt with the annealing treatment and morphology of the obtained films.

MATERIALS AND METHODS

Sample Preparation

Nickel monoxide thin films were successfully fabricated onto glass substrates with employment of SPT. An aqueous solution of nickel (II) chloride tetrahydrate ($NiCl_2$ $[H_2O]_4$) (Sigma make, with a purity of 99.9%) were used for spraying process with a fixed concentration of 0.01 M that dissolved in distilled water. The glass substrates which type of micro slides with dimensions (75×25×0.5) mm. Which were ultrasonically cleaned for 20 min when immersed in a heated distilled water at 70°C. The prepared solution was sprayed through a metallic nozzle with a radius of 0.35 mm onto heated glass substrates, for regarding a uniform thin film's deposition. So, an evaporation and decomposition could happen, thereby resulting in a formation of nickel oxide thin films according to the chemical reaction equation [10]:

$$NiCl_2 \cdot 4H_2O \xrightarrow{heat} NiO + 2HCl\uparrow + 3H_2O\uparrow$$

It's worth mentioning that, the flow rate, substrate temperature, deposition time, nozzle to substrate distance was kept fixed throughout the deposition process. Meanwhile, the substrate temperature was kept at 350±5 °C and the average solution flow rate was maintained at 0.16 mL per sec, for each spray pulse. Therein, the aqueous solution was sprayed on the substrate with a compressed air as a carrier gas. When the deposition process has finished, the substrate was left onto hotplate until it reaches the room temperature. Whereas, for make sure the chemical interaction has finished. Afterwards, one of the fabricated samples has been annealed to the selected deposition temperature for 15 min.

Sample Analysis

The crystal structural analysis was carried out using X-ray diffractometer (D2 PHASER, by BRUKER, Germany), with a wavelength of CuKα1 at λ=1.54056 Å, as a source of incident radiation. The thickness of NiO thin films was measured using an optical interferometer method, employing a green laser (wavelength of 532 nm). Wherein, this method depends on the interference of the laser beam that reflected from the thin film surface and its substrate. Within, the thickness has been determined using the formula [11].

$$t = \frac{\lambda}{2} \times \frac{\Delta x}{x} \qquad (1) \text{ (1)}$$

Where x is the fringe width, Δx is the consecutive separation distance of fringes, and λ is the laser wavelength.
FTIR spectra were recorded by Fourier transformation spectrophotometer (IR Prestige-21, by Shimadzu, Japan). UV-Vis spectra of the samples were obtained at room temperature using K-MAC SV2100 spectrophotometer (Korea Material & analysis, Korea). For an optical microscopic investigation, a digital camera of the 5 MB resolution was

used to connect with a microscope of type MOTIC B Series (Malaysia) that has employed for examining the surface topography of NiO thin films.

RESULTS AND DISCUSSION

The structural characterizations of NiO thin films have been examined by X-ray diffraction technique, to divulge the variations of the crystallinity. The XRD patterns of NiO thin films are shown in Figure (1). Which displayed the curve line of two cases; which are as deposit and annealed. It is noticed that the samples in both cases were polycrystalline in a cubic phase of NiO. The reflection peaks were growth along (111), (200) and (202) planes, at $2\theta = 37.280°$, 43.297°, and 62.916°, respectively. The strongest reflection intensity was observed at the first one, for deposit and annealed cases. XRD patterns were ensured in comparison with ICDD card No. (04-0835) [7]. After which, the 'd' values of the XRD were investigated with the standards that taken from the diffraction data file, as listed in the table (1). There is a good agreement in the observed and standard values of d-spacing which verified that the annealed state of NiO thin films. There is an accuracy of about 99.5% in the matching process of XRD data with the database. Moreover, NiO thin films identity has been verified. Crystallite size can be measured using FWHM of the XRD spectrum. The of broadening of the FWHM is inversely proportional to the average crystallite size (D). Which could be predicted by the Scherrer's formula [12], where, D is the grain size that given by:

$$D = \frac{K\lambda}{\beta \cos(\theta)} \qquad (2)$$

where β is the observed full width at half maximum intensity of the peak. An average value of β has been taken to calculate D. where, it's found that 20.57 nm, 21.32 nm for as deposit state and annealed, respectively.The spectra of the NiO samples are shown in Figure (2). The spectrum shows numerous absorption peaks that recorded within the range of 4000 cm^{-1} to 400 cm^{-1}. It's worth mentioning that, the broad absorption band nearby 3450 cm^{-1} which assigned to O–H stretching vibrations.

Whereas, the band at 1630 cm^{-1} is attributable to the H–O–H bending vibration mode. Therein, one can indicate the existence of traces of water in the sample. Moreover, it has not completely removed after the annealing process.The absorption bands that observed in the region of 430–490 cm^{-1} were definitely assigned to Ni–O stretching modes, as its previously termed by other researchers as mention in reference [13]. By investigating the FTIR spectrum, after the annealing process, an enhancement was clearly observed in the absorbance of NiO thin films. This could be an essential feature when it used for solar absorber applications. Furthermore, many of researchers were focused on the applications of the high absorbance thin film layers [14]. Subsequently, thickness values of the prepared samples were found out about (166, 175) nm which referred to as deposit and annealed, respectively. The thickness of prepared NiO films has been directly affected by the annealing treatment. Therefore, annealed NiO films can be further employed for solar cells application [15]. This increase was attributed to the crystallite size aggregate that actually observed after heating treatment. The UV–Vis spectra of NiO thin films were displayed in Figure (3).

The spectroscopic investigation in the UV-vis range was observed absorption peaks in the range of 350-380 nm. this result was in a good agreement with the researchers [1]. Furthermore, the morphology of the surfaces of the prepared film was depicted in figure (4). As can topography be seen, there is a uniform distribution of deposition on the substrate surface. Which, is one of best features of spray pyrolysis deposition technique. An important physical parameter that also has been investigated, which is the energy band gap. Using the absorbance data and according to Tauc formula [17], $(ahυ)^2$ versus incident photon energy (hυ), plots were obtained. The graph is epitomized in Figure (5). The energy band gap values were calculated to be 3.48 eV for the NiO film for as deposit and annealed, which is in a good agreement with that attained for normal bulk NiO (3.6-4.0) eV [18].

CONCLUSIONS

Spray parameters have been optimized for depositing films of Nickelous Oxide. The annealing process was employed. The prepared films are adherent to glass substrates. The crystalline cubic structure has been observed from XRD studies. Nano sized grains were carried out. FTIR have mentioned that absorbance was enhanced after annealing. Film thickness was in nanoscale. Absorption was increased by heat treatment. The films were in rough surface morphology. Energy ban gap of NiO films was in Eg range of NiO bulk mater.

REFERENCES

1. Önen Ü., Botsalı F. M., Kalyoncu M., Şahin Y. and Tınkır M., "Design and Motion Control of a Lower Limb Robotic Exoskeleton" , Des. Control Appl. Mechatron. Syst. Eng., 2017; 135–152.
2. Ukoba K. O., Eloka-Eboka A. C. and Inambao F. L., "Review of Nanostructured NiO Thin Film Deposition Using the Spray Pyrolysis Technique" , Renew. Sustain. Energy Rev., 2018; 82 (July) 2900–2915.
3. Mosiori C. O., *Inorganic Ternary Thin Films:Analysis of Optical Properties*; 2015;
4. Vasu V., and Subrahmanyam A., "Electrical and Optical Properties of Pyrolytically Sprayed SnO2 Film-Dependence on Substrate Temperature and Substrate-Nozzle Distance" , Thin Solid Films, 1990; 189 (2) 217–225.
5. Benramache S., Belahssen O., Arif A. and Guettaf A., "A Correlation for Crystallite Size of Undoped ZnO Thin Film with the Band Gap Energy - Precursor Molarity - Substrate Temperature" , Optik (Stuttg)., 2014; 125 (3) 1303–1306.
6. Sriram S., and Thayumanavan A., "Structural, Optical and Electrical Properties of NiO Thin Films Prepared by Low Cost Spray Pyrolysis Technique" , Int. J. Mater. Sci. Eng., 2014; 1 118–121.
7. Perednis D., and Gauckler L. J., "Thin Film Deposition Using Spray Pyrolysis" , J. Electroceramics, 2005; 14 (2) 103–111.
8. Patil P. S., "Versatility of Chemical Spray Pyrolysis Technique" , Mater. Chem. Phys. Mater. Chem. Phys., 1999; 59 185–198.
9. Ashour A., Kaid M. A., El-Sayed N. Z. and Ibrahim A. A., "Physical Properties of ZnO Thin Films Deposited by Spray Pyrolysis Technique" , Appl. Surf. Sci., 2006; 252 (22) 7844–7848.
10. Mahmoud S. A., Akl A. A., Kamal H. and Abdel-Hady K., "Opto-Structural, Electrical and Electrochromic Properties of Crystalline Nickel Oxide Thin Films Prepared by Spray Pyrolysis" , Phys. B Condens. Matter, 2002; 311 (3–4) 366–375.
11. A. Alias M. F., M. Rashid K. and A. Adem K., "Optical Properties for Ti Doped Thin Zno Films Prepared By PLD" Int. J. Innov. Res. Sci. Eng. Technol., 2014; 03 (08) 15538–15544.
12. Lang A. R., "X-Ray Diffraction Procedures for Polycrystal-Line and Amorphous Materials" , Acta Metall., 1956; 4 (1) 102.
13. Anandan K., and Rajendran V., "Morphological and Size Effects of NiO Nanoparticles via Solvothermal Process and Their Optical Properties" , Mater. Sci. Semicond. Process., 2011; 14 (1) 43–47.
14. Essa M. S., Chiad B. T. and Shafeeq O. S., "Macro Controlling of Copper Oxide Deposition Processes and Spray Mode by Using Home-Made Fully Computerized Spray Pyrolysis System" , AIP Conf. Proc., 2017; 1888 (1) 020021.
15. Ukoba O. K., Inambao F. L. and Eloka-Eboka A. C., "Influence of Annealing on Properties of Spray Deposited Nickel Oxide Films for Solar Cells" , Energy Procedia, 2017; 142 244–252.
16. Rahdar A., Aliahmad M. and Azizi Y., "NiO Nanoparticles: Synthesis and Characterization" , J. Nanostructures, 2015; 5, 145–151.
17. Greenwood D. A., "Amorphous and Liquid Semiconductors" , Opt. Acta Int. J. Opt., 1970; 17 (12) 952–952.
18. Akaltun Y., and Çayir T., "Fabrication and Characterization of NiO Thin Films Prepared by SILAR Method" , J. Alloys Compd., 2015; 625 144–148.

Table (1): 'd' values and d_{hkl} for hkl indices in case of as deposit and Annealed state.

hkl	Theoretical		As deposit		Annealed	
	2θ	d_{hkl}	2θ	d_{hkl}	2θ	d_{hkl}
111	37.280	2.4100	37.352	2.4056	37.273	2.4105
200	43.297	2.0880	43.261	2.0896	43.386	2.0839
220	62.916	1.4760	62.896	1.4765	62.143	1.4925

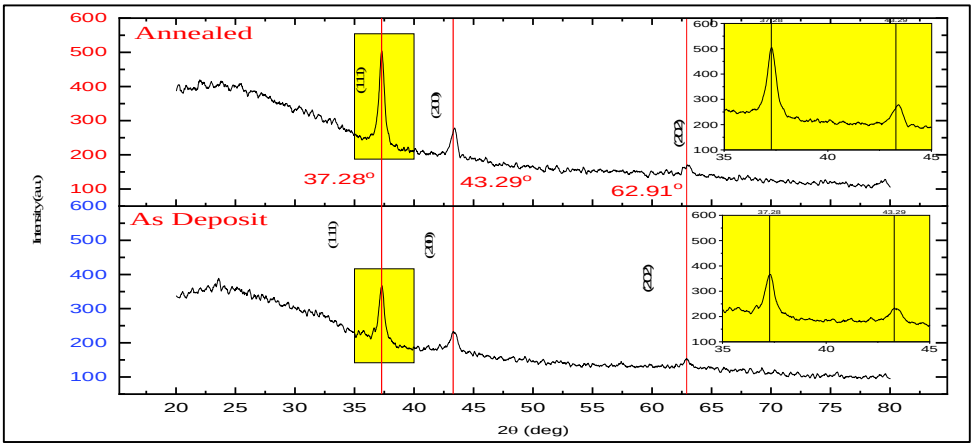

Figure (1): XRD patterns of NiO thin films.

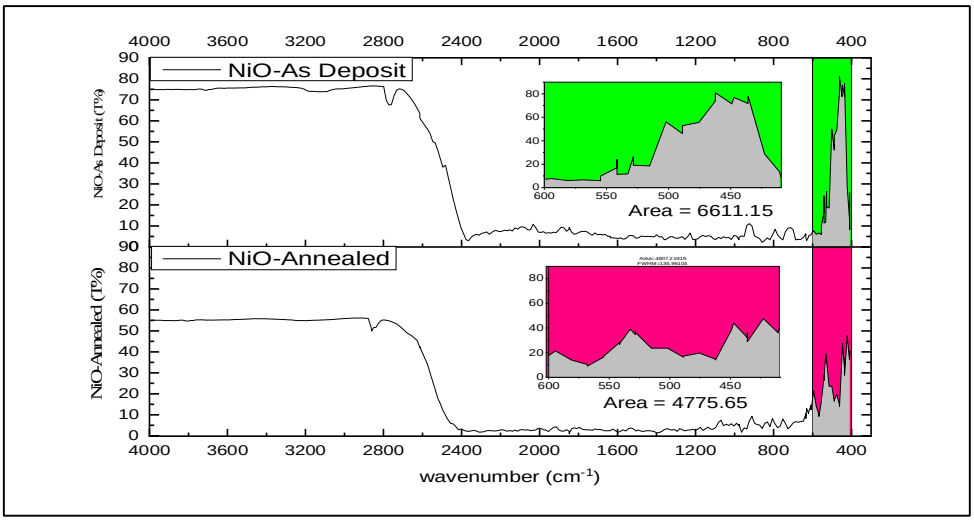

Figure (2): FTIR spectra of NiO thin film

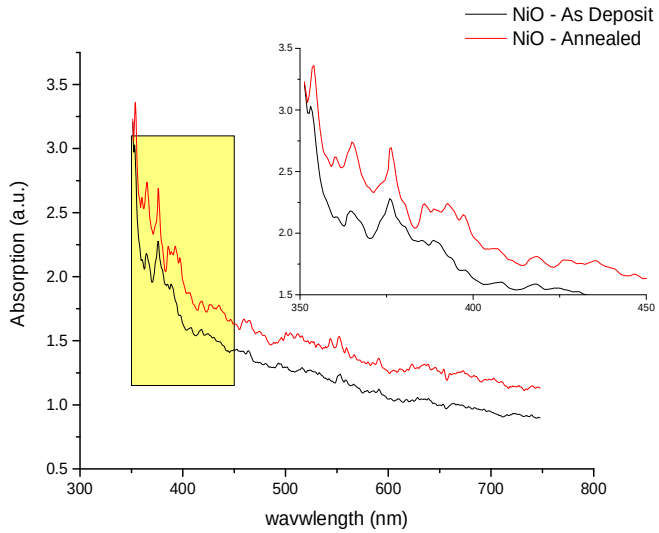

Figure (3): UV–vis spectra of NiO thin film

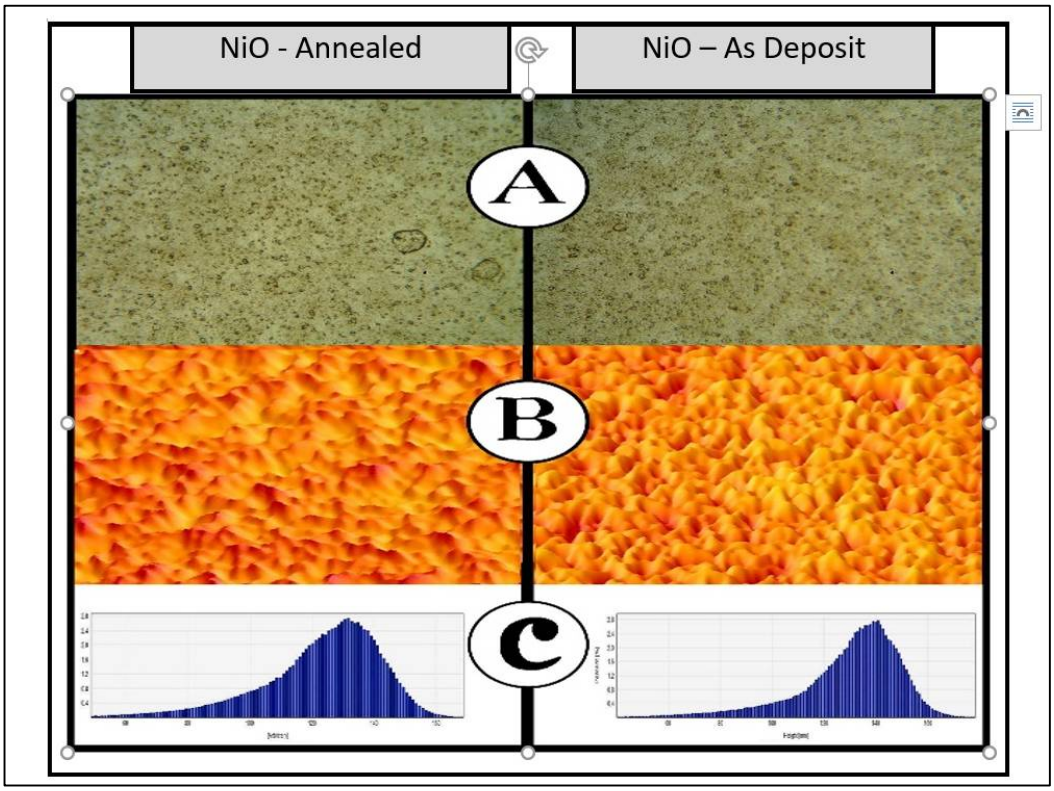

Figure (4): Optical of NiO thin film; A) optical photo, B) Morphology distribution, c) Roughness histogram.

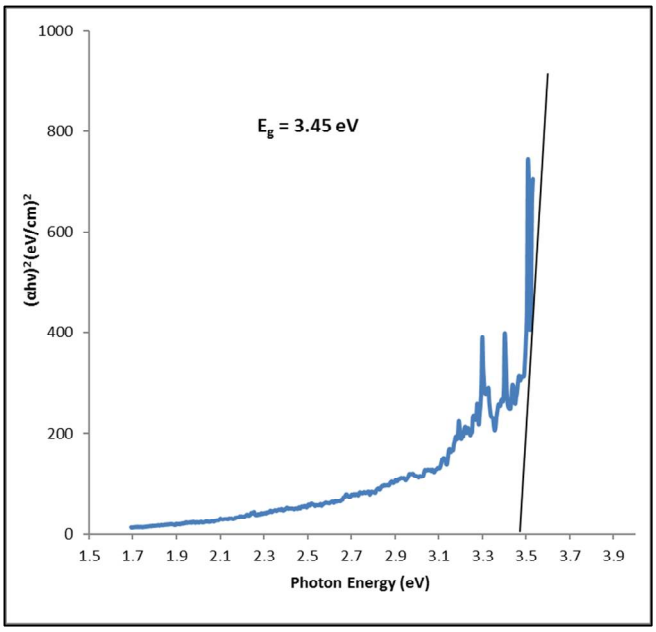

Figure (5): represents (ahυ)² vs hυ, the plot for NiO film.